CORA Cork Open Research Archive
Cartlann Taighde Oscailte Chorcaí

Title	Real-time early detection of allergic reactions based on heart rate variability
Authors	Gutiérrez-Rivas, Raquel
Publication date	2016
Original Citation	Gutiérrez-Rivas, R. 2016. Real-time early detection of allergic reactions based on heart rate variability. PhD Thesis, University College Cork.
Type of publication	Doctoral thesis
Rights	© 2016, Raquel Gutiérrez-Rivas. - http://creativecommons.org/licenses/by-nc-nd/3.0/
Download date	2026-10-26 23:22:03
Item downloaded from	https://hdl.handle.net/10468/4047

UCC
University College Cork, Ireland
Coláiste na hOllscoile Corcaigh

University of Alcalá

National University of Ireland, Cork

Joint PhD

PhD Program in Electronics: Advanced Electronic Systems.
Intelligent Systems.

Doctoral Thesis

Real-Time Early Detection of Allergic Reactions based on Heart Rate Variability

Raquel Gutiérrez Rivas

2016

University of Alcalá

National University of Ireland, Cork

Joint PhD

PhD Program in Electronics: Advanced Electronic Systems.
Intelligent Systems.

Real-Time Early Detection of Allergic Reactions based on Heart Rate Variability

Author

Raquel Gutiérrez Rivas

Supervisors

Professor William P. Marnane (University College Cork)

Dr Juan Jesús García Domínguez (University of Alcalá)

Head of Department: Professor Nabeel Riza (University College Cork)

PhD Program Coordinator: Professor Manuel Mazo Quintas (University of Alcalá)

July, 2016

Y pensar, pensar que allí nomás, desde donde pa' cualquier lao se mira adentro,
donde la luz y la sombra se juntan pa' algo más que pa' que pase un día […]
Allí nomás la vi sentada, con sus ojos tan quietos,
con el tiempo metido hasta en las uñas, con el sosiego entero escrito en el espinazo:
la estatua de carne que enarbola siglos de olvido y de miseria.
Me sentí tan pequeño ante tanta grandeza.
¿De qué vale mi canto sin tu algo?

José Larralde (1969). Estatua de Carne.

Agradecimientos

A mi familia, vuestro apoyo y confianza me han empujado a afrontar cada reto teniendo la certeza de que estaríais sujetándome si algo salía mal. Soy consciente de la suerte que tengo al teneros tan cerca a pesar de los kilómetros y espero hacer que os sintáis orgullosos de mí con cada una de mis decisiones.

A Marce, mi ancla con el mundo y el principal sufridor de mis "picos y valles" durante estos cuatro años. Gracias por todo: los consejos, los consuelos, las horas de escucha e, incluso, las "reprimendas". Algún día seré yo la que esté al otro lado y espero poder corresponderte.

A David… *no hasta dos, ni hasta tres, sino contar conmigo*. No creo que sepas cómo ni cuánto me has ayudado estos años ¡gracias compae!

A Juan Jesús García Domínguez, por haber puesto su confianza en mí desde mi primer proyecto hace ya más de 7 años. Por las horas de correcciones sacadas de donde no había. Por ver el vaso siempre medio lleno.

To Liam Marnane for supporting this thesis and for his advices, corrections and congratulations. To Niall Twomey, Andriy Temko, Emanuel Popovicci, Jonathan Hourihane and people at UCC for their help.

Al grupo GEINTRA US&RF del que siempre me sentiré parte, por muy lejos que me vaya. Gracias por la formación transversal y humana. Siempre recordaré con cariño, quién lo habría dicho, las reuniones semanales y los nervios antes de cada presentación. Gracias a los que de una forma u otra han colaborado en este trabajo. A Edel Díaz, que toma el relevo, muchísimo ánimo.

A todo el equipo de la sección de alergología del Hospital Universitario de Guadalajara, sin el que esta tesis no podría haberse llevado a cabo. A Arantza Vega Castro, por su implicación y fe en el proyecto. A Isabel y Ana, enfermeras del servicio, por su paciencia y su buena disposición para colaborar en la recolección de datos.

Resumen

La popularización del concepto “Internet de las cosas” ha fomentado el rápido desarrollo de aplicaciones centradas en la obtención de información relativa a personas. Por este motivo, y gracias a la disponibilidad de la capacidad de cálculo de los *Smartphones*, a lo largo de los últimos años se han comercializado diversos dispositivos económicos y aplicaciones a través de los que analizar la salud de los usuarios. En esta tesis se propone el uso de la señal electrocardiográfica para la detección precoz de reacciones alérgicas. Con este objetivo, se ha diseñado en primer lugar un nuevo algoritmo de detección de latidos cardiacos capaz de trabajar en tiempo real. La precisión de dicho algoritmo es similar a los propuestos en la literatura, sin embargo, su complejidad computacional y consumo de recursos son muy reducidos, lo que lo hace idóneo para ser empleado en plataformas portátiles de recursos limitados.

En un estudio previo, se analizó el efecto que las reacciones alérgicas provocaban en la variabilidad del ritmo cardíaco, demostrando que dicho efecto es detectable incluso antes de la aparición de síntomas físicos en la mayoría de los pacientes alérgicos estudiados. Sin embargo, el método propuesto en dicho trabajo no puede emplearse para detectar alergias en pruebas reales, puesto que la complejidad computacional del modelo diseñado necesita horas de análisis para realizar dicha detección. Además, el estudio se centró únicamente en pruebas de provocación de alergias alimentarias en niños menores de 12 años.

En este trabajo se continúa el estudio de la variabilidad del ritmo cardíaco en pacientes realizando pruebas de provocación con dos objetivos principales: el diseño de un algoritmo capaz de detectar alergias en tiempo real, y la extensión del estudio para incluir adultos y pruebas de provocación de alergias a medicamentos. El algoritmo resultante de dicho estudio tiene una precisión similar al propuesto en el trabajo previo, así como la reducción de la cantidad de alérgeno que los pacientes alérgicos deben consumir y de la duración de las provocaciones. Sin embargo, la nueva propuesta puede implementarse en un dispositivo autónomo y portátil y, lo que es más importante, es capaz de realizar las detecciones de reacciones alérgicas en tiempo real.

A pesar de que los resultados obtenidos son prometedores, este estudio debe interpretarse como el inicio de una investigación mayor, puesto que es necesario emplear más tiempo y esfuerzo en la adquisición de nuevos datos para obtener una muestra representativa de toda la población de pacientes alérgicos a alimentos y medicamentos.

Abstract

The popularisation of the concept of “Internet of Things” has promoted the fast increase of applications focused on obtaining information regarding people. For this reason, and thanks to the availability of the computing capacity of smartphones, over the last years a large number of low cost devices and applications have been marketed for analysing the health of users. In this thesis it is proposed to use ECG signals for early detection of allergic reactions. With this aim, a new QRS complex detection algorithm has been designed able to work in real time. This algorithm achieves an accuracy similar to those proposed by other authors, by reducing their computational complexity and the needed resources, which make it able to be implemented in portable platforms.

In a previous study the effect that the occurrence of an allergic reaction causes in the heart rate variability was analysed, showing that it is noticeable even before the appearance of physical symptoms in most of the cases in which patients suffered an allergic reaction. However, the method proposed in this previous study is not suitable for detecting allergic reactions during real tests, since the computational complexity of the model designed requires hours of analysis to perform that detection. Moreover, the previous study only focused on food provocation tests in children under 12 years old.

The study of the heart rate variability of allergic and non-allergic patients during provocation tests is continued in this work, with two main objectives: the designing of an algorithm capable of detecting allergic reactions in real time, and the extension of the study to include adults and drug provocation tests. The resulting algorithm has an accuracy similar to that proposed in the previous work and the achieved dose and length reduction of the provocation tests is similar as well. However, this algorithm is able to be implemented in a standalone portable device with limited resources and, what is more important, to perform the allergy reactions detection in real-time.

Although the results are promising, this study should be interpreted as the beginning of further research, since it is necessary to spend more time and effort in acquiring new data to get a representative sample of the entire population of allergic patients in the case of both food and drug allergies.

Contents

Chapter 1. Introduction 1

1.1 Structure of the thesis 3

1.2 Thesis Background 5

Chapter 2. Background, Problem Statement and Objectives 7

2.1 Basics of QRS complex detection 8

2.1.1 The electrocardiographic signal 9

2.1.2 ECG sources of noise, interferences and artefacts 11

2.1.2.1 Power-line interference 12

2.1.2.2 Motion artefact 14

2.1.2.3 Muscle noise 16

2.1.2.4 Wandering baseline 16

2.1.3 QRS complex detection structure 17

2.1.3.1 Pre-processing techniques 18

2.1.3.2 R-peaks detection techniques 21

2.2 Heart Rate and Heart Rate Variability 24

2.3 Introduction to allergies and allergy detection 27

2.4 Previous work 30

2.4.1 Dataset 30

2.4.2 Feature set 32

2.4.3 Automated allergy detection 34

2.5 Problem statement and Thesis objectives 37

Chapter 3. QRS Complex Detection 41

3.1 Benchmark databases 43

3.2 Metrics 44

3.3 Pan & Tompkins' algorithm 45

3.3.1 Pre-processing stage 45

3.3.2 Thresholding stage 48

3.3.3 Search-back stage 49

3.4 Proposed QRS detection algorithm 50
3.4.1 Pre-processing stage 51
3.4.2 R peaks detection stage 52
3.4.3 Parameter selection 54
3.5 QRS complex detection evaluation 56
3.5.1 Accuracy evaluation using floating-point representation 56
3.5.2 Accuracy evaluation using fixed-point representation 64
3.5.3 Computational complexity evaluation 64
3.5.4 Fixed point implementation 68
3.6 Conclusions 69

Chapter 4. Automated Allergy Detection 71
4.1 Evaluation methods 72
4.1.1 T-value and p-value analysis 72
4.1.2 Area under the Receiver Operating Characteristic curve (AUC) 74
4.2 HRV feature selection 76
4.2.1 Diagnostic ability study 76
4.2.2 Complexity analysis 81
4.2.3 Feature selection 83
4.3 Allergic reaction detection algorithm 85
4.4 Results 88
4.5 Conclusions 91

Chapter 5. Artefact Detection and Positioning 93
5.1 Introduction to the new trial 94
5.1.1 Differences between protocols 94
5.1.2 Data collection set-up 95
5.2 Test of the Allergy Detection algorithm 97
5.3 Movement artefact reduction 100
5.3.1 First approach: Measurement of the chest movement 101
5.3.2 Second approach: Detecting subject posture and activity 107
5.3.2.1 Pocket Navigation system 107
5.3.2.2 Test of the Pocket Navigation System 110
5.4 Conclusion 114

Chapter 6. Extension of the Algorithm Application 117
6.1 Description of the new dataset 118
6.2 Analysis of the new dataset 120
6.2.1 Group [Children, Drugs] 120
6.2.2 Group [Adults, Food] 121
6.2.3 Group [Adults, non-NSAID] 122
6.2.4 Group [Adults, NSAID] 123
6.3 Adaptation of the allergy detection 125
6.4 Conclusions 128

Chapter 7. Conclusions and Future Works 131
7.1 Contributions 131
7.1.1 Novel real-time QRS complex detection algorithm 131
7.1.2 Development of an algorithm based on HRV for the early detection of allergy reactions .. 132
7.1.3 Study of the HRV signal in adults and children exposed to food and drugs allergens 133
7.2 Future Works 134
7.3 Publications Derived from the Thesis 135
7.3.1 International Journals 135
7.3.2 International Conferences 135

Appendix A – HRV Features 137
A.1 Time domain features 138
A.1.1 Mean Heart Rate Variability 138
A.1.2 Standard Deviation 138
A.1.3 Coefficient of Variation 138
A.1.4 Root Mean Square 138
A.1.5 NN50, pNN50, pNN25 139
A.1.6 Histogram Index 139
A.1.7 Positive and Negative trends (STPP, STNN) 140
A.2 Graphical domain features 140
A.3 Frequency domain features 141

Appendix B – SoC-based architecture for the proposed QRS complex detection algorithm 143

B.1 Low-level peripheral 144

B.2 High-level peripheral 147

B.3 Test of the proposed architecture 147

Appendix C – t-value level of significance limit depending on the degree of freedom 149

Appendix D – Mean HRV of the subjects from the CUH database during the OFCs 151

Appendix E – Ethical approval documents 161

Appendix F – Informed consents 175

F.1 Informed consent for a Food Allergy Test 176

F.2 Informed consent for a Drug Allergy Test 178

F.3 Informed consent for the data collection process 180

Bibliography 183

List of Figures

Figure 2.1-1. Left: anatomy of the human heart [Ownw00]; Right: electrical system of the heart [Madh06] 9

Figure 2.1-2. ECG peaks, waves and interval representation 10

Figure 2.1-3. Example of the ECG signal during the occurrence of an atrial flutter. Subject iaf5 from the Intracardiac Atrial Fibrillation (iafdb) Database in [GAGH00]. The wrong activation of atria electrical nodes, makes them produce additional heartbeat. 11

Figure 2.1-4. Example of the ECG signal during an atrial fibrillation. Subject iaf2 from the Intracardiac Atrial Fibrillation (iafdb) Database in [GAGH00]. The atria contract very fast and irregularly, provoking an irregular heartbeat and a desynchronization with the ventricles. 11

Figure 2.1-5. Power spectra of the main waves of the ECG signal, muscle noise and motion artefacts based on an average 150 beats. Figure extracted from [Afon93]. 12

Figure 2.1-6. Einthoven Triangle configuration 12

Figure 2.1-7. ECG signal with 50 Hz interference 13

Figure 2.1-8. Features of the notch filter 13

Figure 2.1-9. ECG filtered with a notch filter 13

Figure 2.1-10. Motion artefact effect 14

Figure 2.1-11. ECG without LL, LA or RA electrode 15

Figure 2.1-12. ECG spectrum without LL, LA or RA electrodes 15

Figure 2.1-13. ECG with muscle noise 16

Figure 2.1-14. Wandering baseline effect 17

Figure 2.1-15. Structure of a QRS complex detector algorithm 18

Figure 2.1-16. Wavelet denoising example 19

Figure 2.1-17. Wavelet coefficients and denoised wavelets 19

Figure 2.1-18. Example of Hilbert Transform of an ECG signal 20

Figure 2.1-19. EMD de-noising example 22

Figure 2.1-20. Example of the Empirical Mode Decomposition of an ECG signal into 5 Intrinsic Mode Functions 22

Figure 2.1-21. Example of pre-processing stage 23

Figure 2.1-22. Result of the pre-processing stage 24

Figure 2.1-23.Example of double adaptive threshold and detection of the R peaks 24

Figure 2.2-1. Heart Rate Variability of a healthy subject performing different physical activities. 25

Figure 2.3-1. Example of immediate hypersensitivity skin test or prick test (left, extracted from [Beea00]) and delayed hypersensitivity test preparation (right, extracted from [Grou15]) 28

Figure 2.3-2. Flowchart of an Oral Food Challenge (OFC) at CUH 30

Figure 2.4-1. Modified OFC process 32

Figure 2.4-2. Epoch definition for the computation of each feature 34

Figure 2.4-3. Block diagram of the automated allergy detection based in the analysis of the 18 features of the HRV signal proposed in [Twom13] 35

Figure 2.4-4. Example of likelihood signal achieved with the novelty classifier for an allergic subject 36

Figure 2.4-5. Example of likelihood signal achieved with the novelty classifier for a non-allergic subject .. 36

Figure 2.5-1. Groups for the allergy detection study 39

Figure 3.3-1. Block diagram of the Pan & Tompkins algorithm 46

Figure 3.3-2. Pan & Tompkins QRS detection algorithm block diagram 46

Figure 3.3-3.Signals generated during the pre-processing stage of the Pan and Tompkins algorithm 47

Figure 3.3-4. Input and output of the pre-processing stage 47

Figure 3.3-5. Comparison between ECG and pre-processed signal without delays 48

Figure 3.3-6. Example of Pan and Tompkins algorithm's Signal and noise level estimation and set of Thresholds 49

Figure 3.3-7. Search-back technique example 50

Figure 3.4-1. Block diagram of the proposed QRS complex detection algorithm 51

Figure 3.4-2.Block diagram of the pre-processing stage 51

Figure 3.4-3. Pre-processing result 52

Figure 3.4-4. State machine diagram 53

Figure 3.4-5. Correspondence between the FSM states and the ECG phase 53

Figure 3.4-6. Proposed algorithm's parameters v. sampling frequency 55

Figure 3.4-7. Definition of R-peak slope interval 55

Figure 3.5-1. Example of ECG signal, x [n], with motion artefacts. Subject 3 of the ADB database 61

Figure 3.5-2. Pan & Tompkins. QRS complex detection for record no. 100 (Se=100%; +P=100%; FS=200 Hz) 62

Figure 3.5-3. Proposed algorithm. QRS complex detection for record no. 100 (Se=100 %; +P=100 %; FS=360 Hz) 62

Figure 3.5-4. Pan % Tompkins. QRS complex detection for record no. 108 (Se=98.525 %; +P=88.083 %; FS=200 Hz) 63

Figure 3.5-5. Proposed algorithm. QRS complex detection for record no. 108 (Se=98.411 %; +P=95.96 %; FS=360 %) 63

Figure 4.1-1. Example of ROC curves with different AUC 75

Figure 4.2-1. T-value for the six statistical parameters for the studied HRV features 77

Figure 4.2-2. (1 - p-value) of the six statistical parameters for the studied HRV features 78

Figure 4.2-3. AUC for the six statistical parameters for the studied HRV features 80

Figure 4.2-4. Relative computational time needed to compute each feature 82

Figure 4.2-5. Comparison between mean HRV of allergic (red) and non-allergic (blue) subjects using (a) mean, (b) median, (c) mode, (d) range, (e) standard deviation and (f) interquartile range 83

Figure 4.2-6. AUC, p-value, t-value of the standard deviation of all the features and relative computational time needed to obtain them. 84

Figure 4.2-7. ECG (a); Heart Rate Variability (b), and mean Heart Rate Variability signal examples 84

Figure 4.3-1. MRR signal of an allergic (a) and a non-allergic (b) subject. Purple dotted line represents the mean value of the MRR signal during each "background" period, or MBG signal 85

Figure 4.3-2. Flow chart of the proposed allergy detection algorithm 87

Figure 4.3-3. Normalized MRR (NMRR) signal for an allergic (a) and a non-allergic (b) subject 87

Figure 4.3-4. Maximum MeanPeak value for each subject of the Allergy Database 88

Figure 4.4-1. Subject 18's mean HRV signal during the OFC 90

Figure 5.1-1. Shimmer3 unit and orientation of the inertial sensors 97

Figure 5.2-1. PDF of the standard deviation of the MRR for the training and testing datasets 98

Figure 5.2-2. ROC of the standard deviation of the new dataset 99

Figure 5.2-3. MRR signal of the subject GU053 99

Figure 5.3-1. Example of MRR signal variations depending on the subject's physical activity or posture: standing (red), sitting (purple), walking (green), walking downstairs (cyan) and walking upstairs (orange). 101

Figure 5.3-2. Example of False Positive due to the presence of movement artefacts. a) MRR signal of the Subject GU069; b) Movement of the subject; and c) MRR signal corrected with the movement with GAcc=50 103

Figure 5.3-3. Sensitivity and Specificity obtained depending on GAcc and Th values 104

Figure 5.3-4. Time gain obtained with several combinations of GAcc and Th parameters 104

Figure 5.3-5. Maximum MeanPeak value comparison between allergic and non-allergic subjects, before and after the artefact reduction 105

Figure 5.3-6. MRR of the subjects GU118 during the OFC, corrected using the chest movement 106

Figure 5.3-7. Accel of subject GU118 during the OFC 106

Figure 5.3-8. Shimmer allocation for the second approach 107

Figure 5.3-9. Block diagram of the inertial pocket navigation system 108

Figure 5.3-10. Roll, Pitch and Yaw angles definition 109

Figure 5.3-11. Example of pitch angle depending on the subject posture and physical activity; (cyan) seated, (red) standing, (blue) walking, (green) walking upstairs and (purple) walking downstairs 110

Figure 5.3-12. Trajectory followed by the subject during the testing experiment. 111

Figure 5.3-13. The upper subfigure shows the pitch angle estimation for the 10-minutes-walk at the hospital. The lower subfigure shows the MRR signal, measured in beats per minute, for the same walk. 111

Figure 5.3-14. MRR signal of the subject with which the Pocket Navigation System was tested 112

Figure 5.3-15. Pitch angle and physical activity classification during the first false alarm 113

Figure 5.3-16. Pitch angle and physical activity classification during the second false alarm 113

Figure 5.3-17. Pitch angle estimation and physical activity classification during the third and fourth false alarms 113

Figure 6.1-1. Classification of the subjects from the database 119

Figure 6.2-1. PDF of the MRR's standard deviation of allergic and non-allergic children exposed to food, and non-allergic children exposed to drugs 121

Figure 6.2-2. PDF of MRR's standard deviation of adults and children exposed to food 122

Figure 6.2-3. PDF of MRR's standard deviation of adults exposed to food and non-NSAID 123

Figure 6.2-4. PDF of MRR's standard deviation of adults exposed to non-NSAID and NSAID 124

Figure 6.3-1. PDF of the Children group 126

Figure 6.3-2. PDF of the group [Adults, non-NSAID] including food 126

Figure 6.3-3. PDF of the [Adults, NSAID] group 126

Figure 6.4-1. Division of the database subjects depending on the algorithm's results 129

Figure A- 1. Example of HRV histogram and Histogram index computation 139

Figure A- 2. Representation of the relationship between the difference between each RR pair and the previous one 140

Figure A- 3. Representation of the relationship between the difference between each RR pair and the previous one 141

Figure A- 4. Example of Power spectrum in the VLF, LF and HF bands 142

Figure B- 1. General block diagram of the proposed SoC architecture 145

Figure B- 2. Block diagram of the proposed low-level peripheral 145

Figure B- 3. Block diagram of the configurable FIR filter 145

Figure B- 4. Block diagram of the moving average block 146

List of Tables

Table 2.4-1. Main features of the test from which the ECG signals of the database used were extracted 31

Table 3.1-1. Databases used to test the algorithm performance 43

Table 3.4-1. ADB and NSRDB obtained results 55

Table 3.5-1. Results of the proposed QRS detection algorithm with the MITDB 57

Table 3.5-2. Results of the Pan & Tompkins algorithm with the MITDB 58

Table 3.5-3. Comparison of accuracy results for some proposals with the full MITDB databases 59

Table 3.5-4. Comparison of accuracy results for some proposals with several signals of the MITDB databases 59

Table 3.5-5. Comparison between P&T and proposed algorithm performances over all the databases 60

Table 3.5-6. Results of the fixed-point version of the proposed QRS detection algorithm with the MITDB 65

Table 3.5-7. Results of the fixed-point version of the P&T algorithm with the MITDB 66

Table 3.5-8. Relative error computation for the different signals involved in the QRS complex detection algorithm 67

Table 3.5-9. Relative error computation for the different signals involved in the P&T QRS detection 67

Table 3.5-10. Complexity analysis results obtained by both algorithms 68

Table 3.5-11. Resource consumption of the proposed system in a Zynq XC7Z010 FPGA 68

Table 3.5-12. Comparison between the results obtained with the floating-point version of the proposed QRS complex detection algorithm and with the proposed SoC architecture 68

Table 4.1-1. Statistical parameters used for evaluating each HRV feature 75

Table 4.2-1. T-values obtained with the performed t-test for the 6 statistical parameters of the HRV features 78

Table 4.2-2. P-values ($\cdot 10^{-3}$) obtained with the performed t-test for the 6 statistical parameters of the HRV features 79

Table 4.2-3. Confidence level obtained with the performed t-test for the 6 statistical parameters of the HRV features 79

Table 4.2-4. AUC obtained for the 6 statistical parameters of the HRV features 81

Table 4.3-1. Statistical differences between an allergic subject and a non-allergic one 86

Table 4.4-1. Performance of the Allergy detection algorithm 89

Table 4.4-2. Statistical parameters of subjects 14 and 15 89

Table 5.1-1. Features of the new dataset 96

Table 5.2-1. Results obtained with the new dataset 98

Table 5.3-1. Results of the allergic reactions detection algorithm with the artefact reduction 105

Table 6.1-1. Subjects (Allergic/non-allergic) divided by age and type of allergen 118

Table 6.1-2. Prevalence of allergic subjects depending on their age and the type of allergen 120

Table 6.2-1. Mean and standard deviation of each one of the groups analysed in this chapter 124

Table 6.3-1. Evaluation of the standard deviation of the mean HRV depending on the group 125

Table 6.3-2. Evaluation of the allergy detection algorithm with the defined groups 127

List of Acronyms

+P	Positive predictivity
ADB	Allergy Database
ANS	Autonomic Nervous System
AUC	Area Under the Curve
AV	Atrioventricular
BIH	Beth Israel Hospital arrhythmia laboratory
bpm	beats-per-minute
BSN	Body Sensor Network
CHn	Channel n
CNS	Central Nervous System
CSI	Cardiac Sympathetic Index
CUH	Cork University Hospital
CV	Coefficient of Variation
CVI	Cardiac Vagal Index
CWT	Continuous Wavelet Transform
DWT	Discrete Wavelet Transform
ECG	Electrocardiogram
EMD	Empirical Mode Decomposition
FFT	Fast Fourier Transform
FN	False Negative
FP	False Positive
Fs	Sampling frequency
FSM	Finite-State Machine
GMM	Gaussian Mixture Model
GUH	Guadalajara University Hospital
HF	High Frequency
HPF	High-Pass Filter
HR	Heart Rate
HRV	Heart Rate Variability
IgE	Immunoglobulin E
IMF	Intrinsic Mode Function

IMU	Inertial Measurement Unit
IQR	Interquartile Range
LA	Left Arm
LF	Low Frequency
LFHF	ratio Low Frequency to High Frequency
LL	Left Leg
LOO	Leave One Out
LPF	Low-Pass Filter
MBG	Mean Background
MI	Myocardial Infarction
MIT	Massachusetts Institute of Technology
MITDB	MIT-BIH Arrhythmia Database
MRR	Mean RR
NMRR	Normalised Mean RR
NPKI	Noise Peak Level
NSAID	NonSteroidal Anti-Inflammatory
NSRDB	MIT-BIH Normal Sinus Rhythm Database
OC	Oral Challenge
OFC	Oral Food Challenge
P&T	Pan & Tompkins
PDF	Probability Density Function
PMV	Predicted Mean Vote
PNS	Parasympathetic Nervous System
QSWT	Quadratic Spline Wavelet Transform
RA	Right Arm
RMSSD	Root Mean Square of the Difference between adjacent RR intervals
ROC	Receiver Operating Characteristic
RRHL	RR High-Limit
RRLL	RR Low-Limit
RRML	RR Missed-Limit
SA	Sinoatrial
Se	Sensitivity
SNS	Sympathetic Nervous System

SoC	System on Chip
SPKI	Signal Peak Level
SpO2	Peripheral capillary Oxygen Saturation
STD	Standard Deviation
STDNN	Standard Deviation of the RR intervals
STNN	Sequential Trend Negative
STPP	Sequential Trend Positive
SWT	(discrete) Stationary Wavelet Transform
TG	Time Gain
TN	True Negative
TP	True Positive
UKF	Unscented Kalman Filter
VLF	Very-Low Frequency
WT	Wavelet Transform

Lista de Acrónimos

Es	Especificidad
FC	Frecuencia Cardíaca
FN	Falso Negativo
FP	Falso Positivo
MVC	Media de la Variabilidad Cardíaca
PdE	Prueba de Exposición
SatO2	Saturación de Oxígeno (en sangre)
Se	Sensibilidad
TA	Tensión Arterial
VC	Variabilidad Cardiaca
VN	Verdadero Negativo
VP	Verdadero Positivo
VP-	Valor Predictivo Negativo
VP+	Valor Predictivo Positivo

Chapter 1.

INTRODUCTION

The level of miniaturizing of electronic devices achieved during the last 30-40 years has led to the development of portable devices that are able to perform relatively complex tasks, powered by a battery, operating with increasing autonomy. This fact has had a significant impact on most areas of technological development. However, the areas to benefit most are the ones related to remote monitoring. As a result, the so-called "motes" have emerged [YaSQ13]. These devices, in their most basic version, include a power source, a microcontroller, a transceiver and one or more sensors. The reason for their popularity is that they solve big challenges with systems that do not affect the environment they are deployed in, such as industrial processes monitoring [JZLQ15], environment control [SLYJ14] or smart spaces development [TeEB15].

One of the areas to benefit most from this evolution is that of medicine, since the appearance of these devices has encouraged the emergence of several technological proposals. Although motes do not automate the diagnosis, they greatly reduce the time required and facilitate the work of the medical staff. The use of devices and applications for remote patient monitoring (or Telemedicine) does not affect negatively to any extent the standard procedures followed in hospitals. On the contrary, these systems add a large number of advantages for both hospitals and patients as they allow the continuous and remote access to different physiological parameters.

Besides, in some cases patients will be able to stay in their own homes during monitoring with a higher level of mobility. This will significantly increase their quality of life and reduce waiting lists, the economic costs of the hospitals and the workload of the medical staff. In general, a telemedicine system is provided with some *intelligence*, that allows, among others, the signal filtering, the signal conditioning and the analysis of the measurements made on those parameters. It is also possible to add other features such as the ability to locate patients, generate alarms, etc. Thus, telemedicine systems provide two main advantages: on the one hand, the quantity and quality of the extracted information is larger than the one obtained nowadays, which greatly helps doctors; on the other hand, they significantly increase the patient safety, since the control of their health can be as comprehensive as necessary. Although the doctors should always make the last decision, the inclusion of computational intelligence in the monitoring systems can simplify the diagnosis processes in a very significant way.

The use of motes implies, however, some drawbacks. Due to the fact that they are powered by a battery, and the resources are usually limited, it is necessary to reduce as much as possible the computational complexity of their firmware. The tasks that they can carry out have a limited complexity as well. Besides, the applications in which they are usually employed, have real-time requirements which need to be taken into consideration.

This thesis is focused on remote monitoring of patients, or telemedicine systems[JiCh15]. Several works have been published in the area of the analysis, control and/or monitoring of people's health thanks to the consolidation of "Internet of things" [TrDu15]. In this area many parameters regarding the state of people's health have been used for, among other applications: increasing the elderly safety by monitoring their motion [SuMu14]; analysing the evolution of a particular disease by measuring one physiological parameter [PBDT14]; or analysing the behaviour, increasing the comfort of the users of smart spaces or saving the energy consumption of the elements controlled by smart spaces by acquiring a large quantity of information [HJHJ15].

Particularly, in this work the health of patients will be observed through the measurement of their electrocardiographic signal (ECG). Due to its importance and the easiness to measure it, the ECG is one of the most studied physiological signals. It is possible to observe, not only the cardiovascular system state, but also the behaviour of different physiological systems through the analysis of the Heart Rate Variability (HRV) signal, which represents the time intervals between consecutive heartbeats. In this thesis, the relationship between HRV variations and the existence of allergic reactions will be studied.

Nowadays, the gold standard for the detection of allergies is the so called provocation tests, in which the patients are required to take some doses of the suspected allergen. The danger of this process could be reduced by detecting the allergies before the appearance of the physical symptoms. A previous investigation carried out by Niall Twomey at University College Cork (Ireland) [Twom13] demonstrated that it is possible to relate variances of the HRV with the existence of allergic reactions, and, what is more important, that it is possible to detect them before the health of the patient is compromised. However, that process was not able to work in real-time due to its computational complexity, and so, the early detection could not be achieved during the provocation tests.

This thesis proposes the continuous monitoring of the ECG for the early detection of allergies in real-time during the provocation tests. With this aim, information regarding the performance of the heart will be extracted from this signal during several provocation tests, and the differences between allergic and non-allergic patients will be defined and used for the development of an allergy alarm system. This novelty implies the reduction of the risk the patients are exposed to by warning the medical staff before the allergy reactions are noticeable.

1.1 Structure of the thesis

The rest of this thesis is organized as follows:

- Chapter 2: "*Background, Problem Statement and Objectives*". In this chapter, the basics of the knowledge areas covered by this thesis are introduced. The main concepts of heartbeat detection are explained here: how the ECG signal is generated, the main noises that complicate the heartbeat detection, the state of the art on detection algorithms, etc. Then, the importance of the HRV signal is shown through the analysis of several current works in which this signal is employed in a variety of applications.
  The concepts of allergy and the allergy diagnostics methods used nowadays are outlined next. The previous work carried out at University College Cork is summarized in this chapter. The specific problems that comprise the motivation of this work, such as the need for computationally efficient algorithms, real-time requirements or portable devices constraints, are listed and finally the objectives of this thesis are introduced.

- Chapter 3: "*QRS Complex Detection*". In this chapter, a novel real time heartbeatdetection algorithm for use in low resource hardware "motes" is proposed. With this algorithm, it is possible to obtain a sensitivity and specificity above 99.5% with a reduced computational complexity. The algorithm has been tested over standard and non-standard databases, sampled at different frequencies for patients with different health conditions. All these tests allow the performance of the proposed algorithm to be verified under different conditions and a comparison made to the results of other methods.

- Chapter 4: "*Automated Allergy Detection*". As a first contribution, in this chapter the set of HRV features used in the previous work for the detection of allergic reactions is analysed in order to classify the 18 features of the set depending on their computational complexity and diagnostic ability. The results provided by these tests make it possible to distinguish between the features that give information related to allergic reactions and those that can be considered useless for this application. This study has been performed on a dataset obtained during the initial study that consists of 23 children who underwent a food allergy provocation test at Cork University Hospital. Once the proper feature has been selected, it should be studied how an allergy reaction affects it. This study leads to the second contribution of Chapter 4, which is the proposal of a novel real-time early detection of allergies. In Chapter 4 this algorithm is explained, as well as the results obtained with the 23 subjects that compose the database.

- Chapter 5: "*Artefact detection and Positioning*". The algorithm presented in the previous chapter has been tested during food allergy provocation tests (Oral Food Challenges, OFC) with patients that were required to remain on a bed during the tests. However, depending on the hospital and the medical protocol, the subjects may be able to move freely. This condition will affect the performance of the proposed allergy detection algorithm and so, its effects need to be defined.
  With this aim, another dataset has been recorded at the Guadalajara University Hospital (Spain) where the patients are not confined to a bed during the OFC. This chapter investigates the differences arising from these two situations, which are mainly provoked by the patients' movement. The effect of movement on the HRV signal can be considered here as an artefact.

Two artefact-reduction methods are proposed in this chapter: firstly, the absolute movement of the patients is measured by placing a 3-axis accelerometer on the chest. The second solution consists of placing an Inertial Measurement Unit (IMU) in the patients' pocket in order to detect the physical activity they are performing. Thus, this chapter provides two contributions. First one is the proposal of an early detection algorithm based on the HRV and movement of the subjects; second one is an early detection algorithm based on the HRV and movement of the patients and the ability to track their position during the OFCs.

- Chapter 6: "*Extension of the Study*". This chapter investigates the allergy detection performance when the target of the study is changed in different ways. During the data collection, the ECG signal of adults undergoing OFC, as well as children and adults exposed to drug allergies provocation tests have been acquired. In this Chapter, the features of those groups are analysed and the allergy detection algorithm is tested with them. However, as will be explained, a big effort needs to be made in this way to establish a detection pattern for each one of the groups based on the HRV response to allergens in the case of allergic patients. Thus, the results provided by this chapter can be taken into account as the starting point to further research in this area.

- Chapter 7: "*Conclusions and Future Works*". This chapter presents the most significant conclusions of this thesis, and the publications derived from it are listed. Finally, some research lines that might be investigated in the future are proposed.

1.2 Thesis Background

This thesis has been carried out as a joint PhD between the Electronics Department of the University of Alcalá (Spain) and the Electric and Electronic Department of University College Cork (Ireland). It has been developed under the auspices of the research projects LEMUR (ref. TIN2009-14114-C04-01) and LORIS (ref. TIN2012-38080-C04-01), both supported by the Spanish Ministry of Science and Innovation. It has also been economically supported by the University of Alcalá grant program FPI/UAH (ref. FPI/UAH2012) and by the University of Alcalá mobility program. Three research stays were carried out thanks to the mobility program, all of them at University College Cork, in Ireland.

One of the goals of LEMUR and LORIS projects was the development of cooperative systems for the positioning of people and mobile robots in diverse environments. The research presented in this thesis was carried out as part of the subtask named "*integration of the positioning networks with another networks (BSN and Smart grid)*", in particular with the *interaction of the positioning networks with Body Sensor Networks (BSN)*.

The thesis describes original work developed at the GEINTRA Research Group of the University of Alcalá and at the Biomedical Engineering research group of University College Cork.

Chapter 2.

BACKGROUND, PROBLEM STATEMENT AND OBJECTIVES

This chapter introduces the basics of the heartbeat detection, Heart Rate Variability signal analysis, and allergy. Section 2.1 details how the electrocardiographic signal is generated and the main sources of noise that affect it. This analysis will help to understand the challenges faced when detecting QRS complexes. An overview of the current state of the art regarding the QRS complex detection is explained in order to justify the necessity of designing a new algorithm despite the fact that there are many methods proposed during the last 40 years.

It is important to know that the Autonomous Nervous System (ANS) controls Heart Rate Variability (HRV) depending on the necessities of several physiological systems. Thanks to this fact it is possible to extract from the HRV, information related to the behaviour of those physiological systems. Section 2.2 explains some examples of the use of the HRV signal to provide diagnostic information for several conditions which are not directly related to the heart health. These examples give a clear idea of the great number of applications in which this signal can significantly improve several diagnostic methods that are used nowadays.

The allergy definition is given in section 2.3, as well as the existing methods used to detect different kinds of allergies. The so-called Oral Food Challenge (OFC) procedure is detailed in this section, as to increase the safety of the patients undergoing it, is one of the main objectives of this Thesis. Section 2.4 explains the starting point of this work; the Thesis carried out by Niall Twomey [Twom13] which is summarized. Once defined the background of this work, the main limitations of the explained methods and technologies are listed in section 2.5. The overcoming of these limitations shapes the motivation of this study and lead to the objectives and proposals of this Thesis, which are listed in section 2.6.

2.1 Basics of QRS complex detection

Due to its inherent importance, software QRS detection has been a research topic for more than four decades. As a result of this interest, many algorithms have been published that reflect the evolution of computer technology [KöHO02]. The computational load determined the complexity and therefore the performance of the first proposals, whereas recent work is focused on performance of the algorithm, as computers are becoming faster, more powerful and more reliable. Nevertheless, with the appearance of wearable technology, where low-power battery-driven devices are required, is changing to the original idea of developing low computational load algorithms [GFJC11, LANC14, ZDPL14] as is stated in [Kenn13].

Thanks to the evolution of technologies, there are some new alternatives available, allowing real-time analysis of the ECG signal to be performed. One of the latest is the use of cloud computing as is proposed by Xia et al. in [XiAZ13]. However, this proposal needs a permanent internet connection to achieve truly real-time results. Another possibility is the use of a host system to analyze the ECG signal measured by a remote device, in order to avoid the restrictions derived from its limited computational resources. In this case, a new problem arises related to the communication requirements, as the ECG signal has to be sent continuously to the analysis unit. To avoid these problems, it is necessary to compress, transmit and reconstruct all the data [LeKL11, MKAV11]. Another approach is the design of an ECG monitoring and analysis device for a particular application, as the one proposed by Chou et al. in [CTCL11] .

In the next subsections, the challenges of QRS complex detection will be explained, as well as the techniques used more frequently to face those challenges.

2.1.1 The electrocardiographic signal

The ECG represents the electrical activity of the heart. It has several electrical nodes (Figure 2.1-1) which are able to generate synchronized electrical impulses to activate its valves sequentially, thus allowing the blood to flow correctly through its chambers.

The ECG signal shows the addition of all the action potentials[1] generated by the electrical conduction system of the heart. Figure 2.1-2 represents the ECG waveform. Each one of its peaks: Q, R and S; waves: P, T and QRS complex; segments: PR and ST; and intervals: PR and QT; has correspondence with a state of the heart during each temporal phase of the heartbeat. These peaks, intervals, waves and segments have been studied and their features, both in time and amplitude domains, have been bounded.

However, all these values have a strong dependency on the patients' physiology, the measurement equipment, the position of the electrodes, etc. Depending on the application, those ECG's features might have more or less importance (e.g. QT variability related to stress situations [KIKP14] or QT-RR interval co-variability differences on diabetic patients [FMSN14]). Usually the R peaks or the QRS complexes are used to define the instant in which the heartbeat occurs, as they represent the depolarization of both ventricles after they are contracted and the blood is pumped out of the heart.

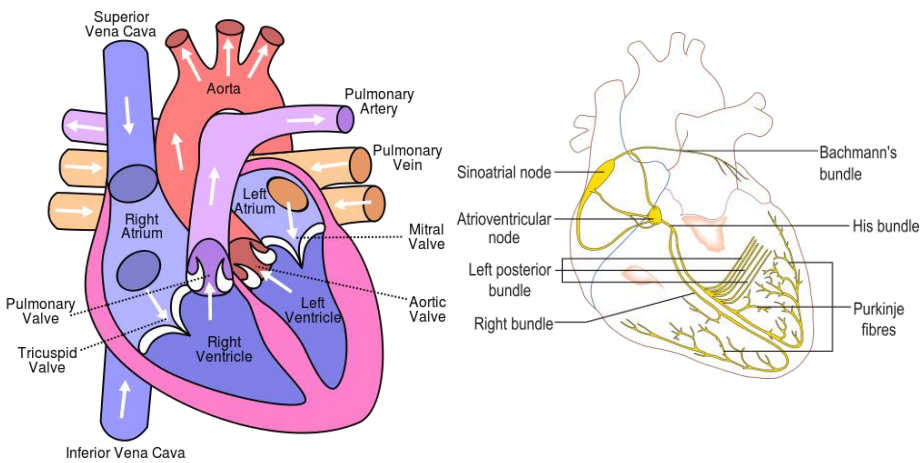

Figure 2.1-1. Left: anatomy of the human heart [Ownw00]; Right: electrical system of the heart [Madh06]

[1] Action Potential: "The Action Potential is the electrical signal that accompanies the mechanical contraction of a single cell when it is stimulated by an electrical current. It is caused by the flow of Sodium (Na^+), Potassium (K^+), Chloride (Cl^-), and other ions across the cell membrane. It provides information about the nature of physiological activity at the single-cell level" [Rang01]

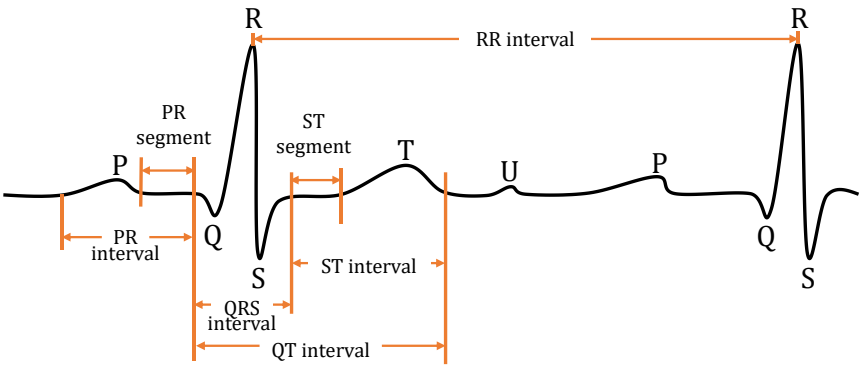

Figure 2.1-2. ECG peaks, waves and interval representation

As is explained above, different nodes are able to generate an electrical impulse. The natural pacemaker of the heart is the sinoatrial node, but, due to a bad functioning of the heart, it could be generated also at the Atrioventricular (AV) node, or at the Purkinje net. This is the cause or the consequence of a heart malfunction. Some examples are:

- Atrial flutter: An electrical loop is formed between both atria, which produces heart beats at a very high rate, but in a regular form. Figure 2.1-3 shows an example of the ECG signal during an atrial flutter. In these cases, the atria beat faster than the ventricles, which provokes the appearance of additional heartbeats, as shown in the figure.
- Atrial fibrillation: Random electrical impulses are generated at the atria. These impulses could be so fast and irregular that the atria cannot contract completely but they tremble as is shown at the Figure 2.1-4. In this situation, the atria cannot impulse enough blood through the arteries.
- Atrioventricular block: Dysfunction occurs between atria and ventricles. It could be first-grade block (the impulses reduce their speed when go from atria to ventricles), second grade (part of the impulses that pass through the AV node are blocked), or third grade (all the impulses are blocked at the AV node). Some P waves appear that are not followed by a QRS complex, so a low heart rate (or bradycardia) is detected.

These and other kinds of heart malfunctions can produce an irregular heart rate, or extra heartbeats or, even, missing heartbeats. It is important to take them into account when designing an algorithm for the detection of the heartbeats position.

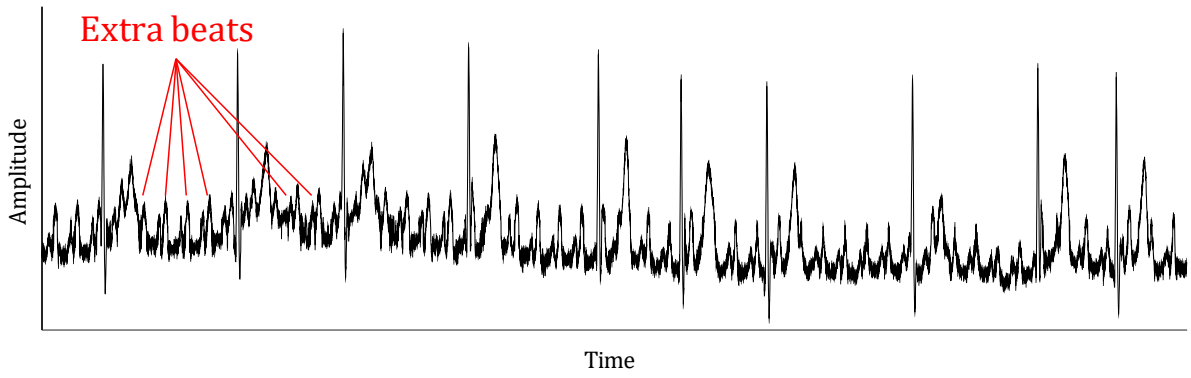

Figure 2.1-3. Example of the ECG signal during the occurrence of an atrial flutter. Subject iaf5 from the Intracardiac Atrial Fibrillation (iafdb) Database in [GAGH00]. The wrong activation of atria electrical nodes, makes them produce additional heartbeat.

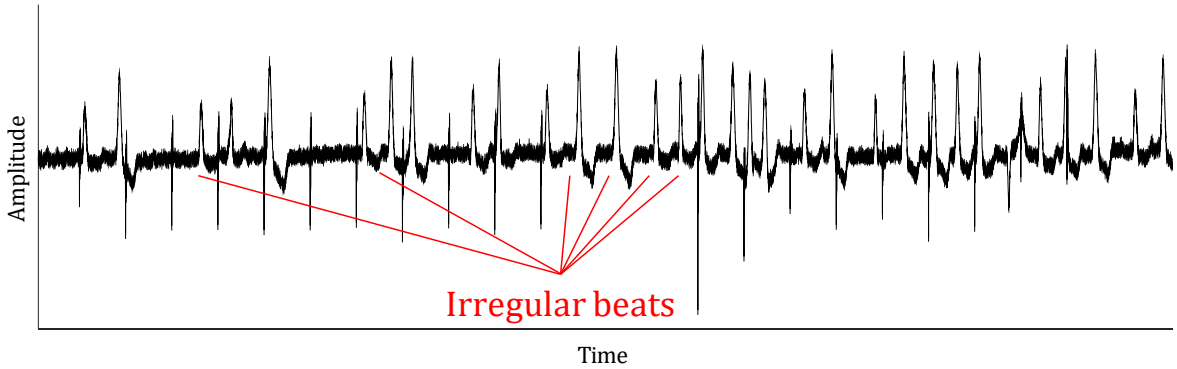

Figure 2.1-4. Example of the ECG signal during an atrial fibrillation. Subject iaf2 from the Intracardiac Atrial Fibrillation (iafdb) Database in [GAGH00]. The atria contract very fast and irregularly, provoking an irregular heartbeat and a desynchronization with the ventricles.

2.1.2 ECG sources of noise, interferences and artefacts

The main challenge facing the QRS detection process is to perform an accurate heartbeat detection even with the presence of several artefacts. In [FJJY90] the features of the most important artefacts involved in the QRS complex detection were analysed. Most of these noises are easily removed, since their bands of frequencies are far away from the frequency band of interest. However, some of these interferences have features very similar to those of the ECG waves (Figure 2.1-5) such as the artefacts provoked by the movement of the patient. The most important sources of noise will be explained next. For all the ECG recordings it has been employed a 3-lead configuration, with the electrodes arranged in the Einthoven Triangle configuration [WiJK47] as shown in Figure 2.1-6.

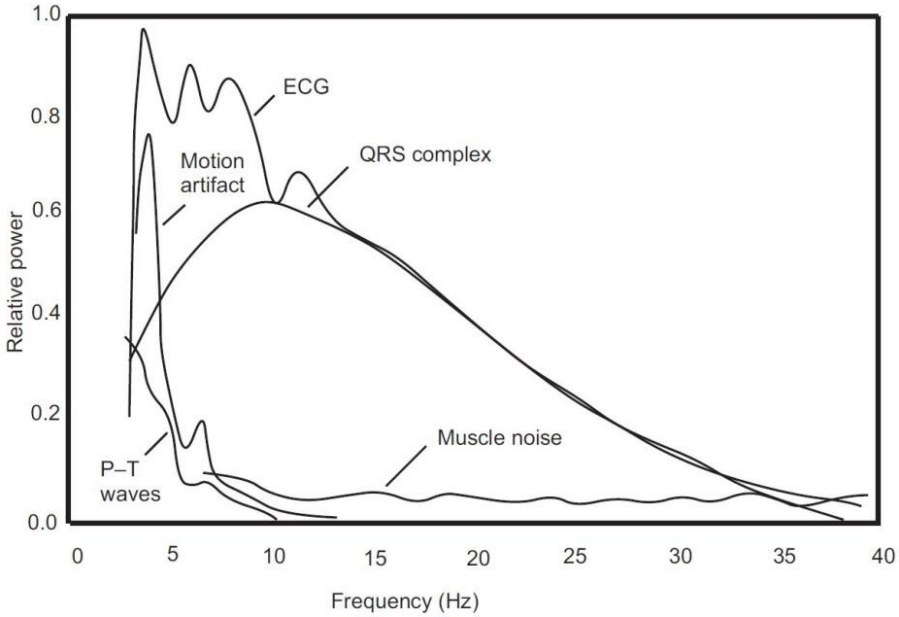

Figure 2.1-5. Power spectra of the main waves of the ECG signal, muscle noise and motion artefacts based on an average 150 beats. Figure extracted from [Afon93].

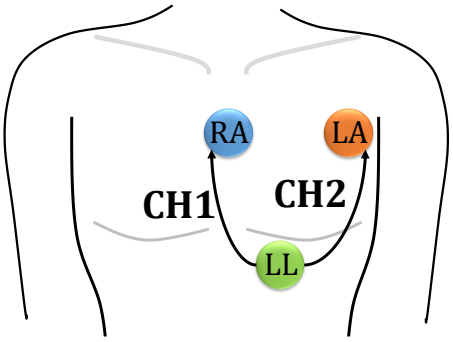

Figure 2.1-6. Einthoven Triangle configuration

2.1.2.1 Power-line interference

This interference will affect the ECG signal when any part of the equipment is connected to the mains, but it could appear even if the equipment is isolated due to the capacitive coupling [ChPa00]. As can be observed in the Figure 2.1-7 a frequency component of 50 Hz appears. Due to its features, it is necessary the use of a notch filter to remove this interference. Figure 2.1-8 shows an example of 2nd order notch filter and Figure 2.1-9 the resulting filtered signal. This filter barely removes information concerning the QRS complex.

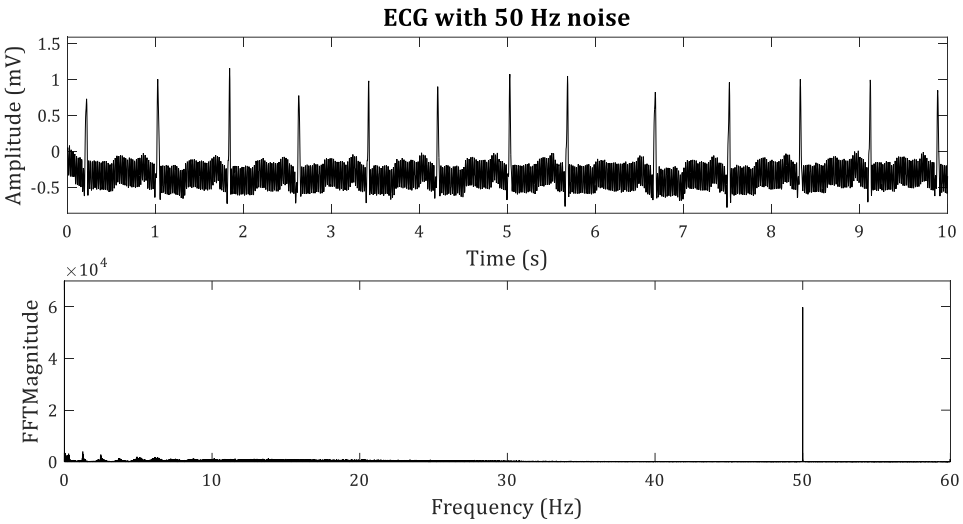

Figure 2.1-7. ECG signal with 50 Hz interference

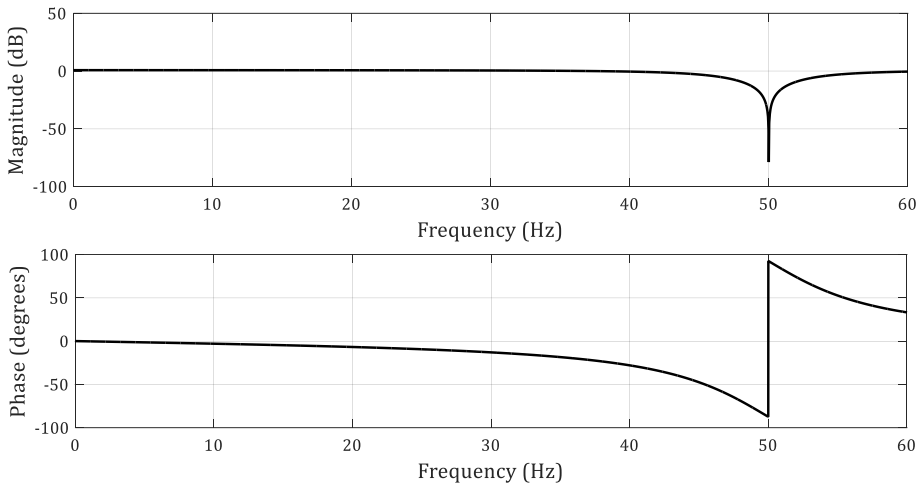

Figure 2.1-8. Features of the notch filter

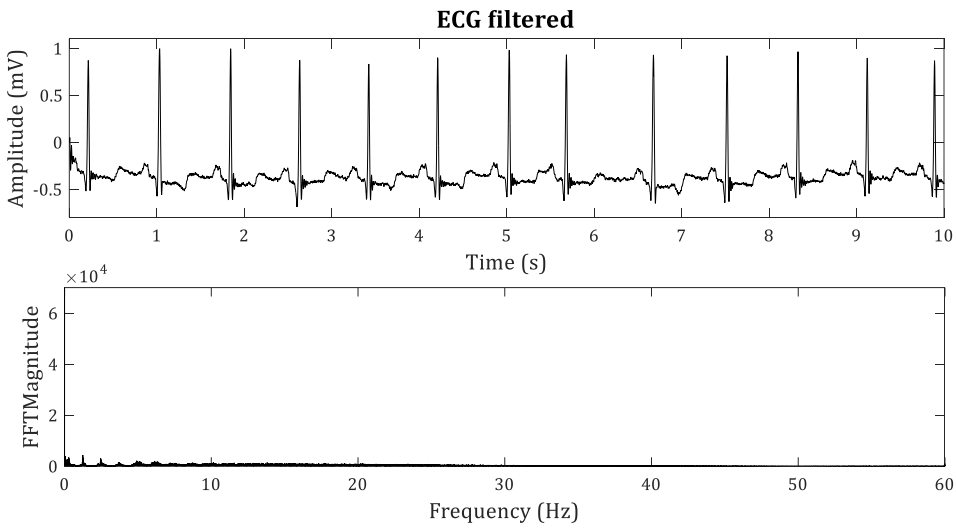

Figure 2.1-9. ECG filtered with a notch filter

2.1.2.2 Motion artefact

This artefact is produced because of a poor contact between any of the electrodes with the skin. Movements due to changing the posture usually provoke this bad contact, or the electrodes are deformed and they lose contact with the skin. As can be seen in Figure 2.1-10, motion artefacts produce high frequency peaks (as the one occurred before second 86) similar to R peaks, which could be misclassified as heartbeats by a QRS complex detection algorithm. In this example, the 50 Hz interference is noticeable as well, due to the fact that the unconnected electrodes act as antennas. The power spectrum components of this noise have a frequency very similar to the interesting band frequency, which makes the filtering stage more complicated.

The effects of detaching each one of the electrodes are plotted on Figure 2.1-11. In the first case, when the reference electrode is removed (LL electrode), the noise level of the ECG signal is increased. In the second case, the LA electrode has been detached, so when the operation CH1-CH2 is executed, the common mode noise is not removed. Also, because the LA electrode is still connected to the measurement device, more interferences have been added. Finally, when the RA electrode is detached (which is usually the electrode capturing more signal), the ECG signal amplitude is decreased and it becomes less immune to any type of noise. In any of these three cases, the noises and interferences added to the ECG signal have frequencies similar to the ECG frequency, so they might make the QRS detection more difficult.

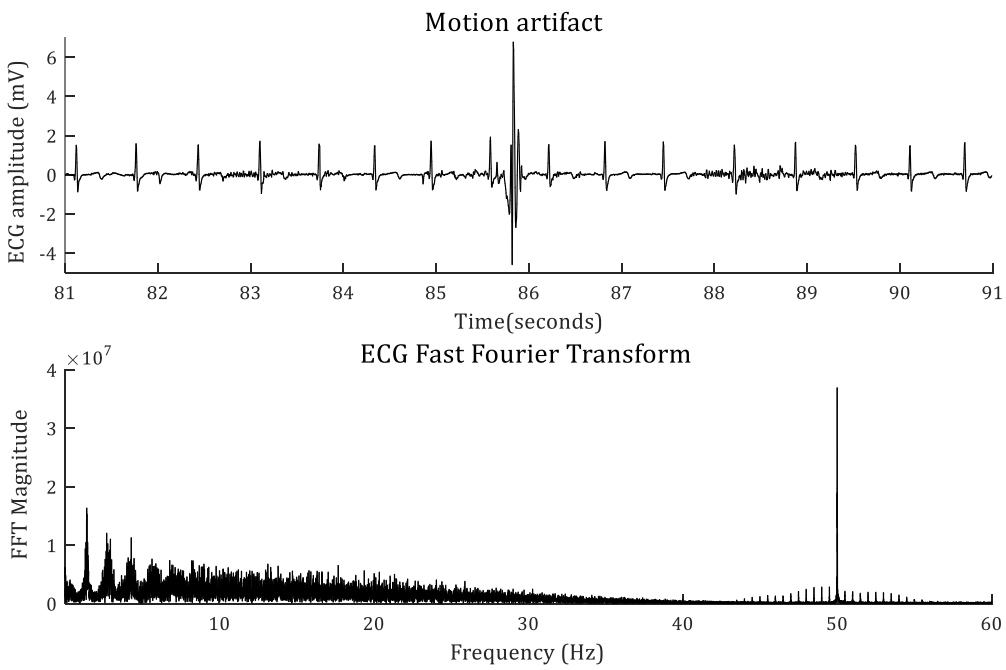

Figure 2.1-10. Motion artefact effect

Finally, Figure 2.1-12 depicts the ECG power spectrum for these three cases. Even though the measurement equipment is completely isolated of the power line, a 50 Hz component appears. This happens because the electrodes are acting as antennas for this interference.

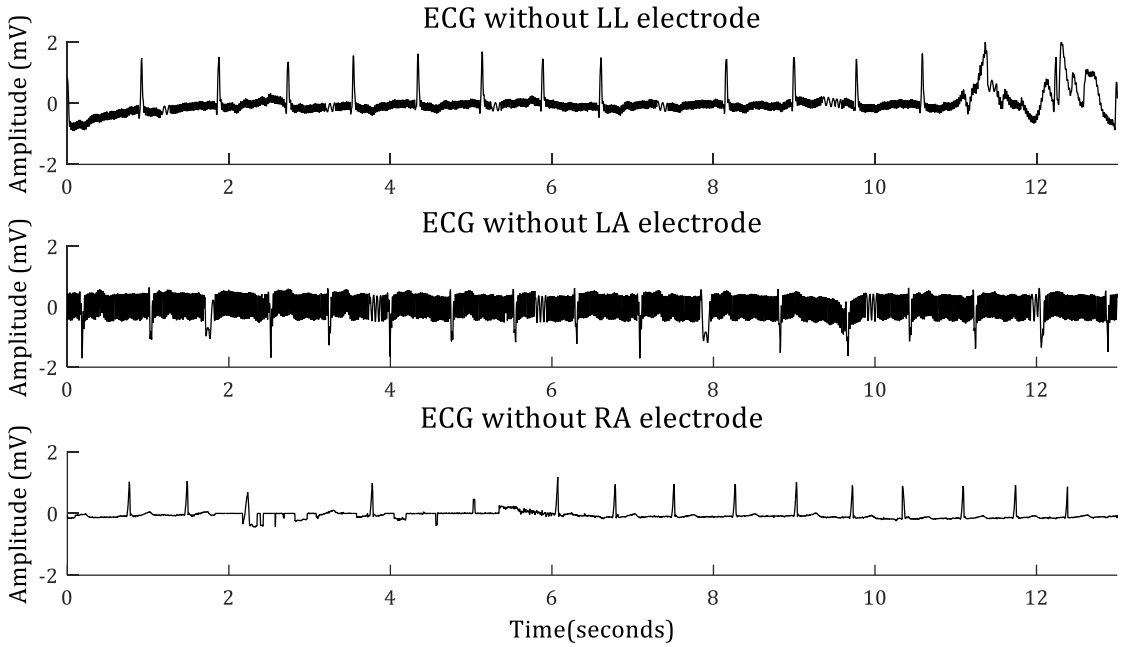

Figure 2.1-11. ECG without LL, LA or RA electrode

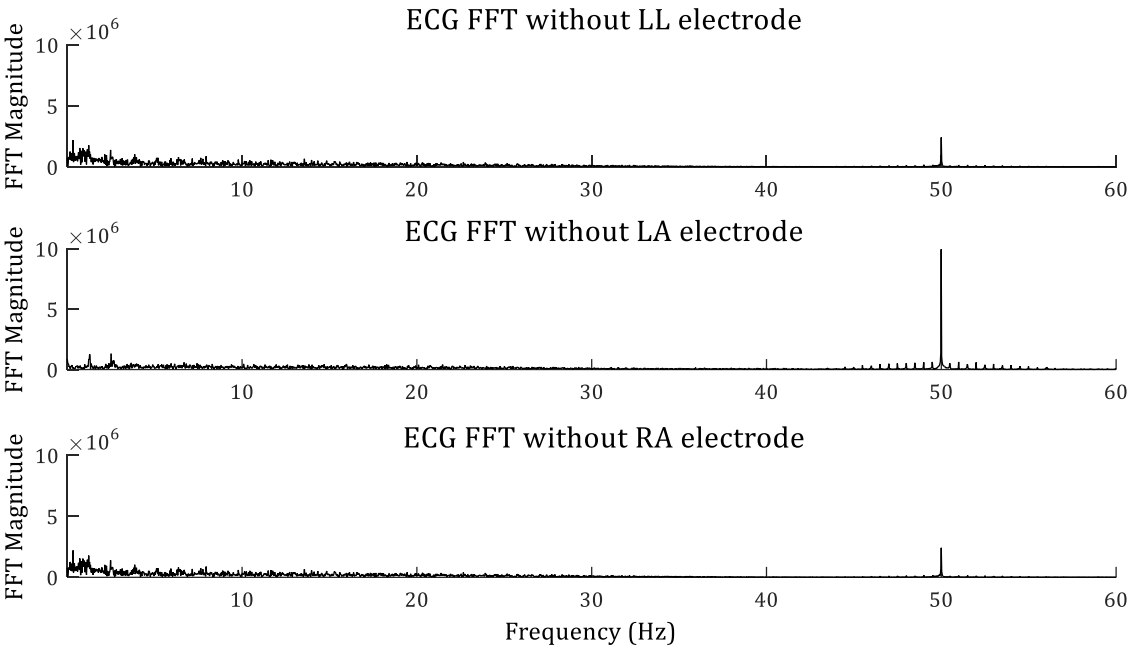

Figure 2.1-12. ECG spectrum without LL, LA or RA electrodes

2.1.2.3 Muscle noise

This noise appears due to the activity of the muscles close to the electrodes. In many cases, when there is a muscle contraction, the produced impulse completely hides the ECG signal. As can be seen in the Figure 2.1-13, the temporal effect of a muscle activation consists on the increasing of the background noise, which hinds the R peaks detection. In the frequency domain, the muscle activation produces the increasing of the low frequency band, which can be removed by obtaining the derivative signal. The most problematic effect of this noise is the presence of high frequency components, as they could be confused with R peaks when the R detection is carried out.

2.1.2.4 Wandering baseline

This effect produces a low-frequency variation of the ECG signal baseline (Figure 2.1-14). There are several sources of this artefact, such as subject movement, poor contact or disconnection of an electrode, respiration effect, etc. Its frequency is very low, so it can be easily removed without losing important information from the ECG signal.

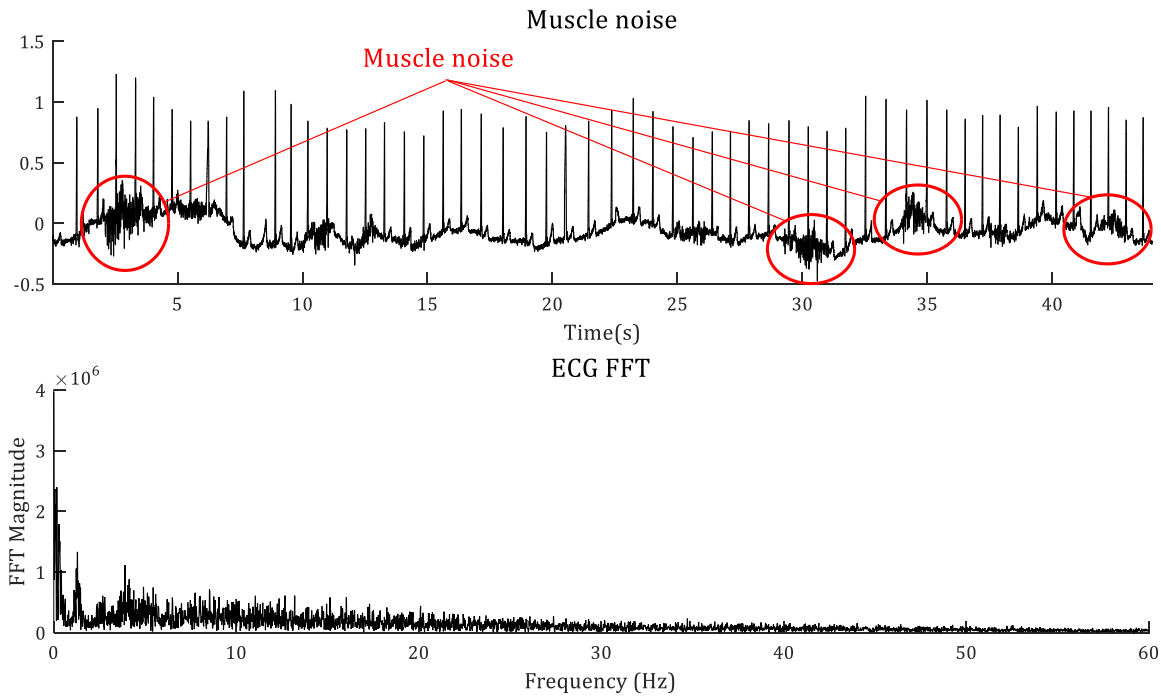

Figure 2.1-13. ECG with muscle noise

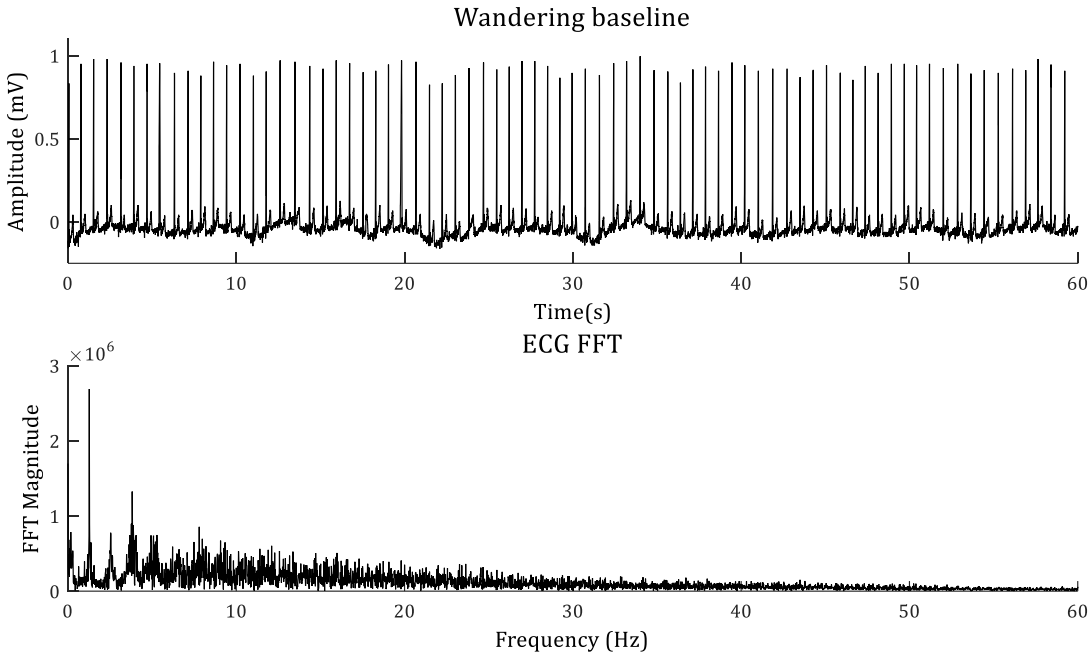

Figure 2.1-14. Wandering baseline effect

2.1.3 QRS complex detection structure

Each one of the above interferences and noises has a different effect on the ECG signal, which may hinder the detection of QRS complexes, so the process for eliminating each one of them is different as well. For instance, the power-line interference (Figure 2.1-7) could be removed by applying a notch filter. This filter barely removes important information from the ECG signal as long as it is only necessary to detect the position of the R peaks. However, the peaks due to motion (Figure 2.1-10) have frequencies and morphologies which could be mistaken for R peaks. This makes the process of the R peak detection more complex, thus, for a correct detection, it is necessary to take into consideration the possible maximum and minimum time interval between R peaks or the study of the detected peaks morphologies.

The R peaks detection algorithms are generally based on two main blocks (Figure 2.1-15): a pre-processing stage, which attempts to reduce or remove most part of the noise; and the detection stage, in which the R peaks of the ECG signal are detected. Considering this structure, most algorithms could be classified depending on the techniques that the authors propose for implementing each block. However, since the pre-processing stage techniques are more easily defined as they are based on concrete mathematical methods, the R peaks detection techniques depend on the features of the signals obtained with the first process. Most of them are based on the existence of a threshold.

2.1.3.1 Pre-processing techniques

Wavelet Transform (WT)

With the use of WT, it is possible to obtain information simultaneously in time and frequency domains. Through this technique, the ECG signal can be decomposed into a set of basic functions called wavelets (time-limited waves) by segmenting the ECG signal and applying the Discrete WT (DWT) to each segment. The length of the segments depends on a trade-off between accuracy and time-consumption. Then the wavelets that do not provide valid information are removed. Figure 2.1-16 plots an example of raw ECG signal, sampled at 360 Hz and the result of applying an 8-level Discrete Stationary Wavelet Transform (SWT). The bottom figure shows the residual signal, which is the removed part of the raw ECG signal.

In the Figure 2.1-17, the left column depicts the detail coefficients of the approximation; and the right column the result of the de-noising process over the coefficients. In this example, the coefficients d8, d7, d2 and d1 have been completely removed; a threshold has been applied to the coefficient d3, and coefficients d4, d5 and d6 have not been filtered. The resulting de-noised ECG signal is the addition of the signals of the left column.

There are several kinds of WT which are commonly used to pre-process the ECG signal such as Dyadic [PZZX09], DWT [ChCC06], DWT with Cubic Spline interpolation [ZhWu08], Quadratic Spline (QSWT) [IeVM08], Continuous (CWT)[GhGG08]. As the QRS complex information is within the frequency band from 5Hz to 22Hz, the WT is often used together with a filtering stage in order to reduce high and/or low frequency noises. Which increases both, the computational complexity and the resources this process needs for the filtering of the ECG signal.

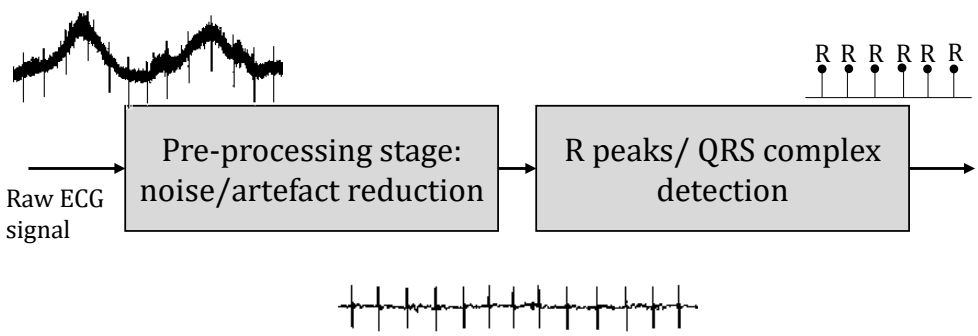

Figure 2.1-15. Structure of a QRS complex detector algorithm

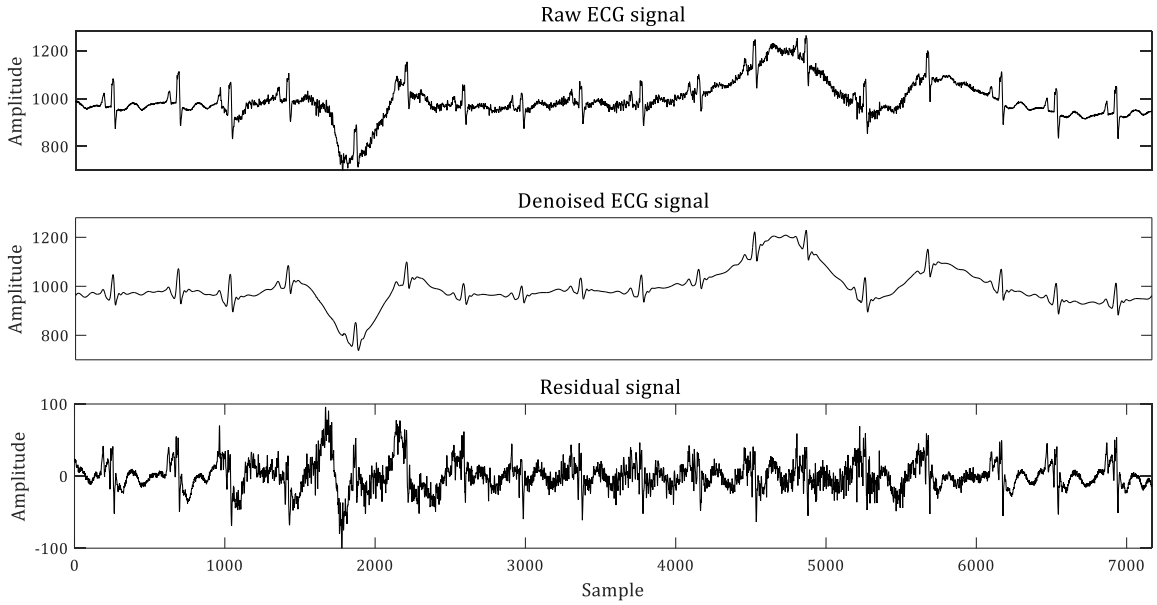

Figure 2.1-16. Wavelet denoising example

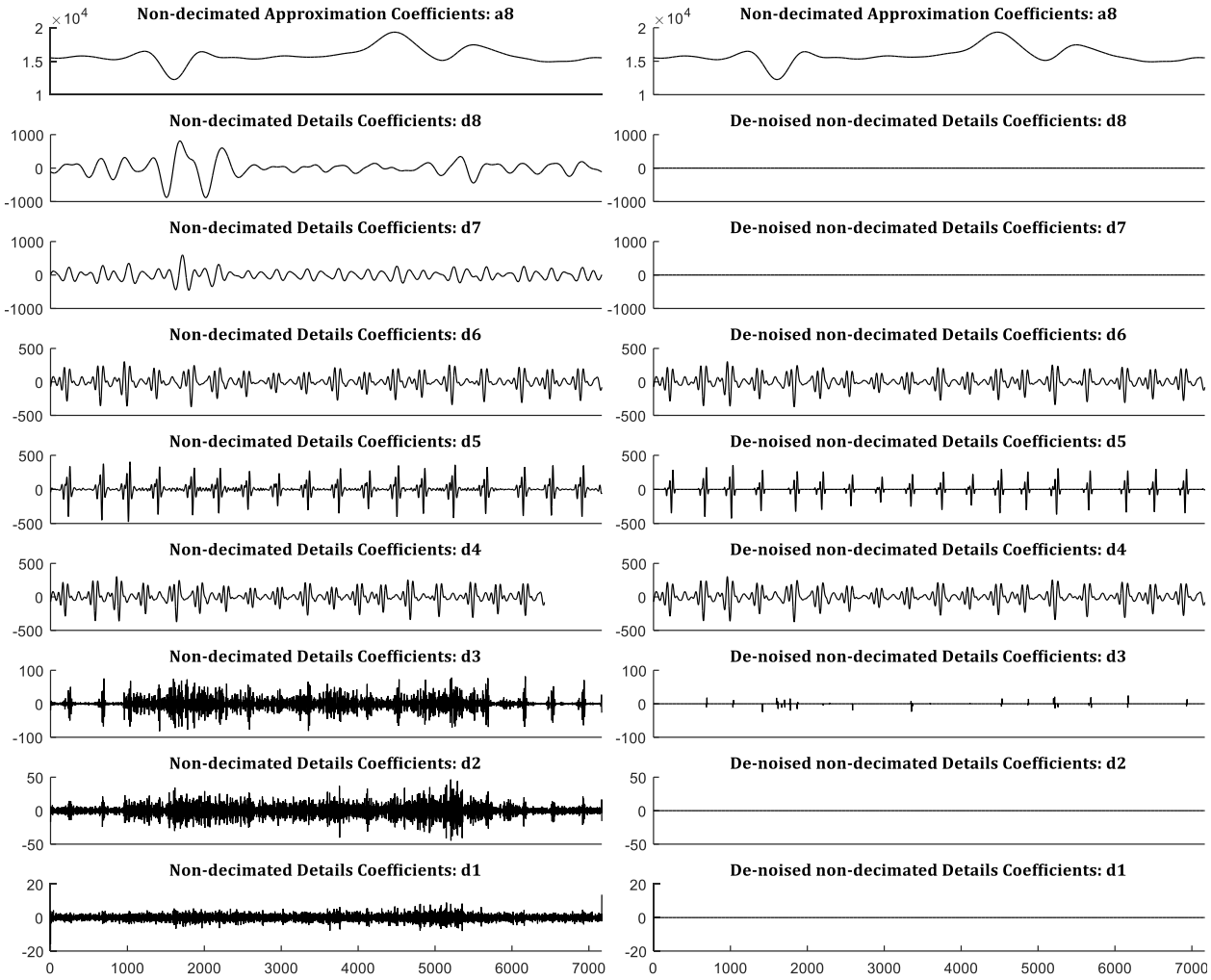

Figure 2.1-17. Wavelet coefficients and denoised wavelets

Hilbert Transform

One interesting property of this transform is that it is zero while the signal is constant and provides a zero-crossing every time there is an inflexion in the raw signal (Figure 2.1-18). Due to the morphological properties of the QRS complexes, a set of rules can be established to identify the position of the R waves. However, the features of several artefacts that are commonly present in the ECG signal could be mistaken as R peaks. For this reason, the Hilbert Transform is normally used together with another pre-processing stage. This other stage can be composed by a cascade of differentiations, integrations, etc. [MuMM13]; or they can be applied after [ZhLi09] or before [FFRM12] a WT.

Techniques based on differentiation

Differentiation emphasizes the dramatic changes that occur in a signal, as those provoked by the QRS complexes. These techniques are based on the well-known Pan and Tompkins algorithm [PaTo85]. Although these are the most efficient techniques from a power consumption and computational complexity point of view, usually they are not able to remove all the noises affecting the ECG signal. For this reason, they require the use of less noisy acquisition platforms and a more complex detection technique for avoiding the false positives. Some examples can be found in [ChKS12].

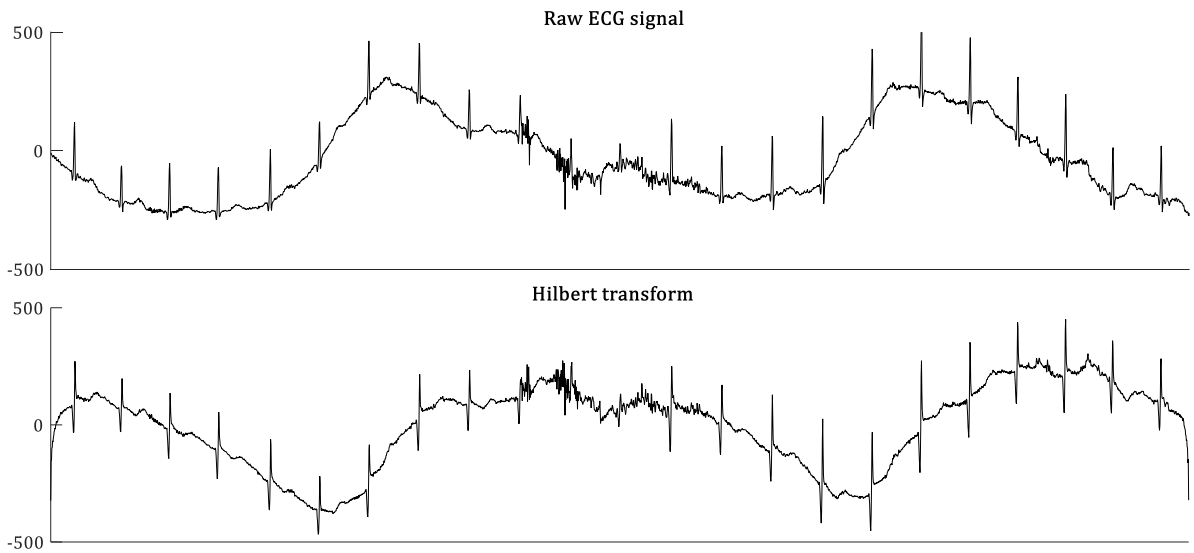

Figure 2.1-18. Example of Hilbert Transform of an ECG signal

Empirical Mode Decomposition (EMD)

As WT, EMD[PBTK10] decomposes the signal into a sum of oscillatory functions (Intrinsic Mode Functions, IMFs) whose oscillations have lower frequencies than the preceding one. Each IMF met the following conditions: First, the sum of maxima and minima of each IMF is the same as the number of zero-crossings; and, secondly, at any point of the IMF, the mean value of the envelope defined by the local maxima and the envelope defined by the local minima should be zero. Then the IMFs that do not contain information about the ECG signal are removed and the ECG is reconstructed with the non-removed IMFs. Figure 2.1-19 shows an example of EMD de-noising of an ECG signal. Figure 2.1-20 depicts the raw input signal and the result of applying the algorithm proposed in [ZoCh09], which is a fusion of EMD decomposition and Hilbert transform for filtering the ECG signal. Some authors combine this technique with WT [KhBJ13] as well, in order to improve the detection performance.

2.1.3.2 R-peaks detection techniques

With regard to the detection stage, the most used techniques are: analysis of the ECG morphology (slope analysis, zero-crossing detections, etc.); search for the maxima; and single, dual or even triple dynamic or adaptive thresholds to detect the amplitude of the ECG signal and the time between R peaks. Depending on the pre-processing technique employed, the most appropriate detection stage will be different. According to the published works, the most common combination is the use of the wavelet decomposition with a double dynamic threshold [PuLL12] to detect the R peaks.

There are some online QRS detectors that only use one dynamic threshold [IMLD12, NEBA12], obtaining an accurate detection. Their results can be improved if the Pan-Tompkins' search-back technique is included, as in [ZAAB12]. The Search-back technique consists of the storage of all the peaks found after the detection of an R peak, even if they do not meet the requirements to be an R-peak. If a new R-peak is not found within a determined time interval after the last detection, the stored peaks are analysed in order to find which of them can be classified as a heartbeat. This technique, as well as the Pan and Tompkins' algorithm, is detailed in Chapter 3.

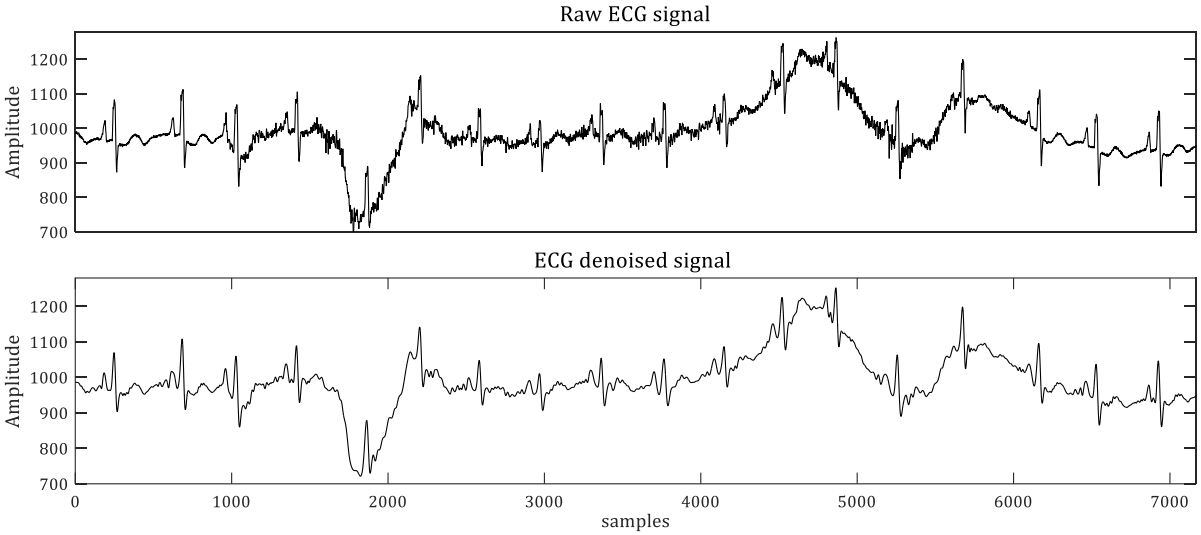

Figure 2.1-19. EMD de-noising example

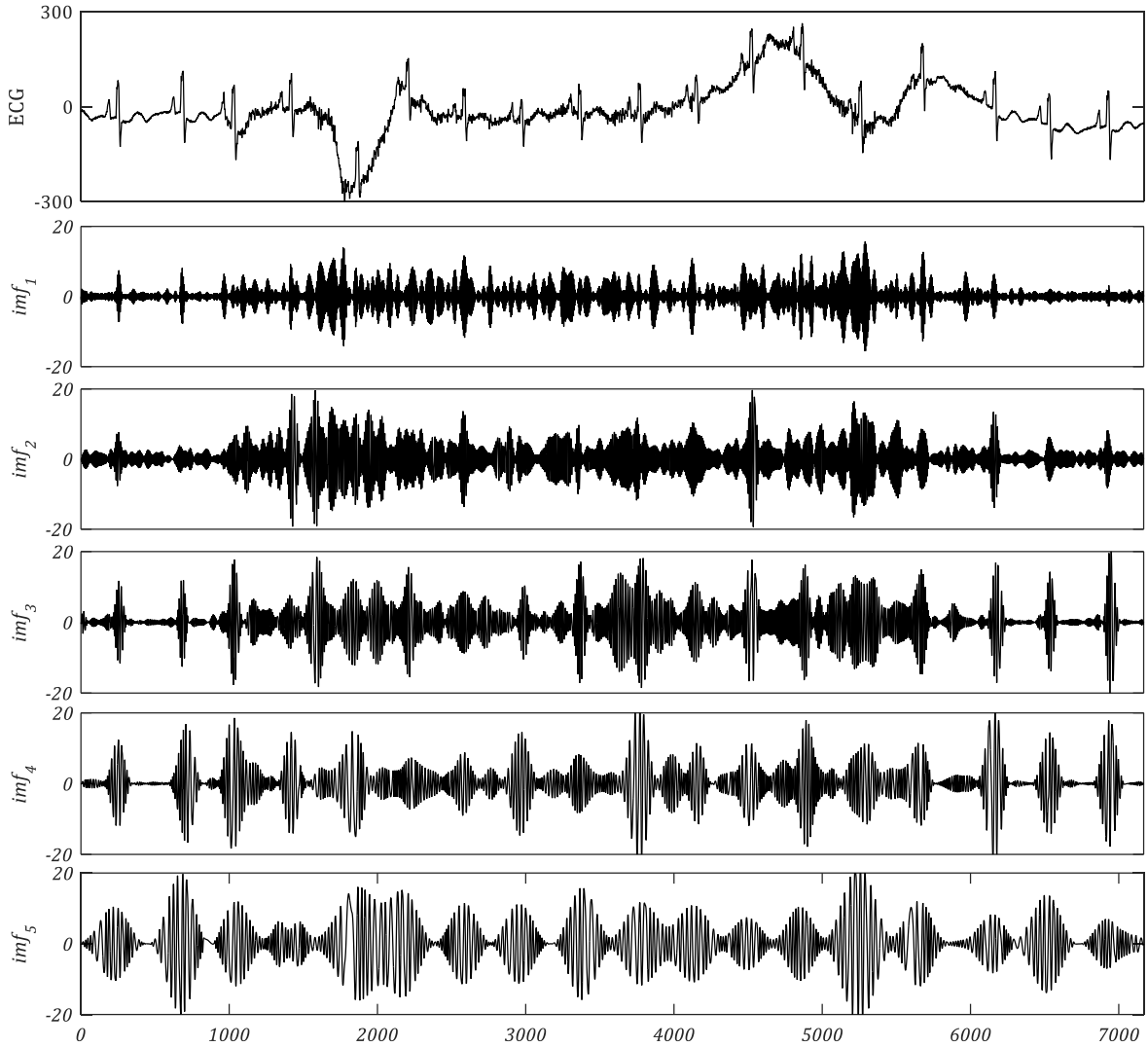

Figure 2.1-20. Example of the Empirical Mode Decomposition of an ECG signal into 5 Intrinsic Mode Functions

Next will be explained an example of a QRS complex detection algorithm proposed in [GSGM14]. The pre-processing stage of this algorithm is based on a drift estimation and a low-pass FIR filter (Figure 2.1-21). The resulting signal is depicted by Figure 2.1-22; the detection stage is based on a dual threshold to detect the positive and negative peaks of each QRS complex within the resulting processed ECG signal. The value of both thresholds is updated each second based on the amplitude of the positive and negative peaks as shown in Figure 2.1-23. The R peak is detected each time both thresholds are crossed by the signal within a predetermined time interval.

Regarding the pre-processing methods, as is mentioned above, usually the transform-based ones (Wavelet, Hilbert and EMD) need an additional stage for filtering the raw ECG signal, while the differentiation technique does not need any additional filtering. For this reason, usually the differentiation techniques are less complex and require less resources. However, these techniques need a more complex detection stage, since the artefacts and noises are not completely removed.

The correct technique to be used depends on several factors such as: the platform employed to implement the solution, the quality of the measurement system (and so, the level of noise), the movement of the patients, etc. Usually, Wavelet, Hilbert or EMD transforms achieve better results regarding the reduction of noises than techniques based on differentiation. However, the need of additional stages and high-order filters makes them unsuitable to be implemented in reduced-resources platforms.

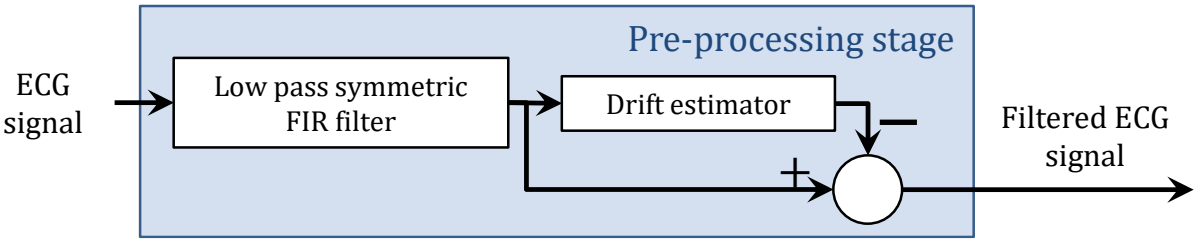

Figure 2.1-21. Example of pre-processing stage

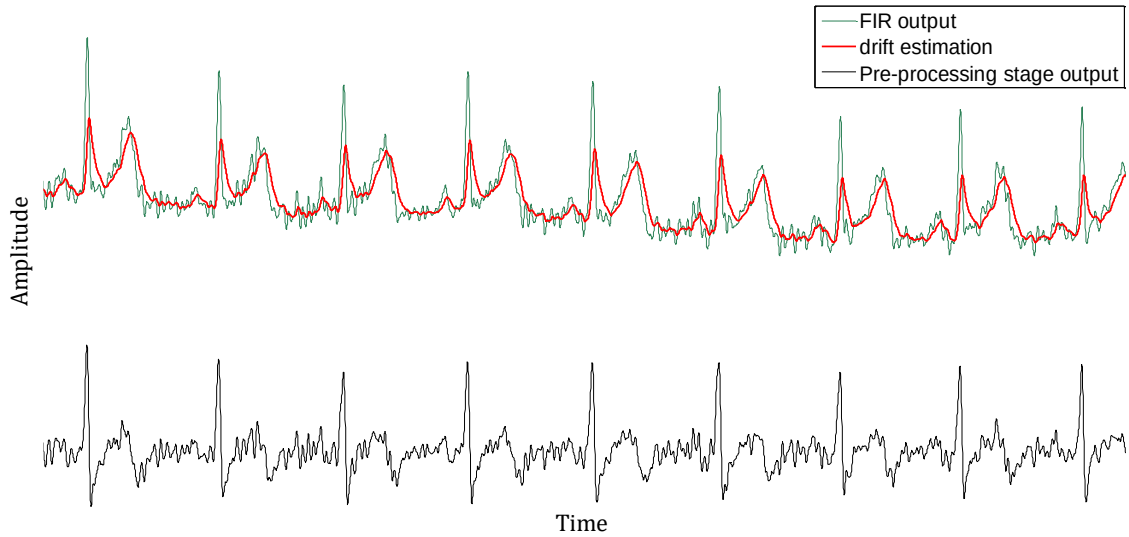

Figure 2.1-22. Result of the pre-processing stage

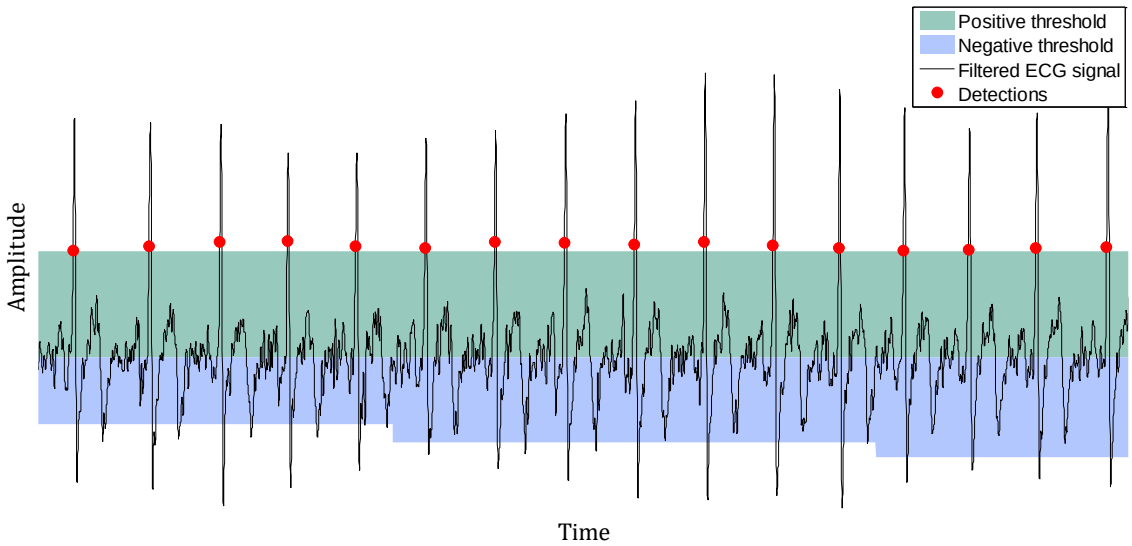

Figure 2.1-23.Example of double adaptive threshold and detection of the R peaks

2.2 Heart Rate and Heart Rate Variability

Heart Rate (HR) is defined as the number of heart beats per minute. This rate is controlled by the Autonomic Nervous System (ANS), which is composed of the Parasympathetic (PNS) and the Sympathetic Nervous Systems (SNS). The SNS prepares the body for stress situations, while the parasympathetic controls it within normal states. Thus, the heart rate varies depending on the demands of both systems following a cycle. Each of them have different requirements based on the necessities of several physiological systems [BTEG97]:

- Thermoregulatory system: changes in the difference between the environment and body temperatures produce very low frequency variations in the heart rate.
- Vasomotor system: heart rate varies with changes in blood pressure.
- Respiratory system: heart rate increases during the inspiration and decreases during the exhalation.
- Central Nervous System (CNS): depending on the subject's mood (stress, happiness, sleep stage, relaxation), the heart rate is high or low

Thus, for healthy people under normal circumstances, the more the heart rate varies the healthier is the subject.

Due to the relationship between the heart rate with other physiological systems behaviour, it is possible to analyse those systems by observing the HR variations. Usually these changes are analysed beat-by-beat, i.e. by computing the HR, which is equivalent to the time interval between each pair of adjacent heartbeats (RR intervals, Figure 2.1-2). The obtained signal is the so-called Heart Rate Variability (HRV) signal. Figure 2.2-1depicts an example of HRV signal of a healthy subject performing different activities, as can be distinguished by observing the mean value of the HRV (~80 bpm while sitting and ~110 while walking). During the same activity, the HRV does not have a constant value, its variation is approximately of ±10 bpm. This variance reflects the continuing adaptation of the body performed by the ANS.

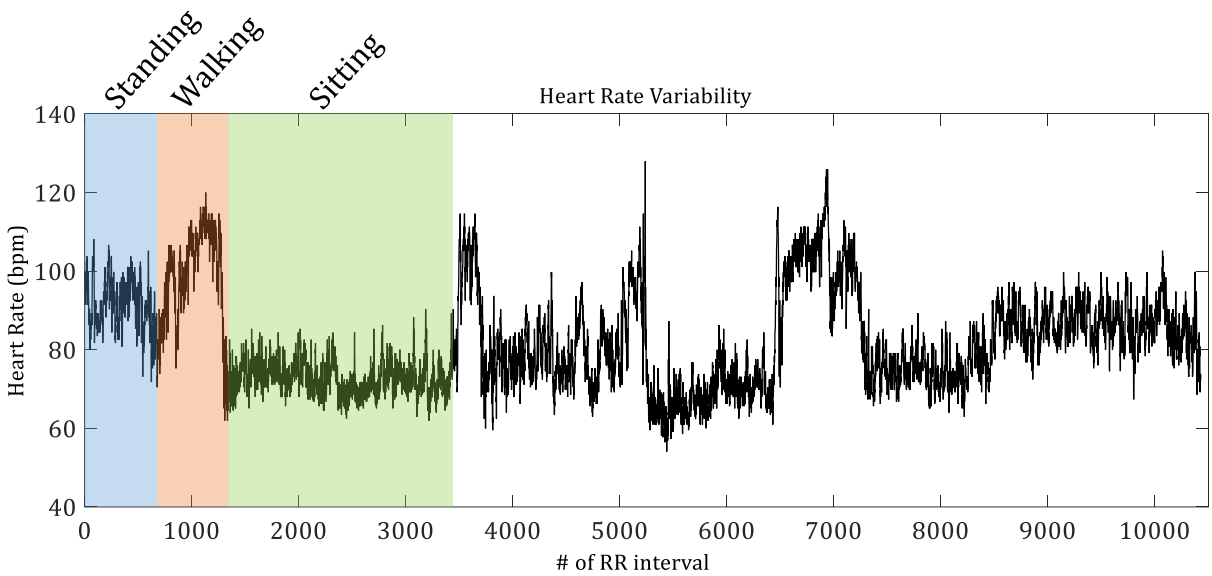

Figure 2.2-1. Heart Rate Variability of a healthy subject performing different physical activities.

Depending on the application, the HRV signal can be analysed in different ways. Thanks to its popularity, several features have been extracted, studied and their values or variations bounded for different health conditions. A large number of features can be extracted in time, frequency, graphical, etc. domains. In this work, a group of 18 features [Twom13] is analysed. The way these features are computed is explained in Appendix A.

The continuous observation of the heart rate allows the detection of cardiac diseases such as arrhythmias [GKLE12, HWCT12]. As proposed in [LWSG12], it is possible to develop an alarm system which could reduce considerably the risk the patients are exposed to by linking the HRV monitoring device with a positioning system.

Thanks to the accessibility of this signal and the reduced number of resources needed to obtain it, HRV has become a very useful tool to not only analyse the heart's health [MILP12, PMSB11], but also to study other physiological systems [HNVB07] and even to help to diagnose non-cardiac diseases in a non-invasive way [BEDD11, MILP12]. The study of HRV can give more information during the realisation of physical stress tests [BGIC13, GSCR12], this information could be a great tool to predict the recovery of the subjects depending on their characteristics such as their ages, gender, weight, etc. The usefulness of the Heart Rate Variability is demonstrated through the numerous and varied applications in which it has been used: assessment of prolonged pain states in the neonatal care context [JRLJ11], detection of seizures of new-borns [MaMe09], study and classification of individuals' mental state [KWVK07] or mood [VaLS12], stress detection [BeAF12], analysis of the sleeping phase [EyDB12], detection of apnea [HWSS11], etc.

Due to the fact that the performance of various and varied physiological systems can be observed and analysed through the measurement of the HRV signal it can be used to aid the diagnosis of certain diseases, in which case, the alternative observation method might be highly invasive. Additionally, it can be measured continuously with economic user-friendly devices that do not disturb the normal behaviour of the patients, allowing the access to information about the health status of the individuals during daily situations and familiar context, which greatly increases the quality and quantity of information available.

2.3 Introduction to allergies and allergy detection

"Allergy" is the name given to the abnormal reaction of the immune system to foreign substances that are, generally, harmless. To develop allergy, it is necessary to have a previous contact with the allergen and that development can take place any time the person is exposed to it. In these cases the body generates a response; the most frequent is that related to antibody called IgE (immunoglobulin E) which is in the surface of mast cells and basophils. At this moment, the person is "sensitized" to the allergen; this means that they can develop an allergic reaction in a further contact. In a future exposure to that substance, the allergen joins the specific IgE, activating these cells. This joining makes the body to release substances (mediators) that trigger the allergic reactions.

"Allergen" is a substance able to induce an immune reaction. Substances that could be allergens are pollen, dust mites, mould spores, animal hair, foods (milk, nuts, egg, fruits, etc.) or drugs (penicillin, antibiotics, insulin, etc.).

The severity of the allergic reactions varies from minor symptoms like pruritus, rash or hives; to more serious reactions, such as rhinitis, conjunctivitis, vomiting, abdominal cramp, or generalized reactions called anaphylaxis. Anaphylaxis provokes difficulty to breathe, hypotension and cardiorespiratory arrest.

It is believed that the susceptibility for developing allergy is related both to each subject's features such as heredity, age and gender; and to different environmental factors like pollution, amount of allergen, dietary changes or exposure to infectious diseases.

There is no test to know who, from sensitized people, will become allergic, that means will develop an allergic reaction. There is not a defined pattern that can help the physicians to predict which subject is allergic to which substance or, more importantly, what kind of symptoms they will suffer. Usually allergic reactions produced by food or drugs are more dangerous than those produced by other kind of allergens.

In case of suspicion of an allergic disease, the physicians perform different tests that expose the subject to the allergen and record the result. There are different tests that can be used:

- Immediate hypersensitivity skin tests (prick and Intradermal tests): These tests are carried out over the skin, by inserting a small quantity of the possible allergen. If the subject is sensitized, a wheal with erythema will appear in 15 or 20 minutes. A positive result means sensitization but is not necessary related to allergic symptoms with that allergen.
- Delayed hypersensitivity allergy tests (epi-cutaneous test): Physicians paste some patches impregnated with the possible allergens over the subject's back for 48 hours. Then, they remove them and evaluate the reaction of the skin. These tests measure delayed cell mediated allergic reactions.
- Blood testing: The concentration of specific IgE antibodies in the patient's blood is measured in a laboratory. Through this tests it is possible to identify antibodies to several kinds of allergens and, unlike the skin tests, it does not depend on subject's age, skin state, drugs, etc. As was the case of skin tests, sensitization does not mean allergic symptoms.
- Provocation tests or Oral Challenges for food[Ito13] or drug[ABRB03] allergies detection: These are the gold standard tests in allergy. The person is exposed to the allergen using increasing doses, until a full dose (a normal food portion or a therapeutical dose) is achieved. It is used to confirm a food or a drug tolerance and in certain cases to confirm allergy. It is a high-risk procedure that must be carried out in a hospital setting. If symptoms appeared the test is stopped and symptoms are treated. The challenge test can be performed oral, subcutaneous, intramuscular or intravenously.

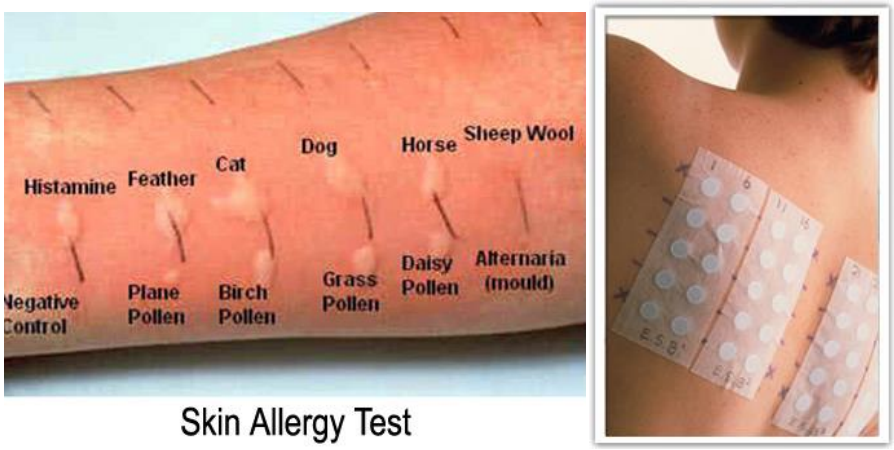

Figure 2.3-1. Example of immediate hypersensitivity skin test or prick test (left, extracted from [Beea00]) and delayed hypersensitivity test preparation (right, extracted from [Grou15])

This work is focused on the food allergy detection through allergy provocation tests, or Oral Food Challenges (OFC). Figure 2.3-2 summarizes the way these tests are conducted nowadays at the Department of Paediatrics and Child Health in the Cork University Hospital (CUH). As will be explained later on, there could exist some differences in how the OFC are performed. However, the philosophy is the same in all of them. The stages of this process are the following ones:

1. Before the test starts, the base line health status of the subject is checked. This is done by measuring several physiological parameters of the subject, such as blood pressure, heart rate and blood oxygen saturation. Physicians also look for any health condition that could be mistaken later with an allergic reaction.
2. A dose of the substance is then divided into several portions of different sizes. Usually, each portion is one half of the next one, being the maximum one half of the whole dose. The number of portions depends on the kind of allergen and the subject's features and clinical history.
3. The medical staff gives the smallest portion to the subject.
4. During a time interval of 10 to 20 minutes (again depending on the subject and allergen's features) the subject remains under observation. The medical staff is trained to detect both physiological and behavioural changes that might indicate the imminent appearance of an allergic reaction. Typically, the physicians look for skin problems, breathing difficulties, itchy tongue, red eyes, etc.; or with regard to behavioural changes, a decrease in physical activity. If the subject does not show any symptom, the next dose is given to him/her.

Successively, the observation periods are interspersed with the subsequent administrations of the allergen until the patient reacts, in which case the symptoms are treated and the patient is classified as allergic (he/she fails the test); or until all the portions have been administered to the patient. In the last case, as a delayed reaction can take place, the patient remains under observation at the hospital for the next two hours. If no symptom appears during this period, the patient is said to have passed the tests, i.e. classified as non-allergic.

As can be deduced, these tests present a high risk to the subjects' health. It is necessary for the appearance of a reaction to occur for diagnosing the allergy, if any. Therefore, even with the continuous observation of expert nurses, in some cases the subjects required the administration of adrenaline due to the severity of their reactions. Besides, the detection of the symptoms depends on the visual inspection of the subjects and on what they report that they feel, which sometimes can be confusing both, for the patients and for the medical staff.

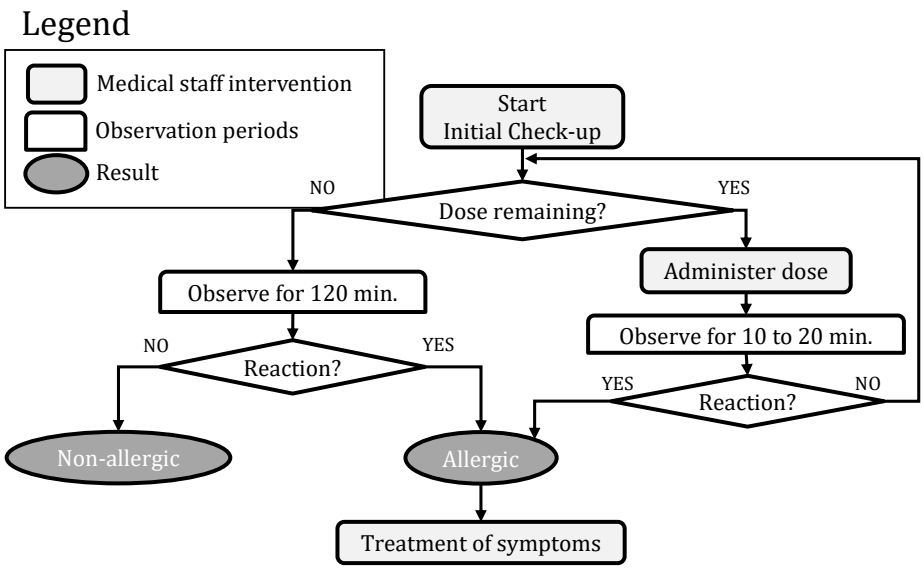

Figure 2.3-2. Flowchart of an Oral Food Challenge (OFC) at CUH

2.4 Previous work

This Thesis presents research which is the continuation of a research carried out in the Department of Electrical and Electronic Engineering at the National University of Ireland, Cork (Ireland), "Digital Signal Processing and Artificial Intelligence for the Automated Classification of Food Allergy" [Twom13, TTHM14]. The main objective of that Thesis was the automation of the allergy detection through the measurement and analysis of the HRV signal. This work will be summarized next.

2.4.1 Dataset

The Department of Paediatrics and Child Health at the Cork University Hospital performs OFCs in order to confirm the existence of food allergies. A collaboration between University College Cork and the Cork University Hospital was established with the aim of studying the ECG signal during the provocation tests, for which the approval of the Hospital ethics committee was obtained. The participation in the data-collecting process was voluntary for the patients, who gave their legal consent through their guardian signing the pertinent informed consent. Since the patients are underage, if the guardian did not want them to participate in the data collection, the OFC proceeded as usual. 23 children (age range 9 months – 10 years) were studied during routine OFC. The use of the remote sensing ECG monitoring was in addition to routine care and supervision.

TABLE 2.4-1. MAIN FEATURES OF THE TEST FROM WHICH THE ECG SIGNALS OF THE DATABASE USED WERE EXTRACTED

ID	Age	Gender	Allergen	OFC length	Total doses	Result
1	18 months	M	Wheat	0h. 14min.	1	Fail
2	6 years	M	Peanut	1h. 40min.	5	
3	9 years	M	Egg	1h. 34min.	5	
4	12 months	M	Milk	1h. 44min.	4	
5	8 years	M	Peanut	2h. 13min.	7	
6	9 years	F	Peanut	0h. 36min.	1	
7	6 years	M	Soy	0h. 57min.	3	
8	5 years	M	Peanut	1h. 45min.	5	
9	8 years	F	Egg (cake)	0h. 50min.	2	
10	3 years	M	Milk	1h. 23min.	3	
11	6 years	F	Peanut	1h. 25min.	5	
12	5 years	F	Milk	0h. 41min.	2	
13	3 years	F	Milk	1h. 46min.	5	
14	8 years	M	Soy	0h. 33min.	1	
15	9 years	F	Wheat	1h. 37min.	7	
16	12 months	M	Milk	2h. 10min.	4	Pass
17	6 years	M	Egg	1h. 42min.	5	
18	10 years	M	Egg (cake)	2h. 09min.	9	
19	4 years	F	Soy	2h. 11min.	8	
20	6 years	M	Peanut	1h. 51min.	8	
21	4 years	F	Wheat	1h. 29min.	6	
22	2 years	M	Peanut	1h. 03min.	4	
23	18 months	F	Milk	1h. 33min.	6	
Mean				**1h. 25min.**	**4.5**	

Termination of OFC was according to the existing unit protocols and clinical staff never had access to the ECG data. Fifteen of the 23 subjects of this study reacted to the given substance, while the other eight passed the tests. For each one of the tests, the allergen, age and gender of each subject, number of administered doses, total duration of the tests and result are summarized in Table 2.4-1.

A wireless Shimmer device[Shim00a] was used to record the ECG signal. The Shimmer device is a wearable platform composed of a MSP430F5437A microprocessor and several internal sensors. Some of the peripherals are: a 3-axis low noise accelerometer array, a 3-axis wide range accelerometer array, a 3-axis gyroscopes, 3-axis magnetic sensor, a relative pressure sensor and a temperature sensor as well as a Bluetooth antenna and a Micro SD Card socket. In addition, there are several expansion boards for adding capabilities to the basic platform. For this research, the Shimmer's ECG daughter board [Shim00b] was used to obtain a 3-lead ECG signal.

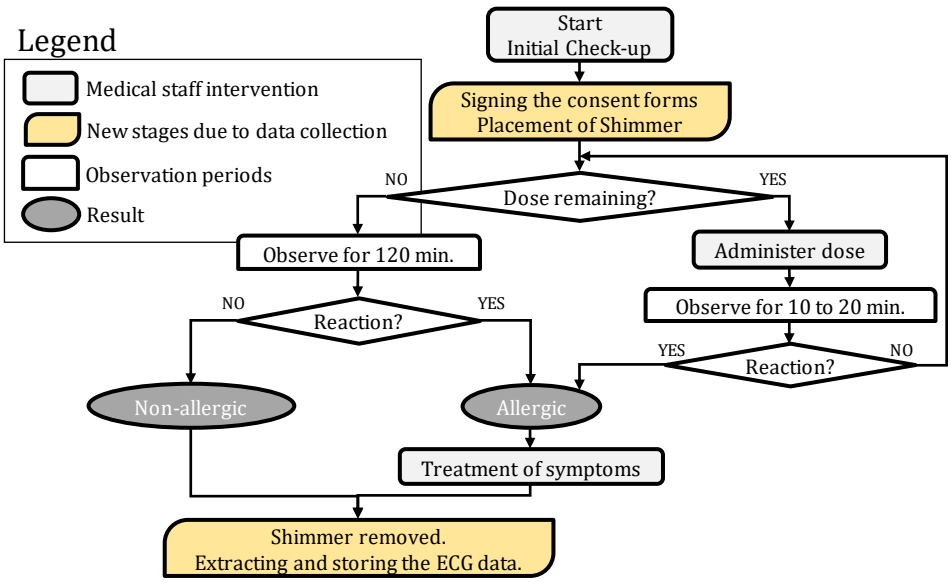

Figure 2.4-1. Modified OFC process

In each test, a shimmer was placed with a strap around the trunk and its electrodes arranged in the Einthoven triangle configuration (Figure 2.1-6). A sampling frequency of F_S = 256Hz was used to measure the ECG signal, as recommended in [RiKW01] for a paediatric population. The changes in the normal OFC procedure include the allocation of the Shimmer after the tests started, and its removal when the tests had finished. The rest of the process progressed as normal, as Figure 2.4-1 depicts.

2.4.2 Feature set

Once the ECG signal was obtained, the HRV of each subject was calculated in order to identify differences between allergic and non-allergic subjects. As is explained above, there exist a large number of HRV features that have been used to classify different health conditions. For this work 18 of the most popular features from different domains were studied, since it was unknown which body mechanism was necessary to observe.

The group of features were computed using different epoch (or temporal interval) windows as explained in the Figure 2.4-2, it can be observed how each second, the 18 features are obtained from each epoch regardless its duration. Different lengths were considered in that work: 60, 120, 180 and 300 seconds because the effect of the allergy was not characterized before. Shorter epochs measure the immediate effects, whilst longer ones analysed longer term variations of the HRV signal. **Appendix A** details the computation of each one of the considered features, which are the following ones:

- Time domain
  a. Mean of the RR intervals within each epoch (MRR)
  b. Standard deviation of the RR intervals (STDNN)
  c. Coefficient of variation: Standard deviation divided by the mean of the HRV (CV)
  d. Root mean square of the differences between adjacent RR intervals (RMSSD)
  e. NN50: Number of consecutive RR intervals differing by more than 50 ms.
  f. pNN50: Percentage of consecutive RR intervals that differ for more than 50ms.
  g. pNN25: Percentage of consecutive RR intervals that differ for more than 25 ms.
  h. Histogram index: Total number of RR intervals divided by the height of the histogram of RR intervals of the window measured on a discrete scale with bins of 1/128 seconds

- Sequential domain
  i. Positive trend (STPP): Percentage of consecutive increasing RR intervals
  j. Negative trend (STNN): Percentage of consecutive decreasing RR intervals

- Graphical domain: These features are extracted from the Poincaré representation. Poincaré represents the relationship between each RR interval with the previous RR interval. The RR intervals form an ellipse-shape cluster. Minor axis, SD1, represents the beat-to-beat variability; while the mayor axis, or SD2, is related to the long-term variability. From this plot, the next features have been analysed:
  k. Cardiac sympathetic index (CSI) is obtained as SD1/SD2
  l. Cardiac vagal index (CVI) as SD1*SD2
  m. SD1
  n. SD2

- Frequency domain
  o. Very low frequency power (VLF): Total power of the HRV spectrum in the very-low frequency band (0 to 0.04 Hz)
  p. Low frequency power (LF): Total power of the HRV spectrum in the low frequency band (0.04 to 0.15 Hz)
  q. High frequency power (HF): Total power of the HRV spectrum in the high frequency band (0.15 to 0.4 Hz)
  r. Ratio Low-High frequency (LFHF): Ratio between LF and HF power

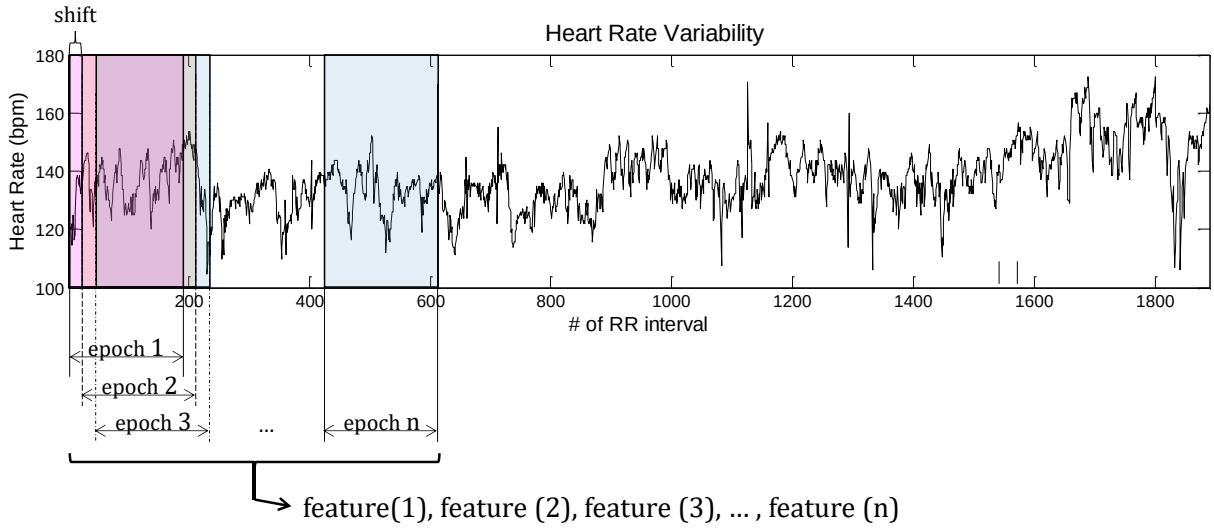

Figure 2.4-2. Epoch definition for the computation of each feature

2.4.3 Automated allergy detection

The previous work investigated the suitability of the machine-based technics to identify automatically signatures of food allergy based on the measurement and analysis of the HRV signal. The motivation to carry out that work was the observations of two allergists who conduct oral food challenges. These allergists observed that subjects had the tendency of becoming quiet before the onset of an allergic reaction, and their heart rate tended to change as well before the occurrence of the allergic reactions.

An energy expenditure estimator was designed based on the measurement of the subject's movement using a 3-axis accelerometer. Subjects performing OFC at the Cork University Hospital are required to stay quiet and relaxed during the test, so the activities they could perform were limited. For this reason, there was not a significant difference between allergic and non-allergic subjects regarding the energy expenditure.

The final approach was based on the analysis of the previous explained HRV's features. First, Principal Component Analysis [Webb93] is used to de-correlate the feature set. This process reduces the dimensionality of the feature vector. The only set of labelled data available was the data corresponding to the background interval, i.e., the data corresponding to the time in which any of the subjects had not had the allergen yet. For this reason, a novelty classifier based on a Gaussian Mixture Model (GMM) was employed.

The output of the classifier is the likelihood of each sample of belonging to the background class: if the likelihood is high, the data belongs to the known class, which is non-allergic; otherwise, the data belong to a different class, which in this case it is allergic. Figure 2.4-3 shows the block diagram of the system.

Figure 2.4-4 depicts an example of the likelihood signal obtained with the novelty classifier for an allergic subject (Subject 7) and Figure 2.4-5 for a non-allergic subject (subject 23). The background interval is the grey zone, while each blue zone represents a check-up period in which a new dose was given to the subjects, except for the last one, which is the end of the tests. If the likelihood value is below a threshold (red line) for more than a determined time, it is considered the representation of an allergic reaction. The value of the threshold is based on the mean and standard deviation of each subject as stated by *eq 2.1*. As can be seen in Figure 2.4-4, for the subject 7 before the end of the test (around minute 52) there was an event that can be considered an allergic reaction.

For each one of the subjects, it is necessary to set the following parameters: percentage of the information retained by the PCA, the number of Gaussians composing the GMM model, the multiplicative factor *n*, and the time the likelihood should be below the threshold, *d*. For each subject these parameters were selected based on the data of the rest of the subjects within the database by using an internal Leave One Out (LOO) (to select PCA and GMM parameters) and external LOO (to set *n* and *d*).

$$th = \mu - n\sigma \qquad \textit{(eq. 2.1)}$$

Where *n* is a multiplicative factor that is adapted to each patient's features.

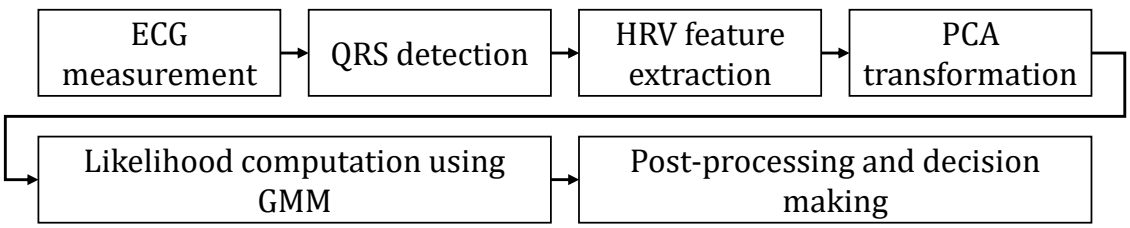

Figure 2.4-3. Block diagram of the automated allergy detection based in the analysis of the 18 features of the HRV signal proposed in [Twom13]

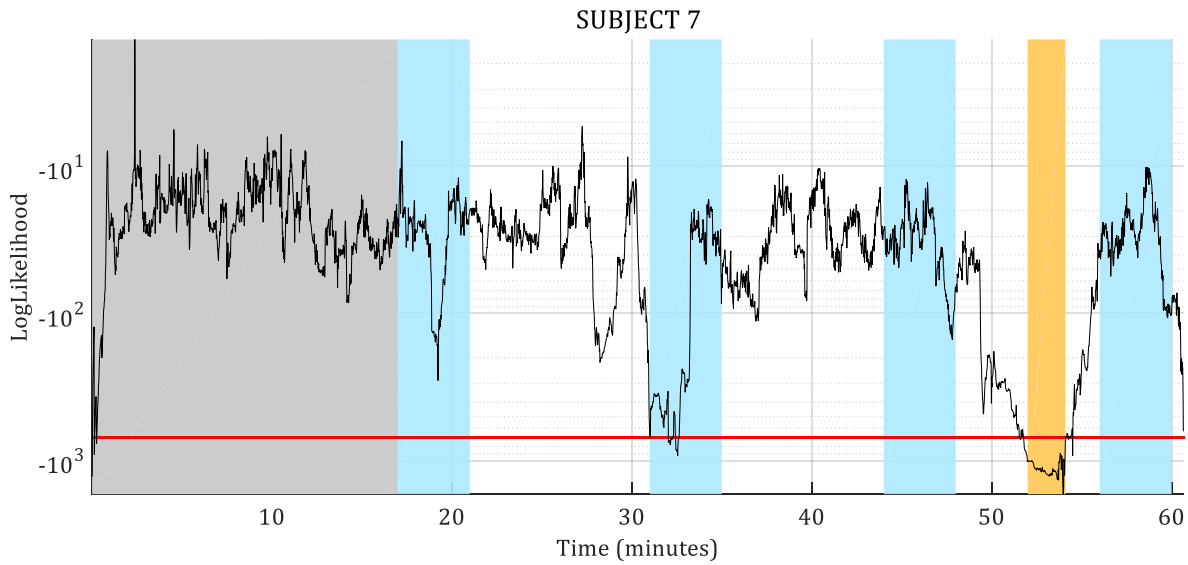

Figure 2.4-4. Example of likelihood signal achieved with the novelty classifier for an allergic subject

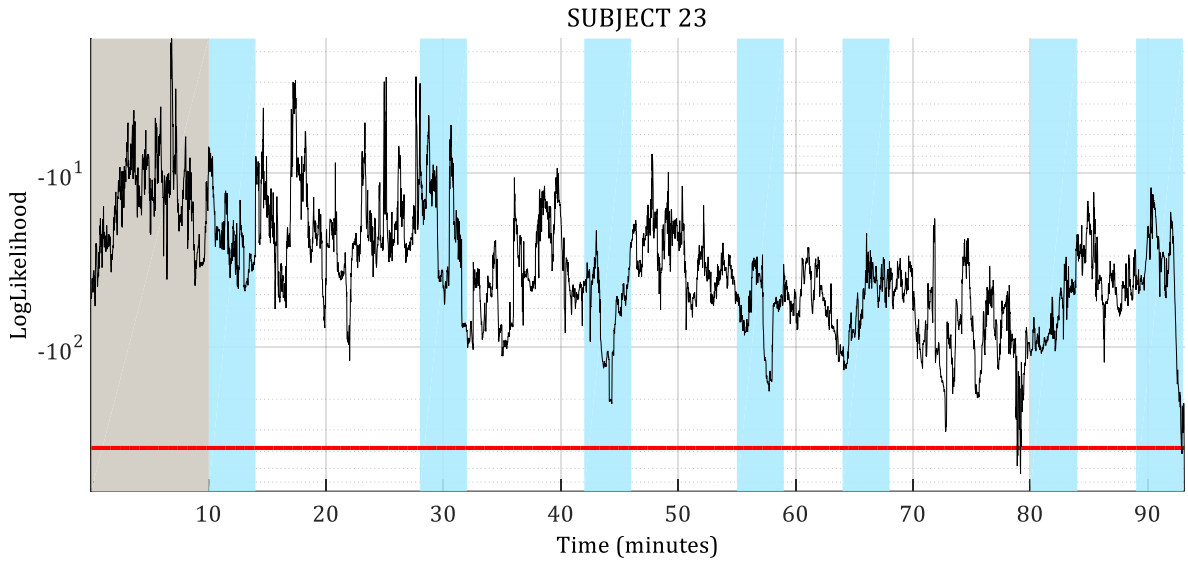

Figure 2.4-5. Example of likelihood signal achieved with the novelty classifier for a non-allergic subject

The designed algorithm could correctly classify all the non-allergic subjects (100% specificity) and detect 14 out of 15 allergic subjects (93.33 % sensitivity). An important fact that should be taken into consideration is that, the designed algorithm, resulted in a mean time of 39 minutes less than the mean length of the Oral Food Challenges. This implies a reduction of 30% of the total duration of the tests, which leads to the detection of the allergic reactions before the appearance of the physical and noticeable symptoms and so, a great reduction in the danger of a severe reaction.

For this work, the ECG signals were manually annotated. Several QRS complex detection algorithms were studied here. By using the one with the best performance, the sensitivity with the fully automated routine was reduced to 80%. The final results were obtained by fusing the partial results obtained by computing the features with the four different epochs (60, 120, 180 and 300 seconds).

The need of analysing 18 features of the Heart Rate Variability with 4 different epochs implies a computational load which makes this system unable to work in real-time during the Oral Food Challenges and so, renders it unusable for the medical staff during real OFCs. It is necessary to reduce this computational complexity in order to get a real-time allergy detection system able to warn to the medical staff of the likely occurrence of an allergic reaction.

Due to the process followed for designing this algorithm, the small number of patients available makes it necessary to select the parameters of the classification model for each subject. This selection is based on the data of the rest of patients. For this reason, if a new patient is analysed, the results cannot be predicted.

2.5 Problem statement and Thesis objectives

It has been demonstrated that allergic reactions affect the HRV in a particular manner. Besides, these effects take place, in many cases, before the appearance of the physical symptoms. This finding can be used to considerably reduce the stress the patients are exposed to and, what is more important, the risk of suffering a severe reaction.

Neither the QRS complex detection, nor the allergy detection process employed in the previous research worked in real time. On the contrary, the QRS complex detection algorithm needed the whole ECG signal to set the threshold and so, to detect the QRS complexes; the allergy detection algorithm, on the other hand, was based on the selection of a unique model for each subject, but the parameters of that model depended on the data of the rest of the subjects. This means that for the analysis of a new patient it was necessary to get a new model based on the whole database whose results are unknown.

Thus, the main issues to be specifically addressed by this Thesis, while fulfilling all the other general requirements, are:

- **Real-time and motes' limitations focus**. As has been explained, it is aimed to design a system able to work in real-time during real tests which should be taken into account during all the algorithm design process. Due to the motes' limitations regarding computation capabilities and resource availability, and the need of getting online information, every algorithm proposed in this work should be computationally efficient.

- **Develop a new QRS complex detection algorithm.** Despite the great number of proposed algorithms, most of them require many resources and computational capabilities. This thesis is focused on the remote monitoring of patients for whom it is mandatory to use portable devices. There are two drawbacks of working with portable devices: first, the computational capabilities are reduced and, secondly, the energy consumption should be as low as possible to extend their autonomy. The QRS complex detection will work together with a high level algorithm that must produce a result in real-time. Then, the QRS complex detection algorithm should analyse the ECG signal and detect the R peaks in real-time as well, minimizing the use of resources.

- **Design of a real-time allergy detection algorithm.** Once it is demonstrated that it is possible to detect an allergic reaction through the analysis of the HRV signal, it is necessary to design an allergy detection algorithm able to set an alarm if an abnormal situation is detected during the tests. This will allow the medical staff to take advantage of the findings of the previous work during a real OFC. For this objective, it should be determined which particular feature or group of features provides information about the physiological changes produced by an allergic reaction and reduce the set of features. If the way this feature or group of features changes during an allergic reaction is modelled, it is possible to design an allergy detection algorithm able to work in an online mode and so, warn to the medical staff of the future appearance of physical reactions.

- **Test of the proposed method under different conditions.** The dataset available at the beginning of this research consisted of 23 children exposed to food allergies (Table 2.4-1). Due to the protocol followed at the Cork University Hospital to perform OFC, the patients were required to remain on a bed. A new set of data has been obtained from the Guadalajara University Hospital, in which the OFC protocol is different, as will be explained in Chapter 5. Although the number of doses and their sizes are similar, the observation periods are longer and so is the total length of the OFC. More importantly, the patients are

allowed to move freely within the allergy room, which influences their heart rate and so, hinders allergy detection based on HRV. It should be studied how the movement of the patients affects the results of the proposed allergy detection method and. The energy expenditure estimator proposed by Twomey in the last work has not been considered here, since there are more factors that affect how much the children move, like their age or the activity they are performing. Due to the fact that the tests are longer in this new process, the activity will change along the whole test regardless the result of the OFCs.

- **Extension of the study.** There exist great quantities of allergy types with which the body must deal with. Nowadays, it is not possible to predict which kind of reaction a patient will have depending on his/her features (age, gender, health status, etc.) or on the features of the allergen (kind, quantity, etc.) due to the large number of variables to consider. In this thesis, a simplification has been made in order to define six groups depending on the age of the patients (children, adults) and the type of the allergen (food, NonSteroidal Anti-Inflammatory Drugs –NSAID-, and non-NSAIDs), as is listed in Figure 2.5-1. The conclusions from the analysis made on [Children, food] group will be tested on the other groups. In this way, it is possible to get a better definition of the proposed allergy detection method in terms of applicability.

	Allergen		
Age	Children, food	Children, NSAID	Children, non-NSAID
	Adult, food	Adult, NSAID	Adult, non-NSAID

Figure 2.5-1. Groups for the allergy detection study

Chapter 3.

QRS COMPLEX DETECTION

The first step in developing a real time automated allergy detection system for implementation on a mote and for use in a hospital setting, is to develop a real time low computational complex algorithm for QRS complex detection. This algorithm must maintain the performance of the state of the art algorithms. As was advanced in Chapter 2, even though there are a large number of proposed QRS complex detection algorithms, most of them are focused on the complete removal of the different noises affecting the ECG signal.

For this task, complex processes, high order filters, and a great number of resources are required. However, for applications based on the information regarding the instant in which a heartbeat occurred, the computational effort employed in most of the proposed algorithms is not required. Moreover, this thesis is focused on remote monitoring systems in which devices with limited resources are used to measure and analyse the ECG signal. Most of the existing algorithms are not suitable for use on these devices and/or do not provide the required information in real-time.

The information regarding the positions of the R-peaks is not important by itself, but the analysis performed over them (analysis of the HRV signal). It is important to keep in mind, mainly when working in real-time, that this kind of algorithm will be part of a higher level application, and so,

the available resources will be shared. Furthermore, the devices used for telemedicine or remote monitoring applications are typically portable devices, so the optimization of the processes execution will increase their autonomy. Thus, the challenge here consists of designing a QRS complex detection algorithm with the following features:

- ✓ Able to work in real-time. The higher level application will need the information regarding the positions of the R-peaks as soon as they are produced.
- ✓ Low resources consumption. This algorithm will be implemented on a portable device together with other applications, so it is needed to optimize the number of resources (memory cells, multipliers, adders, etc.) required. Furthermore, the reduction of the number of operations implies a reduction of the power consumption, and so an increase in the devices autonomy.
- ✓ High accuracy. The proposed QRS detection should detect as many R-peaks as possible whilst not detecting noise peaks as R-peaks i.e., the number of false negatives (FN) and false positives (FP) should be reduced.

Jiapu Pan and Willis J. Tompkins published their algorithm in 1985 as "A real-time QRS detection algorithm" [PaTo85]. This algorithm has been the main reference for most of the proposed algorithms designed to work in real-time since it was published 30 years ago. For this reason, it can be considered as a gold standard in this area. It was able to run on the 8-bit microprocessors Z80 (Zilog) and NSC800 (National Semiconductors). Both microprocessors had a master clock of up to 4 MHz and a memory capacity of 64 kB. Even with these constraints, it managed to obtain an accuracy of 99.3 % on the detection of all the R peaks within one of the currently most used databases (MIT database), working in real-time. As a consequence of its feature and despite the fact that it was published 30 years ago, this algorithm is still today one of the most referenced real-time QRS complex detection algorithms. However, it presents a large number of false detections in the case of ECG signals affected by high frequency artefacts, as will be shown later.

This chapter proposes a new real-time low-cost QRS complex detection algorithm to be implemented on devices with a reduced number of resources. With the aim of establishing a comparative element, the Pan & Tompkins algorithm is also described. Both algorithms are analysed under the same conditions in order to obtain their performance and computational complexity.

3.1 Benchmark databases

Several standard ECG databases are available to evaluate QRS complex detection algorithms. The use of these well annotated and validated databases provides reproducible and comparable results in terms of accuracy. These databases contain a large variety of selected ECG signals that allow the testing of the algorithms under different conditions, from records with clear R-peaks and few artefacts to others with abnormal shapes, noise and lots of artefacts that make it difficult to achieve an accurate detection. These databases will be used for evaluating the performance of both algorithms with ECG signals presenting different features.

The most used ECG database is MIT-BIH Arrhythmia Database, MITDB [MoMa01]. This database has been extracted from the PhysioNet Website [GAGH00]. It contains 48 ECG recordings, each with a duration of 30 minutes, at a sampling rate F_S of 360Hz. This set represents different types of phenomena that arrhythmia can provoke in ECG signals. The MIT-BIH Normal Sinus Rhythm Database (NSRDB) will be used as well. This database is composed of 130-minutes long ECG signals from 18 healthy adults (aged from 20 to 50), at a sampling frequency F_S of 128Hz. Furthermore, the authors have obtained another database (Allergy Database, ADB) from the Paediatrics Section of Cork University Hospital (Cork, Ireland). It is composed of 24 ECG signals with different lengths (from 13 minutes to more than 130 minutes), sampled at 256Hz.

TABLE 3.1-1. DATABASES USED TO TEST THE ALGORITHM PERFORMANCE

Database	*F_S (Hz)*	*# of signals*	*Total length*	*Marked feature*
NSRDB	128	18	24h 4min	Almost ideal database
ADB	256	24	10h 13min	Very high level of motion artefacts
MITDB	360	48	15h 3min	• "Random" beat-to-beat changing times • Early beats amplitudes • Changing QRS morphology
ApneaECG	100	69	191h 40min	ECG measured during apnoea episodes
Fantasia	250	20	22h 13min	10 young and 10 elderly subjects resting in supine position
Challenge	250	100	16h 40min	ECG related to subjects on different health status

All the subjects in this database are children (aged 7 months to 10 years old), and most of these ECG signals are affected by several motion artefacts. In addition, three more databases have been obtained from PhysioNet: ApneaECG, Fantasia and Challenge 2014 databases. All the ECG signals employed here are annotated, i.e. the real positions of all the R-peaks are known. Table 3.1-1 summarizes the main features of the databases used.

There are several reasons to use so many databases: firstly, if an algorithm is successfully checked with as much data as possible, a higher level of robustness can be concluded; secondly, the acquisition conditions are different for each database, so it allows the analysis of the dependency between these conditions and the algorithm parameters; and finally, most authors validate their algorithms with the MIT-BIH Arrhythmia Database, so it is needed to use this standard database for comparing the results with previous works.

3.2 Metrics

According to the Association for the Advancement of Medical Instrumentation (AAMI) [Asso98], for evaluating a QRS detection algorithm the next metrics and definitions should be used:

- True Positive (*TP*): R-peak correctly detected.
- False Negative (*FN*): Non-detected R-peak.
- False Positive (*FP*): Artefact or noise mistaken for R-peak.
- Sensitivity (*Se*): Ability to detect the existent R-peaks; percentage of the existent R-peaks which are correctly detected *(eq. 3.1)*.
- Positive predictivity (*+P*): Ability to discriminate between R-peaks and interferences or noises, i.e. percentage of the detected peaks which are R-peaks *(eq. 3.2)*.

$$Se = \frac{TP}{TP + FN} \qquad \textit{(eq. 3.1)}$$

$$+P = \frac{TP}{TP + FP} \qquad \textit{(eq. 3.2)}$$

When comparing the results of two different QRS complex detection algorithm, the minimum between *Se* and *+P* will be used, as is the most common method.

3.3 Pan & Tompkins' algorithm

Most of the R-peaks detection algorithms can be divided into two main blocks: pre-processing stage and R peaks detection stage. Taking into account the classification made in chapter 2, the pre-processing stage of the Pan & Tompkins (P&T) algorithm is based on differentiation, and the detection stage uses a triple adaptive threshold: two amplitude thresholds, and one temporal threshold. P&T also includes a third block (searchback block in Figure 3.3-1) which is responsible for checking the features of the detected R-peaks and correcting any errors. These three blocks are detailed in the next subsections.

3.3.1 Pre-processing stage

This block prepares the ECG signal before it is analysed by the R-peaks detection block by reducing the noises and artefacts that appear on it. Firstly, two filters remove the high and low frequency components of the signal. Then, a derivative is applied to remove the wandering baseline. Next, the squaring block makes the signal positive. The ideal value of the resulting signal is zero between QRS complexes, and has two rises representing each QRS complex, as can be seen in Figure 3.3-3. Finally, the integration window makes those two peaks form a trapezoid representing the ECG QRS complex. Figure 3.3-2 shows the block diagram of the pre-processing stage. Each one of the operations carried out within this phase is implemented through the following difference equations:

- **Low-pass filter (LPF)** main purpose is the elimination of the power line interference following *(eq. 3.3).*
- **High-pass filter (HPF)** is implemented by obtaining an all-pass filter with delay *(eq. 3.5)* and subtracting a first order low-pass filter *(eq. 3.4).*
- The **derivative** *(eq. 3.6)* extracts information about the slopes.
- The **window integral** *(eq. 3.7)* integrates all the peaks produced during a QRS complex if the length, N, is correctly set. The authors set the length of the window to 160 ms. For the sample frequency, F_S, used by them of 200 Hz, it implies 32 samples.

A more detailed description of the features of the employed filters can be obtained in the book "Biomedical signal processing", chapter 12 [Afon93].

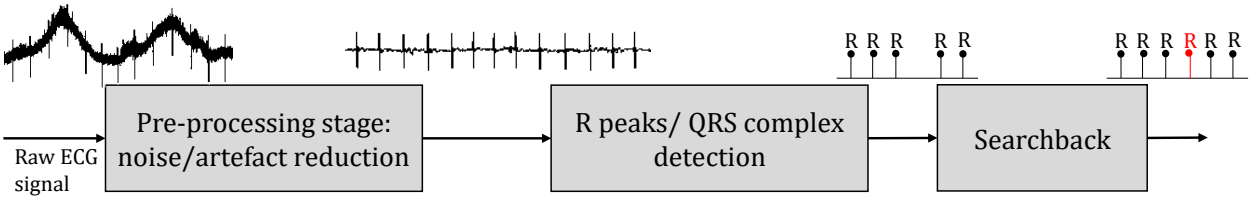

Figure 3.3-1. Block diagram of the Pan & Tompkins algorithm

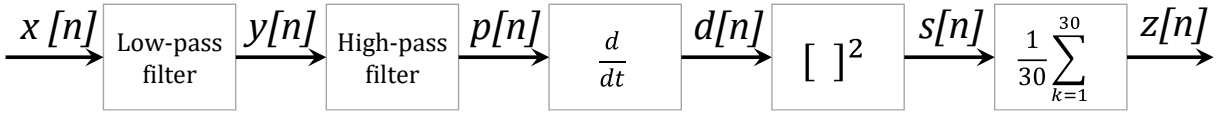

Figure 3.3-2. Pan & Tompkins QRS detection algorithm block diagram

$$y(n) = 2y(n-1) - y(n-2) + x(n) - 2x(n-6) + x(n-12) \qquad \textit{(eq. 3.3)}$$

$$p_{lp}(n) = p_{lp}(n-1) + y(n) - y(n-32) \qquad \textit{(eq. 3.4)}$$

$$p(n) = p_{lp}(n-16) - \frac{1}{32}[p(n-1) + p_{lp}(n) - p_{lp}(n-32)] \qquad \textit{(eq. 3.5)}$$

$$d(n) = \frac{2p(n) + p(n-1) - p(n-3) - 2p(n-4)}{8} \qquad \textit{(eq. 3.6)}$$

$$z(n) = \frac{1}{N}\left[s\big(n-(N-1)\big) + s\big(n-(N-2)\big) + \cdots + s(n)\right] \qquad \textit{(eq. 3.7)}$$

Figure 3.3-3 shows the signals generated within the pre-processing stage. Figure 3.3-4 depicts the comparison between the ECG signal, *x(n)*, and the pre-processed signal, *z(n)*. The amplitude of the pre-processed signal has been magnified by 10 to easily compare both signals. As can be seen in that figure, there exists a latency, which is the addition of all the delays produced in each one of the stages of the pre-processing phase. Removing this delay (Figure 3.3-5), it can be seen that the position of the R-peak corresponds with the position of the half positive slope of the pre-processed signal trapezoid. The total duration of the QRS complex can be obtained by measuring the duration of one of the slopes.

Figure 3.3-3.Signals generated during the pre-processing stage of the Pan and Tompkins algorithm

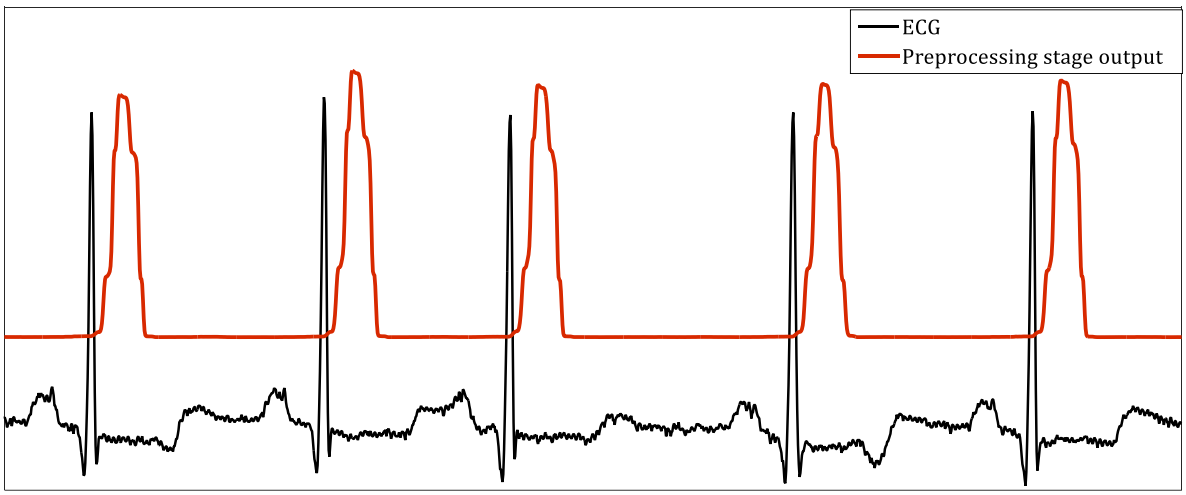

Figure 3.3-4. Input and output of the pre-processing stage

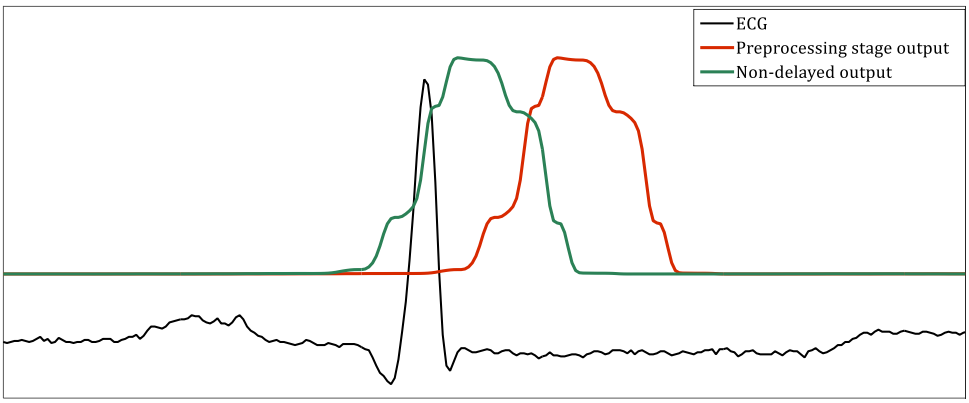

Figure 3.3-5. Comparison between ECG and pre-processed signal without delays

3.3.2 Thresholding stage

Pan and Tompkins algorithm has a learning phase for estimating the amplitude of the R-peaks (signal level, *SPKI*) and the noise peaks (noise level, *NPKI*). To initialize the estimated values, it needs approximately 2 seconds at the beginning of the analysis. After the initialization, their values are continuously updated during the ECG analysis. Each detected peak is classified as R-peak, or noise peak. Depending on this decision, the algorithm updates the value of *SPKI (eq. 3.8)* or *NPKI (eq. 3.9)*. To be classified as an R-peak, the amplitude of the detected peak has to be higher than a threshold, the value of which is computed in *(eq. 3.10)*. *Threshold2 (eq. 3.11.)* is used instead of *Threshold1* if the search back technique is applied (subsection 3.2.3). Figure 3.3-6 shows an example of *SPKI* and *NPKI* estimation and the corresponding value of both thresholds.

$$SPKI\ [n] = 0.125 * PeakAmplitude + 0.875 * SPKI\ [n-1], if\ the\ peak\ is\ an\ R\ peak \qquad (eq.\ 3.8)$$

$$NPKI\ [n] = 0.125 * PeakAmplitude + 0.875 * NPKI[n-1], if\ the\ peak\ is\ a\ noise\ peak \qquad (eq.\ 3.9)$$

$$Threshold1\ [\mathrm{n}] = NPKI + 0.25(SPKI\ [n] + NPKI\ [n]) \qquad (eq.\ 3.10)$$

$$Threshold2\ [\mathrm{n}] = 0.5 \cdot Threshold1[n] \qquad (eq.\ 3.11)$$

In order to avoid False Positives (i.e. noise peaks classified as R-peaks) two temporal restrictions are applied. First, a peak cannot be found within the next 200 ms so, the algorithm does not look for a peak until this time has passed. Secondly, if a peak is found during the time interval 200-360 ms after the last detection it could be an elevated T-wave, so it is only classified as an R-peak if the maximal slope of this waveform is higher than the half of that of the previous R-peak.

3.3.3 Search-back stage

The final block stores the amplitude and position of each R-peak, and each noise peak found since the last detected R-peak. It computes the RR average of two sets of RR intervals:

- RR_{Avg1} is the average of the last 8 RR intervals
- RR_{Avg2} is the average of the last 8 intervals whose values fell in the range *RRLL* (RR low limit, *(eq. 3.12)*), *RRHL* (RR high limit, *(eq. 3.13)*).

Whenever an R-peak is not found *RRML* seconds *(eq. 3.14)* before the last detection, the maximum stored noise peak whose amplitude is higher than *Threshold2* is classified as R-peak. In this situation the signal level is adjusted using *(eq. 3.15).* The multiplicative factors used in the following equations were empirically selected by the authors.

$$RRLL = 0.92 * RR_{Avg2} \qquad \textit{(eq. 3.12)}$$

$$RRHL = 1.16 * RR_{Avg2} \qquad \textit{(eq. 3.13)}$$

$$RRML = 1.66 * RR_{Avg2} \qquad \textit{(eq. 3.14)}$$

$$SPKI = 0.25 * PeakAmplitude + 0.75 * SPKI \qquad \textit{(eq. 3.15)}$$

Where RR_{Avg2} represents the mean of the last 8 RR-intervals whose durations were in the range *RRLL-RRHL*.

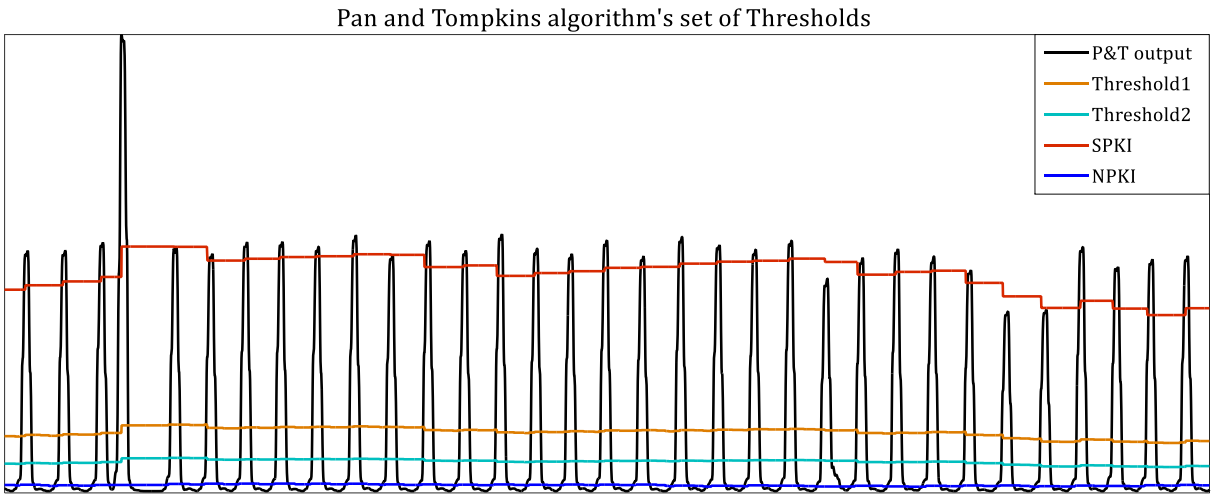

Figure 3.3-6. Example of Pan and Tompkins algorithm's Signal and noise level estimation and set of Thresholds

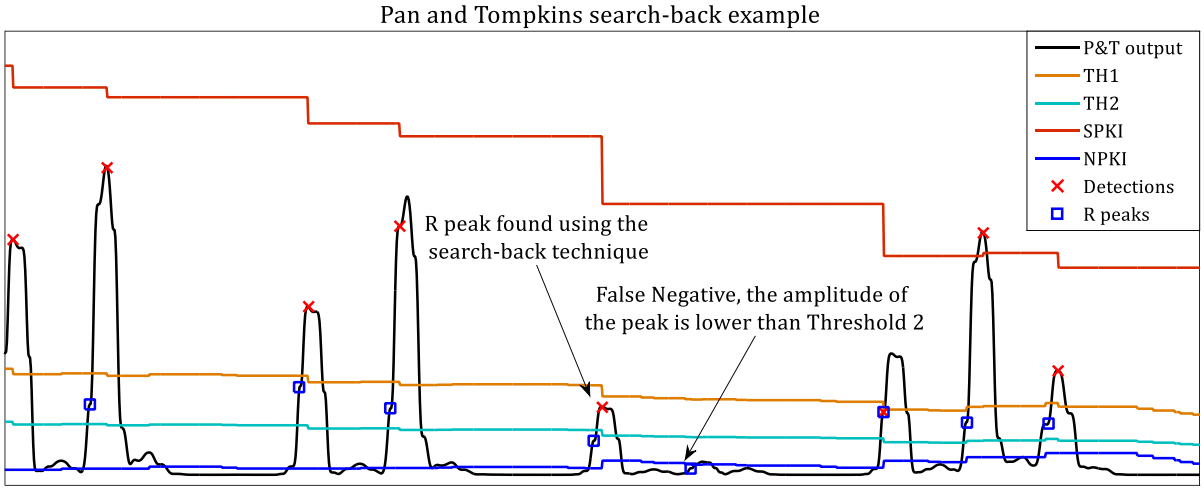

Figure 3.3-7. Search-back technique example

Figure 3.3-7 shows an example of the use of the search-back technique. In this case there are two R peaks whose amplitudes are below *Threshold1 (TH1)*. The time interval *RRML* has passed since the last detected R-peak and the amplitude of the first peak is higher than *Threshold2 (TH2)*, so it is classified as R-peak. The amplitude of the second peak is below *Threshold2* so it is not classified as R-peak, even if the conditions for applying the search-back technique are met. In this situation, the value of *SPKI* is decreased faster than when a high-amplitude R-peak is found, and so is the case of the *Threshold1* as can be observed in the Figure 3.3-7.

3.4 Proposed QRS detection algorithm

The aim is to reduce the computational complexity of the P&T algorithm, while maintaining its performance. The complexity of the P&T algorithm can be reduced in two ways: first, the pre-processing stage could be simplified by reducing the filtering stage, as well as removing the integration window; secondly, a single threshold could be used for detecting the position of the R peaks. Instead of using the Search back technique, the threshold adaptation algorithm will be designed with the goal of reducing the number of false negatives. The block diagram of the proposed algorithm is shown in Figure 3.4-1. It is composed of two main stages. The ECG signal is derived and integrated at the pre-processing stage, which is based on the Pan and Tompkins' pre-processing; then, the processed ECG samples are analysed by the R-peaks detection stage, which is based on a dynamic threshold whose level is controlled by a Finite State Machine (FSM).

Even though it is based on the P&T stages, the resources and number of operations required for the proposed algorithm are less, as will be demonstrated in this chapter. In addition, the designed algorithm can be adapted to the sampling frequency of the input ECG signal without recalculating all the parameters, which makes it able to work in different applications.

3.4.1 Pre-processing stage

Figure 3.4-2 shows the block diagram of the pre-processing stage. In order to reduce low-frequency noises, the first step of the pre-processing stage is the derivation of the input ECG signal $x[n]$ according to *(eq. 3.16)*. This process mainly reduces the wandering baseline effect produced by respiration. Then, an integration operation is carried out to remove the high-frequency artefacts from the signal $y_0[n]$, following *(eq. 3.17)*. As is shown later, the value of N is very small, so this stage is acting as a low pass filter (Moving Average) whose integration window length, N, depends on the sampling frequency F_S. Finally, in order to emphasize the R-peaks, every sample $y_1[n]$ is squared *(eq. 3.18)*. For a better understanding of the proposed algorithm, the result for every stage is represented by using the ECG record for subject 108m of the MIT-BIH Arrhythmia Database (see Figure 3.4-3).

$$y_0[n] = x[n] - x[n - N_d] \qquad \textit{(eq. 3.16)}$$

$$y_1[n] = \frac{1}{N-1}\sum_{k=0}^{N-1} y_0[n-k] \qquad \textit{(eq. 3.17)}$$

$$y[n] = y_1[n]^2 \qquad \textit{(eq. 3.18)}$$

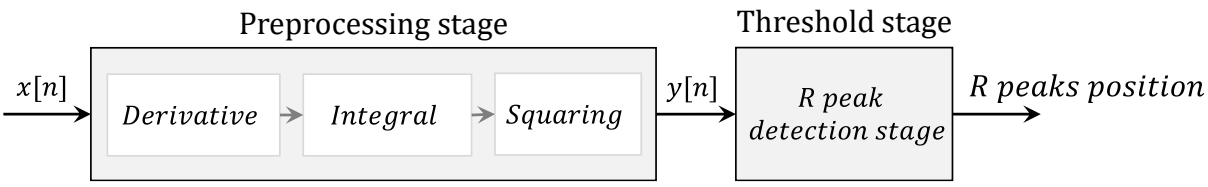

Figure 3.4-1. Block diagram of the proposed QRS complex detection algorithm

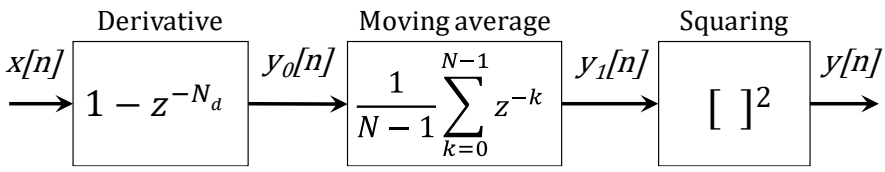

Figure 3.4-2.Block diagram of the pre-processing stage

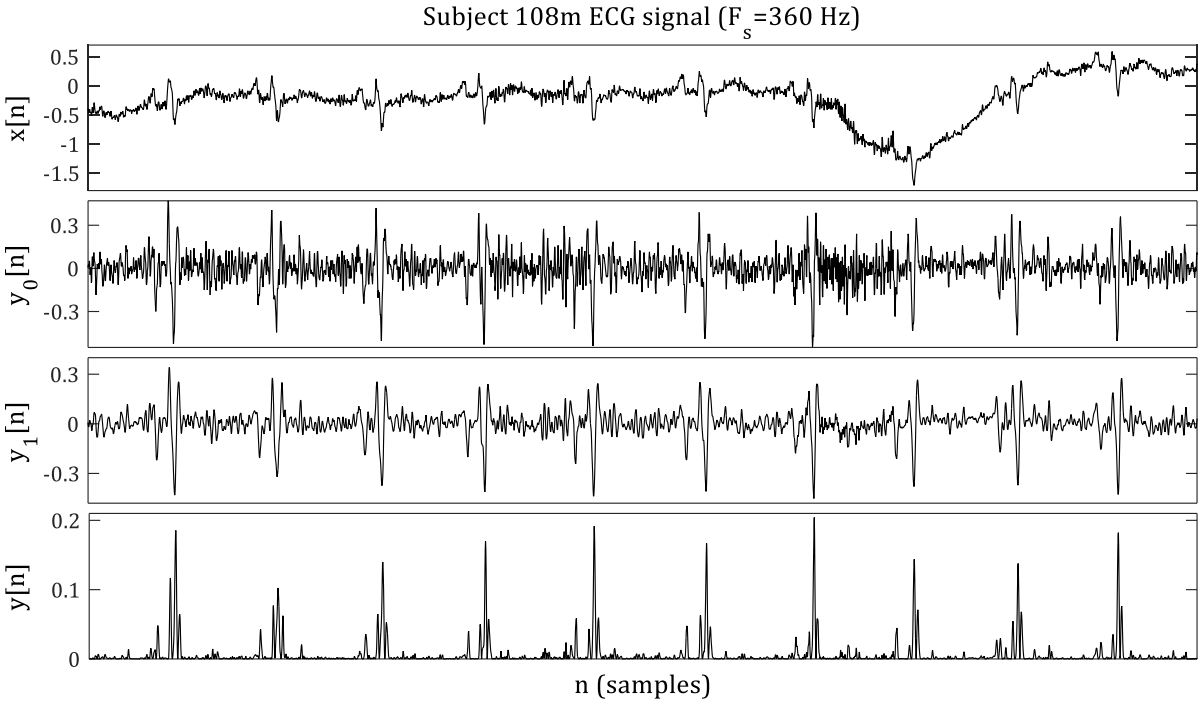

Figure 3.4-3. Pre-processing result

3.4.2 R peaks detection stage

For this stage, it is very common to use an adaptive threshold, as used by most of the recently published real-time QRS detection algorithms. This adaptation capability of the threshold is essential when the pre-processing stage cannot remove all the artefacts and mainly in those signals with large T-waves, since they could be misclassified as R-peaks. In this proposal, the threshold value is controlled by a FSM, according to the following 3 states:

- **State 1: Looking for a maximum peak**. During a time interval, equal to the minimum feasible RR interval RR_{min} plus the standard duration of a QRS complex QRS_{int} (typically 60ms), the algorithm searches for the maximum peak of the signal. It is considered here, a maximum heartrate of 300 bpm, so the minimum RR interval is set as RR_{min}=200ms. The maximum found during this state will be classified as R-peak. The machine changes to the following state when the interval $RR_{min}+QRS_{int}$ ends. At the end of this state the threshold amplitude is the mean $R_{peak}Amp$ of the amplitudes of all the R-peaks found.
- **State 2: Waiting state**. The duration of this state depends on the position $R_{peak}Pos$ where the R-peak was found in State 1. The FSM is waiting for a time equal to RR_{min} less the time between the position of the last R-peak and the end of State 1. Through it, the false detections can be avoided during the interval RR_{min} after the last peak was detected, as this is the period when a long T-wave could be misclassified as R-peak.

- **State 3: Threshold decreasing.** When State 2 finishes, the initial value of the threshold *th[n]* is computed as the mean value of all the previous detected R-peaks. In this state, the threshold value *th[n]* is reduced with every new sample from the input ECG signal *x[n]*, according to *(eq. 3.19)*. The way the threshold varies with each new sample has been chosen experimentally. The value of the parameter P_{Th} varies depending on the sampling period T_S as is explained below. This state ends when the level of the ECG signal *x[n]* is higher than the threshold value *th[n]*.

$$th[n] = th[n-1] \cdot e^{-P_{th} * T_S} \qquad \textit{(eq. 3.19)}$$

Figure 3.4-4 summarizes how the finite state machine FSM works, and Figure 3.4-5 shows the correspondence between the states of the FSM and the phase of the ECG signal.

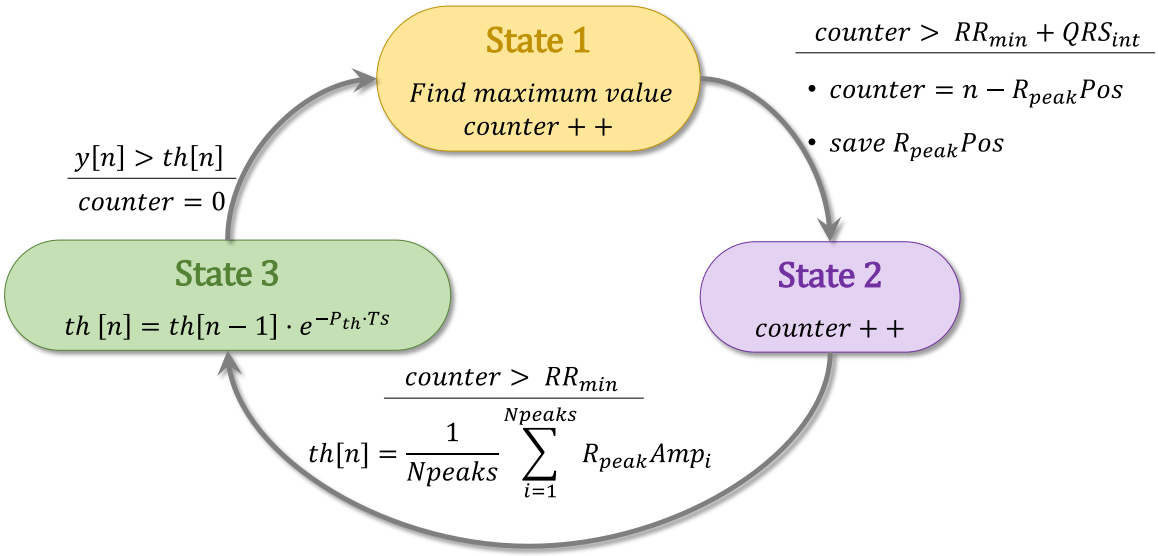

Figure 3.4-4. State machine diagram

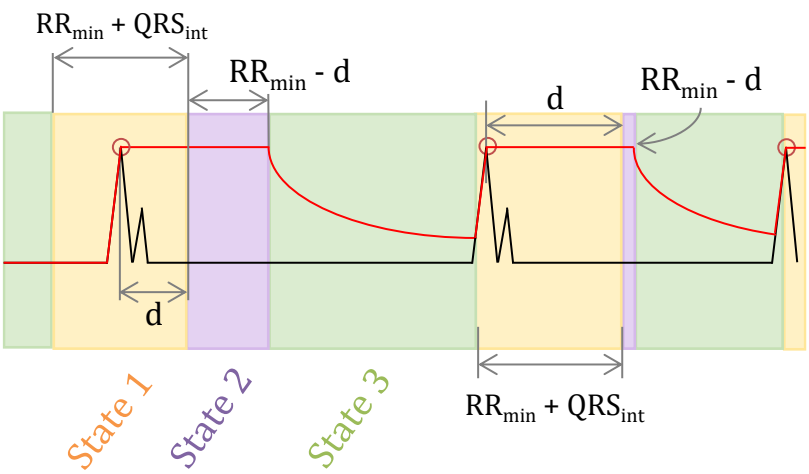

Figure 3.4-5. Correspondence between the FSM states and the ECG phase

3.4.3 Parameter selection

The proposed QRS complex detection algorithm is based on three parameters:

- Nd: represents the order of the sample that has to be subtracted from the current one
- N indicates the number of samples that are included in the integration window
- P_{Th} defines the speed with which the threshold value *th[n]* is decreased.

As these parameters depend on the sample frequency of the ECG signal, to fix their values, a sensitivity, *Se (eq. 3.1)*, and positive predictivity, *+P (eq. 3.2)*, tests have been carried using two databases: NSRDB and ADB. Signals from the first database are almost ideal, since they belong to healthy subjects and the noise is almost null. Second database has been used due to its sample frequency (256 Hz) is proportional to the one used for the NSRDB (128 Hz).

The most suitable configuration for parameters N, N_d and P_{Th} has been searched using 10 integer values for N (1 to 10), 10 integer values for N_d (1 to 10), and 21 values for P_{Th} (4.5 to 6.5 in steps of 0.1). Then, the performance was compared by using the minimum value between *Se* and *+P* (*min (Se, +P))* for each combination of these three parameters in the best achieved case. The combination with the best result for the NSRDB was N=3, N_d=2, and P_{Th}=5.4 (F_S=128Hz); whereas in the case of ADB, it was N=6; N_d=5 and P_{Th}=6.1 (F_S=256 Hz). These results are summarized in Table 3.4-1. Assuming that the parameters N, N_d and P_{Th} have a linear dependency with F_S, these parameters can be defined mathematically by *(eq. 3.20)*, *(eq. 3.21)* and *(eq. 3.22)*, respectively, by applying a linear interpolation with the sampling frequency F_S. According to these equations, the parameters for MITDB (F_S=360Hz) are obtained: N=8, N_d=7 and P_{Th}=6.6. Figure 3.4-6 shows the estimated optimal values for the parameters N, N_d, and P_{Th}, in relation with the sampling frequency F_S, for values different than 128Hz and 256Hz considered in NSRDB and ADB, respectively. Furthermore, it can be also concluded from the results how the definition of N implies a fixed time of 3/128 seconds (23.4ms), which is approximately the mean time of the R-peak slope (Figure 3.4-7), computed for the MITDB, NSRDB and ADB (24.07ms).

$$N = round\left(\frac{3 \cdot F_S}{128}\right) \qquad \textit{(eq. 3.20)}$$

$$N_d = round\left(\frac{3 \cdot F_S}{128}\right) - 1 = N - 1 \qquad \textit{(eq. 3.21)}$$

$$P_{Th} = \frac{0.7 \cdot F_S}{128} + 4.7 \qquad \textit{(eq. 3.22)}$$

TABLE 3.4-1. ADB AND NSRDB OBTAINED RESULTS

Database	N	N_d	P_{Th}	TP	FN	FP	Se (%)	+P (%)
NSRDB	3	2	5.4	192329	61	12	**99.968**	99.994
ADB	6	5	6.1	195887	1024	1421	99.380	**99.280**

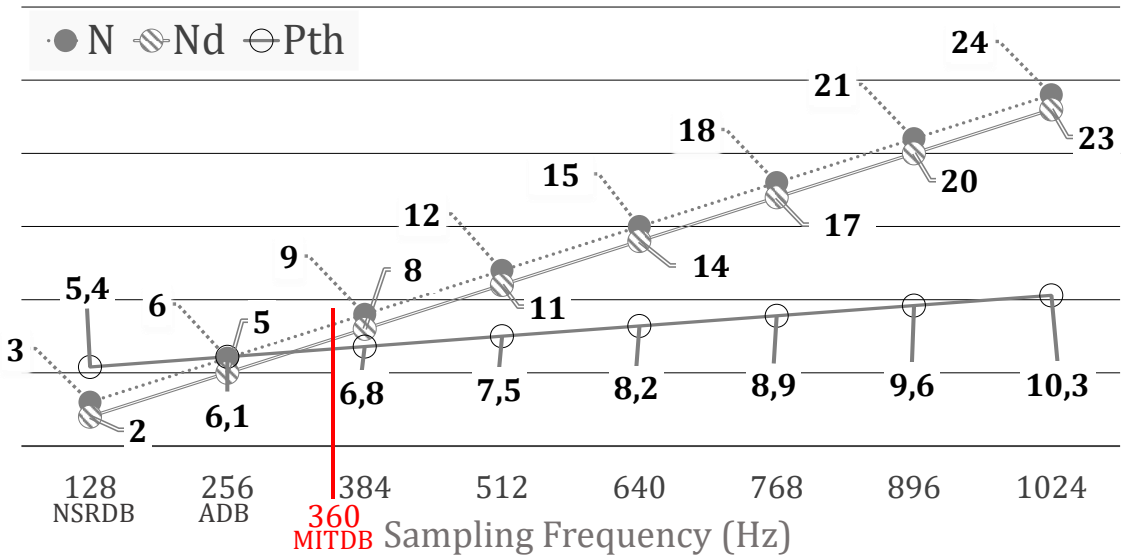

Figure 3.4-6. Proposed algorithm's parameters v. sampling frequency

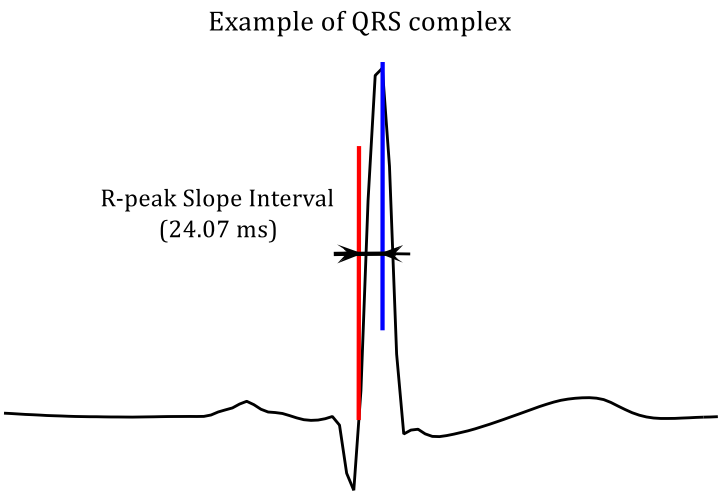

Figure 3.4-7. Definition of R-peak slope interval

3.5 QRS complex detection evaluation

As was previously stated, the proposed algorithm requires a reduced amount of hardware resources for its implementation, keeping at the same time a similar accuracy level as the most accurate algorithms currently published. Nevertheless, it is not possible to carry out a detailed comparison about the implementation or the processing time for the different approaches, since most of the previous algorithms are implemented in software.

In [KöHO02] some algorithms are compared with respect to the computational load, being classified into three categories: low, medium and high computational load. So, for the sake of a hardware and complexity evaluation of the proposed algorithm, both algorithms have been simulated on MATLAB® and tested with the available data. Floating-point and fixed point representations were used. Both simulations were performed analysing the ECG samples one-by-one, following the same steps as if it was working in real-time, i.e. by using the same sequential processes and operations as if it was running on a portable device.

3.5.1 Accuracy evaluation using floating-point representation

The use of any QRS complex detector algorithm in medical devices requires a rigorous evaluation of its performance. Table 3.5-1 shows the results obtained by the proposed algorithm with all the records of the MITDB database, where the average values are *Se*=99.73% and *+P*=99.77%; results obtained by the P&T algorithm implementation for the same database are shown in Table 3.5-2. Here the average results are *Se*= 99.53%, and *+P*=99.29%. Subjects 100 m and 108m represent how the two algorithms work with a normal ECG signal, and with a ECG presenting special features, respectively. Both examples are analysed below.

As can be noticed by the reader, there is a slightly difference between the results obtained here using the P&T algorithm and the ones reported by the authors on their publication (*Se*=99.75%; *+P*=99.54%). Although the P&T's detection stage has been implemented following the steps indicated in the original work, some of the details are not given (e.g. the initial value of the threshold, criteria to find a peak, etc.) and some assumptions have been made resulting in such a difference.

TABLE 3.5-1. RESULTS OF THE PROPOSED QRS DETECTION ALGORITHM WITH THE MITDB

ID	# Annotation	TP	FN	FP	S_e (%)	+P (%)	min (S_e, +P)
100m	2272	2272	0	0	100,00	100,00	100,00
101m	1866	1865	1	3	99,946	99,839	99,839
102m	2187	2187	0	0	100,00	100,00	100,00
103m	2084	2084	0	0	100,00	100,00	100,00
104m	2228	2228	0	27	100,00	98,803	98,803
105m	2573	2561	12	36	99,534	98,614	98,614
106m	2027	2025	2	0	99,901	100,00	99,901
107m	2138	2135	3	0	99,860	100,00	99,860
108m	1763	1735	28	72	98,412	96,015	96,015
109m	2531	2531	0	0	100,00	100,00	100,00
111m	2125	2124	1	0	99,953	100,00	99,953
112m	2539	2539	0	0	100,00	100,00	100,00
113m	1795	1795	0	0	100,00	100,00	100,00
114m	1880	1880	0	4	100,00	99,788	99,788
115m	1953	1953	0	0	100,00	100,00	100,00
116m	2391	2386	5	4	99,791	99,833	99,791
117m	1534	1534	0	0	100,00	100,00	100,00
118m	2278	2278	0	0	100,00	100,00	100,00
119m	1987	1987	0	0	100,00	100,00	100,00
121m	1864	1863	1	1	99,946	99,946	99,946
122m	2476	2476	0	0	100,00	100,00	100,00
123m	1519	1516	3	0	99,803	100,00	99,803
124m	1620	1619	1	0	99,938	100,00	99,938
200m	2598	2597	1	1	99,962	99,962	99,962
201m	1962	1945	17	0	99,134	100,00	99,134
202m	2136	2130	6	0	99,719	100,00	99,719
203m	2980	2883	97	21	96,745	99,277	96,745
205m	2656	2652	4	0	99,849	100,00	99,849
207m	1842	1840	2	10	99,891	99,459	99,459
208m	2954	2939	15	1	99,492	99,966	99,492
209m	3005	3005	0	0	100,00	100,00	100,00
210m	2650	2587	63	3	97,623	99,884	97,623
212m	2747	2747	0	0	100,00	100,00	100,00
213m	3250	3247	3	0	99,908	100,00	99,908
214m	2262	2259	3	1	99,867	99,956	99,867
215m	3363	3358	5	0	99,851	100,00	99,851
217m	2208	2202	6	1	99,728	99,955	99,728
219m	2154	2154	0	0	100,00	100,00	100,00
220m	2048	2048	0	0	100,00	100,00	100,00
221m	2427	2424	3	0	99,876	100,00	99,876
222m	2483	2482	1	0	99,960	100,00	99,960
223m	2605	2604	1	0	99,962	100,00	99,962
228m	2053	2050	3	62	99,854	97,064	97,064
230m	2256	2256	0	0	100,00	100,00	100,00
231m	1571	1571	0	0	100,00	100,00	100,00
232m	1780	1780	0	0	100,00	100,00	100,00
233m	3078	3072	6	0	99,805	100,00	99,805
234m	2753	2752	1	0	99,964	100,00	99,964
Average	**109451**	**109157**	**294**	**247**	99,731	99,774	99,731

TABLE 3.5-2. RESULTS OF THE PAN & TOMPKINS ALGORITHM WITH THE MITDB

ID	#Annotations	TP	FN	FP	S_e (%)	+P (%)	min (S_e, +P)
100m	2268	2268	0	0	100,00	100,00	100,00
101m	1862	1860	2	5	99,893	99,732	99,732
102m	2183	2183	0	2	100,00	99,908	99,908
103m	2080	2079	1	0	99,952	100,00	99,952
104m	2225	2220	5	5	99,775	99,775	99,775
105m	2568	2549	19	59	99,260	97,738	97,738
106m	2024	2022	2	0	99,901	100,00	99,901
107m	2133	2125	8	1	99,625	99,953	99,625
108m	1760	1712	48	254	97,273	87,080	87,080
109m	2527	2526	1	0	99,960	100,00	99,960
111m	2121	2120	1	2	99,953	99,906	99,906
112m	2535	2535	0	0	100,00	100,00	100,00
113m	1791	1791	0	1	100,00	99,944	99,944
114m	1877	1860	17	95	99,094	95,141	95,141
115m	1950	1950	0	0	100,00	100,00	100,00
116m	2387	2382	5	5	99,791	99,791	99,791
117m	1532	1527	5	21	99,674	98,643	98,643
118m	2274	2274	0	0	100,00	100,00	100,00
119m	1983	1983	0	0	100,00	100,00	100,00
121m	1860	1859	1	0	99,946	100,00	99,946
122m	2471	2470	1	1	99,960	99,960	99,960
123m	1515	1515	0	0	100,00	100,00	100,00
124m	1617	1616	1	2	99,938	99,876	99,876
200m	2594	2593	1	1	99,961	99,961	99,961
201m	1957	1946	11	167	99,438	92,097	92,097
202m	2133	2125	8	3	99,625	99,859	99,625
203m	2975	2838	137	20	95,395	99,300	95,395
205m	2651	2641	10	0	99,623	100,00	99,623
207m	1838	1837	1	6	99,946	99,674	99,674
208m	2950	2931	19	5	99,356	99,830	99,356
209m	3000	2993	7	3	99,767	99,900	99,767
210m	2644	2602	42	2	98,411	99,923	98,411
212m	2742	2742	0	0	100,00	100,00	100,00
213m	3244	3243	1	0	99,969	100,00	99,969
214m	2258	2254	4	1	99,823	99,956	99,823
215m	3357	3353	4	0	99,881	100,00	99,881
217m	2204	2199	5	1	99,773	99,955	99,773
219m	2150	2150	0	2	100,00	99,907	99,907
220m	2044	2044	0	0	100,00	100,00	100,00
221m	2422	2418	4	0	99,835	100,00	99,835
222m	2479	2351	128	103	94,837	95,803	94,837
223m	2601	2600	1	0	99,962	100,00	99,962
228m	2049	2038	11	8	99,463	99,609	99,463
230m	2252	2252	0	0	100,00	100,00	100,00
231m	1567	1567	0	2	100,00	99,873	99,873
232m	1777	1776	1	3	99,944	99,831	99,831
233m	3073	3071	2	0	99,935	100,00	99,935
234m	2748	2748	0	0	100,00	100,00	100,00
Average	**109252**	**108738**	**514**	**780**	**99,530**	**99,288**	**99,288**

Table 3.5-3 and Table 3.5-4 shows a comparison among the results obtained by some works previously described using all or some, respectively, of the ECG signals of the MITDB; These tables are sorted by the minimum value between *Se* and *+P*, which is the most common way to compare QRS complex detection algorithms. As can be observed, the accuracy of the proposed algorithm is in the range of the other previous works, it should be noted than the first two references of the table published the results based on less than 50% of the signals within the MITDB. The first algorithm of the database, is a "pseudo-real-time" improvement of the other proposal published in the same work (which is in the 9th row of the table) consisting of a technique similar to the searchback proposed by P&T.

TABLE 3.5-3. COMPARISON OF ACCURACY RESULTS FOR SOME PROPOSALS WITH THE FULL MITDB DATABASES

Authors	***Proposed algorithm***		***Results***			***Database***
	Pre-processing stage	***Detection stage***	***Se***	***+P***	***Min***	
Christov alg II [Chri04], *(2004)*	Moving averaging filter	3 Dynamic thresholds	99,78	99,78	**99,78**	Full MITDB
Proposed	**Differentiation**	**Dynamic threshold**	**99,73**	**99,77**	**99,73**	**Full MITDB**
Ghaffari et al. [GhGG08], *(2008)*	Wavelet	Dynamic threshold	99,91	99,72	**99,72**	Full MITDB
Zidelmal et al. [ZAAB12], *(2012)*	Wavelet	Dynamic threshold	99,64	99,82	**99,64**	Full MITDB
Adnane et al. [AdJC09], *(2009)*	Differentiation	3 dynamic thresholds	99,77	99,64	**99,64**	Full MITDB
Phyu et al. [PZZX09], *(2009)*	Wavelet	Dynamic threshold	99,63	99,89	**99,63**	Full MITDB
Nielsen et al. [NEBA12], *(2012)*	Wavelet	Dynamic threshold	99,63	99,63	**99,63**	Full MITDB
Zheng et al. [ZhWu08], *(2008)*	Wavelet	Dynamic threshold	99,68	99,59	**99,59**	Full MITDB
Christov alg I [Chri04], *(2004)*	Moving averaging filter	3 dynamic thresholds + Searchback technique	99,56	99,76	**99,56**	Full MITDB
Pan & Tomp. [PaTo85], (1985)	**Differentiation**	**2 dynamic thresholds**	**99,56**	**99,76**	**99,56**	**Full MITDB**
Chen et al. [ChCC06], *(2006)*	Wavelet	Dynamic threshold	99,55	99,49	**99,49**	45 signals of MITDB
Ieong et al. [IMLD12], *(2012)*	Wavelet	Dynamic threshold	99,31	99,70	**99,31**	Full MITDB
Moraes et al. [MFVC02], *(2002)*	Differentiation	2 dynamic thresholds	99,22	99,73	**99,22**	Full MITDB
Laila et al. [AhMA12], *(2012)*	Wavelet + Hilbert	Dynamic threshold	96,30	97,83	**96,3**	Full MITDB

TABLE 3.5-4. COMPARISON OF ACCURACY RESULTS FOR SOME PROPOSALS WITH SEVERAL SIGNALS OF THE MITDB DATABASES

Authors	***Proposed algorithm***		***Results***			***Database***
	Pre-processing stage	***Detection stage***	***Se***	***+P***	***Min***	
Pal et al. [PaMi12], *(2012)*	EMD	Morphological analysis	99,88	99,96	**99,88**	21 signals of MITDB
Das et al. [KhBJ13], *(2013)*	EMD + Wavelet	Dynamic threshold	99,81	99,96	**99,81**	17 signals of MITDB
Chen et al. [ChCC06], *(2006)*	Wavelet	Dynamic threshold	99,55	99,49	**99,49**	45 signals of MITDB

Finally, both P&T and the proposed algorithm have been tested over the rest of the databases, in order to compare both performances, Table 3.5-4 depicts the results. With the NRSDB, both algorithms get *Se* and *+P* close to 100%. With the Allergy database, which is composed of 24 ECG signals with a high level of noise, both algorithms get the worst performance: *min(Se,+P)*=98.327% with P&T and 99.28% with the proposed algorithm. With the other three databases, the results are slightly better with the proposed algorithm than with the P&T. Apart from its results, it should be taken into consideration that the main advantage of the proposed algorithm is the reduced number of resources used to analyse the ECG signals.

As is explained above, the worst performance of both algorithms is obtained with the Allergy database, since the ECG signals are corrupted with lots of movement artefacts. Figure 3.5-1 shows an example of the effect that these artefacts can cause to the ECG signal. It can be observed that it is difficult to find the position of the R peaks even visually. Even with this drawback, the mean sensitivity of the proposed algorithm is 99.48% and the positive predictivity is 99.28%. With P&T sensitivity is 98.33%, and 98.54%.

TABLE 3.5-5. COMPARISON BETWEEN P&T AND PROPOSED ALGORITHM PERFORMANCES OVER ALL THE DATABASES

Database	Algorithm	#Ann	TP	FN	FP	S_e (%)	+P (%)	min (S_e,+P)
NSRDB	P&T	192314	192271	43	25	99,978	99,987	99,978
	Proposed	192390	192329	61	12	99,968	99,994	99,968
ADB	P&T	196806	193514	3292	2870	98,327	98,539	98,327
	Proposed	196911	195887	1024	1421	99,480	99,280	99,280
Fantasia	P&T	79380	79375	5	317	99,994	99,602	99,602
	Proposed	79445	79436	9	48	99,989	99,940	99,940
ApneaDB	P&T	761351	760846	505	4724	99,934	99,383	99,383
	Proposed	761593	760813	780	1838	99,898	99,759	99,759
Challenge	P&T	72026	71992	34	161	99,953	99,777	99,777
	Proposed	72277	72230	47	111	99,935	99,847	99,847

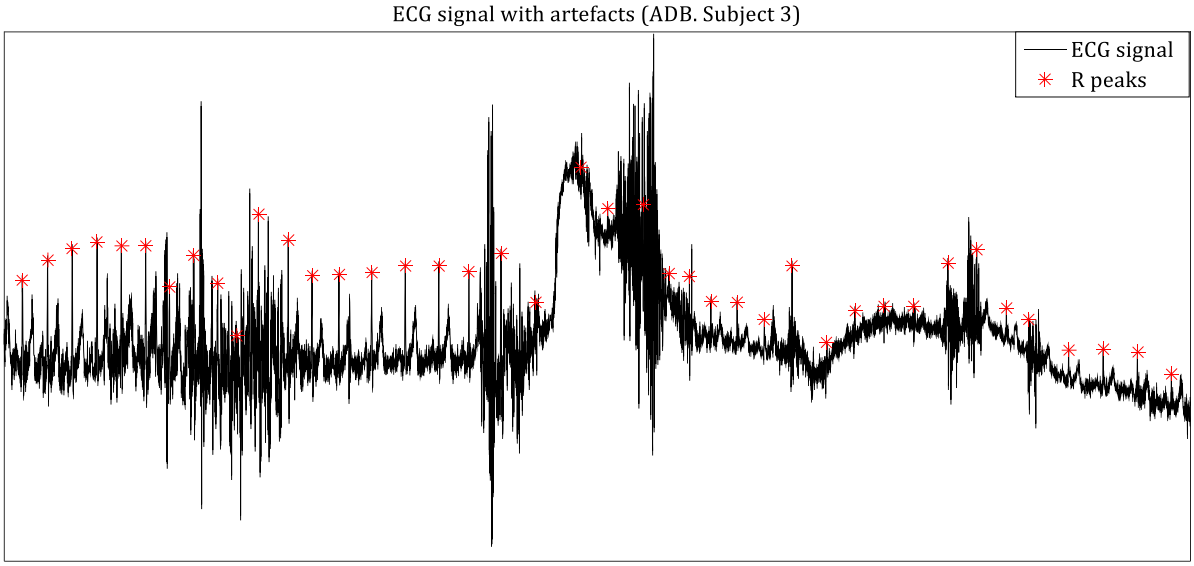

Figure 3.5-1. Example of ECG signal, x [n], with motion artefacts. Subject 3 of the ADB database

To conclude with the comparison, Figures 3.5-2 to 3.5-5 show the detection results for two different ECG segments of both algorithms. The signals are taken from records no. 100 and no. 108 of the MITDB, commonly used for showing the difference between a clear ECG signal (record no. 100) and a very difficult one (record no. 108). These results show again a better detection by the proposed algorithm, especially with noisy recordings (see Figure 3.5-4). On the other hand, P&T's algorithm integrates the samples to obtain the final trapezoid in which the R peaks are detected. In the cases in which the number of noise peaks is high this integration fuses all of them, so, the resulting signal gets trapezoids produced by noise peaks which are misclassified as R peaks. In other cases, if the QRS complex is too wide (as in the case of the 108m subject, see Figure 3.5-4), the pre-processing stage generates two trapezoids for each QRS complex. This implies one False Positive for each wide-QRS-complex, which decreases drastically the positive predictivity.

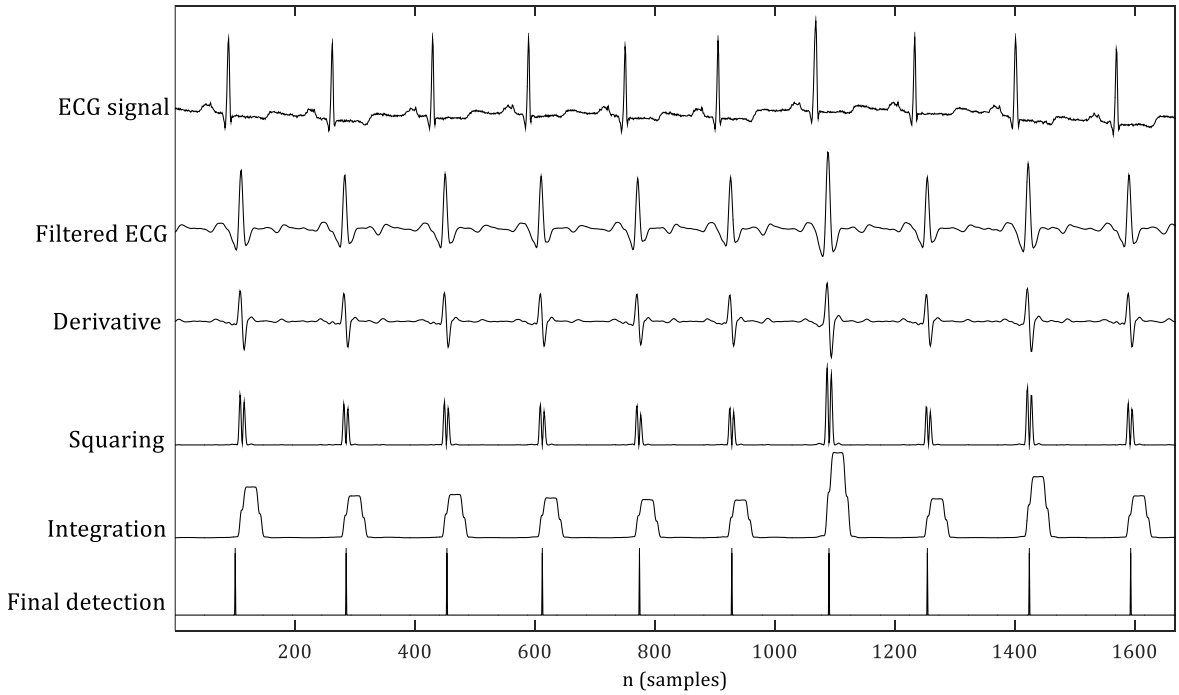

Figure 3.5-2. Pan & Tompkins. QRS complex detection for record no. 100 (Se=100%; +P=100%; FS=200 Hz)

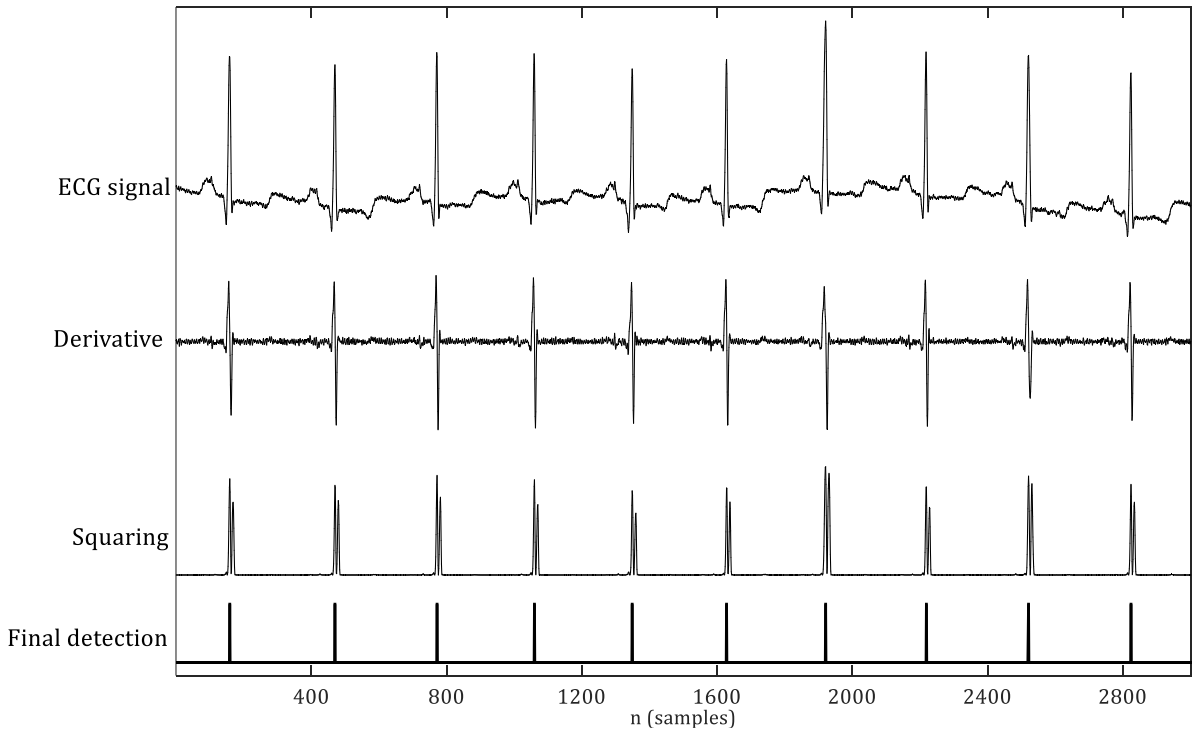

Figure 3.5-3. Proposed algorithm. QRS complex detection for record no. 100 (Se=100 %; +P=100 %; FS=360 Hz)

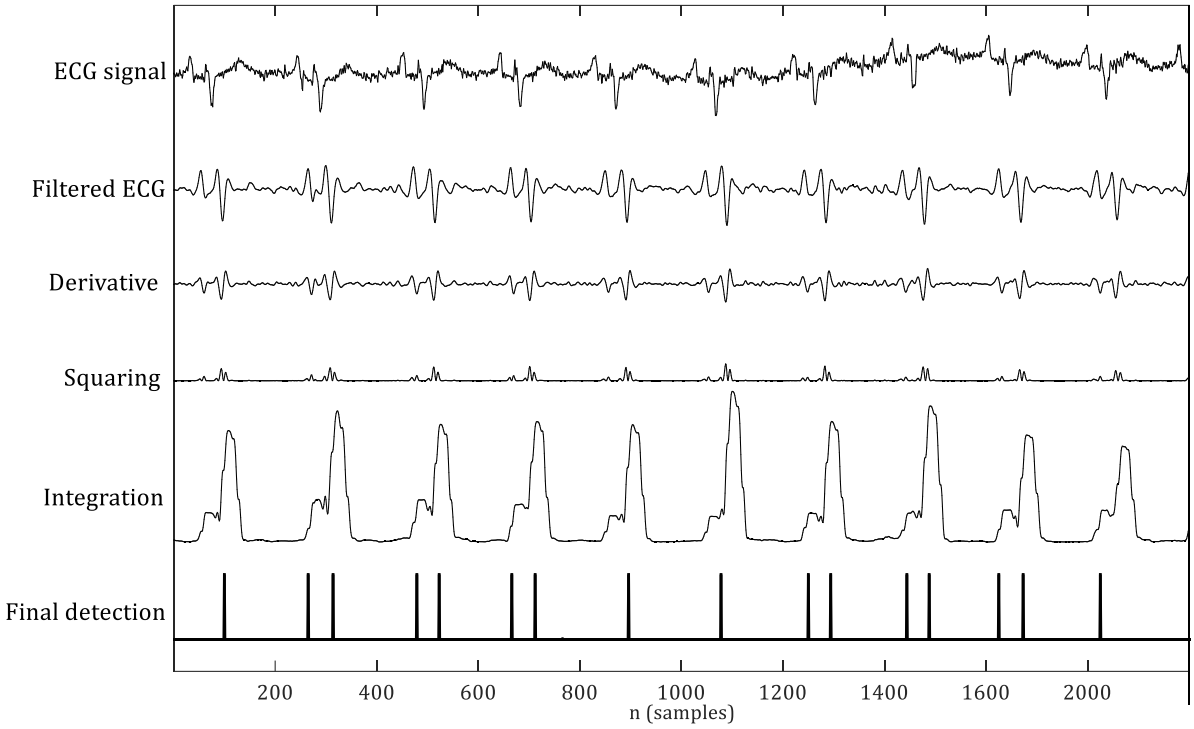

Figure 3.5-4. Pan % Tompkins. QRS complex detection for record no. 108 (Se=98.525 %; +P=88.083 %; FS=200 Hz)

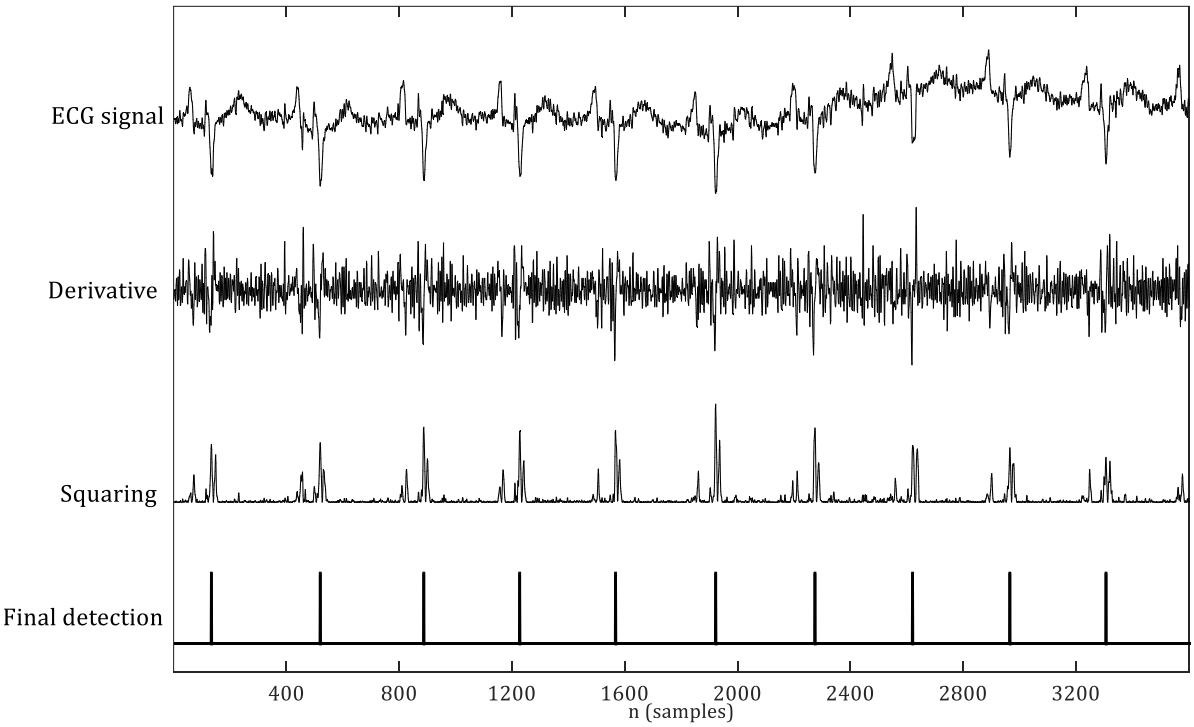

Figure 3.5-5. Proposed algorithm. QRS complex detection for record no. 108 (Se=98.411 %; +P=95.96 %; FS=360 %)

3.5.2 Accuracy evaluation using fixed-point representation

In a real-platform all the data, factors and calculations are made using a fixed-point arithmetic. This change of the representation can provoke a reduction of the original accuracy due to the loss of precision which produces a quantization error (difference between the real and the converted value). Table 3.5-8 lists the quantization error, related to the original value of the samples, of each signal involved in the QRS complex detection for the proposed algorithm, and Table 3.5-9, for the P&T.

Table 3.5-6 and Table 3.5-7 list the results obtained in MATLAB analyzing the MITDB with the fixed-point version of both algorithms. Sensitivity of the new QRS complex detection algorithm has been decreased from 99.731% to 99.638%; and the positive predictivity has been increased from 99.774% to 99.777%. The number of cases in which the *min(Se, +P)* is higher than 99.8% has been decreased from 35 to 34 and the worst performance is obtained again with the subject 108m, in which case *min(Se, +P)* is 95.962%. In the case of the Pan & Tompkins algorithm, the sensitivity has been increased from 99.568% to 99.658%; and the positive predictivity from 99.327% to 99.345%. The number of cases in which the *min(Se, +P)* is higher than 99.8% is the same, 29; finally, the worst performance has been increased from 87.085 to 87.56%.

Considering the obtained results, it has been considered that the differences between both versions are small enough to consider their effect negligible.

3.5.3 Computational complexity evaluation

The resources required for each algorithm have been estimated by reckoning the mean number of additions and multiplications they need to analyse each sample, and the total number of memory cells used to store the variables used.

First part of Table 3.5-10 shows the results for the performance of both algorithms and the resources required for their implementation. The new algorithm uses less than 25% of the memory cells, 30% of the multipliers, and 12% of the adders used by P&Ts. Another analysed complexity parameter is the number of operations per second (comparisons, additions and multiplications). For the computation of these parameters, all the operations have been made for the 48 30-minutes ECG signals of the MITDB.

TABLE 3.5-6. RESULTS OF THE FIXED-POINT VERSION OF THE PROPOSED QRS DETECTION ALGORITHM WITH THE MITDB

ID	# Annotation	TP	FN	FP	S_e (%)	+P (%)	min (S_e, +P)
100m	2271	2271	0	0	100,00	100,00	100,00
101m	1865	1864	1	3	99,946	99,839	99,839
102m	2186	2186	0	0	100,00	100,00	100,00
103m	2083	2083	0	0	100,00	100,00	100,00
104m	2228	2228	0	20	100,00	99,110	99,110
105m	2572	2556	16	37	99,378	98,573	98,573
106m	2026	2019	7	0	99,654	100,00	99,654
107m	2137	2135	2	0	99,906	100,00	99,906
108m	1774	1735	39	73	97,802	95,962	95,962
109m	2531	2530	1	0	99,960	100,00	99,960
111m	2124	2123	1	0	99,953	100,00	99,953
112m	2539	2539	0	0	100,00	100,00	100,00
113m	1794	1794	0	0	100,00	100,00	100,00
114m	1879	1879	0	2	100,00	99,894	99,894
115m	1952	1951	1	0	99,949	100,00	99,949
116m	2391	2386	5	4	99,791	99,833	99,791
117m	1534	1534	0	0	100,00	100,00	100,00
118m	2278	2278	0	0	100,00	100,00	100,00
119m	1986	1986	0	0	100,00	100,00	100,00
121m	1863	1862	1	1	99,946	99,946	99,946
122m	2476	2476	0	0	100,00	100,00	100,00
123m	1518	1515	3	0	99,802	100,00	99,802
124m	1620	1619	1	0	99,938	100,00	99,938
200m	2597	2596	1	1	99,961	99,961	99,961
201m	1999	1934	65	0	96,748	100,00	96,748
202m	2135	2129	6	0	99,719	100,00	99,719
203m	2979	2867	112	24	96,240	99,170	96,240
205m	2655	2651	4	0	99,849	100,00	99,849
207m	1841	1839	2	9	99.891	99,513	99,513
208m	2953	2937	16	1	99,458	99,966	99,458
209m	3004	3004	0	0	100,00	100,00	100,00
210m	2648	2578	70	4	97,356	99,845	97,356
212m	2746	2746	0	0	100,00	100,00	100,00
213m	3249	3244	5	0	99,846	100,00	99,846
214m	2261	2258	3	1	99,867	99,956	99,867
215m	3362	3357	5	0	99,851	100,00	99,851
217m	2207	2201	6	1	99,728	99,955	99,728
219m	2153	2153	0	0	100,00	100,00	100,00
220m	2047	2047	0	0	100,00	100,00	100,00
221m	2426	2420	6	0	99,753	100,00	99,753
222m	2482	2480	2	0	99,919	100,00	99,919
223m	2604	2601	3	0	99,885	100,00	99,885
228m	2052	2048	4	62	99,805	97,062	97,062
230m	2255	2255	0	0	100,00	100,00	100,00
231m	1570	1570	0	0	100,00	100,00	100,00
232m	1779	1779	0	0	100,00	100,00	100,00
233m	3077	3071	6	0	99,805	100,00	99,805
234m	2752	2750	2	0	99,927	100,00	99,927
Total	**109459**	**109063**	**396**	**244**	**99,638**	**99,777**	**99,638**

TABLE 3.5-7. RESULTS OF THE FIXED-POINT VERSION OF THE P&T ALGORITHM WITH THE MITDB

ID	#Annotations	TP	FN	FP	S_e (%)	+P (%)	min (S_e, +P)
100m	2268	2268	0	0	100,00	100,00	100,00
101m	1862	1861	1	1	99,946	99,946	99,946
102m	2183	2183	0	2	100,00	99,908	99,908
103m	2080	2079	1	1	99,952	99,952	99,952
104m	2225	2222	3	2	99,865	99,910	99,865
105m	2568	2550	18	61	99,299	97,664	97,664
106m	2024	2022	2	1	99,901	99,951	99,901
107m	2133	2127	6	1	99,719	99,953	99,719
108m	1760	1718	42	244	97,614	87,564	87,564
109m	2527	2526	1	0	99,960	100,00	99,960
111m	2121	2120	1	2	99,953	99,906	99,906
112m	2535	2535	0	0	100,00	100,00	100,00
113m	1791	1791	0	3	100,00	99,833	99,833
114m	1877	1860	17	108	99,094	94,512	94,512
115m	1950	1950	0	0	100,00	100,00	100,00
116m	2388	2383	5	5	99,791	99,791	99,791
117m	1532	1532	0	19	100,00	98,775	98,775
118m	2274	2274	0	0	100,00	100,00	100,00
119m	1983	1983	0	47	100,00	97,685	97,685
121m	1860	1858	2	0	99,892	100,00	99,892
122m	2471	2470	1	1	99,960	99,960	99,960
123m	1515	1515	0	0	100,00	100,00	100,00
124m	1617	1616	1	0	99,938	100,00	99,938
200m	2594	2593	1	1	99,961	99,961	99,961
201m	1957	1945	12	138	99,387	93,375	93,375
202m	2133	2128	5	5	99,766	99,766	99,766
203m	2975	2837	138	21	95,361	99,265	95,361
205m	2651	2641	10	1	99,623	99,962	99,623
207m	1838	1838	0	6	100,00	99,675	99,675
208m	2950	2931	19	5	99,356	99,830	99,356
209m	3000	2993	7	5	99,767	99,833	99,767
210m	2644	2618	26	2	99,017	99,924	99,017
212m	2743	2743	0	0	100,00	100,00	100,00
213m	3244	3243	1	0	99,969	100,00	99,969
214m	2258	2255	3	1	99,867	99,956	99,867
215m	3357	3354	3	0	99,911	100,00	99,911
217m	2204	2201	3	1	99,864	99,955	99,864
219m	2150	2150	0	0	100,00	100,00	100,00
220m	2044	2044	0	0	100,00	100,00	100,00
221m	2422	2420	2	1	99,917	99,959	99,917
222m	2479	2448	31	16	98,749	99,351	98,749
223m	2601	2600	1	0	99,962	100,00	99,962
228m	2049	2041	8	11	99,610	99,464	99,464
230m	2252	2252	0	0	100,00	100,00	100,00
231m	1567	1567	0	0	100,00	100,00	100,00
232m	1777	1776	1	6	99,944	99,663	99,663
233m	3073	3071	2	0	99,935	100,00	99,935
234m	2748	2748	0	0	100,00	100,00	100,00
Total	**109254**	**108880**	**374**	**718**	**99,658**	**99,345**	**99,345**

TABLE 3.5-8. RELATIVE ERROR COMPUTATION FOR THE DIFFERENT SIGNALS INVOLVED IN THE QRS COMPLEX DETECTION ALGORITHM

Signal	Mean relative error	Standard deviation of the relative error	Maximum relative error
Input (ECG), *x[n]*	$2.3608 \cdot 10^{-4}$	$3.1043 \cdot 10^{-4}$	$1.0558 \cdot 10^{-2}$
Derivative signal, *y_0[n]*	$4.2761 \cdot 10^{-5}$	$6.6965 \cdot 10^{-3}$	$1.4907 \cdot 10^{-2}$
Integrate signal, *y_1[n]*	$5.1197 \cdot 10^{-4}$	$8.4625 \cdot 10^{-4}$	$3.5833 \cdot 10^{-3}$
Pre-processed signal, *y[n]*	$9.3762 \cdot 10^{-2}$	0.1231	0.4994
Threshold, *Th[n]*	$1.2186 \cdot 10^{-2}$	$8.4823 \cdot 10^{-2}$	0.679

TABLE 3.5-9. RELATIVE ERROR COMPUTATION FOR THE DIFFERENT SIGNALS INVOLVED IN THE P&T QRS DETECTION

Signal	Mean relative error	Standard deviation of the relative error	Maximum relative error
Input (ECG), *x[n]*	$3.3228 \cdot 10^{-4}$	$1.9249 \cdot 10^{-4}$	$1.2541 \cdot 10^{-3}$
Output of the LPF, *y[n]*	$4.4856 \cdot 10^{-4}$	$4.4554 \cdot 10^{-2}$	4.9488
Output of the HPF, *p[n]*	$1.4128 \cdot 10^{-3}$	$2.6829 \cdot 10^{-2}$	0.25
Derivative and squared, *s[n]*	$3.8523 \cdot 10^{-3}$	$2.5616 \cdot 10^{-2}$	0.1936
Output of the preprocessing stage, *z[n]*	$7.4512 \cdot 10^{-3}$	$1.2715 \cdot 10^{-2}$	0.1257
Threshold1, TH1[n]	$8.4942 \cdot 10^{-3}$	$1.6835 \cdot 10^{-2}$	0.1336
Threshold2, TH2[n]	$8.6038 \cdot 10^{-3}$	$1.6835 \cdot 10^{-2}$	0.1336

As can be seen in the second part of the Table 3.5-10, the proposed algorithm makes 1.5 comparisons, similar number of multiplications and less than the 50% of multiplications of the P&T, reducing the total number of operations to 80%. It should be noted that P&T's algorithm was designed to work at a fixed sampling rate F_S=200Hz and so, the order of the filters, value of the coefficients and length of the windows were defined for this frequency; whereas the parameters of proposed one are adjusted automatically to the input sample frequency without changing the resource consumption.

The last part of Table 3.5-10 shows the mean total number of operations each algorithm should perform for getting the value of each sample. It can be seen that the proposed algorithm needs 50% of the total number of operations needed by P&T. This implies that the proposed algorithm needs half of the processing time than P&T's to carry out the same analysis, letting the processor free to perform other tasks.

TABLE 3.5-10. COMPLEXITY ANALYSIS RESULTS OBTAINED BY BOTH ALGORITHMS

Analysis		P&T	Proposed
Resources	Memory cells	123	28
	Multipliers	18	6
	Adders	41	5
Operations / sec.	Comparisons	1416	2163
	Multiplications	1201	1107
	Additions	2817	1205
	Total operations	5434	4475
Operations/sample	Comparisons	7.08	6.01
	Multiplications	6.01	3.08
	Additions	14.09	3.35
	Total operations	27.17	12.43

3.5.4 Fixed point implementation

The fixed point implementation of the proposed algorithm has been implemented in a Xilinx XC7Z010 FPGA [Xili14] using VHDL language. The details of this implementation can be found in **Appendix B**. The resources used to get the real version of the proposed algorithm are listed in Table 3.5-11. The obtained results are similar to those obtained with fixed-point version implemented in MATLAB, as summarized in Table 3.5-12, which validates the real implementation.

TABLE 3.5-11. RESOURCE CONSUMPTION OF THE PROPOSED SYSTEM IN A ZYNQ XC7Z010 FPGA

Resource	Low-level peripheral	High-level peripheral	Global system
DSP48E1	6	0	6 (7%)
RAMB	10	0	17 (10%)
Slices	817	276	2366 (53%)

TABLE 3.5-12. COMPARISON BETWEEN THE RESULTS OBTAINED WITH THE FLOATING-POINT VERSION OF THE PROPOSED QRS COMPLEX DETECTION ALGORITHM AND WITH THE PROPOSED SOC ARCHITECTURE

Parameters	Floating-point version	Fixed-point SoC version
R-Peaks	109451	109948
TP	109157	109391
FN	294	557
FP	247	248
Se	99.731	99.493
P+	99.774	99.774

3.6 Conclusions

A great number of QRS complex detection algorithms have been proposed over the last three decades. Those algorithms have evolved thanks to the new capabilities that technology offers. This evolution has led to a significant improvement in the obtained performance, achieving precisions near 100%. Nevertheless, regarding the remote monitoring of patients, these detectors may become unsuitable due to the lack of resources and computational capabilities. The growing interest on continuous-remote monitoring systems (either for clinical or personal applications), makes necessary the development of efficient algorithms capable to work on portable devices, usually with limited hardware resources.

A very low-complexity QRS complex detector has been proposed, suitable for wearable systems or for its use in telemedicine or remote monitoring systems. In spite of its low complexity, taking into account all the ECG signals previously analysed, it achieves a mean sensitivity of Se=99.843% and a mean specificity of 99.740%, reaching a performance comparable to other proposals. In addition, the algorithm can be tuned online to different sampling rates by changing the value of 3 parameters without increasing the resources needed. The pre-processing block of the algorithm is mainly based on a differentiation to reduce the low-frequency noises and on an integration to smooth the ECG signal. The detection stage is based on a single dynamic threshold, whose value is controlled by a finite state machine.

The behaviour of the algorithm has been tested in mixed conditions, through the cases provided by several databases with ECG signal belonging to patients with assorted features (age, gender, health condition), affected by varied levels of noise and digitized with diverse sampling frequencies. As one of the database is considered to be standard, the obtained performance can be easily compared with previous proposals.

The computational time and the number of resources required by the proposed algorithm to detect all the R-peaks of the MITDB database has been estimated and compared with the well-known P&T algorithm under the same conditions. This comparison shows that the proposed algorithm reduces almost 50% the computational time, 78.6% the number of required resources, and 17.6% the number of operations per second, and 54.3% the number of operations per sample. In spite of this reduction, it provides a better detection with extremely difficult ECG recordings.

The analysis carried out over the proposed algorithm regarding accuracy and resources employed demonstrates its suitability for working on remote monitoring applications, in which it is necessary to get information in real-time and portable devices are used.

Next chapter studies the Heart Rate Variability of a group of patients undergoing Oral Food Challenges. The 18 features used in the previous work are analysed to get the one providing more information about the effect an allergic reaction has on the HRV signal of allergic patients. The comparison of the features of allergic and non-allergic patients under the same circumstances will help to discriminate the HRV variations provoked by reasons different than allergies.

Chapter 4.

AUTOMATED ALLERGY DETECTION

The next step in developing a real time allergy detection algorithm is to reduce the computational complexity at the feature stage. This chapter aims to find out which particular set of HRV features gives information regarding the physiological changes produced by an allergic reaction. This analysis will explain how it is possible to detect an allergic reaction through the measurement and analysis of the HRV signal. From the clinical point of view, this fact implies a significant novelty as, even though the relationship between the HRV and the existence of allergic reactions was already established in the background work, no particular one of the studied features was related to the occurrence of an allergic reaction.

In this chapter the 18 features used in the previous investigation are studied in order to discard those features that do not vary sufficiently due to allergic reactions. This study will improve the results obtained by the previous one in two main ways: first, the quantity of information will be reduced, which will reduce the computational complexity of the allergy detection process, making it able to work in real-time; secondly, knowing which one of the features can be used to predict the onset of an allergic reaction may help the doctors to get more information about the physiological changes produced by them.

Oral food challenge (OFC) is the definitive diagnostic test for food allergy [MHAB14], however, it poses a risk for the health of the patients, due to the incremental consumption of the implicated food allergen. Subtle heart rate changes were detected in children experiencing a positive OFC. In previous works [TTHM14], it has been demonstrated the existence of a relationship between the variations of the HRV signal and the presence of an allergic reaction, as explained in Chapter 2 of this thesis. However, with the previously designed algorithm one unique model for all the patients has not been generated, but a unique model for each one of them is used, with the parameters selected depending on the rest of subjects of the database. For this reason, it is not possible to predict the result that this algorithm would provide with new patients. Besides, the process needed to carry out the mathematical model makes the designed algorithm unsuitable to work in real-time.

Thus, the main objective of this chapter is the reduction of the number of features needed to detect an allergic reaction and design of an allergy detection algorithm able to work in real time during the provocation tests.

4.1 Evaluation methods

The set of features will be evaluated from two points of view: first, their "allergy diagnostic" ability will be obtained; then, as the main objective of this work is the proposal of an algorithm able to work in real-time, the computational load needed to obtain the value of each feature is compared. These two tests will help to select a feature or a reduced group of them to develop a real time allergy detection algorithm based on a trade-off between performance and computational cost. There exist several mathematical tools used in the clinical research area to test the diagnostic ability of a proposed method. These tools mainly evaluate the ability of the studied feature to distinguish between data belonging to people with a specific disease and those belonging to healthy people. In this work, *t-value*, *p-value* and *Area Under the Curve* (AUC) have been used. These metrics ae explained next.

4.1.1 T-value and p-value analysis

These values are obtained by conducting a t-test. This test compares two sets of data and determines if there is a significant difference between their means. It is used when the variances of both sets are unknown and/or the sample sizes are small. Some useful information regarding this test can be found on the *VassarStats* website[Lowr00]. Statistically, the outcome of a t-test is

the rejection of the *null hypothesis*, which says that the mean value of the data from the two groups is equal. A t-test can be:

- Paired or unpaired depending if the two sets are related directly or not. In the first case, the two sets belong to the same population, for instance, data belonging to the same group of patients after and before receiving a treatment.
- One-tailed or two-tailed. This feature depends on the variance of both groups. One-tailed test is performed when the variance of one set is expected to be always higher than the other one. Otherwise, the t-test should be configured as two-tailed test.

The resulting t-value measures the difference between the mean values of both populations. In this case, as the data belong to different subjects, the t-test should be configured as unpaired; and, since it is not known previously if the features during an allergic reaction will have bigger or smaller values than during normal states, t-tests will be configured as two-tailed.

P-value measures the probability of getting a difference higher than the obtained t-value between subjects from the same group. As an example, getting a t-value of 4.5 and a p-value of 0.01 means it is 1% likely that the difference between subjects from the same group is higher than 4.5. In other words, if the difference of two subjects is higher than 4.5, it is 99% likely that these two subjects belong to different groups.

For evaluating the outcome achieved, it is necessary to get the *degrees of freedom* (*df*) of the analysed database, which is related with the level of arbitrariness of the values belonging to each group. Its value is computed depending on the size of both groups according to (*eq. 4.1*), in which N_x represents the size of the group x.

$$df = (N_{group1} - 1) + (N_{group2} - 1) \qquad \textit{(eq. 4.1)}$$

Finally, the *confidence level* (CL) should be selected that must be obtained with the studied method. Typical values are 90%, 95% and 99%. Depending on the CL, the p-value and t-value limits are the ones shown in **Appendix C**. The p-value limit is named *significance level*, α. If the p-value is below α, it is considered that the observed data are inconsistent with the *null hypothesis,* and so, this hypothesis should be rejected.

In this chapter, data belonging to 15 allergic and 8 non-allergic subjects are analysed so *df* is 21. Then, if a CL above 95% is required, α for a two-tailed test is 0.05 (p-value < 0.05) and t-value limit is 2.08.

4.1.2 Area under the Receiver Operating Characteristic curve (AUC)

The *Receiver Operating Characteristic, ROC* [HuLi05] represents the accuracy of the analysed method. It represents the sensitivity, *Se*, (eq. 4.2) as a function of *fall-out* or False Positive Rate, which value is 1-Specificity, *Sp,* (eq. 4.3). The *AUC* measures the diagnostic ability of each parameter: if its value is 50%, the result of the classification is random, and above this value, the greater the AUC the better the diagnostic ability, 100 % being the perfect classification. Figure 4.1-1 depicts three examples of ROC curves: the perfect classification is met when AUC is 1 (green area), and the minimum AUC value is 0.5 (red area), which implies a random classification result; blue area represents a generic classification whose AUC is 0.936. The metrics used for these computations are the following ones:

- True Positive, *TP*: Allergic subject detected
- False Negative, *FN*: Allergic subject not detected
- True Negative, *TN*: Non-allergic subject correctly classified
- False Positive, *FP*: Non-allergic subject classified as allergic
- Sensitivity, *Se* (*eq. 4.2*): Percentage of positives correctly classified.
- Specificity, *Sp* (*eq. 4.3*): Percentage of negatives correctly classified.

$$Se = \frac{\#\ of\ allergic\ subjects\ correctly\ classified}{\#\ of\ allergic\ subjects} = \frac{TP}{TP + FN} \qquad (eq.\ 4.2)$$

$$Sp = \frac{\#\ of\ nonallergic\ subjects\ correctly\ classified}{\#\ of\ nonallergic\ subjects} = \frac{TN}{TN + FP} \qquad (eq.\ 4.3)$$

As was explained in Chapter 2, each feature was obtained using epochs of 60, 120, 180 and 300 minutes with one-second shift. For this work, the smallest epoch has been selected (60 seconds) to compute all the features. The short length of this window allows the immediate or short time effects on the analysed signal to be observed. Thus, for each feature there is a data vector whose length is the number of seconds of the test duration.

In order to test how the values of the HRV features are related with presence of allergic reactions, the metrics described above have been used to evaluate 6 statistical parameters of each feature: mean, median, mode, interquartile range, range and standard deviation. Thus, 23 values of each statistical parameter were obtained (one for each subject, 15 allergic and 8 non-allergic).

The meanings of these statistics are explained in Table 4.1-1. Mean, median and mode analyse the general value of each feature during the whole OFC; while range, interquartile range, and standard deviation yield information about how much the features have changed during the tests.

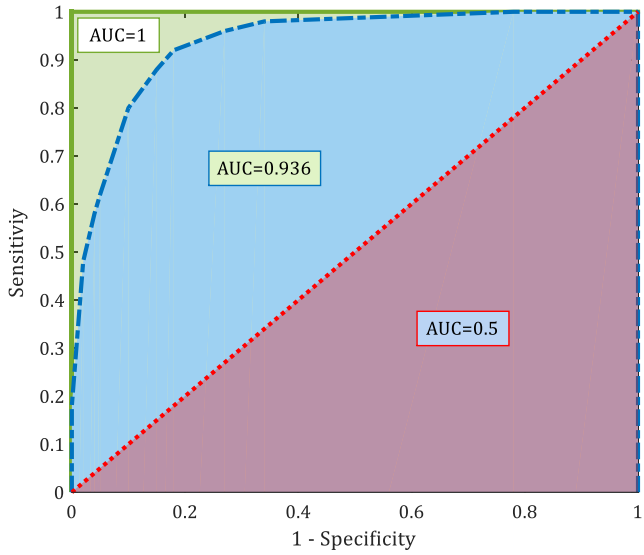

Figure 4.1-1. Example of ROC curves with different AUC

TABLE 4.1-1. STATISTICAL PARAMETERS USED FOR EVALUATING EACH HRV FEATURE

Parameter	*Meaning*
Mean (eq. 4.4)	Average value of the samples.
Median	In a sorted set of values, the median is the value in the central position. If the number of values is even, the median is the mean value of the two central samples. Second quartile of the samples.
Mode	The value that appears most often in a set of data
Interquartile range (IQR)	Difference between the upper and lower quartiles. Measures the statistical dispersion of the samples.
Range	Difference between the maximum and the minimum values of the data.
Standard deviation, std (eq. 4.5)	Quantifies the dispersion of the data.

$$mean = \frac{1}{N}\sum_{i=1}^{N} feat_i \qquad \textit{(eq. 4.4)}$$

$$std = \sqrt{\frac{1}{N}\sum_{i=1}^{N}(feat_i - mean)^2} \qquad \textit{(eq. 4.5)}$$

where N, is the number of elements in the set of data.

4.2 HRV feature selection

4.2.1 Diagnostic ability study

The list of the studied features and the acronyms used are:

- *MRR*: Average HRV
- *STDNN*: Standard deviation of the RR intervals
- *CV*: Coefficient of variance
- *RMSSD*: Root mean square of the RR intervals
- *NN50*: Number of successive pairs of RR intervals differing for more than 50 ms.
- *pNN50/pNN25*: Percentage of successive pairs of RR intervals that differ for more than 50/25 ms. of the RR intervals within the analysed epoch.
- *STPP/STNN*: Number of RR intervals that are longer/shorter than the previous one
- *CSI/CVI*: Cardio Sympathetic/Vagal Index
- *SD1/SD2*: Short/Long axis of the poincaré ellipsis
- *VLF/LF/HF*: Total power in the very low/low/high frequency bands
- *ratioLFHF* or *LFHF*: ratio between LF and HF
- *Histo*: Histogram index

For this study the features obtained in the previous work were used i.e., the QRS complex detection algorithm proposed in Chapter 3 has not been employed to get the RR intervals of the ECG signals in order to isolate the results of the allergy study from the variations that a different QRS complex detection algorithm could introduce. These features were extracted from the HRV signals computed through the manual ECG annotations.

As has been explained in the previous section, the t-test evaluates the differences between data belonging to two different groups. In this case, the database has been divided in 'allergic' and 'non-allergic' groups. The six statistical parameters listed in Table 4.4-1 have been computed for the 18 features of each subject. In this way, for each feature, there are 23 values of each statistical parameter: 15 of them belonging to the non-allergic, and 8 to the allergic. An unpaired, two-tailed t-test has been applied to each statistical parameter of each feature, getting the difference between the allergic and the non-allergic group showed by each feature.

The obtained absolute t-values are shown in Figure 4.2-1, and 1-(p-values) in Figure 4.2-2. Best t-value and p-value are obtained with the standard deviation of the *Mean* (p-value = $6.82 \cdot 10^{-5}$; t-value=4.65) and with the range of the *Mean* (p-value=$8.92 \cdot 10^{-5}$; t-value=4.54). Since *df* in this case is 21, the CL for these two parameters is higher than 99.9%. The next best result is obtained with the standard deviation of *CV* (p-value=0.0133; t-value=2.3837) for which the CL is 95%, followed by the standard deviation of *STDNN* (p-value=0.0339; t-value=1.9263) with a CL of 90%. The exact quantitative results are given following: Table 4.2-1 lists the t-values obtained with all the parameters and Table 4.2-2, the p-values for all the parameters multiplied by 10^3. The CL of each parameter is shown in Table 4.2-3. All the CL below 80% have been set to 0.

The mode of the RMSSD feature is 0 (i.e. the value most repeated). Due to this fact, its p-value and t-value cannot be computed (Not-a-Number, NaN), and its AUC is the minimum possible (0.5).

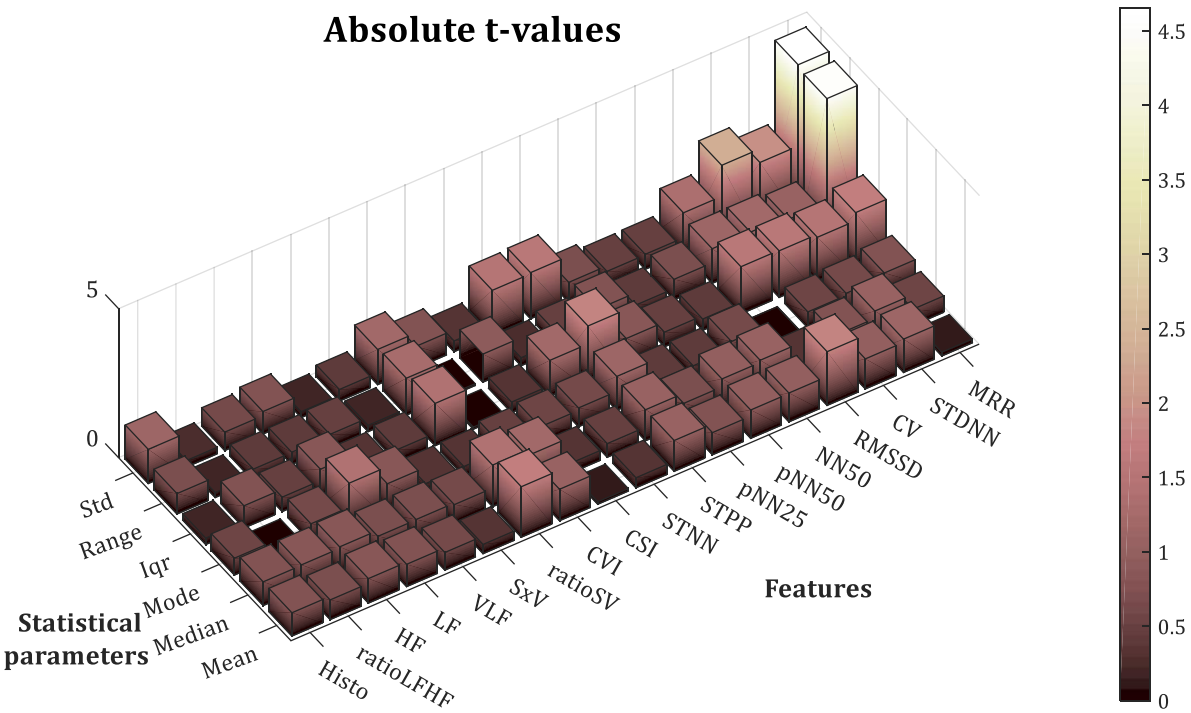

Figure 4.2-1. T-value for the six statistical parameters for the studied HRV features

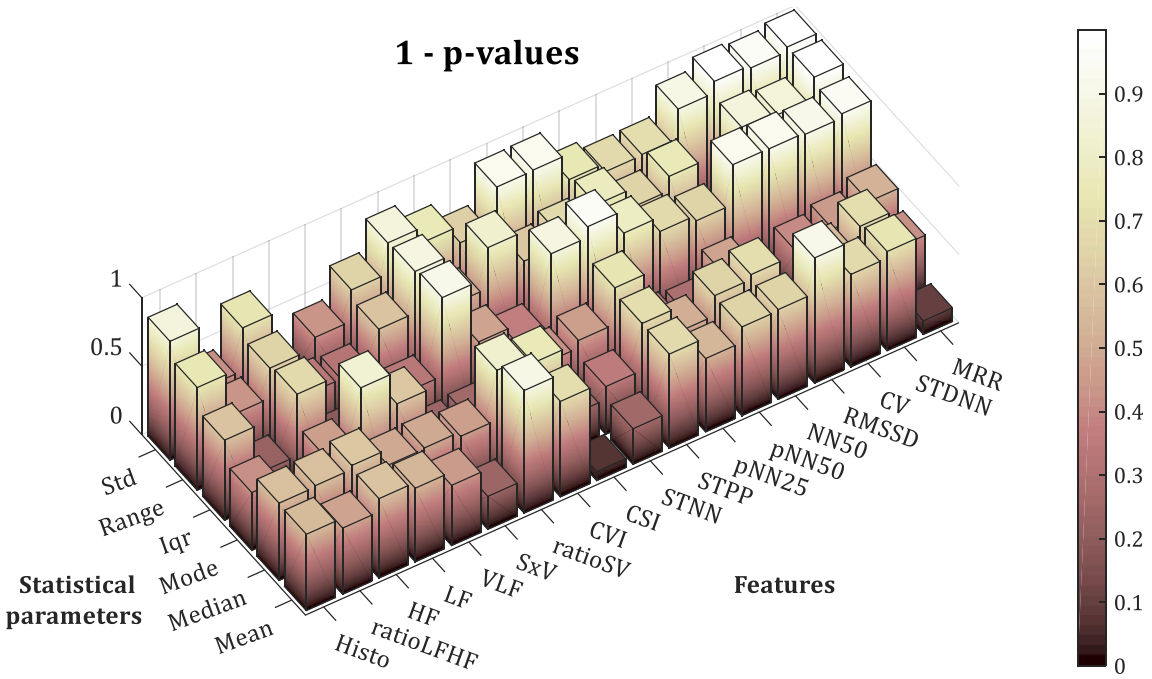

Figure 4.2-2. (1 - p-value) of the six statistical parameters for the studied HRV features

TABLE 4.2-1. T-VALUES OBTAINED WITH THE PERFORMED T-TEST FOR THE 6 STATISTICAL PARAMETERS OF THE HRV FEATURES

HRV feature	Statistical Parameter: Mean	Median	Mode	Iqr	Range	Std
MRR	0,1261	0,5466	0,7366	1,7375	4,541	4,6531
STDNN	1,1174	1,0353	0,6074	1,4641	1,0438	1,9263
CV	1,0077	0,7867	0,537	1,5619	1,1659	2,3837
RMSSD	1,8017	0,36	NaN	1,5811	1,1618	1,3425
NN50	0,9674	1,0428	0,6495	0,3786	0,6865	0,5029
pNN50	0,9502	0,9684	0,3861	0,4915	0,3755	0,484
pNN25	0,7444	0,7021	0,4064	0,8306	0,7889	0,6679
STPP	1,0324	1,0407	1,1352	1,8045	0,4593	1,547
STNN	0,3359	0,4572	0,6312	1,2023	0,2678	1,5056
CSI	0,0826	0,3274	0,5482	0,3562	0,9416	0,3597
CVI	1,0548	1,2026	0,4745	0,0706	0,0605	0,7306
SD1	1,6926	1,3942	0,324	1,4164	1,2386	1,1789
SD2	0,3096	0,6214	0,3026	0,414	0,2108	0,3899
VLF	0,5909	0,6745	0,8503	0,2939	0,4595	0,1987
LF	0,7476	0,6626	1,4235	0,8667	0,4138	0,7544
HF	0,821	0,8624	0,6126	0,4836	0,4008	0,6165
LFHF	0,6587	0,8108	0,0673	0,7459	0,1672	0,2189
Histo	0,7805	0,7938	0,5645	0,2158	0,6838	1,144

TABLE 4.2-2. P-VALUES ($\cdot 10^{-3}$) OBTAINED WITH THE PERFORMED T-TEST FOR THE 6 STATISTICAL PARAMETERS OF THE HRV FEATURES

HRV feature	Statistical Parameter: Mean	Median	Mode	Iqr	Range	Std
MRR	900,8414	590,4451	469,5369	48,4738	0,0891	0,0682
STDNN	276,4551	312,3018	550,0819	78,9936	154,2299	33,8563
CV	325,0716	440,2468	596,9158	66,6293	128,3625	13,3272
RMSSD	85,9684	722,4734	NaN	64,3962	870,8327	96,8877
NN50	344,3449	308,9169	523,0408	354,3982	249,9596	310,1384
pNN50	352,8162	343,8708	703,3234	314,0969	355,5403	316,7001
pNN25	464,9068	490,3009	688,527	207,7846	219,4881	255,7499
STPP	313,6263	309,856	269,0787	42,7614	325,3781	68,4021
STNN	740,2673	652,2195	534,71	121,3073	395,7222	73,5259
CSI	934,9782	746,5969	589,3615	637,3845	178,5419	361,3469
CVI	303,4945	242,5302	640,0557	527,792	476,1757	236,5396
SD1	105,3258	177,8215	749,1526	85,6551	114,5714	125,8168
SD2	759,9192	541,0155	765,1783	658,4505	417,5519	350,2788
VLF	560,8725	507,3479	404,7505	614,1572	674,6846	577,7976
LF	463,0038	514,8191	169,2724	802,0452	658,3944	770,5128
HF	420,8598	398,2163	546,7215	316,8251	346,3118	272,0994
LFHF	517,2189	426,5494	947,0032	768,0012	565,5818	585,5614
Histo	443,8205	436,2051	578,4262	415,6167	250,7965	132,7578

TABLE 4.2-3. CONFIDENCE LEVEL OBTAINED WITH THE PERFORMED T-TEST FOR THE 6 STATISTICAL PARAMETERS OF THE HRV FEATURES

HRV feature	Statistical Parameter: Mean	Median	Mode	Iqr	Range	Std
MRR	0	0	0	90	99,9	99,9
STDNN	0	0	0	80	0	90
CV	0	0	0	80	0	95
RMSSD	90	0	0	80	0	80
NN50	0	0	0	0	0	0
pNN50	0	0	0	0	0	0
pNN25	0	0	0	0	0	0
STPP	0	0	0	90	0	80
STNN	0	0	0	0	0	80
CSI	0	0	0	0	0	0
CVI	0	0	0	0	0	0
SD1	80	80	0	80	0	0
SD2	0	0	0	0	0	0
VLF	0	0	0	0	0	0
LF	0	0	80	0	0	0
HF	0	0	0	0	0	0
LFHF	0	0	0	0	0	0
Histo	0	0	0	0	0	0

Finally, Figure 4.2-3 represents the resulting AUC of each parameter and Table 4.2-4 lists their values. The best AUC is achieved with the standard deviation (0.958) and the range (0.933) of the *Mean*, whose values are 0.958 and 0.933, respectively. There are two more features whose AUC is higher or equal to 0.8: interquartile range of MRR (AUC=0.8), and standard deviation of CV (AUC=0.825). These two features have been discarded due to their small t-values: 1.7375 and 2.3837, respectively.

The obtained results confirm the mean of the HRV signal (MRR) as the best feature to distinguish between allergic and non-allergic subjects. The statistical parameters through which the differences are better observed are the standard deviation and the range, which implies that there exist abrupt variations in the MRR of the allergic children that are not present in the non-allergic ones.

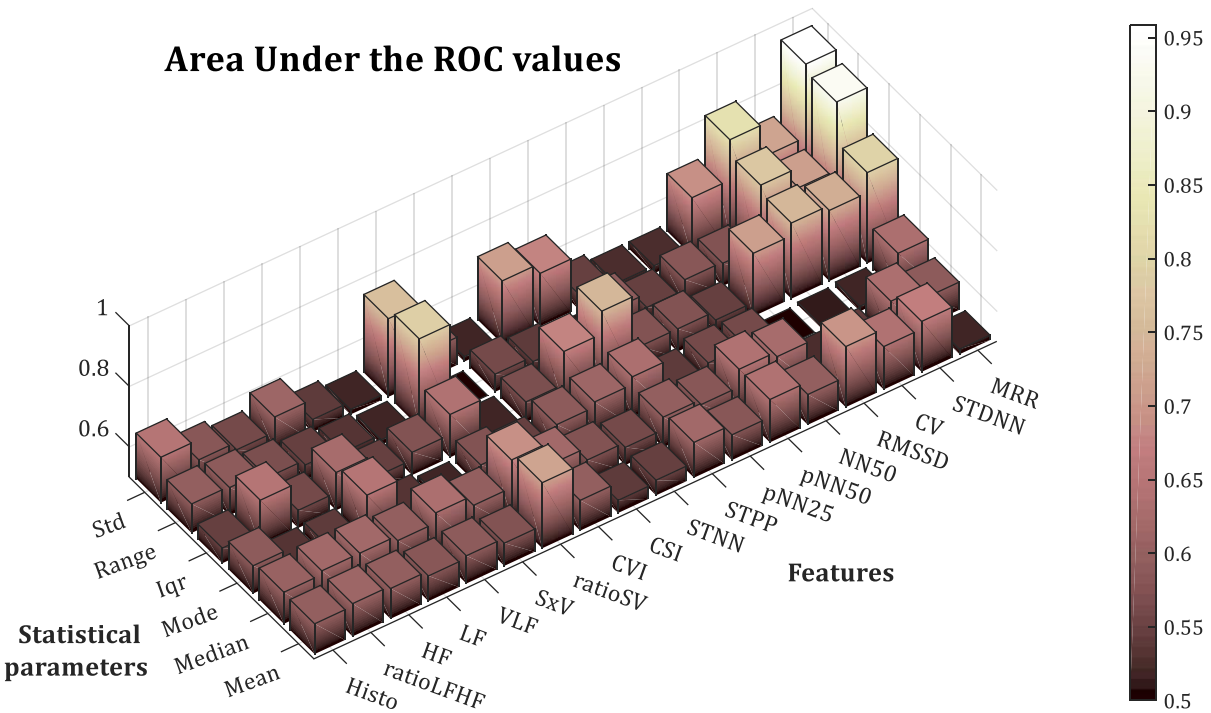

Figure 4.2-3. AUC for the six statistical parameters for the studied HRV features

TABLE 4.2-4. AUC OBTAINED FOR THE 6 STATISTICAL PARAMETERS OF THE HRV FEATURES

HRV feature	Statistical Parameter: Mean	Median	Mode	Iqr	Range	Std
MRR	0,517	0,592	0,633	0,800	0,933	0,958
STDNN	0,667	0,633	0,517	0,733	0,708	0,717
CV	0,642	0,542	0,508	0,750	0,775	0,825
RMSSD	0,700	0,525	0,500	0,708	0,575	0,692
NN50	0,600	0,625	0,558	0,546	0,579	0,525
pNN50	0,642	0,642	0,563	0,575	0,546	0,525
pNN25	0,583	0,583	0,542	0,575	0,592	0,550
STPP	0,617	0,600	0,633	0,750	0,513	0,675
STNN	0,550	0,558	0,608	0,675	0,542	0,708
CSI	0,542	0,575	0,592	0,567	0,558	0,517
CVI	0,600	0,617	0,550	0,517	0,500	0,592
SD1	0,717	0,692	0,575	0,642	0,792	0,758
SD2	0,575	0,600	0,517	0,575	0,517	0,517
VLF	0,592	0,633	0,533	0,550	0,533	0,542
LF	0,583	0,600	0,650	0,625	0,550	0,608
HF	0,600	0,617	0,538	0,558	0,567	0,558
LFHF	0,608	0,617	0,533	0,650	0,592	0,583
Histo	0,600	0,604	0,592	0,550	0,596	0,650

4.2.2 Complexity analysis

The proposed algorithm should be able to work online during real OFCs, so it has to be efficient from a computational cost point of view. The computational cost employed by MATLAB® to compute each feature has been obtained. To do so, all the features were computed and the percentage of the total time employed for getting the value of each one has been used to compare their complexity. Some of the HRV features are obtained directly from the RR intervals, such as the *MRR* or the *RMSSD*. However, to compute other features, previous computations should be performed. For instance, the periodogram of the RR intervals is needed to compute the frequency domain features (*VLF*, *LF*, *HF* and *LFHF*). The whole set of features have been divided into 5 categories on the basis of the previous operations they need:

1. Features obtained directly from the RR measurement: *MRR*, *RMSSD*, *STDNN* and *CV*
2. Features obtained through RR differentiation: *NN50*, *pNN50*, *pNN25*, *STPP* and *STNN*
3. Features obtained by using the auto covariance: *CSI*, *CVI*, *SD1* and *SD2*
4. Features obtained through the periodogram: *VLF*, *LH*, *HF* and *LFHF* ratio
5. Features obtained by computing the histogram: *Histo*

The computational time taken for the initial computations have been considered once for each group. The computational time percentage used to obtain each group of features, and each feature within its group is represented in Figure 4.2-4.

Frequency domain features take the most part of the computational time (97 %) whereas the whole group of features obtained through the computation of the RR differentiation need only 1 % of the total time. For a computer with an Intel® Core™ 2 Quad CPU Q9450 @ 2.66GHz, 4 GB RAM, the total computation of the features takes a mean time of 97.785 ms, including the initialization of the variables involved in the operations. This value is the average time computed for 17 ECG signals, with a total recording of 16 hours, 58 minutes and 41 seconds, which implies 61121 computations for each feature (one each second).

It is important to recall that these operations were performed using MATLAB, taking advantage of its ability to perform matrix calculation. Working on real-time with a portable platform, the time employed to obtain all the features would be much higher. Thus, the study performed here compares the computational cost needed to get these 18 features. The absolute computational time will depend on the specific platform used to run these computations. Taking into account only this comparison, frequency domain features should be avoided from this study, as they need more than 11 times the time employed to compute all the rest of the features together. Besides, they do not present a good diagnostic ability, as shown in section 4.2.1.

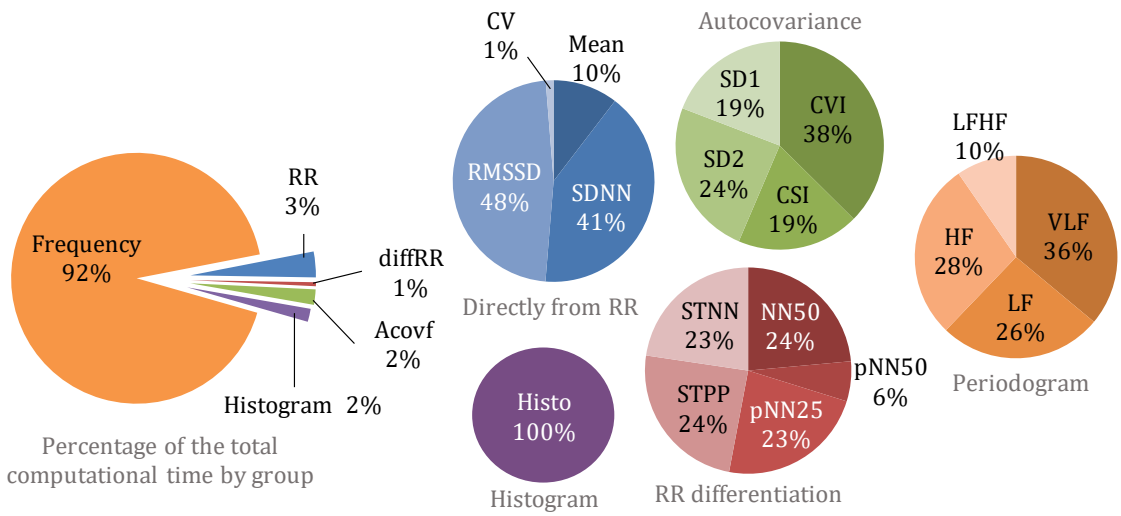

Figure 4.2-4. Relative computational time needed to compute each feature

4.2.3 Feature selection

Figure 4.2-5 shows the differences regarding the normal Probability Density Function (PDF) of the statistics computed for the *MRR*, as well as their boxplot. As it was expected, there are no significant differences between mean, median and mode since there are no background physiological differences between allergic ad non-allergic subjects: age, fitness, health status, etc. On the contrary, the interquartile range, range and the standard deviation are higher in the case of the allergic subjects. This means that in those cases the HRV suffered big changes during the OFC but these changes lasted for short periods of time, then the HRV of the allergic subjects came back to the background range. The allergy detection algorithm should be able to detect that kind of change and distinguish it from HRV changes produced by normal activities.

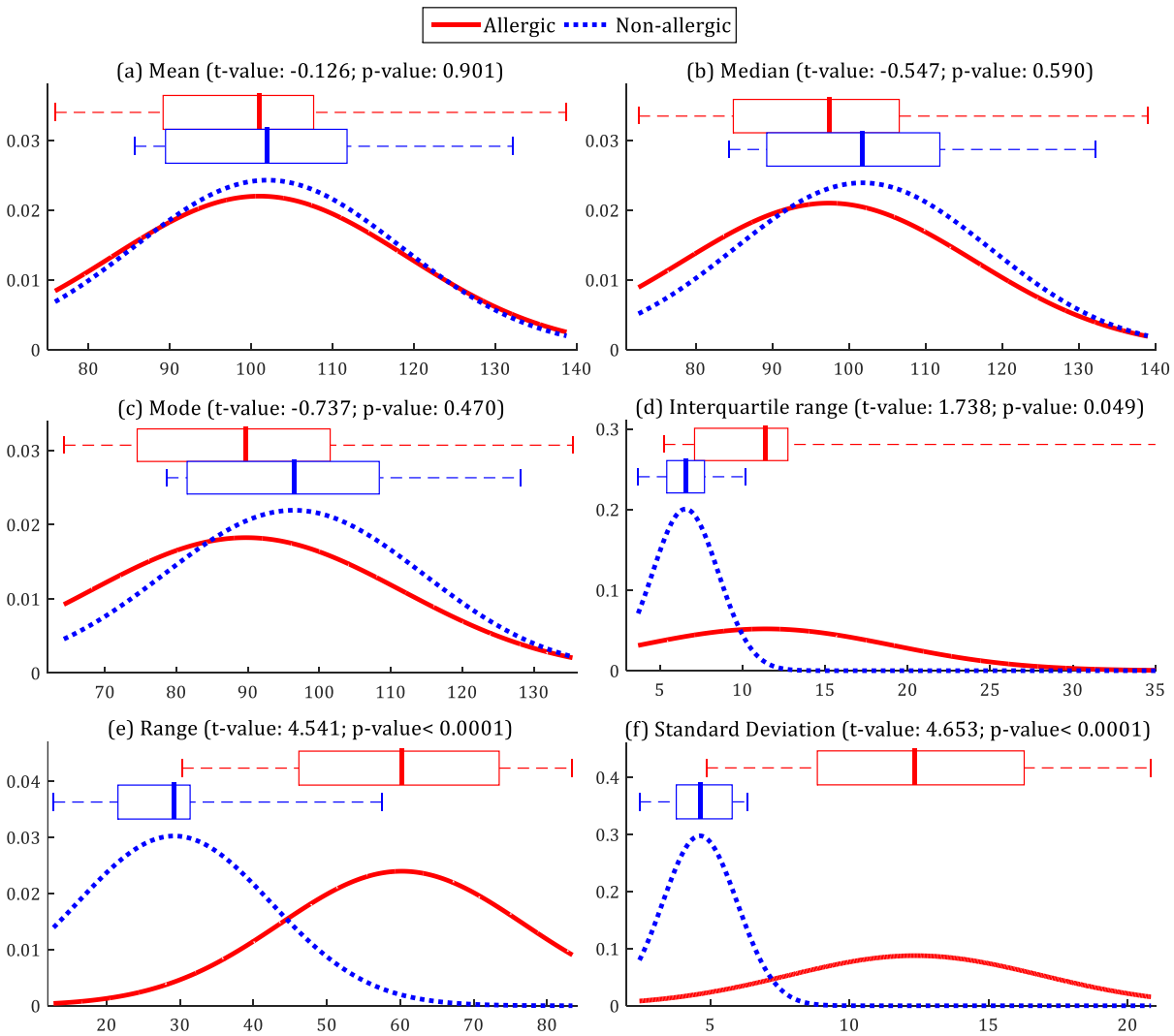

Figure 4.2-5. Comparison between mean HRV of allergic (red) and non-allergic (blue) subjects using (a) mean, (b) median, (c) mode, (d) range, (e) standard deviation and (f) interquartile range

Figure 4.2-6 represents the metrics of the diagnostic ability (t-value, p-value and AUC) attained with the standard deviation of each feature versus the percentage of computational time needed to obtain their values. P-value and t-value have been normalized to easily compare all the parameters. Best AUC (0.958), p-value ($6.82 \cdot 10^{-5}$) and t-value (4.653) is always obtained with the *MRR*. Taking into account these results and that the relative computational load needed to obtain its value is only 3 % of the total time, this feature has been chosen to design the allergic reactions detection algorithm. Figure 4.2-7 shows an example of HRV signal and its corresponding *MRR* feature, computed in a 60-seconds window with 1-second shift.

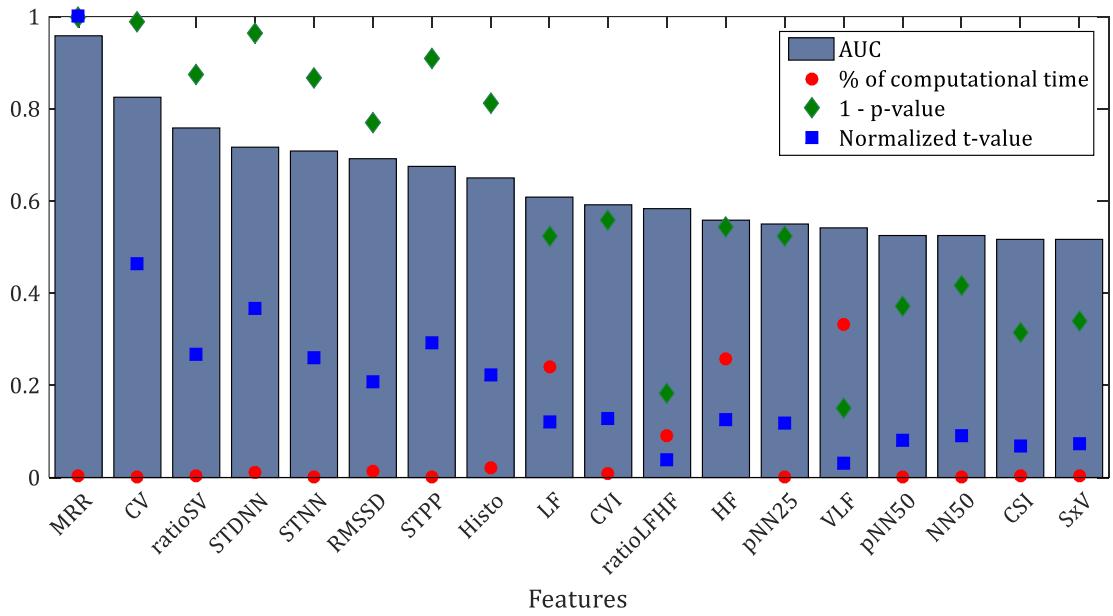

Figure 4.2-6. AUC, p-value, t-value of the standard deviation of all the features and relative computational time needed to obtain them.

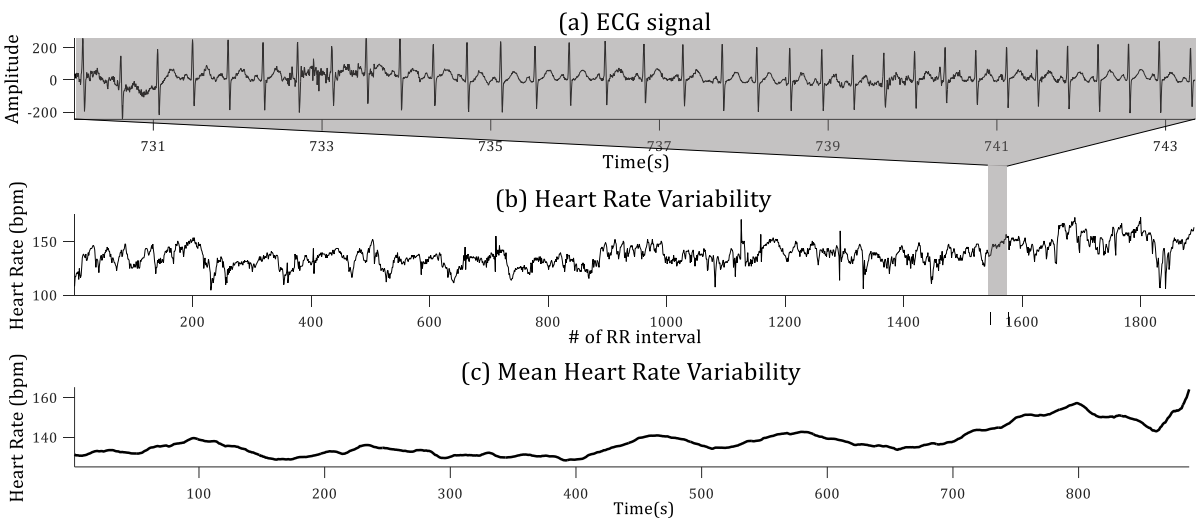

Figure 4.2-7. ECG (a); Heart Rate Variability (b), and mean Heart Rate Variability signal examples

4.3 Allergic reaction detection algorithm

The analysis carried out in the previous section demonstrates that the standard deviation of the mean HRV shows a clear difference in those cases in which the patients suffered an allergic reaction. Besides, the computational load needed to compute its value is low, which allow its analysis in real-time and so, the detection of the allergic reactions in an online mode. This section aims to define the effect an allergic reaction has on the mean HRV signal of allergic patients for its detection. Figure 4.3-1 shows an example of the differences between the MRR signal (black solid line) of an allergic and a non-allergic subject during OFCs. The background data has been shadowed with grey, and each one of the check-up periods (in which new portions of the allergen are given to the subjects) has been coloured with light blue. Table 4.3-1 lists the statistical parameters of both subjects. Mean, median and mode are slightly higher for the non-allergic subject, but the difference is not significant enough. On the other hand, interquartile range is slightly higher for the allergic subject, while the range and standard deviation are much higher in the case of the allergic subject. The reason of these differences are the "peaks" appearing in the MRR signal of the allergic subject, starting on minutes 26 and 46, approximately.

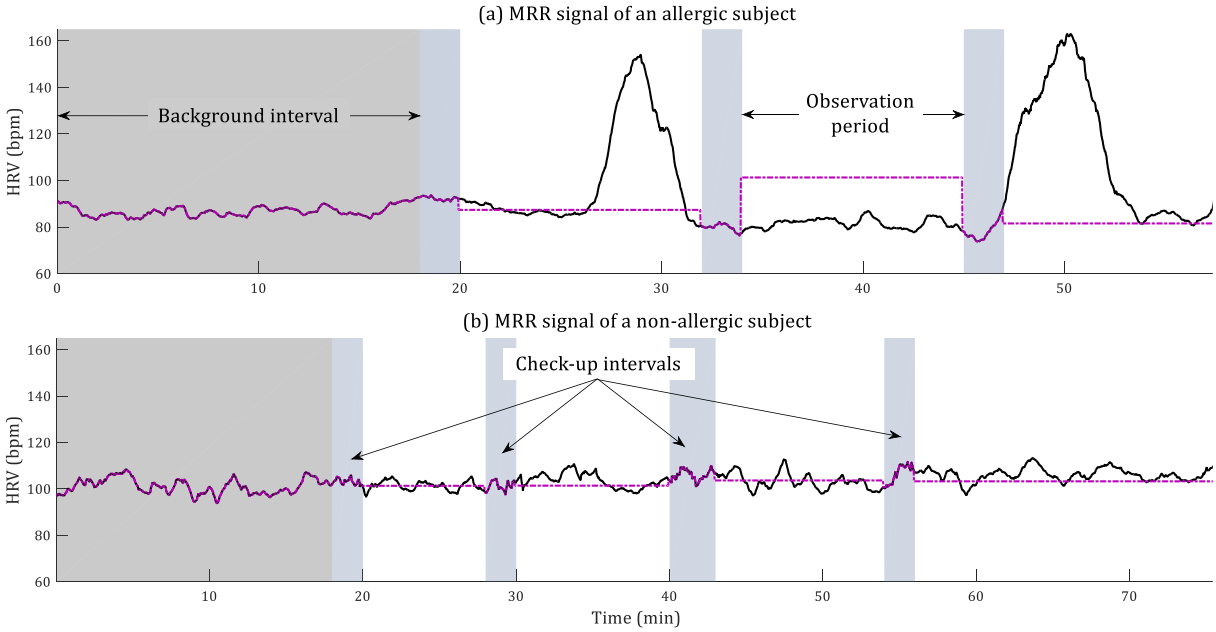

Figure 4.3-1. MRR signal of an allergic (a) and a non-allergic (b) subject. Purple dotted line represents the mean value of the MRR signal during each "background" period, or MBG signal.

TABLE 4.3-1. STATISTICAL DIFFERENCES BETWEEN AN ALLERGIC SUBJECT AND A NON-ALLERGIC ONE

Parameter	***Allergic***	***Non-allergic***
Mean	91.62	104.13
Median	86.28	103.99
Mode	74.31	98.6
Interquartile range	7.54	5.55
Range	83.44	57.45
Standard Deviation	16.49	4.18

Looking at the MRR signal of all the 23 subjects (**Appendix D**) it can be observed that high rises of the MRR signal appear in most of the allergic subjects as will be shown later on, while they are not present in the MRR signals of the non-allergic subjects. This fact provokes the differences between allergic and non-allergic regarding the standard deviation and range of the mean HRV, so they have been considered the representation of the effect an allergen has on the allergic subjects. Following this hypothesis, the detection of an allergic reaction will consist on the detection of those rises of the HRV. As was stated in Chapter 2, the HRV signal of a healthy person does not have a constant value, but it should increase and decrease continuously. For this reason, it is necessary to distinguish normal variations from those representing an allergic reaction. Figure 4.3-2 represents the flow chart of the designed allergy detection algorithm. It is composed of the following stages:

1. When the first check-up ends, the mean of the *MRR* signal since the beginning of the test is computed (MBG signal, displayed by a dotted purple line in the Figure 4.3-1). This period represents the normal HRV of each subject, as they do not take the first portion until it finishes.
2. During the following observation period, the *MRR* signal is compared with the background data, i.e. the *MBG* value is subtracted from each new sample of the MRR signal. The result of this operation is called *NMRR* signal (Normalized *MRR*). This signal represent how different is the *MRR* signal from the background data i.e. how the actual value of the mean HRV differ from the 'normal' mean HRV of the value. Figure 4.3-3 represents the *NMRR* signal for an allergic subject (a) and a non-allergic subject (b).
3. The mean value of the *NMRR* signal during each increase has been computed, the result is called *MeanPeak.* If the value of a *MeanPeak* is higher than a threshold (*Th*), it is considered an allergic reaction.
4. When the next Check-Up starts, the last observation period is considered as the new background interval (as the medical staff did not detect any allergy symptom during it) and the algorithm goes back to the point 1.

The value of *Th* depends on the maximum *MeanPeak* of each subject, from now on, *MaxMeanPeak*. The low limit of the threshold is the maximum *MaxMeanPeak* of the non-allergic subjects and its high limit, the minimum *MaxMeanPeak* of the allergic group.

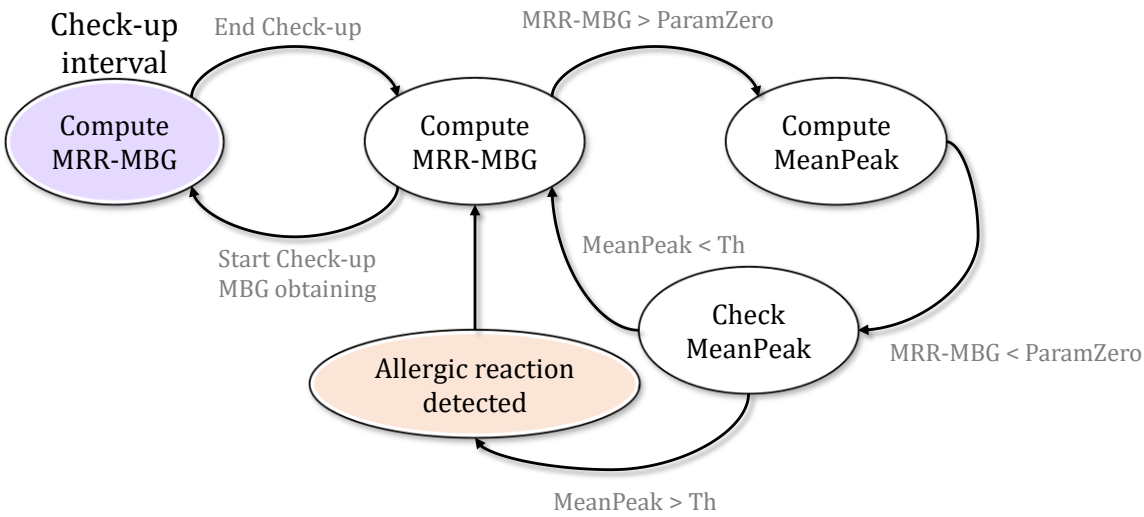

Figure 4.3-2. Flow chart of the proposed allergy detection algorithm

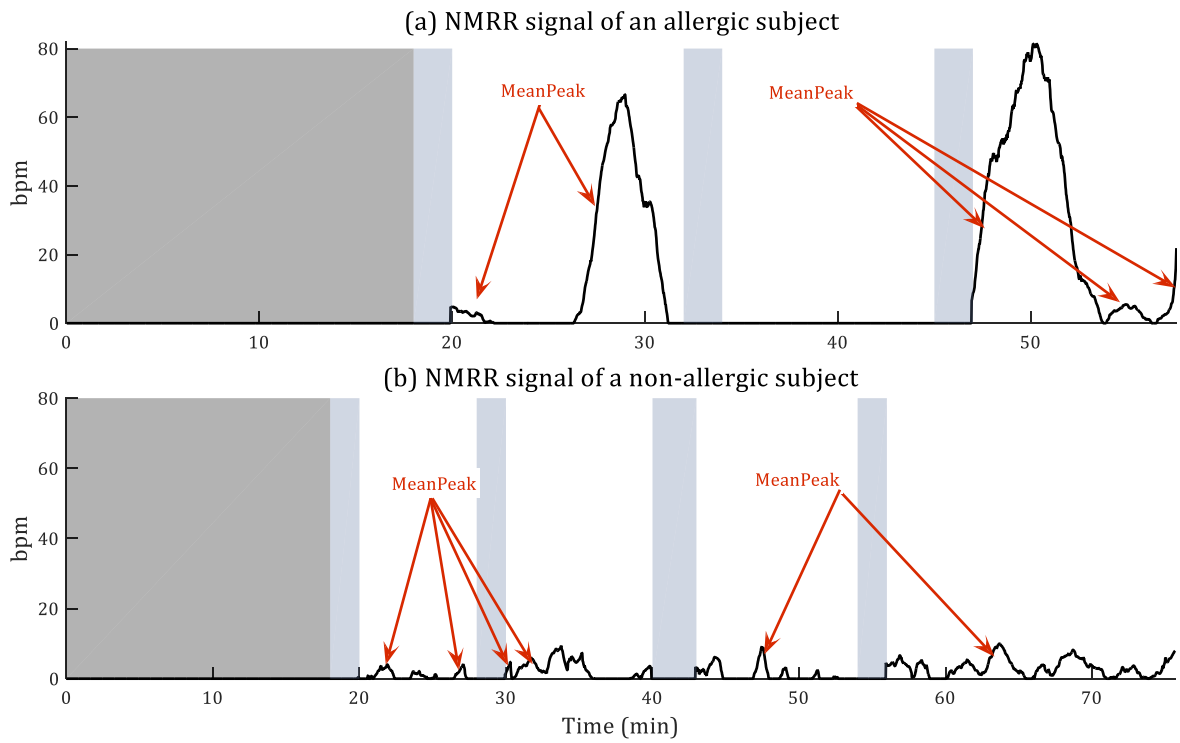

Figure 4.3-3. Normalized MRR (NMRR) signal for an allergic (a) and a non-allergic (b) subject

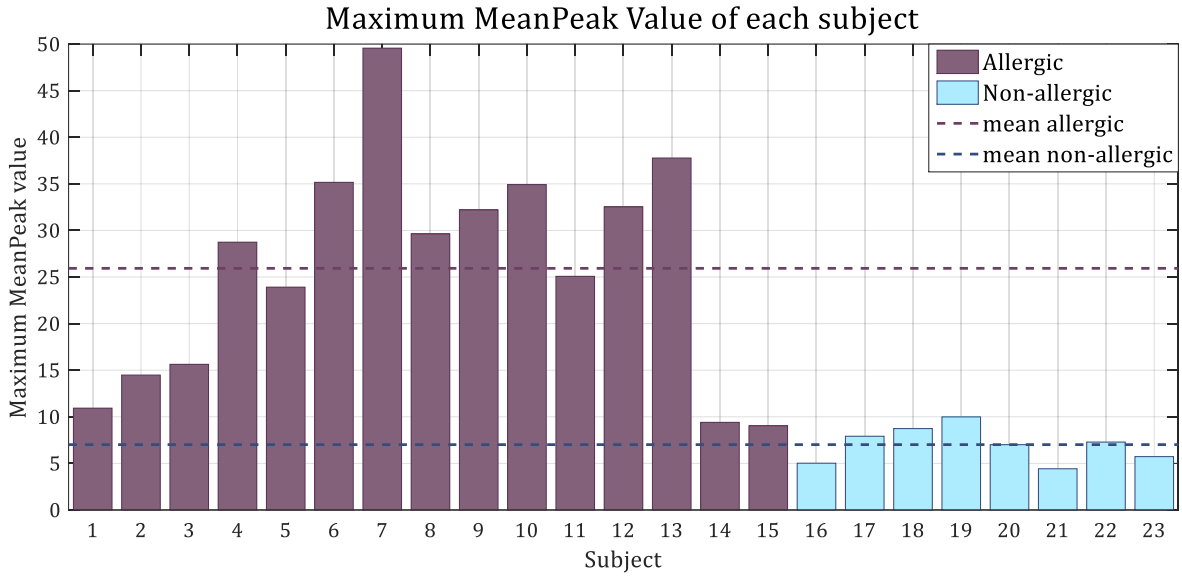

Figure 4.3-4. Maximum MeanPeak value for each subject of the Allergy Database

Figure 4.3-4 shows the *MaxMeanPeak* value for each allergic (purple bars) and non-allergic (blue bars) subject, as well as the mean value for each group (25.93 and 7.01, respectively). It can be observed how these values are much higher in most of the cases for the allergic subjects than for the non-allergic group. However, subjects 14 and 15 present values very similar to those from the non-allergic group even they reacted to the allergen during the OFC (*MaxMeanPeak* 9.40 and 9.03, respectively). To set the value of *Th*, subjects 14 and 15 have not been taken into account. With this consideration, the minimum *MaxMeanPeak* of the allergic subjects is 10.92; and the maximum *MaxMeanPeak* of the non-allergic, 9.99. Thus, the value of the threshold, *Th*, has been set to 10.5, getting 100% of specificity, as all the non-allergic subjects are correctly classified; and 86.67% of sensitivity (13 out of 15 allergic subjects detected).

4.4 Results

Twenty-three children were studied (Table 4.4-1) aged 9 months to 10 years. Fifteen OFC (62%) were positive, confirming food allergy, and eight OFC were negative. OFC duration ranged from 14 to 133 minutes and the mean number of doses they had was 4.5. With the algorithm configured as explained before, it would have been possible to classify correctly all the non-allergic subjects, detect 14 out of 15 allergic ones, and improve their diagnosis by reducing the duration and the number of doses of the OFC, as is summarized in Table 4.4-1.

It has been observed that the features (Table 4.4-2) of the MRR signals belonging to subjects 14 and 15 are more similar to those of the non-allergic group than of the allergic ones. As is represented in Figure 4.3-4, their *MaxMeanPeak* value is below 10, while the mean *MaxMeanPeak* of the allergic subjects is 25.93 (28.5 not considering 14 and 15) and 7.3162 for the non-allergic group. For this reason, these two subjects have been considered as outliers. The mean number of portions that could have been avoided is 1.4 out of 3.73 that were needed. This would imply a 37.5% reduction in the number of doses. The length of the test could have been reduced to the 60% of the mean length employed in the case of the allergic subjects due to the fact that the allergic reactions would have been detected before.

TABLE 4.4-1. PERFORMANCE OF THE ALLERGY DETECTION ALGORITHM

Patient ID	Allergic?	Detected?	Total doses	OFC duration	Doses saved	Time gain
1	Yes	Yes	1	0h. 14min.	0	0h. 00min.
2	Yes	Yes	5	1h. 40min.	3	0h. 56min.
3	Yes	Yes	5	1h. 34min.	3	0h. 58min.
4	Yes	Yes	4	1h. 44min.	1	0h. 50min.
5	Yes	Yes	7	2h. 13min.	2	0h. 32min.
6	Yes	Yes	1	0h. 35min.	0	0h. 14min.
7	Yes	Yes	3	0h. 57min.	2	0h. 26min.
8	Yes	Yes	5	1h. 46min.	2	0h. 44min.
9	Yes	Yes	2	0h. 50min.	1	0h. 22min.
10	Yes	Yes	3	1h. 24min.	0	0h. 01min.
11	Yes	Yes	5	1h. 26min.	2	0h. 35min.
12	Yes	Yes	2	0h. 41min.	1	0h. 09min.
13	Yes	Yes	5	1h. 46min.	4	1h. 07min.
14	Yes	No	1	0h. 33min.	0	0h. 00min.
15	Yes	No	7	1h. 37min.	0	0h. 00min.
16	No	No	4	2h. 10min.	0	0h. 00min.
17	No	No	5	1h. 42min.	0	0h. 00min.
18	No	No	9	2h. 09min.	0	0h. 00min.
19	No	No	8	2h. 11min.	0	0h. 00min.
20	No	No	8	1h. 51min.	0	0h. 00min.
21	No	No	6	1h. 29min.	0	0h. 00min.
22	No	No	4	1h. 03min.	0	0h. 00min.
23	No	No	6	1h. 33min.	0	0h. 00min.
Mean (allergic)			**3.73**	**1h. 16min.**	**1.40**	**0h. 28min.**
Mean (detected)			**3.93**	**1h. 19min.**	**1.61**	**0h. 32min.**
Mean (doses avoided)			**4.42**	**1h. 28min.**	**2.10**	**0h. 40min.**

TABLE 4.4-2. STATISTICAL PARAMETERS OF SUBJECTS 14 AND 15

Parameter	***Subject 14***	***Subject 15***
Mean	138.76	104.79
Median	139	104.85
Mode	134.9	102.24
Interquartile range	6.96	6.33
Range	30.28	31.83
Standard Deviation	4.86	6.65

There are three cases in which the subject only had one dose. In this cases, physical symptoms appeared quicker than usual as happened to subject 1, whose test lasted for 14 minutes. The algorithm detected the reaction at the end of the test, but it was not able to reduce its length. The test of subject 6 lasted for 35 minutes, and the algorithm detected a reaction 14 minutes before its end. In this case, the test might have been reduced to 21 minutes. Finally, in the case of subject 14, the test lasted for 33 minutes and the algorithm was not able to detect any symptom of allergic reaction. Figure 4.4-1 shows the MRR signal of this subject. In this case, the MRR did not present any variation similar to those representing an allergic reaction (as seen in the previous subsection). Consequently, the algorithm was not able to detect the allergic reaction for this subject.

Taking into account only the cases in which the subjects had more than one dose, the algorithm could have decreased the mean number of doses needed from 4.42 to 2.32 (52 % reduction), and the mean length of the OFC from 1h. 28min. to 48 minutes (55 % reduction). These reductions imply as well a reduction of the risk the patients are exposed to. Firstly, as the avoided doses are the last ones, which are the biggest ones, the risk of suffering a severe reaction is lower. Secondly, the medical staff could be warned before the patient gets sick, so they could have acted faster with the use of this algorithm, reducing again the risk of the OFC.

Using only the 60-second epoch, the algorithm developed by Niall Twomey did not get any false positive as well, and detected correctly all the allergic subjects but numbers 1, 3 and 13, getting Se=86.66%. The mean time gain was 22.26 minutes. Using the 4 epoch together, subjects 3 and 13 were correctly detected, increasing the obtained sensitivity to 93.33%. The time gain was increased to 30.8 minutes with this fusion.

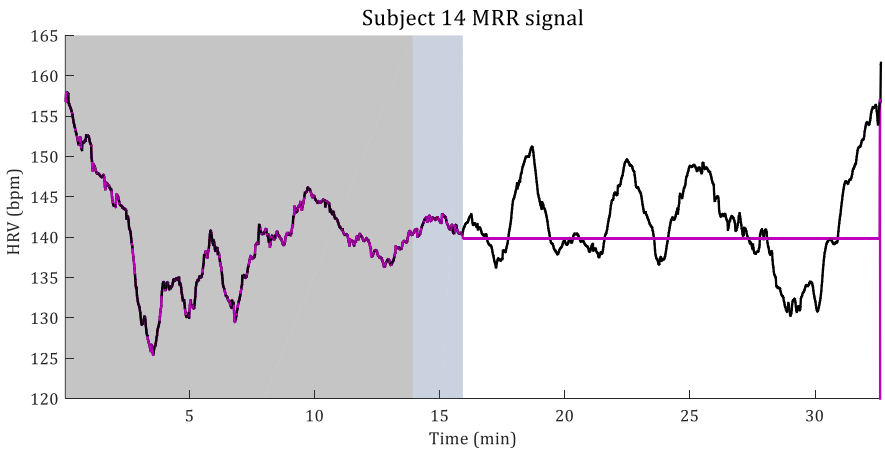

Figure 4.4-1. Subject 18's mean HRV signal during the OFC

4.5 Conclusions

Oral Food Challenge is the definitive test for food allergy. The findings explained in this chapter show distinct differences in routinely measurable electrocardiographic signals relating to heart rate variability that appear unique to subjects whose OFC is positive, not being seen in OFC negative subjects. This retrospective study has suggested HRV is perturbed before objective, evaluable clinical signs are noted, in keeping with the original observation, which had prompted this study, relating to simple elevation of heart rate.

A previous work demonstrated that there exist observable differences between the HRV of an allergic and a non-allergic subject. In that work, classification techniques were used to analyse 18 features of the HRV. A novel detector was designed and it was possible to get 100% of sensitivity and 93.33% of specificity, reducing the length of the tests by 39 minutes and 30% the number of total doses. However, a single model for all the patients was not proposed and the designed classifier was not able to work during real OFCs due to its computational complexity.

Once it is known that the presence of an allergic reaction influences the HRV, it is possible to eliminate uninformative features to simplify the allergic detection algorithm. Six statistical computations of each feature were performed: mean, median, mode, range, standard deviation and interquartile range. The diagnostic ability of each one of these statistical parameters for each feature has been obtained by calculating their t-value, p-value and AUC. These analyses demonstrated that only the *Mean* feature provides useful information regarding the physiological changes produced by an allergic reaction. The comparison between the p-value, t-value and AUC of its statistics confirm the standard deviation (p-value < 0.0001; t-value: 4.653; AUC=0.958) as the best indicator of the presence of allergic reactions.

The reduction of the information needed to detect an allergic reaction has led to the proposal of a new real-time allergy detection algorithm. The designed algorithm improves the first proposal in at least two significant ways: firstly, it uses only one feature of the HRV, which reduces the computational complexity; and, secondly, is completely subject-independent. By using this algorithm, none of the non-allergic patients were misclassified, getting 100% of specificity; and 13 out 15 allergies were detected (Se = 86.66%). Only 60 % of the total number of doses used in real-tests would be required, which implies a 40% reduction of the mean tests length.

The reduction of the computational resources and time needed would enable the development of a user-friendly commercial portable device to implement the proposed algorithm. This device could be composed of a heart rate monitor and a smart phone (tablet, laptop or PC) through which the medical staff can be aware of the patient's HRV changes.

The implementation of HRV assessment and its use in termination of OFC - before the final largest doses are given - could shorten OFC thereby making them safer and more acceptable to hospital units who do not currently offer them to patients, who often worry about OFC safety. It is important to bear in mind that the size of each dose is double that of the previous one, which means that reducing 60 % the number of doses imply a great reduction of the quantity of allergen that the allergic patients need to consume. Thus, the proposed allergy detection algorithm reduces considerably the risk of the allergic patients during the provocation tests.

The allergy detection algorithm proposed in this chapter is based on the data extracted from the HRV signal of 23 subjects performing allergy provocation tests to food allergens. This number of subjects is not enough to establish a behaviour pattern for the whole population. In addition, the conditions in which the patients are during these tests vary depending on the hospital. In the next chapter, a new database is used with which, even the patients have similar features (children exposed to food allergens), the results of the allergy detection algorithm change due to other factors.

Chapter 5.

ARTEFACT DETECTION AND POSITIONING

Chapter 4 proposed a real-time allergy detection algorithm that has been designed based on the information extracted from 23 ECG signals belonging to children undergoing OFCs. Although the algorithm needs to be tested with more subjects, it has been shown that the effect that the allergies have on the HRV of allergic subjects can be detected thanks to the proposed algorithm. However, the ECG signals used for the design of the algorithm belong to children who were required to remain on a bed during the OFCs. As was explained in chapter 2, the HRV can be affected by several factors, with one of the most important for our goal, being the physical activity carried out by the patients.

This chapter introduces a new dataset, which is used as "testing dataset" for the allergy detection algorithm. This new trial was carried out in a different hospital, in which a different protocol is followed during the OFCs. The main difference is that the patients of the second dataset were allowed to move freely. As will be explained in Section 5.3, some categories of movement have an effect on the HRV signal that is quite similar to those provoked by allergic reactions. For this movement, the algorithm misclassifies these events, increasing the number of false positives. To face this new challenge, two approaches based on the measurement of the subjects' movement are proposed in this chapter.

5.1 Introduction to the new trial

A collaboration has been established with the Allergy Section of the Guadalajara University Hospital (GUH) in order to collect new data. This Allergy Section performs an average of 15-20 provocations test every week. However, these tests are not only carried out on children but also adults and not only for food allergens, but also for drug allergy. The required ethical approval from the Ethic Board was obtained to record the ECG of patients exposed to the allergy provocation tests (**Appendix E**). Patients (or legal guardian, if they are underage) willing to participate in the data collection had to sign an informed consent (**Appendix F**).

The provocation tests at the GUH are carried out using the following steps:

1. When the patient arrives to the hospital, his/her health status is checked by measuring his/her blood pressure, heart rate and blood oxygen saturation.
2. The nurses place the Shimmer device on the patient and place the electrodes to allow the ECG to be recorded.
3. A dose of the substance is then divided into several portions of different sizes. Usually, each portion is a half of the next one, the maximum being a half of the whole dose. The number of doses depends on the kind of allergen and the subject's features and clinical history. Usually, the food is divided into 6-7 portions, and drugs into 3.
4. The medical staff give the smallest portion to the subject.
5. For a time interval of 30 minutes (if the allergen is food or certain kind of drugs) or 60 minutes (for the rest of the drugs) the subject remains under observation. If the subject does not show any symptom, the next dose is given to him/her.

When all the doses are finished, the subject remains under medical observation for a further 2 hours and then the Shimmer device is removed. If the patient does not react to the allergen during the provocation test or in the following 24 hours, he/she is classified as non-allergic; otherwise, his/her symptoms are treated and the patient is diagnosed as allergic.

5.1.1 Differences between protocols

As previously indicated, there are some important differences between the protocols followed by the Cork University Hospital (CUH) and the Guadalajara University Hospital (GUH) performing the provocation tests. These differences should be taken into consideration since they modify

significantly performance of the algorithm presented in Chapter 4. The main differences between both protocols are the following:

- Target of the test: At CUH only provocation tests to food allergies in children are performed, while at the GUH, these tests are carried out on both children and adults (every patient older than 12 years). In addition, the provocation test to drug allergies in both children and adults is carried out. This fact provides the opportunity to check the proposed algorithm in those new groups.
- Inclusion criteria: If there is a relative high probability that a patient is allergic, at the GUH they diagnose the allergy and do not carry out the test, trying to minimize the risk of a severe reaction. In the same situation at the CUH they do the provocation test in order to avoid false positives. For this reason, the prevalence of allergic subjects undergoing OFC at the CUH is higher.
- Length of the observation periods: At the CUH the observation periods lasted for 10 to 20 minutes, while at the GUH they usually last for 30 minutes when the allergen is food (30 to 60 minutes when it is a drug).
- Status of the patients: During the observation periods, the patients were required to stay seated and relaxed in the CUH, whereas at the GUH the patients can move freely, provided they do not leave the room. In fact, the children have a "play corner".

From these differences, only movement will result in a significant change in the results, compared to those presented in Chapter 4, whereas the effect of age and allergen on the HRV is investigated in Chapter 6. The movement affects directly the observed physiological parameter, resulting in the HRV changing due to other factors than an allergic reaction. Due to this fact, it will be necessary to detect which HRV variations are provoked by which event.

5.1.2 Data collection set-up

A Shimmer device (Figure 5.1-1, [Shim00a]) was employed for collecting the data during the provocation tests. This device is able to store the measured data in its internal memory card. Furthermore, it measures and stores the data acquired by the internal inertial sensors: 3-axis accelerometer, 3-axis gyroscope and 3-axis magnetometer. For all the signals, the sampling frequency F_s has been set to 256Hz. The main advantage of this system is that once the devices are attached, the patients can move freely. At the end of the tests, the measured data are extracted from the SD cards of the Shimmers and analyzed.

During this data collection at the GUH, the ECG signal for 154 tests was measured, from which 147 were valid. The rest of the signals were discarded because, due to different problems during the measurement (like electrodes detachment), the ECG signals were so corrupted by artefacts that the HRV signal could not be obtained from them. The ECG signals belong to 20 children performing food provocation tests, and 8 drug provocation tests; and 8 adults performing food provocation tests, and 111 drug provocation tests.

Due to the fact that the algorithm presented in Chapter 4 was developed for children exposed to food allergens, the performance of the algorithm on this GUH subgroup will first be assessed. In this case, the testing set is composed of 20 subjects from which 8 resulted in a positive reaction. Table 5.1-1 summarizes the main features of each one of these tests. Due to the fact that the observation periods are longer at the GUH, it can be seen that the mean length of the tests is longer than those from the CUH (1h. 25 min. at CUH) while the mean number of doses is slightly smaller (4.5 at CUH).

TABLE 5.1-1. FEATURES OF THE NEW DATASET

ID	Age	Gender	Allergen	OFC length	Total doses	Result
GU042	3 years	M	Hake	2h. 55min.	2	Allergic
GU053	6 years	M	Egg	0h. 43min.	1	
GU074	5 years	M	Egg	2h. 05min.	3	
GU085	5 years	M	Egg	0h. 30min.	1	
GU091	1 year	F	Milk	4h. 59min.	6	
GU113	8 months	M	Milk	3h. 30min.	6	
GU138	6 years	F	Milk	4h. 15min.	6	
GU178	18 months	F	Milk	2h. 00min.	4	
GU045	12 years	F	Nectarine	3h. 46min.	4	Non-allergic
GU051	7 years	F	Salmon	3h. 35min.	4	
GU056	3 years	M	Milk	3h. 20min.	5	
GU069	3 years	M	Omelet	3h. 17min.	4	
GU080	8 years	M	Tuna	3h. 50min.	4	
GU082	4 years	M	Omelet	3h. 45min.	4	
GU088	12 years	M	Dory	3h. 33min.	4	
GU106	2 years	F	Omelet	2h. 25min.	1	
GU107	8 years	F	Egg	5h. 40min.	7	
GU118	8 years	M	Omelet	3h. 58min.	4	
GU147	5 years	M	Milk	4h. 59min.	7	
GU151	3 years	M	Milk	4h. 23min.	5	
Total	**5.2 ± 3.3 y**	**35% F, 65% M**		**232.4 ± 150.2 min.**	**4.1 ± 1.8**	

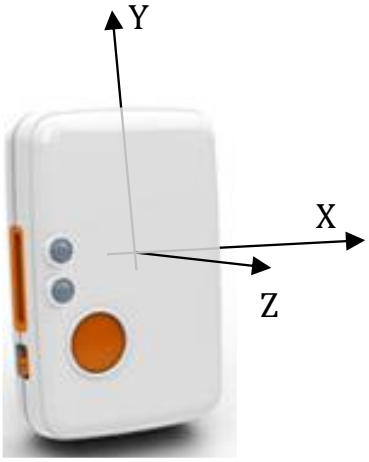

Figure 5.1-1. Shimmer3 unit and orientation of the inertial sensors

5.2 Test of the Allergy Detection algorithm

Choosing the configuration set in Chapter 4 for the allergy detection algorithm for the new data set, 7 out of 8 allergic patients are detected, Se=87.5%; and 4 out of 12 non-allergic patients are correctly classified, getting a Sp=33.3%.

Table 5.2-1 summarizes the results obtained with each subject. Taking into account only the allergic subjects, the number of allergen doses that could be avoided is 12 out of 29 (more than 40 %), with a mean length reduction of 80.88 min. out of 157.12 minutes (more than 50%).

Figure 5.2-1 shows the normal *PDF* of the standard deviation of the *Mean* HRV obtained for the allergic and non-allergic groups of the two datasets. It can be noticed how the new two groups are more similar between them than the original ones. Due to this increase of their similarities, *t-value* has decreased from 4.653 to 2.274; and *p-value* increased from less than 0.0001 to 0.0355, which lead to the reduction of the confidence level from 99.9% to 95%. The AUC has reduced as well, from 0.94 to 0.79 as depicted in Figure 5.2-2. GU053 is the only allergic subject that was not detected. As can be seen in Figure 5.2-3, the *MRR* signal during the observation period has similar features than during the background interval. As a consequence, the maximum *MeanPeak* of this subject is 6.29 which is much lower than the threshold set in the last chapter (*Th=10.5*).

TABLE 5.2-1. RESULTS OBTAINED WITH THE NEW DATASET

ID	Age	Gender	Allergen	OFC length	Total doses	Result	Algorithm result	Doses saved	Time gain
GU042	3 years	M	Hake	2h. 55min.	2	Allergic	TP	0	0h. 48min.
GU053	6 years	M	Egg	0h. 43min.	1		FN	0	0h. 00min.
GU074	5 years	M	Egg	2h. 05min.	3		TP	0	0h. 00min.
GU085	5 years	M	Egg	0h. 30min.	1		TP	0	0h. 43min.
GU091	1 year	F	Milk	4h. 59min.	6		TP	5	4h. 08min.
GU113	8 months	M	Milk	3h. 30min.	6		TP	5	2h. 36min.
GU138	6 years	F	Milk	4h. 15min.	6		TP	2	2h. 29min.
GU178	18 months	F	Milk	2h. 00min.	4		TP	0	0h. 03min.
GU045	12 years	F	Nectarine	3h. 46min.	4	Non-allergic	TN	0	0h. 00min.
GU051	7 years	F	Salmon	3h. 35min.	4		TN	0	0h. 00min.
GU056	3 years	M	Milk	3h. 20min.	5		FP	4	2h. 38min.
GU069	3 years	M	Omelet	3h. 17min.	4		FP	0	0h. 00min.
GU080	8 years	M	Tuna	3h. 50min.	4		FP	2	2h. 35min.
GU082	4 years	M	Omelet	3h. 45min.	4		TN	0	0h. 00min.
GU088	12 years	M	Dory	3h. 33min.	4		FP	3	3h. 00min.
GU106	2 years	F	Omelet	2h. 25min.	1		FP	0	0h. 27min.
GU107	8 years	F	Egg	5h. 40min.	7		FP	1	2h. 06min.
GU118	8 years	M	Omelet	3h. 58min.	4		FP	3	3h. 34min.
GU147	5 years	M	Milk	4h. 59min.	7		FP	5	3h. 49min.
GU151	3 years	M	Milk	4h. 23min.	5		TN	0	0h. 00min.

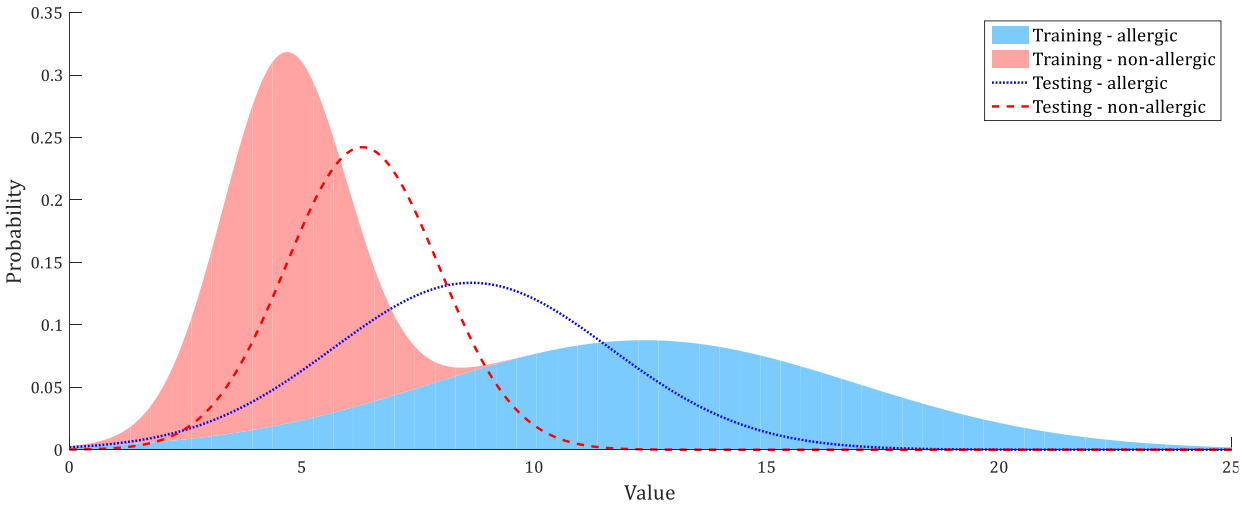

Figure 5.2-1. PDF of the standard deviation of the MRR for the training and testing datasets

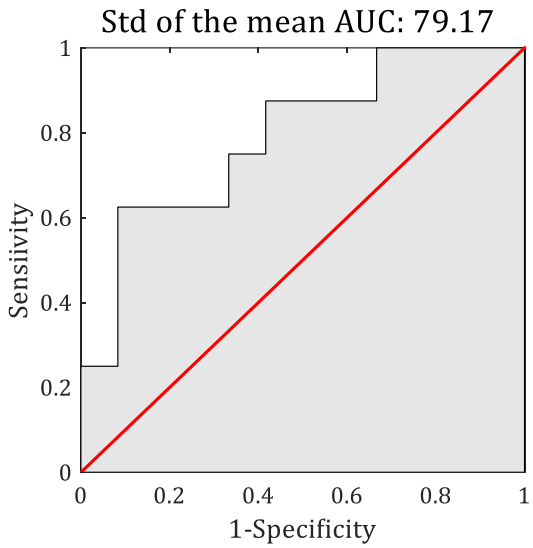

Figure 5.2-2. ROC of the standard deviation of the new dataset

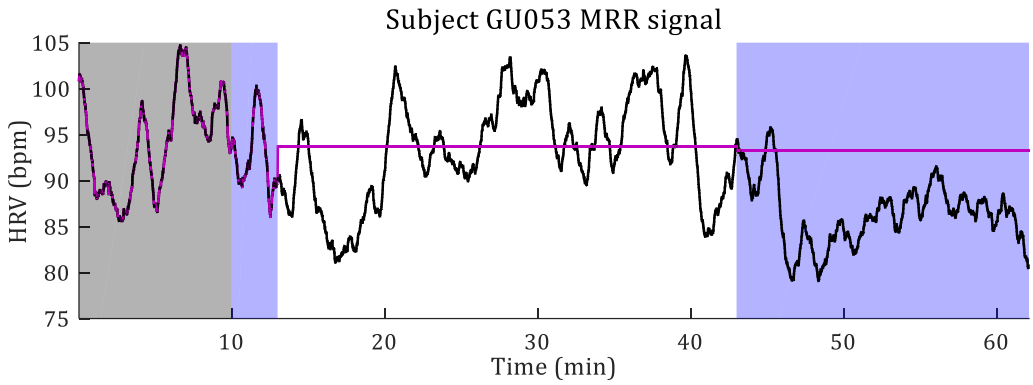

Figure 5.2-3. MRR signal of the subject GU053

Two special cases are GU042 and GU091. These two subjects resulted positive but suffered delayed reactions. Subject GU042 took a new dose of the allergen 6 hours after the end of the OFC at his house. This last portion was bigger than the two taken during the OFC and he reacted to this dose. Therefore, even though no physical symptom appeared during the OFC, the algorithm was able to detect the allergy 72 minutes after the intake of the last dose. Subject GU091 had 6 doses of milk during the OFC and did not present any allergy symptom until 10 hours after the end of the test. The algorithm detected an allergy 4 times during the OFC: once 30 minutes after the first dose, twice after the fourth dose (10 and 24 minutes after); and the fourth reaction 12 minutes after the last dose. In these two cases, the length of the tests could have been reduced from the normal ending (two hours after the intake of the last portion) to the instant in which the algorithm detected the allergen. In these two cases, the appearance of the delayed reactions could have been predicted with the use of the algorithm and the doctors could have prevented the symptoms.

However, there is an unexpected increase of the false positives. It is believed that this increase is due to the fact that the patients were moving during the OFC, rather than for the change on the length of the observation periods. It is known that the physical activity produces an increase of the heart rate, which is reflected in the HRV signal. For this work, the variations of the HR due to other factors than allergic reactions can be considered artefacts. From now on, the effect that the movement has on the HRV signal will be called *motion artefact*, and one the objectives is the reduction of its effect on the HRV signal for improving the accuracy of the allergy detection algorithm.

5.3 Movement artefact reduction

Although there are several factors that can modify the heart rate of a subject, under the circumstances in which the provocation tests are executed, the most important factor affecting the heart rate (aside from the allergic reactions) is the physical activity performed by the subjects. When a subject changes its posture from lying to seated, from seated to standing, from standing to walking, when he/she walks, runs, goes upstairs, etc. variations appear on the measured HRV.

Figure 5.3-1 represents an example of the mean HRV of a healthy individual doing diverse physical activities. A Shimmer device was used to record the ECG signal (F_S=256 Hz), and the proposed QRS complex detection for obtaining the HRV was used. It can be observed that a peak of increase 20 bpm was produced when the subject went from standing to walking, which is likely to be confused as an allergic reaction. When the individual walked upstairs, the mean heart rate increased by more than 50 bpm and then it decreased by more than 70 bpm when the subject sat down again.

Two approaches are proposed next for taking into account movement in the allergy detection algorithm. The first one is based on the measurement of the quantity of movement, and the second one on the detection of the activity and posture of the subject.

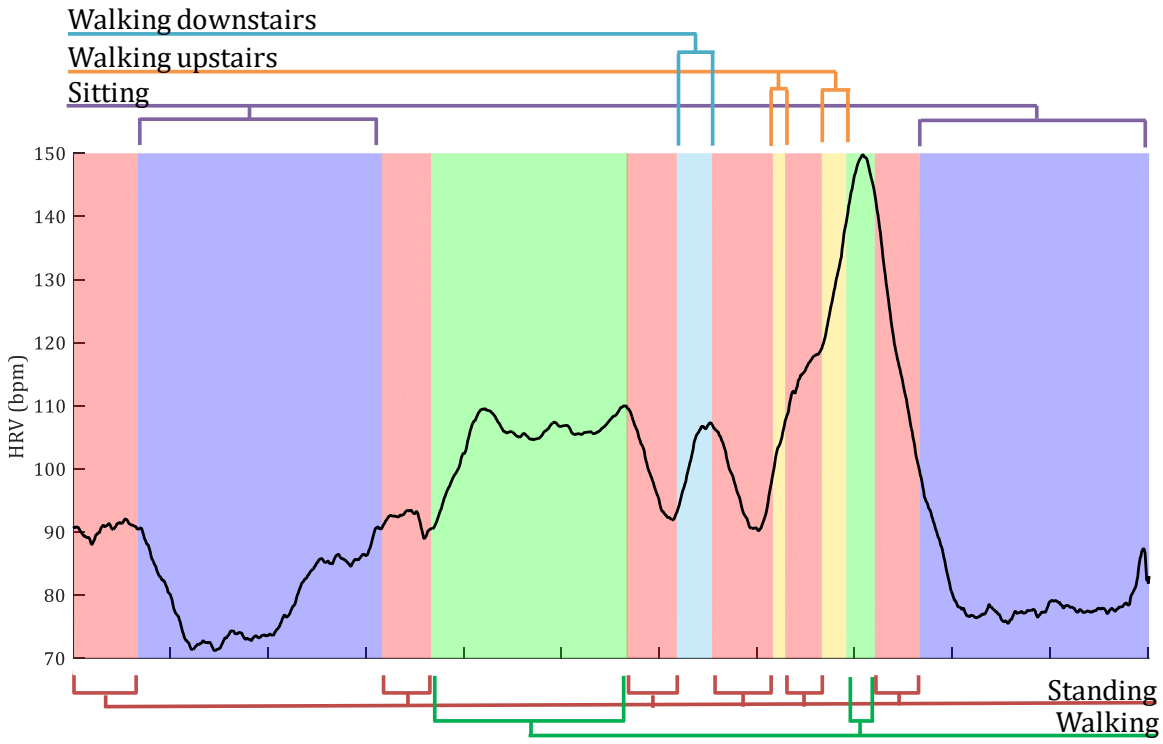

Figure 5.3-1. Example of MRR signal variations depending on the subject's physical activity or posture: standing (red), sitting (purple), walking (green), walking downstairs (cyan) and walking upstairs (orange).

5.3.1 First approach: Measurement of the chest movement

This approach results from the hypothesis that the increase of the HRV is directly proportional to the quantity of movement of the patient. Mathematically, this means that for each unit of movement, the heart rate is increased a fixed number of beats. The factor representing the number of beats per unit of movement has been called *GAcc* (beats/G). In this work, it will be considered that this factor is the same for all the patients of the database. The more similar the patients are, the truer is this assumption. In this case, all the subjects are healthy children aged 12 or less, so their health condition should be similar and so, the response of their heart to the same stimulus. It has been considered as well that this movement can be measured in the centre of the body. For this reason, the position in which the Shimmer was placed for acquiring the ECG (trunk) has been used to measure the movement.

The same device was used to get the acceleration and the ECG signals, so the same sample frequency was used for both measurements, F_S = 256 Hz. Figure 5.3-2.a) shows the MRR signal of the subject GU069. It can be seen that, even if the patient is not allergic, a *MeanPeak* is produced

starting at minute 170 (approx.) whose value is higher than the threshold. As a result, this patient is classified as allergic by the algorithm. Figure 5.3-2.b) represents the root mean square of the 3-axes acceleration (*eq. 5.1*).

$$Accel = \sqrt[2]{Acc_X{}^2 + Acc_Y{}^2 + Acc_Z{}^2} \qquad (eq.\ 5.1)$$

Accel measures the linear acceleration of the subject's chest avoiding the dependency with the shimmers orientation during the measurement. The mean *Accel* signal has been computed in 60-seconds windows with 1-second shift, in the same way that the *MRR* signal is extracted from the HRV. In this way, it is possible to compare both signals, as they represent two magnitudes measured using the same timing. As can be observed, there are several similarities between both signals and most of the times the *Accel* signal changes, the MRR signal changes proportionally. Specifically, during the interval that provokes the false alarm, there is a high rise of the *Accel* signal, which provokes a rise of the MRR signal with a similar shape.

Finally, Figure 5.3-2.c), shows the resulting signal of subtracting from the *MRR* signal 50 beats per unit of acceleration (i.e. *GAcc=50*). With this value of *GAcc*, the corrected *MRR* signal during periods of high movement is lower than in other periods, so the value of *GAcc* should be lower.

In order to set the configuration of the algorithm, an accuracy test has been carried out (based on sensitivity –*eq. 4.1*- and specificity –*eq. 4.2*- values) using 50 values of *GAcc* (from 1 to 50) and 151 values of *Th* (from 5 to 20 in 0.1 steps). Figure 5.3-3 illustrates the obtained results. It is necessary to reach a trade-off between both parameters since, as can be seen in Figure 5.3-3, a high sensitivity implies a small specificity and vice versa. With a large value of *Th*, the algorithm classifies many patients as non-allergic, reducing the number of positives (true and false); on the contrary, if the value of *Th* is small, most of the subjects are classified as allergic, which increases the sensitivity and reduces the specificity.

The combinations of *GAcc* and *Th* that provide the best sensitivity (100%), only one of the non-allergic subjects is correctly classified (Sp=8.33%). Conversely, the maximum sensitivity obtained with 100% of specificity is 50%. The best mean between both metrics that it is possible to obtain is 89.58%, which implies 87.5% of sensitivity (7/8 allergic detected); and 91.67% of specificity (11/12 of the non-allergic correctly classified). The combinations of *GAcc* and *Th* that lead to these results are the ones coloured in blue in the Figure 5.3-4.

Another factor to optimize is the time reduction in the OFC test that can be achieved using the algorithm. This parameter has been evaluated with all the combinations that lead to obtain the maximum mean between the sensitivity and the specificity (Figure 5.3-4). Based on these results, the best combinations within those that provide the best mean (Se, Sp) are (*Th*; *GAcc*) = {(9.5; 31), (9.6; 31)}. These combinations are coloured in dark blue in Figure 5.3-4. Table 5.3-1 lists the results obtained when setting *Th*=9.5 and *GAcc*=31.

Figure 5.3-5 represents the maximum *MeanPeak* of each subject before and after the artefact reduction. Most of the maximum *MeanPeaks* have been reduced using the measurement of the chest movement to reduce the false positives. However, *MeanPeaks* of the non-allergic are now more similar to each other, with the exception of subject GU118, whose value is still higher than without the movement artefact reduction.

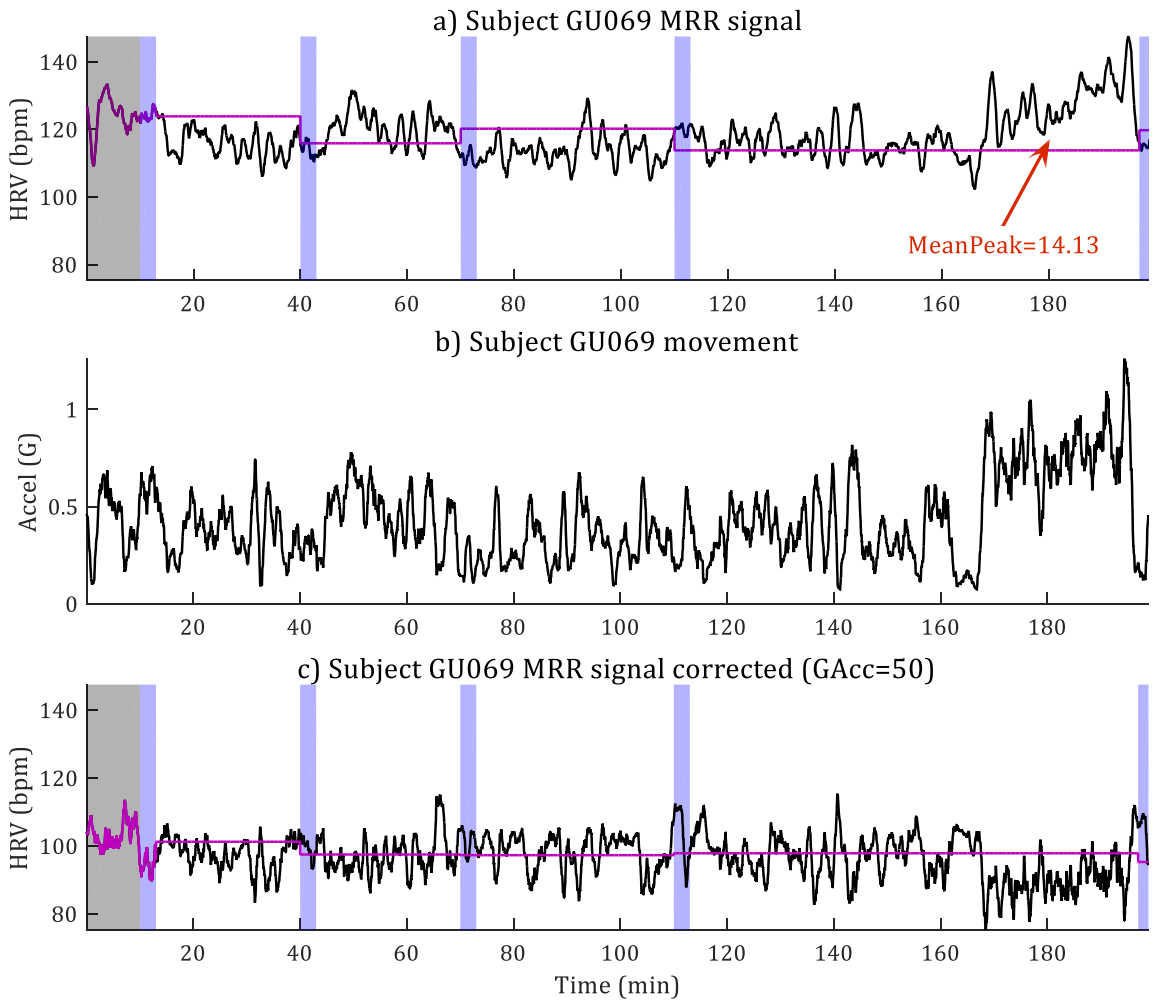

Figure 5.3-2. Example of False Positive due to the presence of movement artefacts. a) MRR signal of the Subject GU069; b) Movement of the subject; and c) MRR signal corrected with the movement with GAcc=50

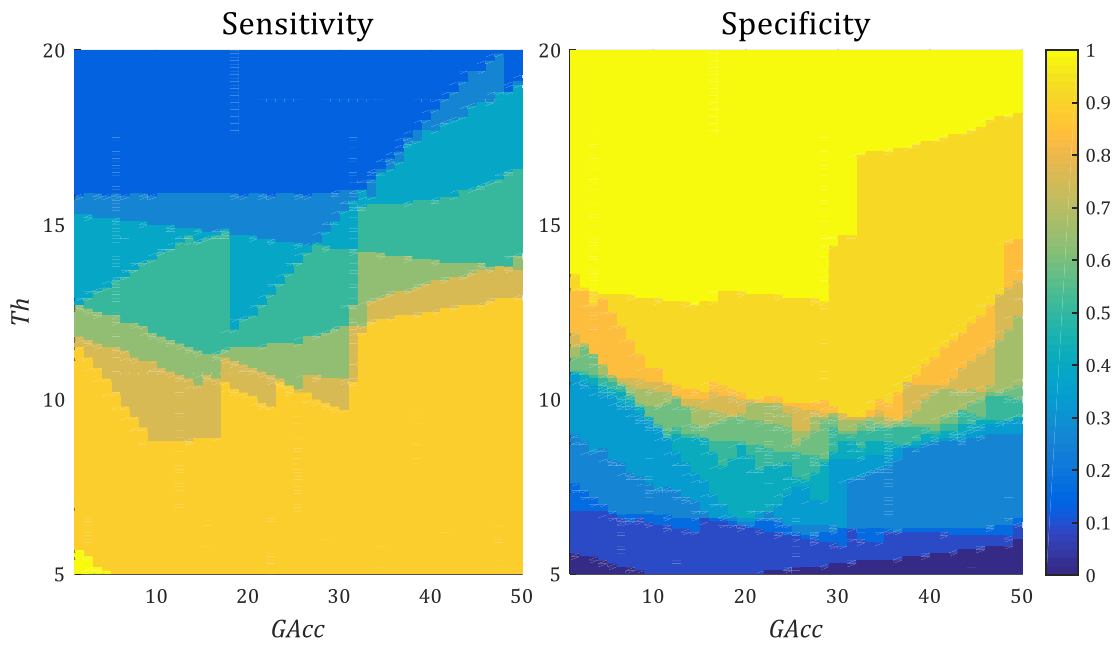

Figure 5.3-3. Sensitivity and Specificity obtained depending on GAcc and Th values

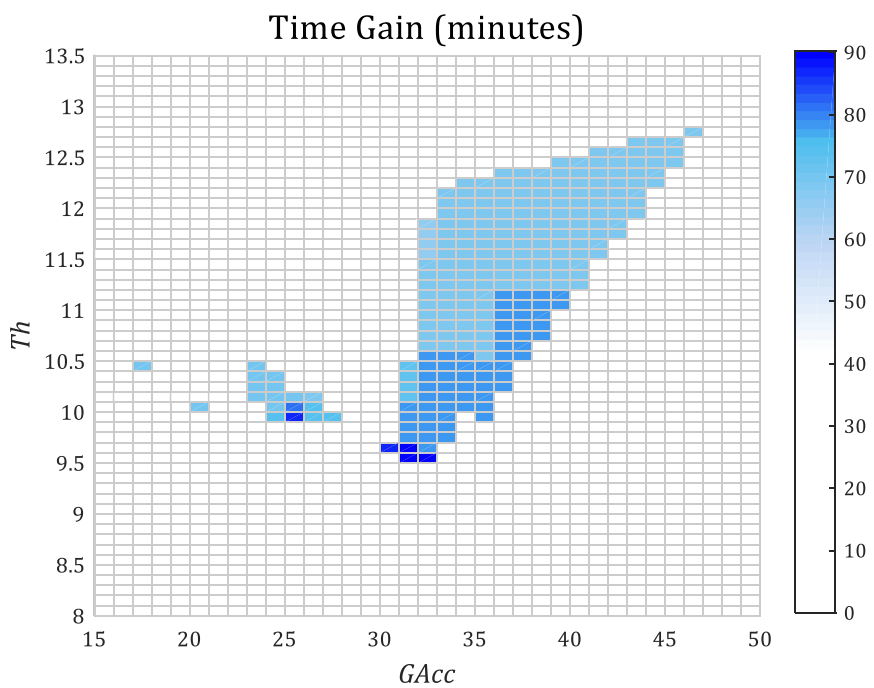

Figure 5.3-4. Time gain obtained with several combinations of GAcc and Th parameters

TABLE 5.3-1. RESULTS OF THE ALLERGIC REACTIONS DETECTION ALGORITHM WITH THE ARTEFACT REDUCTION

ID	OFC length	Total doses	Result	Algorithm result	Doses saved	Time gain
GU042	2h. 55min.	2	Allergic	TP	0	0h. 51min.
GU053	0h. 43min.	1		FN	0	0h. 00min.
GU074	2h. 05min.	3		TP	0	0h. 36min.
GU085	0h. 30min.	1		TP	0	0h. 00min.
GU091	4h. 59min.	6		TP	5	4h. 08min.
GU113	3h. 30min.	6		TP	5	2h. 36min.
GU138	4h. 15min.	6		TP	2	2h. 29min.
GU178	2h. 00min.	4		TP	0	0h. 02min.
GU045	3h. 46min.	4	Non-allergic	TN	0	0h. 00min.
GU051	3h. 35min.	4		TN	0	0h. 00min.
GU056	3h. 20min.	5		TN	0	0h. 00min.
GU069	3h. 17min.	4		TN	0	0h. 00min.
GU080	3h. 50min.	4		TN	0	0h. 00min.
GU082	3h. 45min.	4		TN	0	0h. 00min.
GU088	3h. 33min.	4		TN	0	0h. 00min.
GU106	2h. 25min.	1		TN	0	0h. 00min.
GU107	5h. 40min.	7		TN	0	0h. 00min.
GU118	3h. 58min.	4		FP	3	3h. 36min.
GU147	4h. 59min.	7		TN	0	0h. 00min.
GU151	4h. 23min.	5		TN	0	0h. 00min.
Mean	**3h. 22min.**	**4.1**				

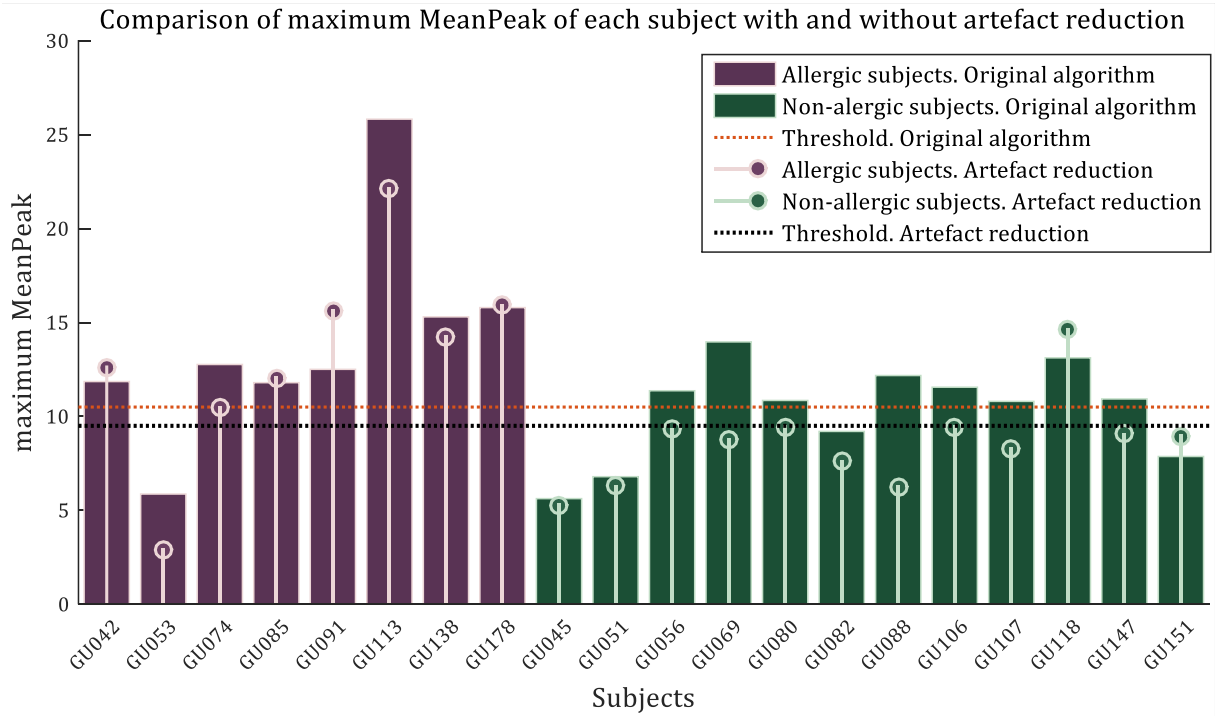

Figure 5.3-5. Maximum MeanPeak value comparison between allergic and non-allergic subjects, before and after the artefact reduction

Figure 5.3-6 shows the mean HRV of the subject GU118 during the OFC corrected with the measurement of the movement. The measurement of its movement during the same time is depicted in Figure 5.3-7. The HRV of this patient increased from the beginning of the test until the minute 120 by almost 40 bpm, while its movement was similar during the whole test. Thus, there is an increase of the HRV but it is not due to the movement, so the algorithm it is not able to correct this variation and classify this subject as allergic (false positive).

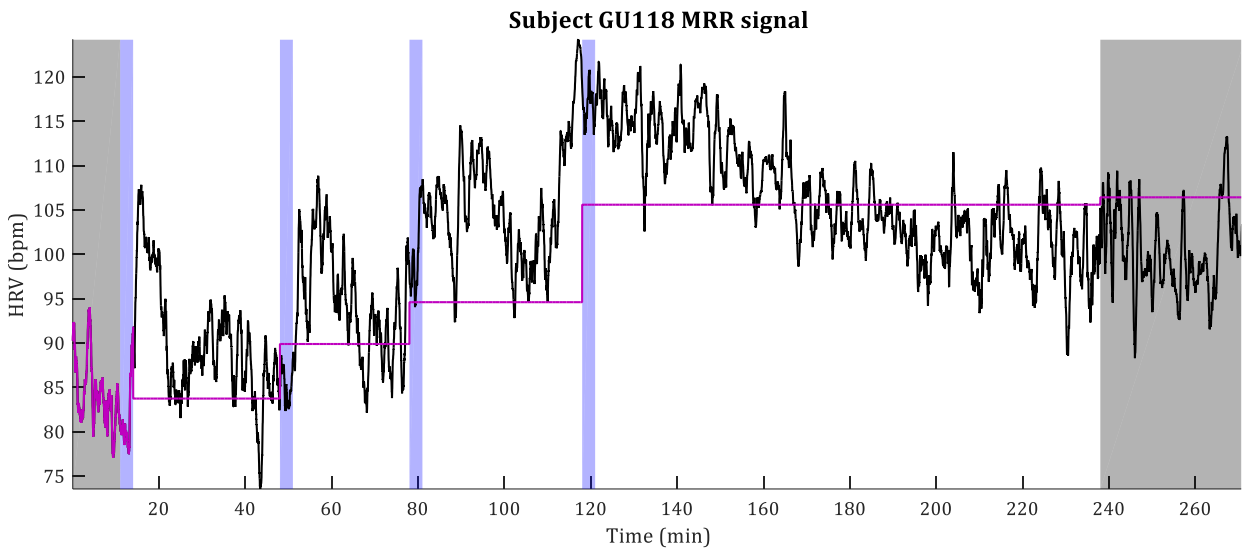

Figure 5.3-6. MRR of the subjects GU118 during the OFC, corrected using the chest movement

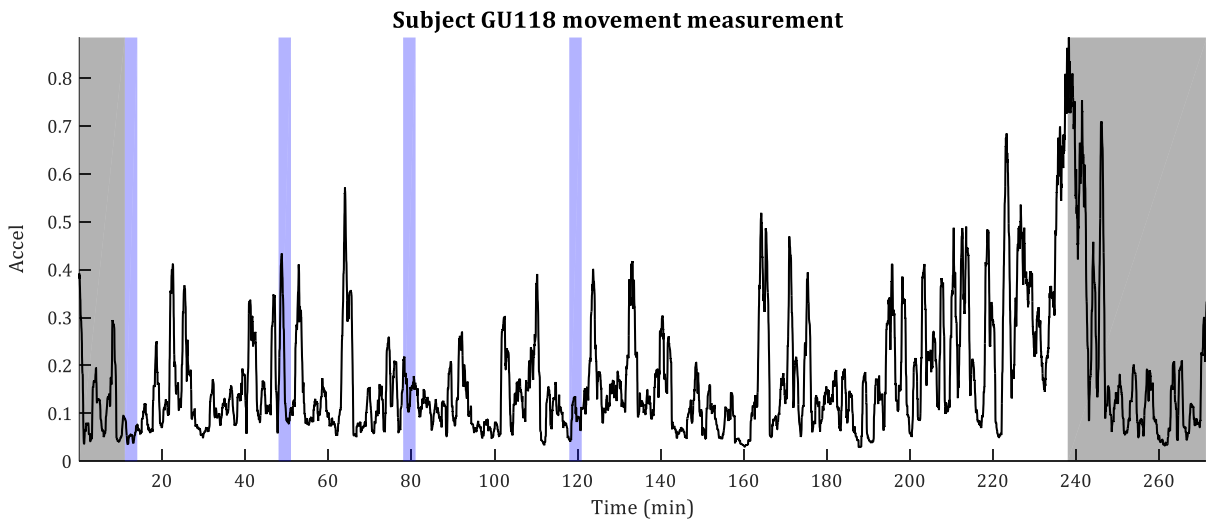

Figure 5.3-7. Accel of subject GU118 during the OFC

5.3.2 Second approach: Detecting subject posture and activity

In the previous section it has been demonstrated that the hypothesis that the movement affects the HRV of the patients analysed here in a similar way is correct. However, if the allergy detection algorithm should be used with a different group of patient, the *GAcc* value should be recalculated based on their physiological differences. The approach presented in this section aims to find a more generic way to remove the movement artefacts, and so the false positives. The hypothesis that leads to this approach is that the movements that provoke larger variations of the HR are the posture changes. If the posture of the subjects is known during the whole test, it is possible to check if it has changed when the allergy detection algorithm produces an alarm. In this approach, if an alarm is generated by the allergy detection algorithm while the subject is changing his/her posture, the false alarm is removed. The Pocket Navigation System proposed by Munoz et al. in [Muno15] will be used to get the information regarding subjects' activity and posture.

5.3.2.1 Pocket Navigation system

The Pocket Navigation System is a personal navigator based on inertial sensors designed to be placed on the upper part of the leg. This location allows the sensor either to be directly introduced in the front pocket of the trousers or to be fastened with an elastic band to the leg, as shown in Figure 5.3-8. The Shimmer device used to measure the ECG also contains as described previously, three mutually orthogonal accelerometers and gyroscopes, therefore the navigation system can be used without the need of additional hardware.

Figure 5.3-8. Shimmer allocation for the second approach

This alternative is not compatible with the first approach, as the position of the Shimmer is different and so the way in which the movement is measured. The pocket navigation system, represented in Figure 5.3-9, is divided into two subsystems: hardware and software. The hardware subsystem corresponds to the left box in the figure and consists of the inertial measurement unit (IMU).

The software subsystem refers to the source code represented in Figure 5.3-9 with the outer right box. The inputs of the software subsystem are the measurements from the accelerometers and gyroscopes, and the output is the patient's position and activity. It has two main parts: the orientation estimation and the position estimation. First block is based on an unscented Kalman Filter (UKF) [Foxl05] whose states are the Euler attitude angles roll (φ) and pitch (Θ) and the heading angle yaw (ψ), defined as depicted by Figure 5.3-10; and the biases of the gyroscope, which are the out values of the gyroscope when it is not moving and should be corrected. The UKF prediction stage integrates the turn rate measurements and applies an autoregressive model for the biases. The UKF update stage makes use of the accelerometer and the gyroscope measurements to correct the orientation and the biases estimation. In [MPJZ15], a detailed explanation of the orientation estimation is given.

The position estimator consists of three algorithms: the step detector, the step length estimator and the vertical displacement estimator [Muno15, MuGo14]. In order to use this algorithm together with the allergy detector, the sample frequency has been set to 256 Hz, so the inertial measurements are sampled at the same time instant as the ECG signal.

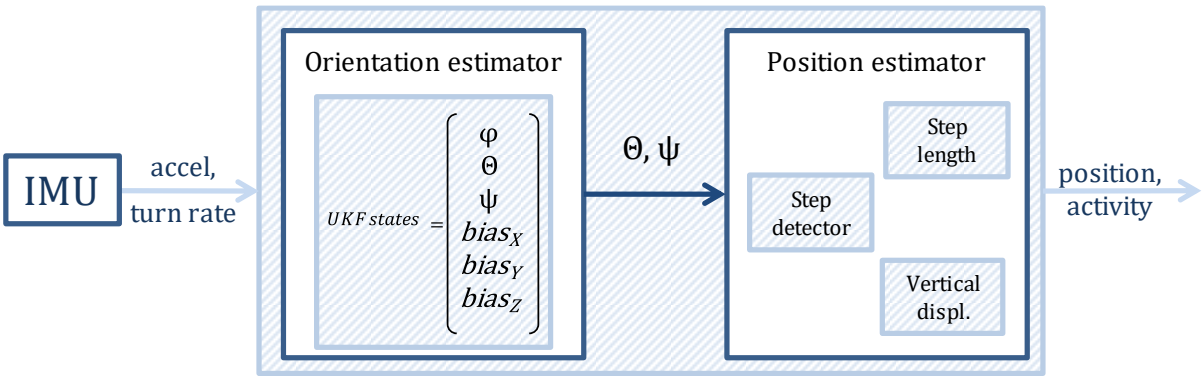

Figure 5.3-9. Block diagram of the inertial pocket navigation system.

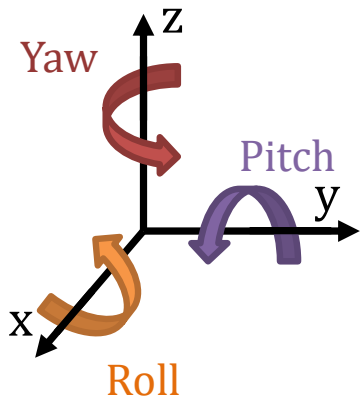

Figure 5.3-10. Roll, Pitch and Yaw angles definition

The pocket navigation system is able to solve 3D positioning by using the aforementioned sensors. The navigation, thus, eliminates the restriction of staying within the same room under the observation of the nurse during the observation periods, which lasts for up to 2 hours, and allows the patient to be located in case of a severe allergic reaction occurring. The pocket navigation system can identify five physical activities, i.e. walking, walking upstairs, walking downstairs, standing and sitting [Muno15]. This set of basic physical activities are the most common activities the patient performs during the provocation tests and, therefore, likely to be confused with allergic reactions.

The pitch angle is used for the posture detection and classification of the physical activity performed by the subjects. Figure 5.3-11 shows an example of the pitch angle estimation during different postures and physical activities. If the subjects are seated, or standing, it remains almost invariable but with different angles (≅ 70° – 90° while sitting; ≅ 0° when standing). Then, the wave form while walking is completely different that the one obtained while the subject is going upstairs or downstairs. The different activities are indicated with colours in the figure.

Even if an inertial navigation system has many advantages, it suffers from long-term errors in the orientation estimation mainly due to the integration of noisy measurements. This error is critical within the provocation tests framework, since they last up to 5 hours. However, doctors and nurses affirm that usually patients are seated most of the time. During these sitting periods the biases of the gyroscope are observable the most of the time, therefore it is possible to keep the orientation error bounded through an accurate biases estimation.

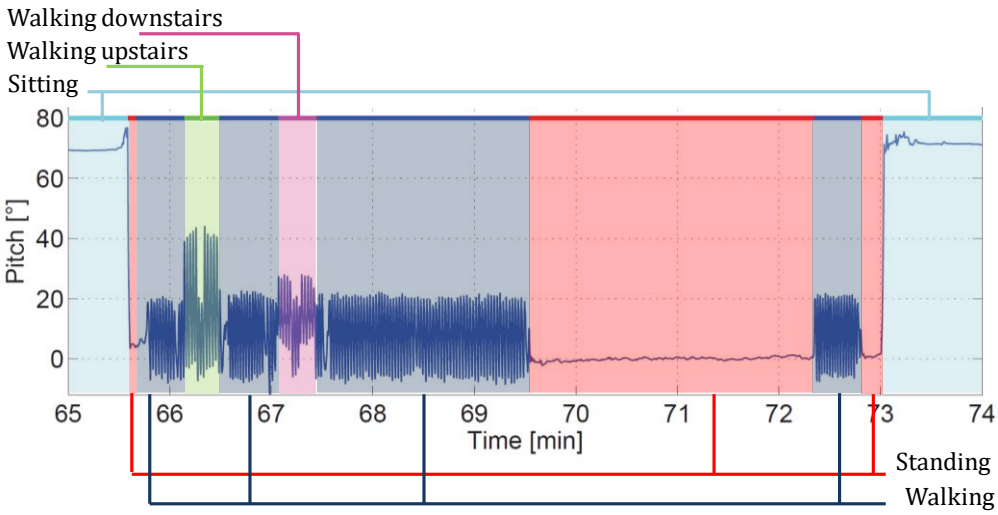

Figure 5.3-11. Example of pitch angle depending on the subject posture and physical activity; (cyan) seated, (red) standing, (blue) walking, (green) walking upstairs and (purple) walking downstairs.

5.3.2.2 Test of the Pocket Navigation System

Test of the physical activity classification and localization ability

A test of the Pocket Navigation System has been carried out at the GUH. In this test, an individual did a representative walk of 10 minutes, in which s/he performed the five activities that the Pocket Navigation System is able to detect. During this experiment, the patient did not take any allergen, so the variations of the HRV are only due to the physical activity. Figure 5.3-12 shows in magenta the trajectory of the patient during the test. The coordinates of the starting point are known, which correspond to the Allergy Unit of the hospital. The initial heading is the direction of the door to leave the room. The patient left the Allergy Unit, which is located on the third floor of the hospital, took the stairs and walked to the restaurant, situated on the ground floor, where s/he queued for a coffee. S/he sat for approximately 1 minute and finally walked back to the Allergic Unit on the third floor.

Figure 5.3-12 shows the stairs up and down as superimposed circular lines. The starting and ending point is the same, as well as the staircase. Therefore, the drift in heading accumulated in the corridor causes a displacement of 4 meters. Figure 5.3-13 shows the pitch angle estimation for the aforementioned walk and the MRR signal measured in beats per minute. The patient's different physical activities are indicated in the figure. As the figure shows, the HRV increases when the patient starts walking and significantly decreases when s/he sits in the restaurant. Moreover, the HRV increases again when the subject starts walking and continues growing because s/he walks upstairs, as expected.

Figure 5.3-12. Trajectory followed by the subject during the testing experiment.

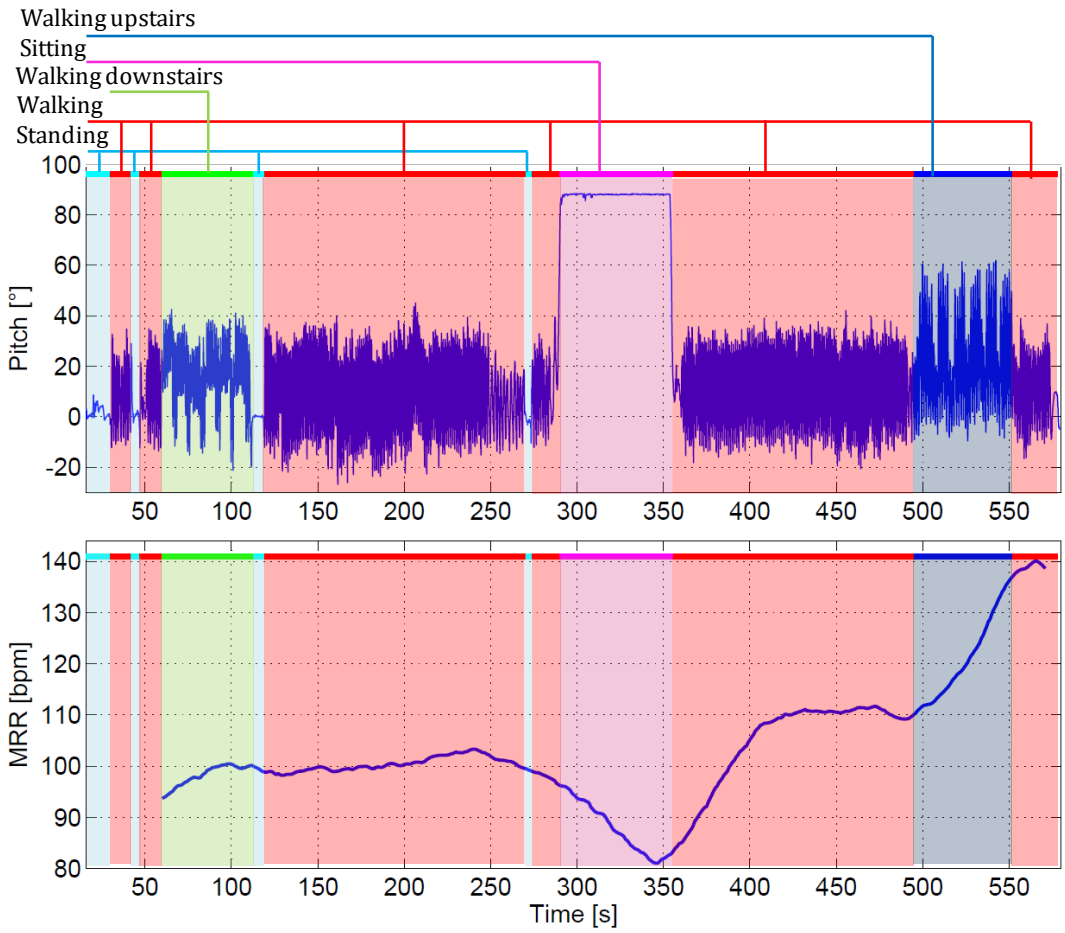

Figure 5.3-13. The upper subfigure shows the pitch angle estimation for the 10-minutes-walk at the hospital. The lower subfigure shows the MRR signal, measured in beats per minute, for the same walk.

Test of the Pocket Navigation system during a provocation test

This system has been tested during a real OFC. The test lasted for 189 minutes, and the subject had 3 doses. This patient resulted in a negative outcome, as he/she did not present any reaction to the allergen. The MRR signal of this subject is showed in Figure 5.3-14. Some *MeanPeaks* appear in the MRR signal which are considered as allergic reactions by the allergy detection algorithm starting on minutes 89, 146, 157 and 159; their values are, respectively, 18.18, 11.52, 17.56 and 14.53 (*Th*=10.5).

However, as can be observed in Figure 5.3-15, Figure 5.3-16 and Figure 5.3-17, these rises of the MRR signal are due to posture changes of the subject from sitting to walking. Between the third and the fourth alarms, the activity of the subject could not be identified by the Pocket Navigation System. However, the change from sitting to walking is correctly detected, which can be used to remove the detection.

This solution makes the result of the algorithm independent of the patient's features. However, in some cases (mainly in the children's tests) the posture of the patient changes many times during the provocations. It should be studied how this kind of filtering affects the cases in which the patient is allergic.

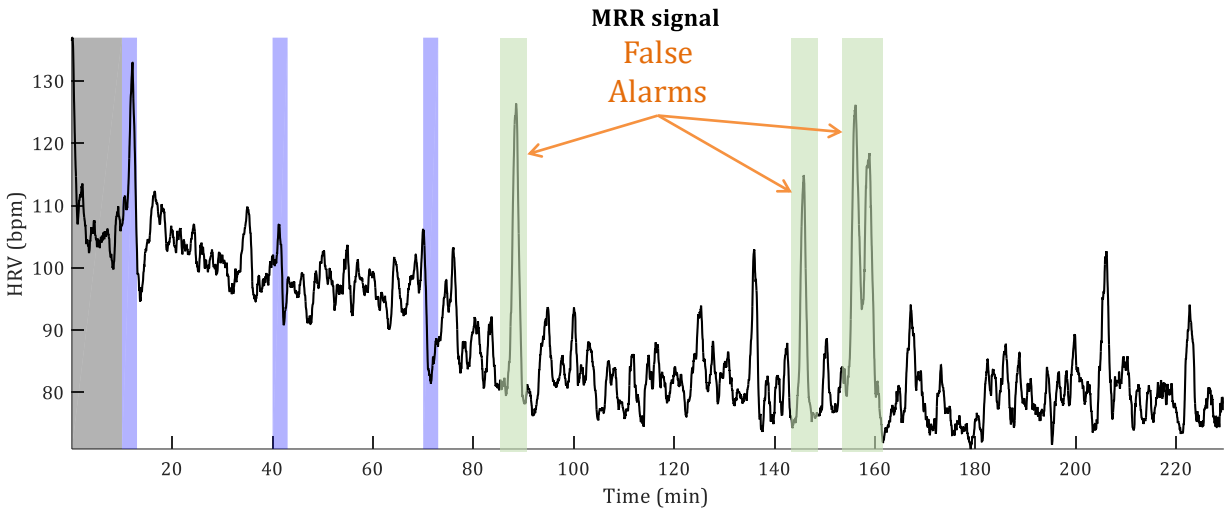

Figure 5.3-14. MRR signal of the subject with which the Pocket Navigation System was tested

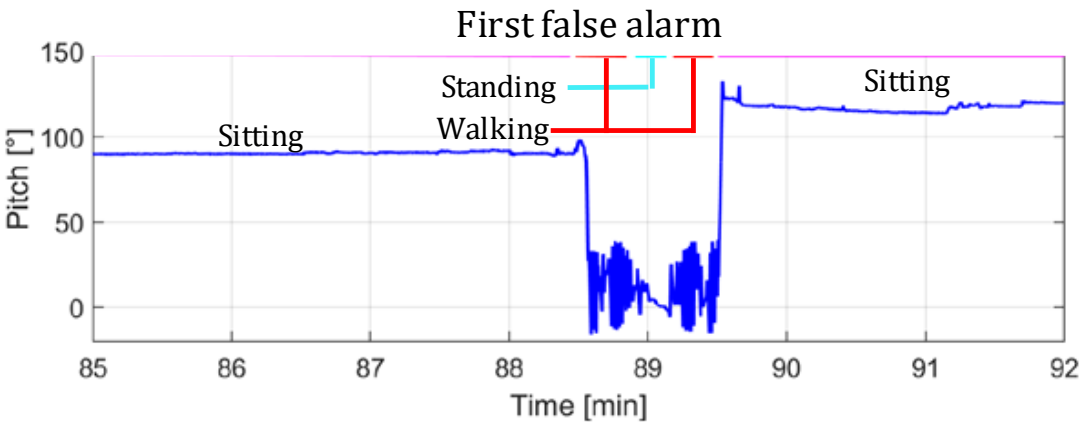

Figure 5.3-15. Pitch angle and physical activity classification during the first false alarm

Figure 5.3-16. Pitch angle and physical activity classification during the second false alarm

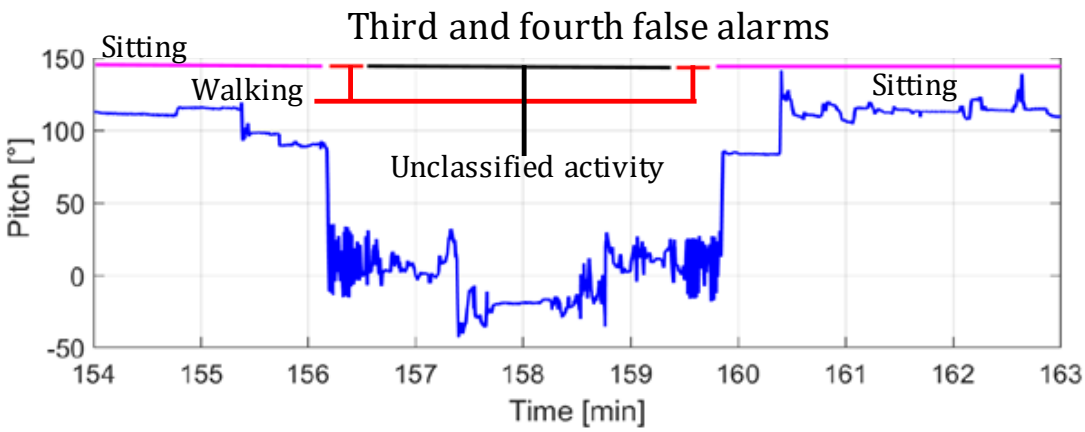

Figure 5.3-17. Pitch angle estimation and physical activity classification during the third and fourth false alarms

5.4 Conclusion

The initial motivation of this chapter was the acquisition of new data for testing the algorithm designed in the previous chapter. However, due to the differences found in the conditions under which the provocation tests were performed for the patients of the new dataset, it was necessary to redesign the original algorithm. It has been shown that the effect that movement has on the mean HRV is similar to that produced by an allergic reaction. For this reason, the preliminary results of the allergy detection algorithm under conditions in GUH show several false alarms when the patients are allowed to move during the OFCs. Thanks to the internal sensors of the Shimmer it is possible to measure how much the subjects move during the tests. However, there are several ways to take into account the movement. Two approaches to remove the movement artefacts have been proposed in this chapter.

The first proposal is based on the measurement of the movement performed by the subjects and correction of the MRR signal. The Shimmer was placed on the trunk of the patients, getting the movement measured on their chest. This approach improves the specificity from 33.33% to 91.67% (from 8 to 1 false detections out of 12 non-allergic subjects). This version shows a clear improvement of the original algorithm, however, its configuration has been tuned depending on the particular features of the new dataset which makes the algorithm specific for these subjects. The number of individuals studied here cannot be considered representative of the whole population. For this reason, the performance of this method should be studied with more patients. It has been assumed for this method that the movement affects in the same manner to all the subjects. This can be considered true if their features are similar, but the proper value of the *GAcc* parameter for patients with different features (such as adults) should be studied and adjusted accordingly.

The second approach is based on the detection of the subjects' posture in order to relate this information with the appearance of allergy alarms. The most important advantages of this proposal are two: first, the algorithm is the same for all the patients; and second, it is possible to locate the patients within the hospital, improving significantly their comfort during the provocation tests, which can last for up to 5 hours. Although the obtained results are promising, it is necessary to check its performance with other patients and further studies need to be done in order to evaluate its suitability for the proposed application. The main weakness of this

approach is that if an allergic subject change his/her posture during the occurrence of an allergic reaction, the alarm would be ignored by the algorithm.

Despite the fact that both approaches are based on the movement to reduce the number of false positives, they cannot be used within the same device. First of all, the Shimmer device needs to be placed in different location for each application and, secondly, the information extracted from the movement is completely different. First approach performs a quantitative analysis (how much the subject is moving), while the Pocket Navigation System does a qualitative analysis (which movement is the subject making). Because of these reasons, two devices need to be used simultaneously for employing the two approaches. Further studies need to be done as well in order to get the best way of fusing the information produced by both systems.

In the next chapter, subjects with different features are analysed: adults and children exposed to food and drugs. The whole group will be divided depending on the age of the subjects and the type of the taken allergen. The features of the groups will be compared in order to find out how the age and allergen affects to the results of the allergy detection algorithm. For the movement artefact reduction, the first proposal of this chapter will be used in Chapter 6.

Chapter 6.

EXTENSION OF THE ALGORITHM APPLICATION

During the data collection carried out at the Guadalajara University Hospital (GUH the ECG signal of children and adults undergoing food and drug allergy provocation tests has been acquired. In the previous chapter, only the children exposed to food allergens were considered. This chapter aims to apply the automated allergy detection algorithm to all the subjects and to study the differences between this group and the rest of the subjects.

The designed allergy detection algorithm is based on the response of the heart to the presence of allergens. In this chapter, the first proposal for the reduction of movement artefacts will be used. For the designing of this approach it was assumed this response of the heart would be the same for all the subjects due to the similarities between them and the features of the tests. However, it is known that the heart performance has a strong dependency on the fitness and health status of each individual. For this reason, the physiological response of the allergic adults is not expected to be the same as that of the children and so, the result of the allergy detection algorithm in these cases is expected to be different. Besides, the allergic reactions to some of the drugs are different to those produced by other drugs or food, which should be reflected in the results as well. In order to adapt the allergy detection to different patterns of patients and

allergens, the whole set of data has been divided depending on the subjects age and the kind of allergen. The adaptation of the algorithm to the differences between those groups is explained below.

6.1 Description of the new dataset

A total number of 147 ECG signals were acquired during the data collection phase, from which those belonging to children undergoing oral food challenges were studied in Chapter 5. Here the rest of the groups will be studied (Table 6.1-1). The new data include 8 children and 111 adults exposed to drug allergens, and 8 adults to food.

As is explained by Kowalski et al. in [KABB13], reactions to NSAID (NonSteroidal Anti-Inflammatory Drugs) can be divided into allergic, when they are immunologically mediated i.e. when the symptoms that the patient suffers are provoked by the immunological system; and non-allergic in the cases in which the drug produces a hypersensitivity reaction in susceptible individuals. For this reason, drugs group will be split into NSAIDs and non-NSAIDs.

The positive cases will be classified based on the reaction and the time in which it appears. Depending on the physiological system affected, the reaction can be digestive (D), vascular (V), dermatological (S), respiratory (R), anaphylaxis (A), conjunctivitis (C) or rhino conjunctivitis (RC). Depending on the time the reaction appears, it is considered immediate (I), if the symptoms started before the end of the tests (until two hours after the intake of the last dose) or delayed (D) if they appeared several hours later. The provocation tests proceed in the same way for all the subjects except for the observation periods when testing some kind of NSAID (such as acetylsalicylic acid), which lasted for 1 hour instead of 30 minutes.

TABLE 6.1-1. SUBJECTS (ALLERGIC/NON-ALLERGIC) DIVIDED BY AGE AND TYPE OF ALLERGEN

		Children	*Adults*
Food		8/12	1/7
Drugs	*NSAID*	0/1	5/43
	Non-NSAID	0/7	1/62

Figure 6.1-1 shows the classification and statistics of all the subjects who have participated in the data collection for this study. The last column indicates the features of the reactions that the positive patients suffered expressed in the format *organ affected/time to appear*. For the rest of the chapter all the subjects will be taken into consideration, including the 23 children exposed to food whose data was analysed in chapters 4 and 5.

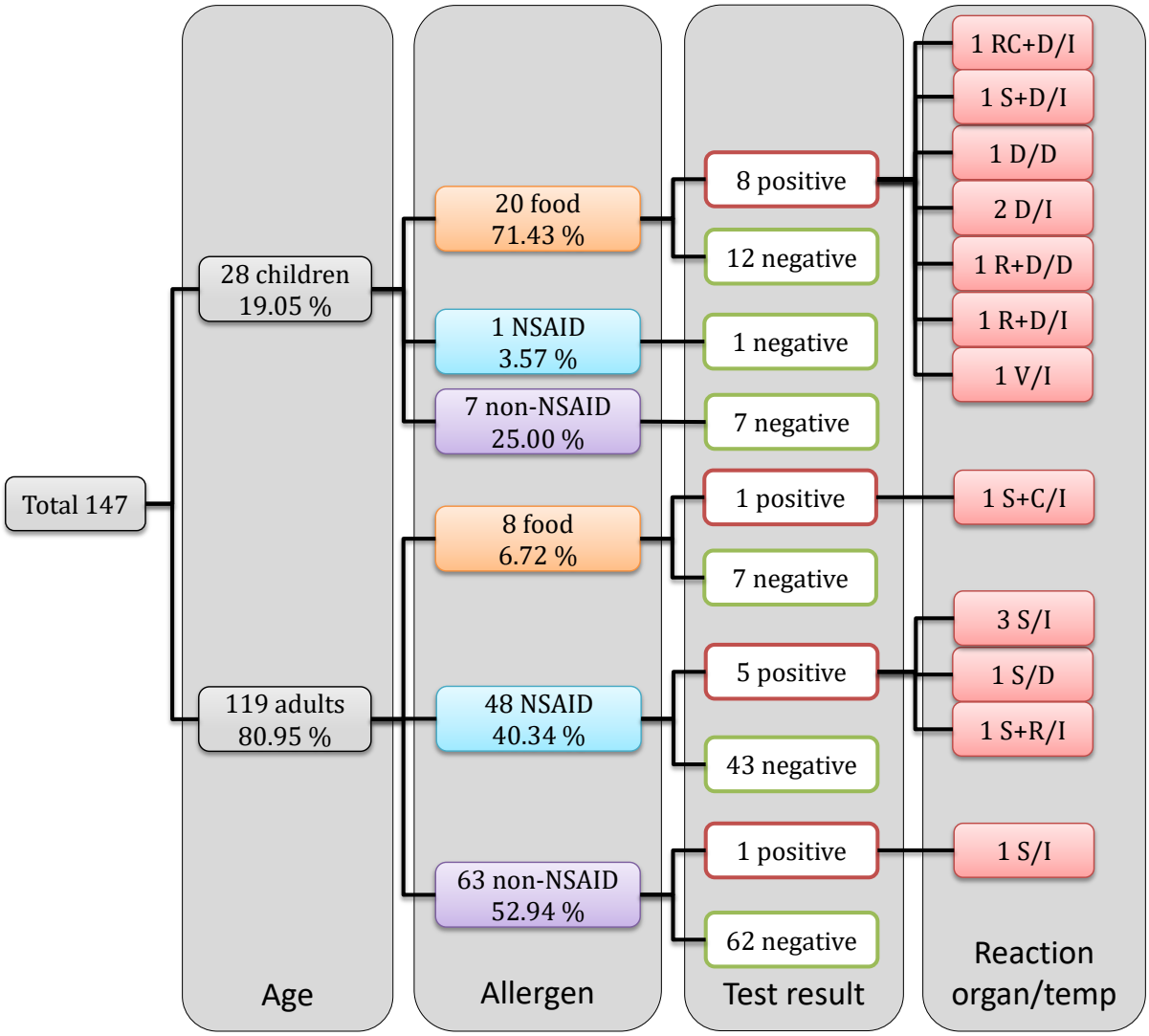

Figure 6.1-1. Classification of the subjects from the database

TABLE 6.1-2. PREVALENCE OF ALLERGIC SUBJECTS DEPENDING ON THEIR AGE AND THE TYPE OF ALLERGEN

		Children	Adults	Total
Food		35%	12.5%	28.6%
Drugs	NSAID	0%	10.2%	10%
	non-NSAID	0%	1.6%	1.4%
	All	0%	5.4%	5%

Several conclusions can be extracted from these data:

- Most of the tests are performed with adults exposed to drugs.
- The number of provocation tests with NSAIDs and non-NSAIDs is similar.
- Only one of the adults exposed to food was allergic. The patient had erythema, localized itching and conjunctivitis 30 minutes after the last dose. Thus, the reaction is classified as *skin+conjunctivitis/immediate*.
- None of the children exposed to drugs (NSAID or non-NSAID) was allergic.
- Only one subject (adult) exposed to non-NSAID resulted positive. Some hives and localized itching affected the patient 2 hours and 30 minutes after the intake of the last dose. This reaction is classified as *skin/immediate.*
- The prevalence of allergic subjects within the initial group (children, food) at GUH is similar to the one in CUH.
- The prevalence of allergic subjects depending on the group is summarized in Table 6.1-2

6.2 Analysis of the new dataset

6.2.1 Group [Children, Drugs]

This group is composed of eight children, and none of them resulted positive. The PDF of the MRR's standard deviation of this group has been compared with the one of allergic and non-allergic children exposed to food. The result is shown in Figure 6.2-1. As expected, the PDF of this group is similar to the non-allergic group exposed to food provocation tests, as they belong to the same group (non-allergic children). A significant difference between these two groups would imply a change of the HRV provoked by drugs, even if the patients were not allergic to them. Due to the lack of data belonging to children allergic to drugs, it is not possible to check if there is any difference between the allergic reactions provoked by a drug and that provoked by food.

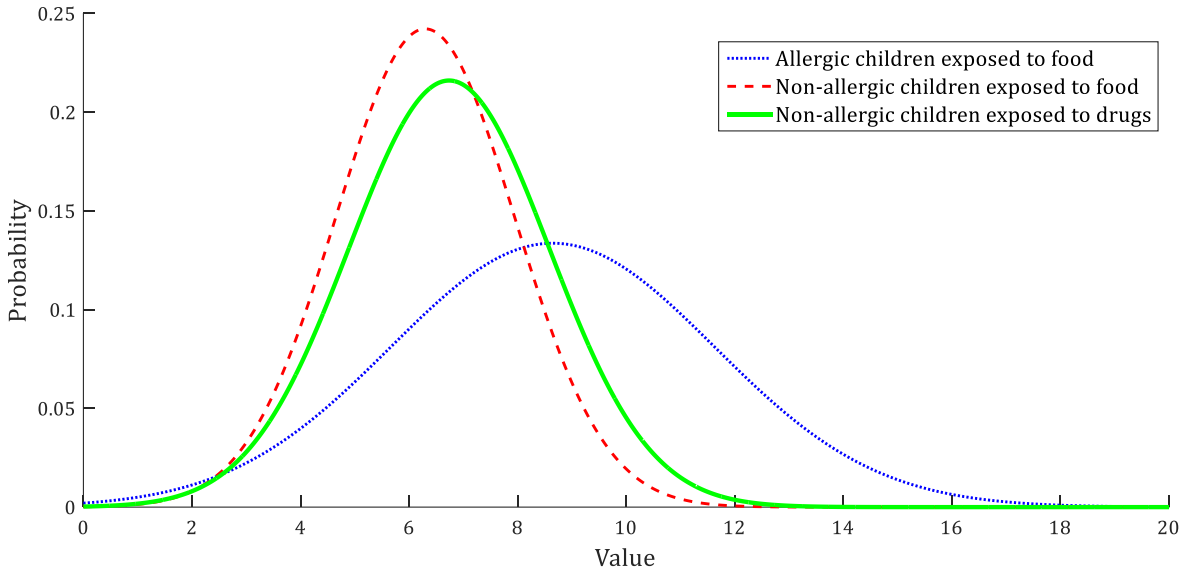

Figure 6.2-1. PDF of the MRR's standard deviation of allergic and non-allergic children exposed to food, and non-allergic children exposed to drugs

6.2.2 Group [Adults, Food]

This group is composed of eight adults, seven of them resulted negative and one reacted to the given substance. The positive patient is a female with age 18 years, and she had an immediate reaction 30 minutes after the 4th dose that affected her eyes and skin. Figure 6.2-2 shows the PDF of the MRR's standard deviation of the seven non-allergic of this group and the data of the positive one, compared with the [children, food] group.

There is a clear difference between adults and children that can be checked by observing the two non-allergic groups. The standard deviation of the *mean HRV* of the adults is much lower than the one of the children, which means that the variance of their heart rate during the provocation test is lower than that of the children's. This difference is probably due to two main factors: firstly, children usually perform more actively physical activities during the provocation test, while the adults are seated during the most part of it; secondly, the variation of the heart rate of the children is higher than the adults' one performing the same activity.

On the other hand, the difference between the allergic and the non-allergic adults is lower than in the case of the children exposed to food, which means that the allergen provoked a more dramatic changes in the HRV of the children, as happens with other stimulus such as the realization of physical activities. Even if the allergic adult suffered an allergic reaction, the standard deviation of her *mean HRV* is lower than the one belonging to the non-allergic children.

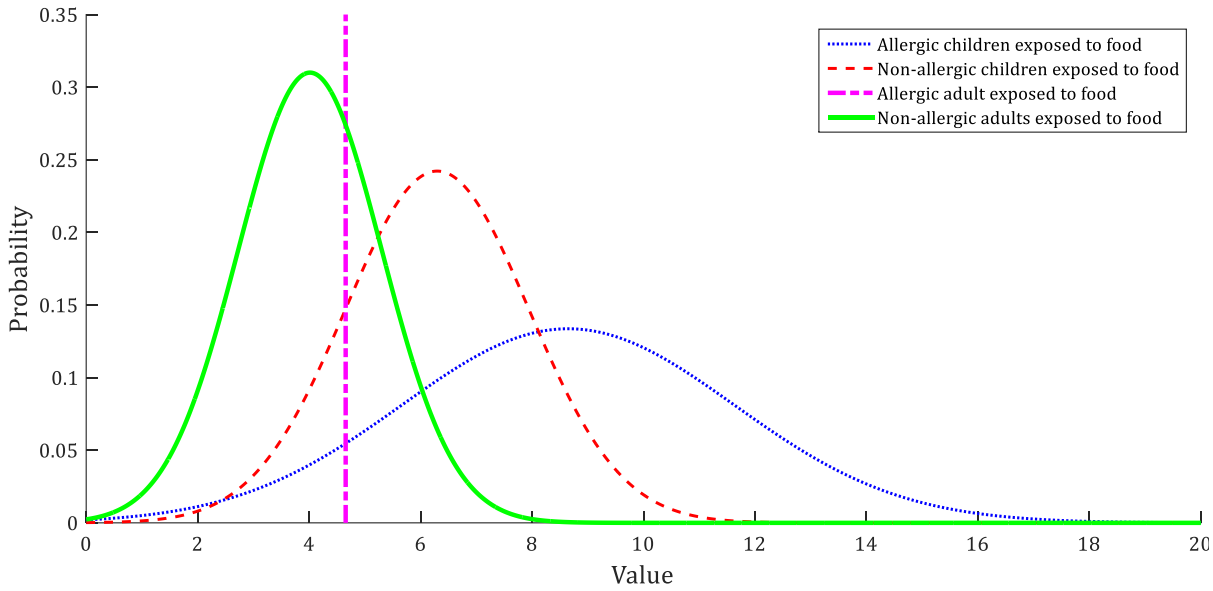

Figure 6.2-2. PDF of MRR's standard deviation of adults and children exposed to food

6.2.3 Group [Adults, non-NSAID]

During the data collection, sixty-three adults underwent allergy provocation tests to non-NSAID. Only one of them resulted positive, a 48 years old female whom symptoms consisted on generalized itching and hives 2 hours and 30 minutes after the third dose. Figure 6.2-3 depicts the PDF of allergic and non-allergic of this group compared to the previous one, i.e. adults exposed to food allergens. Although non-allergic subjects of both groups have similar features, their similarity is lower than in the case of non-allergic children. This is because this group includes individuals with ages from 12[2] to 92 years old, and their fitness and health condition vary considerably. With regard to the allergic subjects, the one in this group is more distinguishable from the non-allergic than in the case of the food.

The features of the reactions that both patients suffered where different, and so their ages, which may explain the differences of their HRV during the provocation test. However, there is not enough information in this or in the previous group regarding the allergic subjects to establish a physiological behaviour pattern. However, as in the case of the previous group, it is not possible to establish a physiological pattern with only one allergic subject.

[2] Regarding the use of drugs, an individual is considered adult when is older than 12 years.

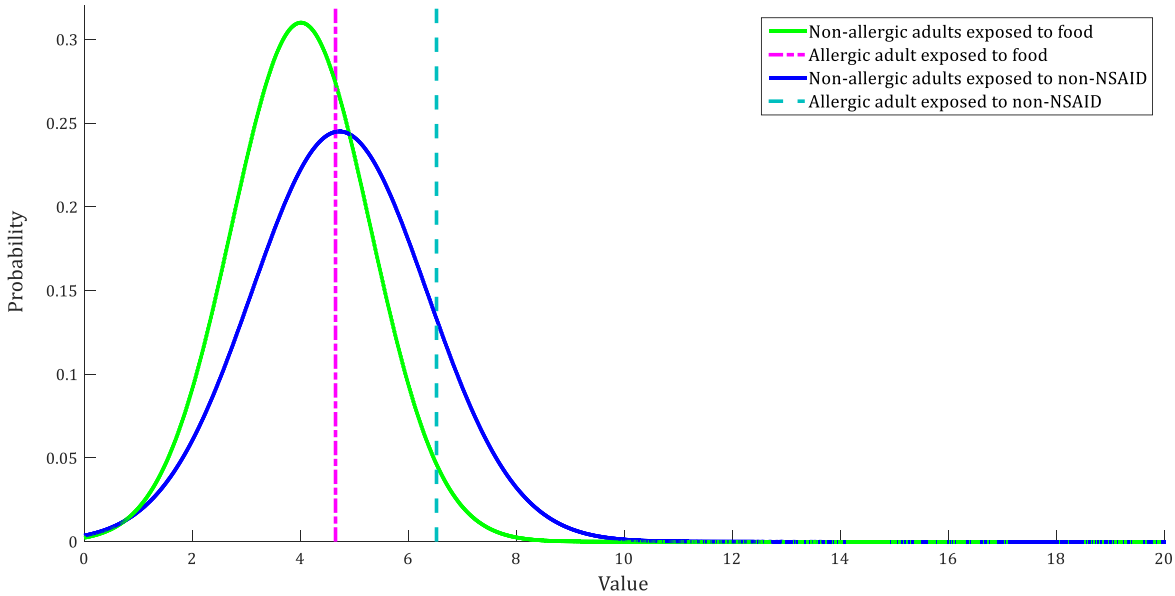

Figure 6.2-3. PDF of MRR's standard deviation of adults exposed to food and non-NSAID

6.2.4 Group [Adults, NSAID]

This group is composed of 48 subjects, and five of them resulted positive. The PDF of these groups are compared with that of [Adults, non-NSAID] group in Figure 6.2-4. The PDF of allergic and non-allergic to NSAID are completely overlapped. As was explained above, the reactions to some NSAIDs are not classified as allergic reactions, but as hypersensitivities to the particular drug in some studies. Furthermore, in some cases, the NSAID does not induce the reaction, but exacerbates the symptoms of an underlying chronic disease that the patients have. For this reason, the subjects from this group should be further studied in order to find out which ones can be grouped and analysed together to find a pattern.

Table 6.2-1 lists the mean and standard deviation of allergic and non-allergic subjects from each one of the groups analysed in this section. As has been graphically shown, through this table it is possible to check quantitatively the differences and similarities of the groups explained above. From this data, two conclusions can be extracted: adults cannot be analysed as children, since their physiological behaviour is different, and so the response of their body to the allergen under test in the case of positive patients.

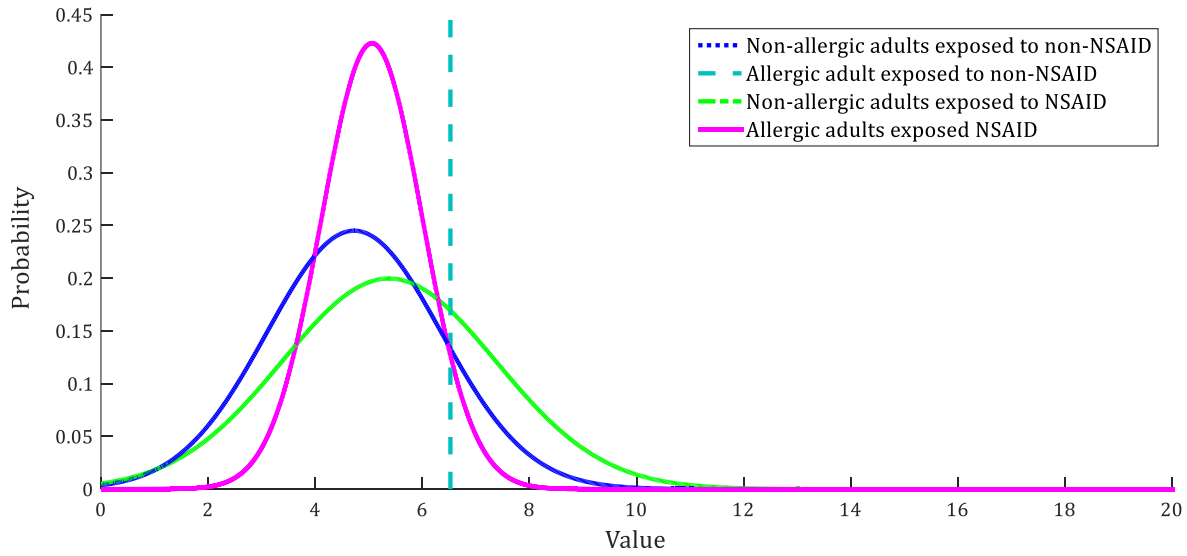

Figure 6.2-4. PDF of MRR's standard deviation of adults exposed to non-NSAID and NSAID

TABLE 6.2-1. MEAN AND STANDARD DEVIATION OF EACH ONE OF THE GROUPS ANALYSED IN THIS CHAPTER

GROUP	SUBGROUP	MEAN	STANDARD DEVIATION
[Children, Food]	Allergic	7.5158	2.3471
	Non-allergic	5.5940	1.6549
[Children, Drugs]	Non-allergic	6.7369	1.8465
[Adults, Food]	Allergic	4.6556	0
	Non-allergic	4.0153	1.2868
[Adults, Non-NSAID]	Allergic	6.5253	0
	Non-allergic	4.7272	1.6281
[Adults, NSAID]	Allergic	5.0609	0.9438
	Non-allergic	5.3788	1.9978

As can be checked in Table 6.2-1, the mean of the non-allergic children is even higher than that of the allergic adults. The second conclusion is that patients exposed to NSAID drugs should be taken out from this study. It should be clarified which one of the patients that suffered a reaction was, actually, allergic to the given substance.

6.3 Adaptation of the allergy detection

It has been shown that there exist differences between adults and children mean HRV during the provocation tests, as was expected due to their physiological differences. For this reason, the allergy detection algorithm should be adapted to such differences. Regarding the analysis carried out in the previous section, the following assumptions have been made:

- There are not allergic children exposed to drugs, so there should not be differences between this group and the non-allergic children exposed to food. For this reason, the configuration set in the previous chapter should work in these cases as it worked previously.
- There is a clear physiological difference between adults and children observable through the data belonging to the non-allergic subjects from both groups. The standard deviation of the adults' *MRR* tends to be lower. This fact implies that there is a smaller variation of the HRV in the adults. For this reason, the configuration of the allergy detection algorithm should be different to the one used with the children.
- It has been demonstrated that the standard deviation of the *MRR* cannot be used to distinguish between allergic and non-allergic subjects undergoing provocation tests with NSAID. Thus, this group should be studied independently from the rest of the adults.

In order to adapt the algorithm to the new subjects, they have been divided into children, adults with NSAID, and adults with non-NSAID (including food as non-NSAID). [Children, food] group will be included in the group *Children* for the rest of the chapter. Table 6.3-1 lists the evaluation of the standard deviation of the *mean HRV* for each one of the defined groups (following the same study carried out in Chapter 4); Figures 6.3-1 to 6.3-3 represent the PDFs of the allergic and non-allergic subjects from each one of the three groups.

TABLE 6.3-1. EVALUATION OF THE STANDARD DEVIATION OF THE MEAN HRV DEPENDING ON THE GROUP

GROUP	SUBGROUP	MEAN	STANDARD DEVIATION	P-VALUE	T-VALUE	AUC
Children	Allergic	7.5158	2.3471	0.1037	1.6913	0.7153
	Non-allergic	6.1020	1.7875			
[Adults, Non-NSAID]	Allergic	5.5904	1.3221	0.4066	0.8349	0.7286
	Non-allergic	4.6357	1.5983			
[Adults, NSAID]	Allergic	5.0609	0.9438	0.7287	0.3490	0.5136
	Non-allergic	5.3788	1.9978			

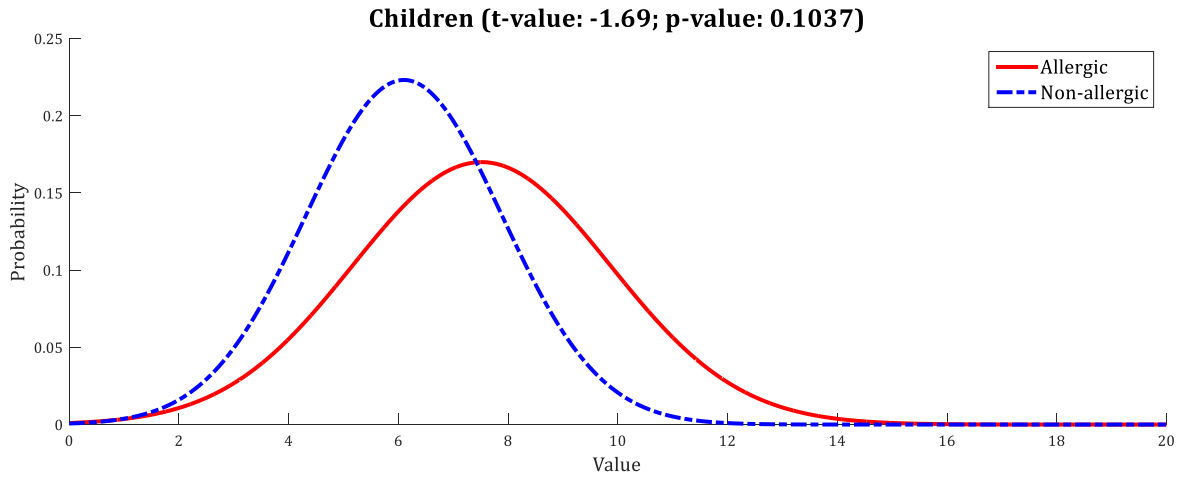

Figure 6.3-1. PDF of the Children group

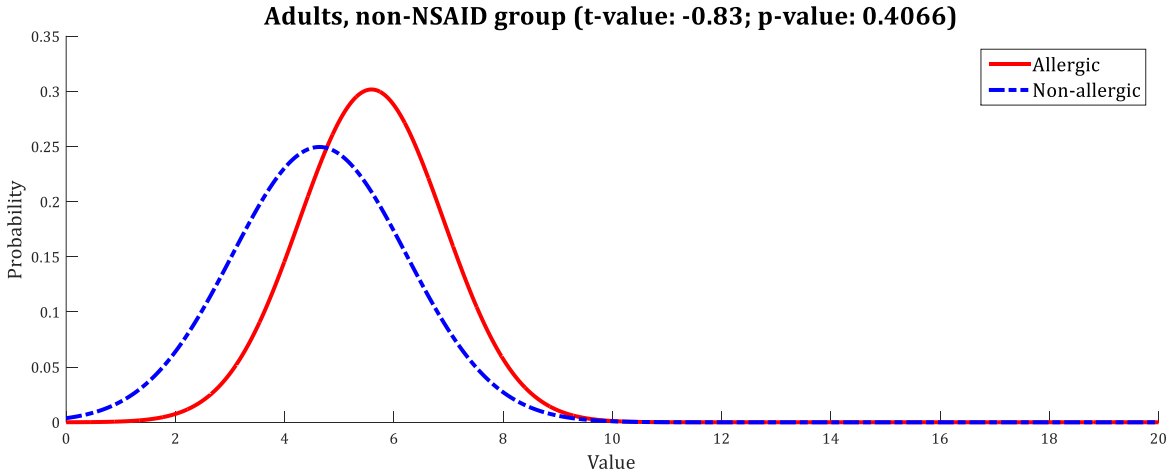

Figure 6.3-2. PDF of the group [Adults, non-NSAID] including food

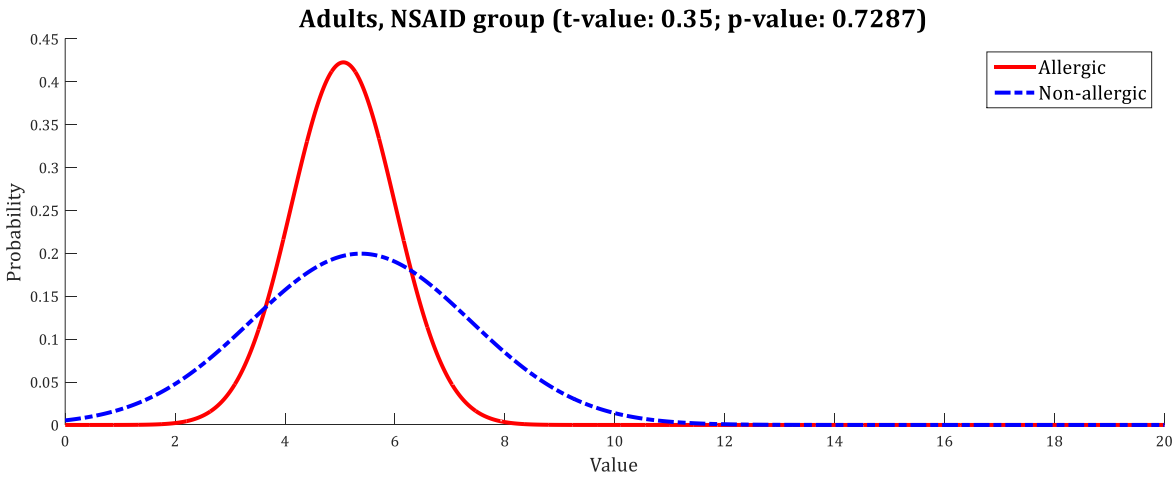

Figure 6.3-3. PDF of the [Adults, NSAID] group

TABLE 6.3-2. EVALUATION OF THE ALLERGY DETECTION ALGORITHM WITH THE DEFINED GROUPS

GROUP	Configuration		TP	FN	TN	FP	Se (%)	Sp (%)	Time gain (total time)	Doses avoided (total doses)
	GAcc	*Th*								
Children	32	10.5	7	1	19	1	87.5	95	69.75min (196.12min)	9 (29)
Adults, non-NSAID	10	12.4	2	0	66	3	100	95.65	88.77min (199.5min)	0 (6)
Adults, NSAID	25	5.4	5	0	20	23	100	46.51	76.6min (226.6min)	1 (15)
Adults, NSAID	10	12.4	1	4	36	7	20	83.72	0 (226.6min)	0 (15)

A performance test of the allergy detection algorithm has been done for the three groups, using 50 values of *GAcc* (from 1 to 50) and 151 values of *Th* (from 5 to 20 in 0.1 steps). The combination that provides the maximum average between Se, and Sp has been considered the best one for each group. With these considerations, the best obtained results and the combination of parameters that provides them are listed in Table 6.3-2.

The algorithm shows a similar performance with children and adults exposed to food and non-NSAID. Seven of the eight allergic children were detected, reducing the required number of doses from 29 to 20 and 30% the length to the tests. Only one of the 20 non-allergic children was misclassified. The algorithm detects the two allergic adults exposed to food and non-NSAID without avoiding any dose, but a mean time of 88.77 minutes before the end of the tests. Sixty-six out of the sixty-nine non-allergic from this group were correctly classified. The threshold has similar value for both groups, while the *GAcc* value of the children is three times higher than of the adults. This implies that the same movement increases the mean HRV of the adults a number of beats 3 times lower than in the case of the children.

One of the subjects of the [adults, non-NSAID] group that was classified by the algorithm as allergic was following an immunotherapy treatment for tolerating the allergen. This subject did not present any physical symptom during the provocation, and so, the result of this test was negative. However, the algorithm did detect an allergic reaction through the HRV, but due to the difference with the provocation, this result is considered a false positive.

Finally, regarding the NSAID group, the best (Se, Sp) average is obtained with Se=100%. This result implies that the algorithm misclassifies 23 out of the 43 non-allergic subjects. Since this group is composed of adults, the same parameters as for the other adults has been tested. With this second configuration only 1 of the patients that had a reaction are classified as allergic, but as

is explained before, it is not possible to know if these subjects were allergic or hypersensitive to the substance they got and so, these results cannot be validated. With this configuration, 36 out of the 43 non-allergic subjects are correctly classified. Figure 6.4-1 shows the classification of the obtained results depending on the age of the subjects, types of the allergen and kind of reaction of the allergic subjects.

6.4 Conclusions

This chapter analyses the differences between the allergic reactions suffered by children and adults exposed to different types of allergens. The original children database has been increased by adding the data of 12 children exposed to drugs (both NSAID and non-NSAIDs). Any of the patients of this new dataset resulted allergic, so they belong to the same group. The parameters of the original algorithm have been tuned according to the new inclusion of children to the original database. The values of the parameters were selected based on the optimization of the average value between sensitivity and specificity, and of the time gain. With this configuration 7 out of the 8 allergic subjects are detected, and all but one non-allergic subjects correctly classified. The value of the parameters should be validated by checking the performance of the allergy detection algorithm over a new and larger database.

As was expected, there is a clear difference between the *mean HRV* of children and adults, regardless the result of the provocation tests. The variability of the adults' heart rate is much lower than that of the children probably due to the lack of movement and to the fact that their heart rate variability varies less with the same physical activity (e.g. change posture from sitting to standing, or walking). The features of allergic and non-allergic adults exposed to NSAID are not distinguishable, which might be due to the fact that likely some of the considered allergic of this group had not an allergic reaction but a hypersensitive reaction. Nevertheless, the NSAID effects have some special features that makes the proposed algorithm unable to detect the allergic reactions provoked by these substances trough the analysis of the *mean HRV*.

Furthermore, the rest of the adults have been grouped together, getting a sensitivity of 100% (two allergic detected) and 95.65 % of specificity. No doses were avoided in this case, but the algorithm was able to detect the allergies a mean time of 88.77 minutes before the appearance of symptoms. However, even taking all these subjects together, there are only two positive cases (prevalence of 2.82%), which is not enough to define a pattern. Besides, this group includes

subjects from a wide range of ages. And as it has been demonstrated comparing children with adults, the age affects the way the HRV is modified by the allergy reactions.

For these reasons, the following tasks should be done in the future to complete this study:

- A new children (exposed to food and drugs) database should be obtained in order to validate the results derived from this study.
- It should be clarified which ones of the adults exposed to NSAID drugs who suffered reactions can be considered allergic to the given substance
- The adults' groups should be divided into smaller groups depending on the fitness/age of the subjects, because these parameters might affect to the response of their heart to an allergic reaction.

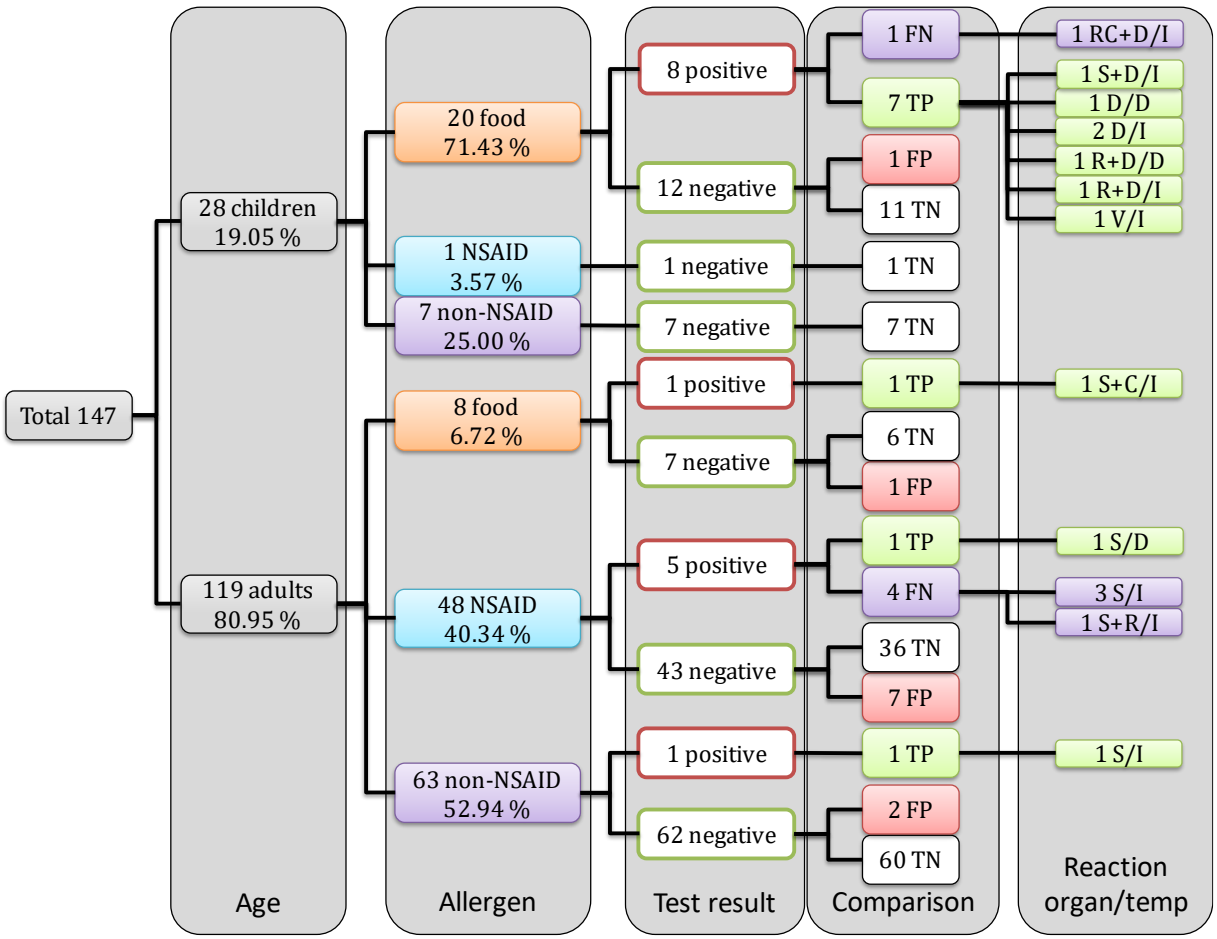

Figure 6.4-1. Division of the database subjects depending on the algorithm's results

Chapter 7.

CONCLUSIONS AND FUTURE WORKS

This chapter summarizes the main contributions of this Thesis. First, the most important conclusions extracted from this work are analysed; then, the publications that have resulted from this research are listed; finally, some future research lines are suggested.

7.1 Contributions

The main objective of this research was to investigate the way of predicting the appearance of allergic reactions based on the analysis of the HRV signal during allergy provocation tests. Thanks to the work carried out during this Thesis, a real-time and low-cost early detection of allergic reactions system has been proposed. The main contributions of this work are summarized below.

7.1.1 Novel real-time QRS complex detection algorithm

In order to achieve one of the primary aims of this Thesis a real-time QRS complex detection algorithm has been proposed. The performance and computational complexity of this algorithm have been evaluated and compared with the Gold Standard of real-time QRS complex detectors, the Pan & Tompkins algorithm. It has been demonstrated that the proposed algorithm maintains

the accuracy of the state of the art algorithms. However, the real benefit of the proposal is its low complexity and resources consumption. Its fixed-point version has been evaluated as well, and it has been implemented on a FPGA, demonstrating that the obtained results are, from a practical point of view, as good as the ones obtained using floating-point arithmetic.

7.1.2 Development of an algorithm based on HRV for the early detection of allergy reactions

For the development of the final allergy detection algorithm, the following steps were followed;

1. Study of the ability of 18 HRV features to distinguish between allergic and non-allergic patients of the 23 subjects participating in the data collection in the Cork University Hospital. The features studied in the previous research [Twom13] have been evaluated by using different metrics. It has been demonstrated that it is possible to extract enough information from the mean HRV to observe the effect an allergen produces on an allergic subject. Furthermore, this effect is observable long before the appearance of physical symptoms and, in several cases, with less doses than needed in the real tests.

2. The effect of the allergic reactions on the mean HRV (MRR) has been modelled in order to design an allergic reaction detection algorithm able to work in real time. This algorithm is verified on 23 subjects (fifteen of them are allergic). All the subjects were younger than 13, and they participated in food allergies provocation tests. 13 allergic subjects were detected, getting 86.67% sensibility; and there were no false alarms, so Sp=100%. The tests could have been reduced for the allergic subjects from a mean length of 1 hour and 16 minutes, to only 48 minutes; and the number of doses from 3.93 to 1.61.

The designed algorithm has been tested on 20 new subjects in the Guadalajara University Hospital (also children exposed to food), 8 allergic and 12 non-allergic. However, at this hospital the provocation tests are carried out under different conditions. The change that affected most this work is the fact that the patients were allowed to move during these tests. This fact leads to the reduction of the specificity from 100% to 33.33%. Two approaches were proposed to deal with these problems, both involving the measurement of the patients' movement or posture:

- First approach corrects the HRV by filtering the movement effect. This filter is made by subtracting a number of beats per unit of movement, assuming this factor is constant and the same for all the individuals. All the false positives but one were removed with this approach, leading to a specificity of 91.67 %, while the obtained sensitivity was 87.5 %. The length of the positive tests could have been reduced from a mean length of 2 hours and 37 minutes to 1 hour and 17 minutes, and the number of doses from 3.63 to 2.12.
- Second approach consists of detecting the subjects' posture. Because the patients stay in the same room during the whole test, it has been considered that the movement that affects most the HRV variability is any change between postures, i.e. from sitting to standing, from standing to walking, etc. This approach proposes the use of this information to remove false alarms. In addition, it is possible to track the movement of the patients and get information regarding their localization within a building. This system would allow them to move freely within the hospital during the observation periods (which can last for up to 2 hours). Although this system has been tested with only one subject, the preliminary results show its suitability for this application.

7.1.3 Study of the HRV signal in adults and children exposed to food and drugs allergens

The same studies carried out over the data belonging to children undergoing OFCs, have been performed with other groups: children exposed to drugs provocation tests, and adults exposed to food and drugs provocation tests. Despite the fact that a big effort has been made at this point, there are not enough subjects from each group to define a pattern, and so, adapt the allergy detection algorithm to each group. Even this information is currently being analysed by an epidemiologist in order to extract as much information as possible, there are some conclusions that can be addressed from the preliminary analyses:

- There is a clear difference between adults and children: standard deviation of non-allergic adults is lower than that of the children.
- The diagnostic ability of the selected feature for the allergy detection is very reduced: the AUC is less than 0.52. This is due to the fact that the reactions to NSAIDs are not always classified as allergies, but in some cases they are defined as hypersensitivities.

7.2 Future Works

In this Thesis a comprehensive study with regard to the use of the mean Heart Rate Variability for the early detection of allergic reactions has been carried out. As it has been shown, there are few works related to this topic. For this reason, this research can be considered the starting point of any forthcoming study in this area. Some of the main potential future works are:

- Increase of the database in order to get enough information for establishing a pattern representing each one of the studied groups. Any of the studied groups has enough number of subjects to consider it representative. Despite the fact that the results in some of these groups are promising, (that is the case of [children, food] group), it is necessary to test the designed algorithm with new data to check its reliability. In the cases in which the results are not considered good ([Adults, NSAID]), a further study should be done in order to find the potential factors that make this group different, maybe including more variables in the study (fitness or/and clinical history of the subjects, particular features of each drug, etc.).

- More subjects performing OFC need to be monitored for the configuration and validation of the Pocket Navigation System. It should be established how the HRV varies with a posture change and whether this variation is similar for subjects with different features. Then, it should be studied how to include this information in the allergy detection algorithm (turning off the analysis of the HRV during a posture change, filtering the HRV signal, etc.)

- Real implementation of the whole allergy detection system. At this time, the QRS complex detection algorithm has been implemented in the Shimmer platform, providing very good results. Shimmer measures the ECG signal and sends the RR intervals to a computer via Bluetooth. The next step will consist on implementing the allergy detection algorithm in Shimmer as well, and the design of a GUI for a computer through which the medical staff would be able to:
    - Connect to the Shimmer devices used during the OFCs
    - Introduce the features of each subject and the tests they are performing
    - Check the localization of each subject
    - Indicate whenever the subjects are having a new dose
    - Be warned when a particular subject is likely to suffer an allergic reaction, his/her posture, localization, level of activity, etc.

- End a test and save the results of each one of the patients electronically

- Development of a health control application for Android. Once the Shimmer is programmed to send the HRV information via Bluetooth, it is possible to change the host from a computer to a smart phone. The number of different applications that can be developed is as high as the number of health factors that are observable through the HRV signal (apnoea detection, mood estimation, glucose level control in diabetic patients, etc.).

7.3 Publications Derived from the Thesis

7.3.1 International Journals

1. R. Gutierrez-Rivas, J. J. Garcia, W. P. Marnane, and A. Hernandez, "Novel Real-Time Low-Complexity QRS Complex Detector Based on Adaptive Thresholding," *IEEE Sens. J.*, vol. 15, no. 10, pp. 6036–6043, Oct. 2015.
2. R. Gutierrez-Rivas, E. Munoz, J.J. García, W. Marnane. (2016), "Heart Rate Variability Analysis and Physical Activity Detection for Improving the Early Detection of Allergic Reactions during Provocation Tests". *IEEE Journal of Biomedical and Health Informatics*. Under review.
3. R. Gutierrez-Rivas, J. Hourihane, J. J. Garcia, and W. P. Marnane, "Loss of Normal Heart Rate Variability during Positive Oral Food Challenges in Children" *International Journal of Medical Informatics*. In preparation.

7.3.2 International Conferences

1. R. Gutierrez, J. J. Garcia, J. C. Garcia, L. Marnane, D. Gualda, S. Fernandez, and E. Garcia, "Activity monitoring and emergency warning with location information of the user," in *2011 IEEE 7th International Symposium on Intelligent Signal Processing*, 2011, pp. 1–6.
2. R. Gutierrez, S. Fernandez, J. Jesus Garcia, J. Carlos Garcia, and L. Marnane, "Monitoring vital signs and location of patients by using ZigBee wireless sensor networks," in *2011 IEEE SENSORS Proceedings*, 2011, pp. 1221–1224.
3. R. Gutierrez Rivas, J. J. G. Dominguez, W. P. Marnane, N. Twomey, and A. Temko, "Real-time allergy detection," in *2013 IEEE 8th International Symposium on Intelligent Signal Processing*, 2013, pp. 21–26.

4. R. Gutierrez, C. Spagnol, J. J. Garcia, L. Marnane, and E. Popovici, "Low complexity QRS detectors for performance and energy aware applications," in *IEEE-EMBS International Conference on Biomedical and Health Informatics (BHI)*, 2014, pp. 256–259.
5. R. Gutiérrez Rivas, J. J. García Domínguez, and W. P. Marnane, "Use of the Heart Rate Variability as a Diagnostic Tool," in *8th International Joint Conference on Biomedical Engineering and Technologies*, 2015, pp. 25–35.
6. R. Gutierrez-Rivas, A. Hernandez, J. J. Garcia, and W. Marnane, "SoC-based architecture for biomedical signal processing," in *2015 37th Annual International Conference of the IEEE Engineering in Medicine and Biology Society (EMBC)*, 2015, pp. 6018–6021.
7. E. Diaz, R. Gutierrez-Rivas, and J. J. Garcia, "Indoor navigation applied to the detection of allergic reactions during provocation tests," in *2015 International Conference on Indoor Positioning and Indoor Navigation (IPIN)*, 2015, pp. 1–7.
8. R. Gutiérrez-Rivas, J. J. García, Liam Marnane, "Study of the Heart Rate Variability Signal during Oral Food Challenges", *in 2016 Global Medical Engineering & Physics Exchanges (GMEPE) / Pan American Health Care Exchanges (PAHCE)*.
9. A. Vega, R. Gutierrez Rivas, A. Alonso, J.M. Beitia, B. Mateo, R. Cárdenas, J.J. Garcia-Dominguez, "Use of an electronic device and a computerized mathematic algorithm to detect the allergic drug reactions through the analysis of heart rate variability*", 7th Drug Hypersensitivity Meeting (DHM),* Málaga (Spain), 21-23 April 2016

APPENDIX A – HRV FEATURES

The Heart Rate Variability signal is a powerful tool to evaluate not only the health of the subject's heart, but also provides several indicators of the subject's general fitness and particular information related with the behaviour of some physiological systems. Its main advantage is that it can be obtained through a non-invasive measurement. Besides, it is computed by counting the time between R peaks, so it is unnecessary the use of complex and expensive acquisition devices.

The HRV signal has been widely studied in order to define which of its features is related with each physiological system. Malik in [Task96] published a comprehensive study of the HRV analysis, explaining some of its more important features: their meanings, clinical implications, ECG recording requirements, standards of ECG measurement, etc. Depending on the application, and the physiological system of interest, a different feature should be selected, which implies a different way of analysing the HRV signal.

This Appendix explains how to obtain the 18 features used in the previous work [Twom13], and studied in Chapter 4. These features will be divided into different categories depending on their domain: time, graphical and frequency domains.

A.1 Time domain features

For all the following equations RR_i represents the ith RR interval and N is the number of RR intervals in the analysed epoch.

A.1.1 Mean Heart Rate Variability

The *Mean* of the Heart Rate Variability *(eq. A.1)* measures the average heart rate over each epoch.

$$Mean = \frac{1}{N}\sum_{i=1}^{N}\frac{60}{RR_i} \qquad \textit{(eq. A.1)}$$

A.1.2 Standard Deviation

This feature measures the variance of the RR intervals within the analysed time interval following *(eq. A.2)*.

$$STDNN = \sqrt{\frac{1}{N}\sum_{i=1}^{N}\left(\frac{60}{RR_i} - Mean\right)^2} \qquad \textit{(eq. A.2)}$$

A.1.3 Coefficient of Variation

The Coefficient of Variation is a normalised measure of the RR intervals variance, and is computed as the ratio between the *Mean* and the *STDNN* features *(eq. A.3)*.

$$CV = \frac{STDNN}{Mean} \qquad \textit{(eq. A.3)}$$

A.1.4 Root Mean Square

The *RMSSD* feature measures the root mean square of the differences between adjacent RR intervals *(eq. A.4)*.

$$RMSSD = \sqrt{\frac{1}{N-1}\sum_{i=2}^{N-1}(RR_i - RR_{i-1})^2} \qquad \textit{(eq. A.4)}$$

A.1.5 NN50, pNN50, pNN25

NNx counts the number of successive pairs of RR intervals that differ for more than *x* ms. In this work, 50ms has been chosen. *pNNx* measures the percentage of *NNx* out of the total pairs of RR intervals *(eq. A.5.)*. 50ms and 25ms limits were used here.

$$pNNx = \frac{NN_x}{N-1} \qquad \textit{(eq. A.5)}$$

A.1.6 Histogram Index

This feature is obtained by computing the histogram of the RR intervals. Usually, the histogram is computed with bins of $1/Fs$ seconds (with Fs=256Hz, the length of the bins is 3.9063 ms). Histogram index is then obtained by dividing the height of the largest bin by the total number of RR intervals *(eq. A.6)*. In other words, the histogram index measures the percentage of RR intervals that have the most common duration. Figure A- 1 plots an example of the histogram computed for an ECG signal which length is 130 minutes approximately. *hist* feature for this example is 0.0424 (630/14873).

$$hist = \frac{h}{N} \qquad \textit{(eq. A.6)}$$

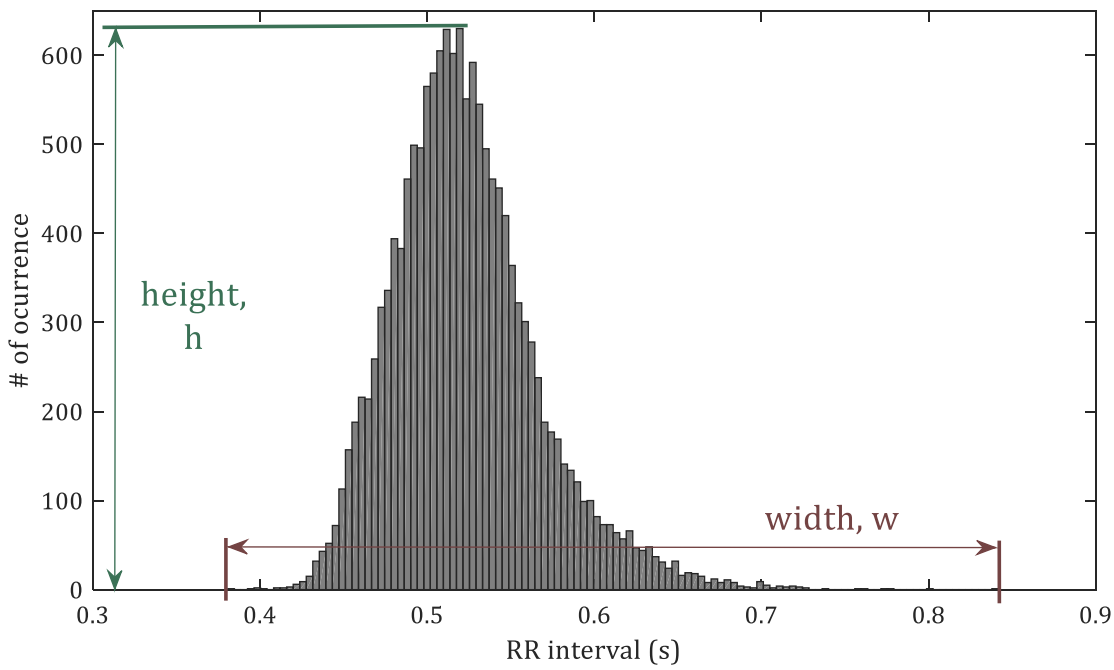

Figure A- 1. Example of HRV histogram and Histogram index computation

A.1.7 Positive and Negative trends (*STPP*, *STNN*)

These features provide information about the inter-beat variability of the HRV, in particular regarding the acceleration (Sequential Trend Positive, *STPP*) and deceleration (Sequential Trend Negative, *STNN*). *STPP* measures the percentage of successive RR interval pairs which are larger than the previous ones, and *STNN* the percentage of those pairs that are shorter than the previous ones. Figure A- 2 shows the relationship between the difference of each RR pairs and the previous one. *STPP* is the percentage of 'points' in the *STPP* quadrant, and *STNN*, the percentage of points in the *STNN* quadrant.

A.2 Graphical domain features

Graphical features are extracted from the Poincaré plot, which depicts the relationship between each RR interval with the following RR interval. As can be seen in the Figure A- 3, the *x* axis indicates a RR interval, and the *y* axis, the immediate posterior RR interval. The representation of all the RR pairs form an elliptic-shaped cluster dispersed along a line oriented at 45° (Figure A- 3). The length of the major axis of the ellipse is the standard deviation in the longitudinal direction, SD2; and the length of the minor axis, the standard deviation in the transversal direction, SD1. SD1 and SD2 quantize the long and short term variability of the HRV, respectively.

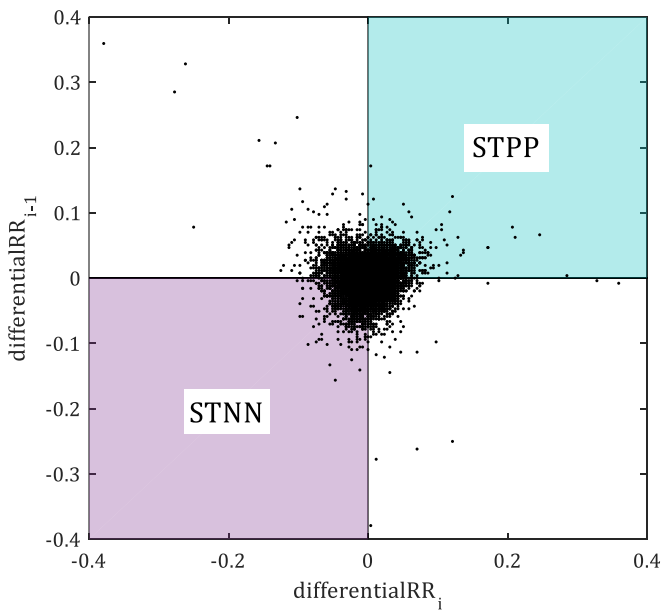

Figure A- 2. Representation of the relationship between the difference between each RR pair and the previous one

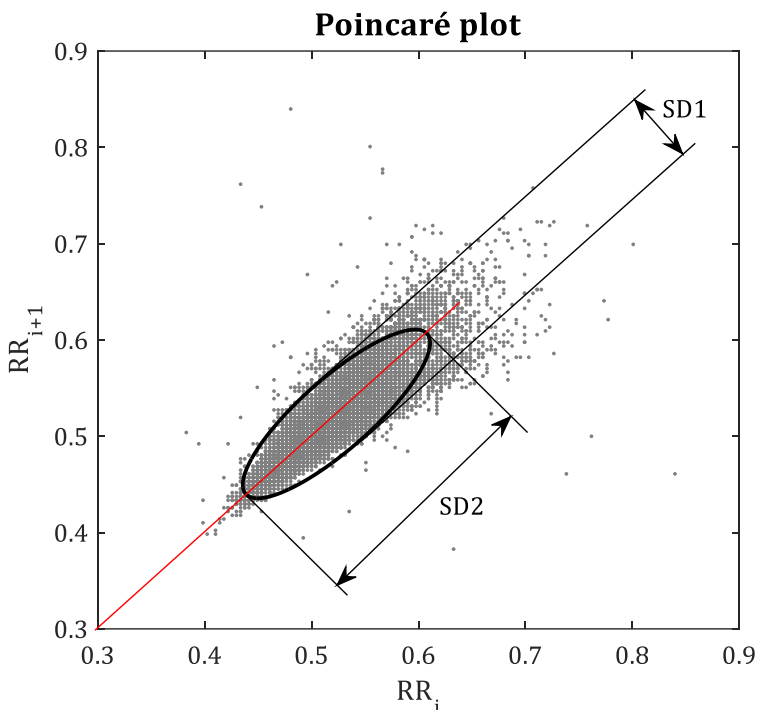

Figure A- 3. Representation of the relationship between the difference between each RR pair and the previous one

The Cardiac Sympathetic Index (CSI) and Cardiac Vagal Index (CVI) provide information about sympathetic and parasympathetic (or vagal) nervous systems and are computed based on both axes of the Poincaré ellipse as depicted by *(eq. A.7)* and *(eq. A.8)*, respectively. The relationship between both indexes has been also measured by analysing the features *ratioSV (eq. A.9)* and *SxV (eq. A.10)*

$$CSI = \log(SD1 \cdot SD2) \qquad \textit{(eq. A.7)}$$

$$CVI = \frac{SD2}{SD1} \qquad \textit{(eq. A.8)}$$

$$ratioSV = \frac{CSI}{CVI} \qquad \textit{(eq. A.9)}$$

$$SxV = CSI \cdot CVI \qquad \textit{(eq. A.10)}$$

A.3 Frequency domain features

For the computation of these features, it should be taken into account that the HRV is an aperiodic signal, so the Fourier Transform (FFT) cannot be applied directly. For this reason, the Lomb periodogram [Lomb76] was employed to estimate the spectrum of the HRV signal. The frequency domain features are:

- VLF: Total power in the very-low frequency band (0.0033 to 0.04 Hz).
- LF: Total power in the low frequency band (0.04 to 0.15 Hz)
- HF: Total power in the high frequency band (0.15 to 0.4 Hz)
- LFHF: Ratio between HF and LF.

An example of the HRV spetrum in the VLF, LF andf HF bands is represented in Figure A- 4.

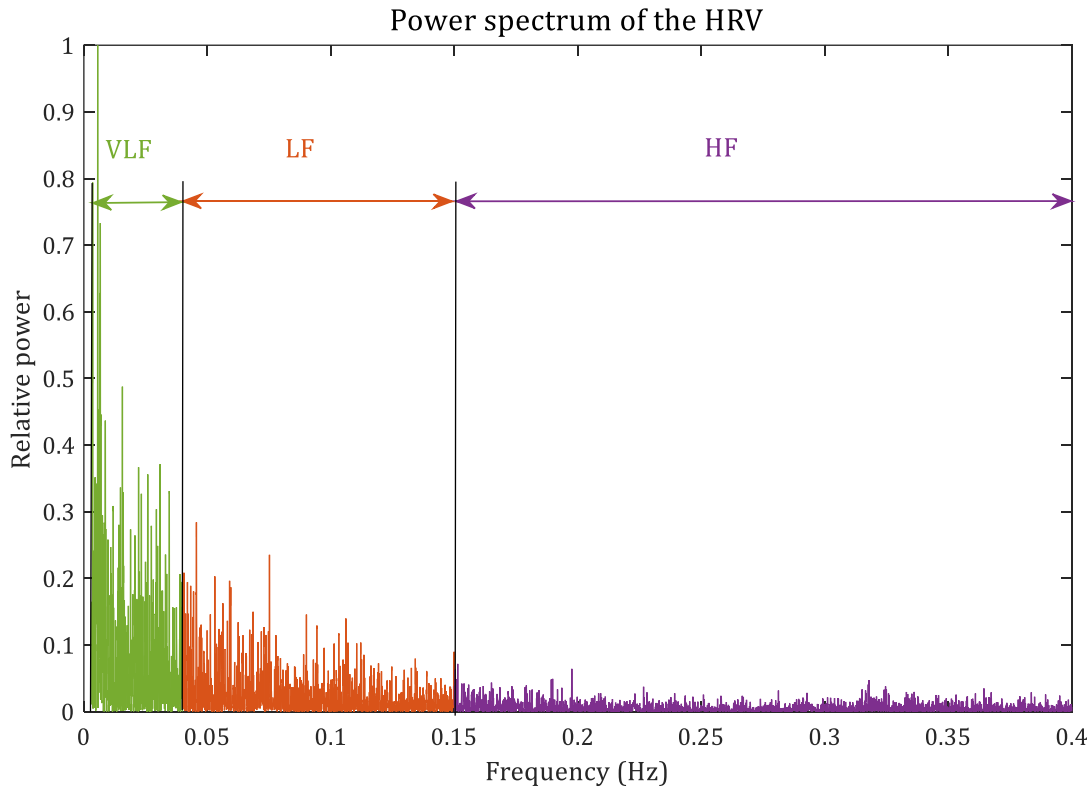

Figure A- 4. Example of Power spectrum in the VLF, LF and HF bands

APPENDIX B – SOC-BASED ARCHITECTURE FOR THE PROPOSED QRS COMPLEX DETECTION ALGORITHM

The proposed QRS complex detection algorithm has been implemented in a Zybo platform by Digilent, Inc, with a Xilinx Zynq XC7Z010 FPGA [Xili14]. This process has helped to both, check the resources the algorithm needs, and design a system able to analyse the HRV signal in real-time.

Thanks to the flexibility of an FPGA, this system has been proposed as a "Biomedical Signal Processor" since, by changing a few parameters it is possible to adapt the whole system for other applications based on the measurement of different biomedical signals. The sampling frequency f_s for input biomedical signals *x[n]* is always far below the common clock frequencies f_{CLK} in current SoC- and FPGA- based designs (f_{CLK}=100MHz for the configurable logic in the device used here). This high frequency ratio between the clock and the sampling frequencies allows time-multiplexed architectures to be proposed, achieving an efficient resource reutilization.

Two advanced peripherals, called low-level and high-level peripherals, have been developed here. The first one is focused on the processing of the biomedical signal *x[n]*, providing basic functions as filtering, integration, moving average, etc. The high-level peripheral operates as a co-processor with the ARM processor to compute advanced tasks. The proposed QRS complex detection algorithm is implemented, then, in the low-level peripheral. The high-level one is in charge of computing the HRV signal and several of its features. Figure B- 1 shows the general block

diagram of the proposed architecture. Both peripherals are connected to the ARM processor through an AXI-lite bus, which allows the definition of a register bank for every peripheral, making it possible to configure them, as well as access to their status and partial results.

The low-level peripheral is capable of sending the input raw signal x[n] to an external DDR3 memory bank, together with the corresponding output signal r[n]. A DMA controller has been included in order not to waste processor time in data moving from peripherals to the external memory. The ARM processor can access the external DDR3 bank to recover the information stored by the peripherals in order to send them to any destination through the Ethernet link available in the system.

B.1 Low-level peripheral

As mentioned above, the proposed biomedical signal processing architecture has been particularized for the proposed QRS complex detection algorithm, which has been implemented in the low-level peripheral following the block diagram shown inFigure B- 2. It is composed of four modules: a configurable FIR filter, a moving average, a squaring module, and an R-peak detection block.

The FIR filter (Figure B- 3) implements the high-pass filtering following *eq. 3.13*. The SOP (Sum Of Products) involved in FIR filtering has been computed by only one DSP48E MAC cell (multiplier + accumulation). The input samples $x[n]$ and the coefficients c_n are stored in slices configured as shift registers SRL16, with a maximum length of 16 coefficients. Both the filter length and the coefficients can be modified in run-time by the processor for any mathematical function. This filter uses the same DSP48E1 cell over time, thanks to the high ratio between the clock frequency f_{CLK} and the sampling frequency, f_s. The latency of this module is 18 cycles.

Next module of the preprocessing stage is a moving average with a configurable length of N samples (*eq. 3.14*). Figure B- 4 depicts the block diagram of this module, based on a buffer with N positions and on a DSP48E1 cell. This buffer is dedicated to accumulation operations, as well as to the division by the number of samples, N. The parameter N can be modified in run-time for a better adaptation. The latency of this block is 7 lock cycles.

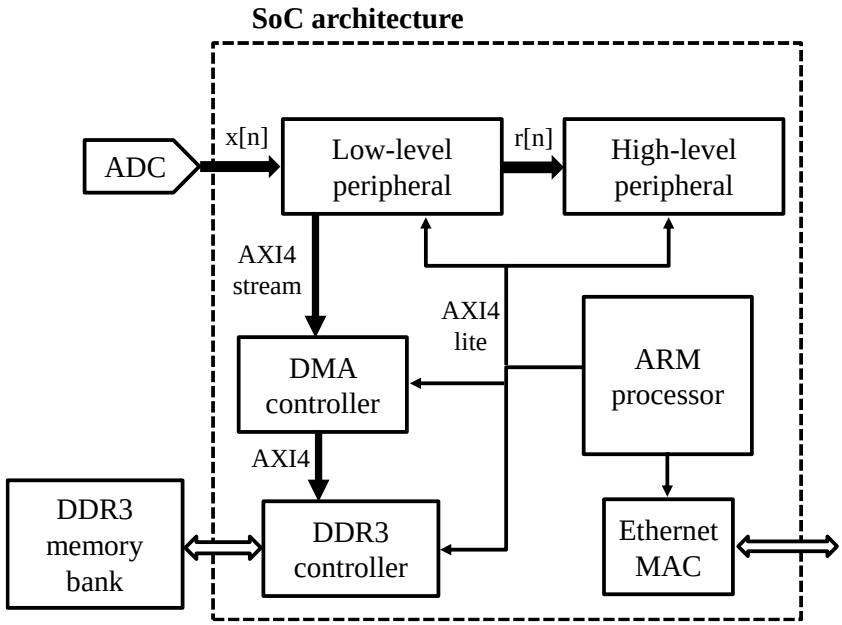

Figure B- 1. General block diagram of the proposed SoC architecture

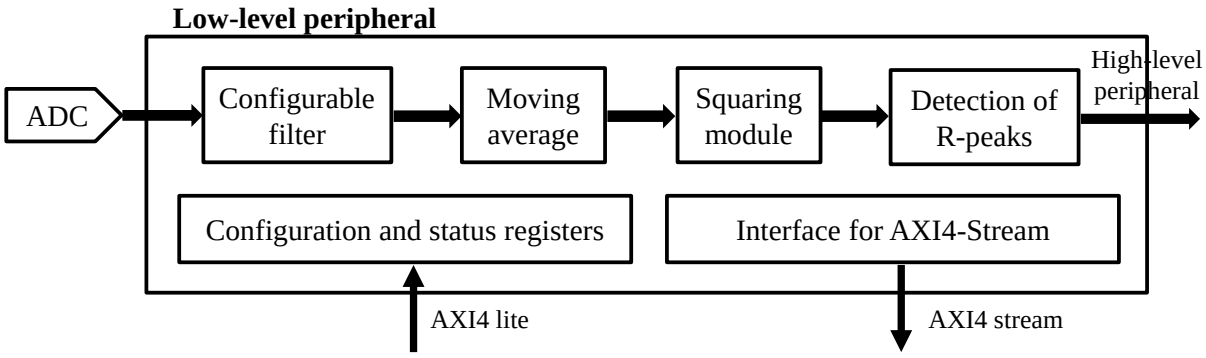

Figure B- 2. Block diagram of the proposed low-level peripheral

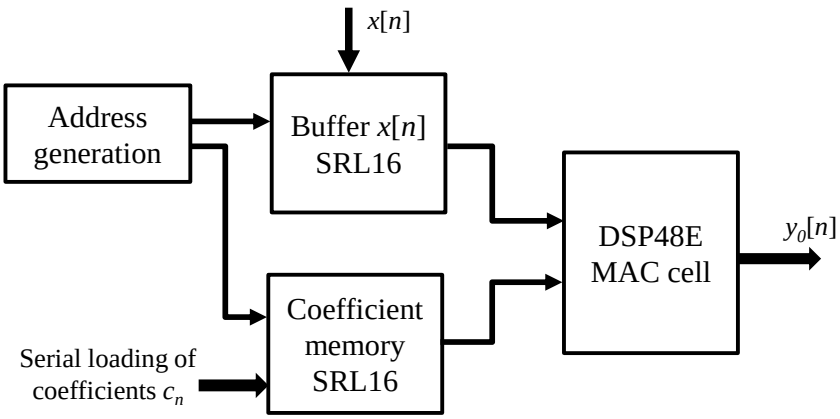

Figure B- 3. Block diagram of the configurable FIR filter

The last part of the pre-processing stage is a squaring module, according to *eq. 3.15*, which is also based on a DSP48E1 cell and with a latency of 5 cycles. The whole preprocessing stage has a latency of 30 clock cycles, which allows the real-time constrains to be met, in order to compute the corresponding sample *y[n]* before the next input sample *x[n+1]* is available, with a sampling frequency of 360 Hz (which is the one used for the MITDB). After this pre-processing stage, the resulting signal *y[n]* is analyzed by a FSM in order to find the position of the R peaks, as explained in chapter 3. The more complex task of this module is likely the exponential function associated to the state no. 3. (*eq. 3.16*). This exponential function has been approximated by a Taylor series with three terms, as shown in *(eq. B.1)*.

$$t_h[n] = t_h[n] \cdot e^{-P_{th} \cdot T_s} \approx t_h[n] \cdot \left(1 + P_{th} \cdot T_s + \frac{(P_{th} \cdot T_s)^2}{2}\right) \qquad \textit{(eq. B.1)}$$

The exponential function requires two DSP48E1 cells, one for the Taylor approximation and the other for the product $P_{th} \cdot T_s$. A third DSP48E1 cell is used in the product $t_h[n] \cdot e^{-P_{th} \cdot T_s}$, all of them involved in the state no. 3. The remaining computing related to the other two states has been implemented using generic adders, not requiring any specific resource from the architecture. The maximum latency of the R-peaks detector is 11 clock cycles. The results of this module (position of the detected R peaks) are sent to the output ports, both for the DMA channel and for the high-level peripheral.

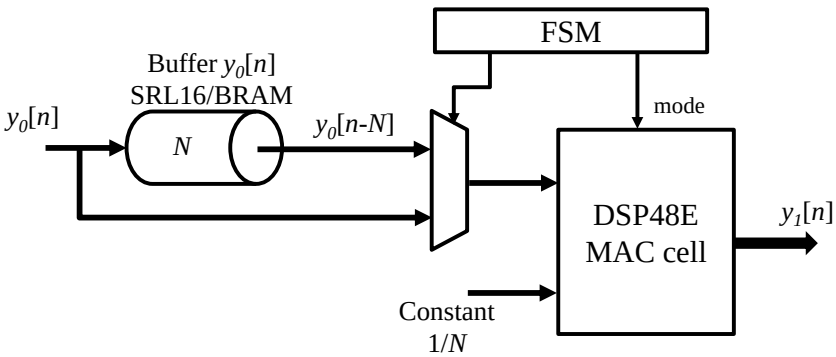

Figure B- 4. Block diagram of the moving average block

B.2 High-level peripheral

This peripheral is responsible for measuring the time interval between consecutive R-peaks, and so, generate the HRV signal. Some statistical HRV parameters are computed in the ARM processor, which could be changed depending on the application. The architecture of this module consists of a counter to measure the timing interval. Whether a new R-peak is identified by the low-level peripheral, the event is notified to the high-level one, where the RR interval is computed and reported to the ARM processor.

B.3 Test of the proposed architecture

The architecture described here implies a fixed-point representation for the proposed ECG signal processing, adapted to the resources available in the FPGA device. This always involves a quantization error on the final result to be analyzed. These errors were computed in MATLAB before the real implementation of the whole system. Chapter 3 explains the details of this quantization.

Table B- 1 describes the word widths defined for the architecture. It should be noted that most of these widths are limited by the size of the input data (18 bits) in the multipliers from the DSP48E1 cells. Table B- 2 summarizes the resource consumption for the different elements in the system. Note that the global system also includes those resources for communications and control of the ADC converter. Although the clock frequency defined by the Zynq device for the configurable logic is 100 MHz, the synthesis tool achieves a critical path for the design of 7.9 ns.

Finally, the design has been successfully verified with the ECG data coming from the MIT database, MITDB. The ECG signal is previously downloaded in an emulation module that provides the ECG signal to the ADC in the SoC device for its real-time processing. The SoC design is also connected to a PC, where all the obtained results are collected and shown in real-time. By comparing the obtained results with those obtained by the floating-point version of the proposed algorithm, in terms of sensitivity, *Se*, and positive predictivity, *+P*, it is possible to observe how the results from the hardware implementation are comparable to the original ones, as shown in Table B- 3.

TABLE B- 1. DATAPATH DIMENSIONS IN THE PROPOSED ARCHITECTURE

Variables	No. of bits	No. of fractional bits
Input $x[n]$	12	11
Coefficients c_n	16	14
Signal $y_0[n]$	18	17
Signal $y_1[n]$	18	17
Signal $y[n]$	18	17
Threshold $t_h[n]$	18	17
Period T_S	9	0
Internal counters	12	0

TABLE B- 2. RESOURCE CONSUMPTION OF THE PROPOSED SYSTEM IN A ZYNQ XC7Z010 FPGA

Resource	Low-level peripheral	High-level peripheral	Global system
DSP48E1	6	0	6 (7%)
RAMB	10	0	17 (10%)
Slices	817	276	2366 (53%)

TABLE B- 3. COMPARISON BETWEEN THE RESULTS OBTAINED WITH THE FLOATING-POINT VERSION OF THE PROPOSED QRS COMPLEX DETECTION ALGORITHM AND WITH THE PROPOSED SOC ARCHITECTURE

Parameters	Floating-point version	Fixed-point SoC version
R-Peaks	109451	109948
TP	109157	109391
FN	294	557
FP	247	248
Se	99.731	99.493
P+	99.774	99.774

APPENDIX C – T-VALUE LEVEL OF SIGNIFICANCE LIMIT DEPENDING ON THE DEGREE OF FREEDOM

Confidence interval	**80 %**	**90 %**	**95 %**	**98 %**	**99 %**	**99.5 %**	**99.8 %**	**99.9 %**
α two-tailed test	0.2	0.1	0.05	0.02	0.01	0.005	0.002	0.001
α one-tailed test	0.1	0.05	0.025	0.01	0.005	0.0025	0.001	0.0005
df					**t-value**			
1	3.078	6.314	12.706	31.820	63.657	127.321	318.309	636.619
2	1.886	2.920	4.303	6.965	9.925	14.089	22.327	31.599
3	1.638	2.353	3.182	4.541	5.841	7.453	10.215	12.924
4	1.533	2.132	2.776	3.747	4.604	5.598	7.173	8.610
5	1.476	2.015	2.571	3.365	4.032	4.773	5.893	6.869
6	1.440	1.943	2.447	3.143	3.707	4.317	5.208	5.959
7	1.415	1.895	2.365	2.998	3.499	4.029	4.785	5.408
8	1.397	1.860	2.306	2.897	3.355	3.833	4.501	5.041
9	1.383	1.833	2.262	2.821	3.250	3.690	4.297	4.781
10	1.372	1.812	2.228	2.764	3.169	3.581	4.144	4.587
11	1.363	1.796	2.201	2.718	3.106	3.497	4.025	4.437
12	1.356	1.782	2.179	2.681	3.055	3.428	3.930	4.318
13	1.350	1.771	2.160	2.650	3.012	3.372	3.852	4.221
14	1.345	1.761	2.145	2.625	2.977	3.326	3.787	4.140
15	1.341	1.753	2.131	2.602	2.947	3.286	3.733	4.073
16	1.337	1.746	2.120	2.584	2.921	3.252	3.686	4.015
17	1.333	1.740	2.110	2.567	2.898	3.222	3.646	3.965
18	1.330	1.734	2.101	2.552	2.878	3.197	3.610	3.922
19	1.328	1.729	2.093	2.539	2.861	3.174	3.579	3.883
20	1.325	1.725	2.086	2.528	2.845	3.153	3.552	3.850
21	1.323	1.721	2.080	2.518	2.831	3.135	3.527	3.819
22	1.321	1.717	2.074	2.508	2.819	3.119	3.505	3.792
23	1.319	1.714	2.069	2.500	2.807	3.104	3.485	3.768
24	1.318	1.711	2.064	2.492	2.797	3.090	3.467	3.745
25	1.316	1.708	2.060	2.485	2.787	3.078	3.450	3.725
26	1.315	1.706	2.056	2.479	2.779	3.067	3.435	3.707
27	1.314	1.703	2.052	2.473	2.771	3.057	3.421	3.690
28	1.313	1.701	2.048	2.467	2.763	3.047	3.408	3.674
29	1.311	1.699	2.045	2.462	2.756	3.038	3.396	3.659
30	1.310	1.697	2.042	2.457	2.750	3.030	3.385	3.646
32	1.309	1.694	2.037	2.449	2.738	3.015	3.365	3.622
34	1.307	1.691	2.032	2.441	2.728	3.002	3.348	3.601
36	1.306	1.688	2.028	2.434	2.719	2.991	3.333	3.582
38	1.304	1.686	2.024	2.429	2.712	2.980	3.319	3.566
40	1.303	1.684	2.021	2.423	2.704	2.971	3.307	3.551
42	1.302	1.682	2.018	2.418	2.698	2.963	3.296	3.538
44	1.301	1.680	2.015	2.414	2.692	2.956	3.286	3.526
46	1.300	1.679	2.013	2.410	2.687	2.949	3.277	3.515
48	1.299	1.677	2.011	2.407	2.682	2.943	3.269	3.505
50	1.299	1.676	2.009	2.403	2.678	2.937	3.261	3.496
60	1.296	1.671	2.000	2.390	2.660	2.915	3.232	3.460
70	1.294	1.667	1.994	2.381	2.648	2.899	3.211	3.435
80	1.292	1.664	1.990	2.374	2.639	2.887	3.195	3.416
90	1.291	1.662	1.987	2.369	2.632	2.878	3.183	3.402
100	1.290	1.660	1.984	2.364	2.626	2.871	3.174	3.391
150	1.287	1.655	1.976	2.351	2.609	2.849	3.145	3.357
200	1.286	1.652	1.972	2.345	2.601	2.839	3.131	3.340
300	1.284	1.650	1.968	2.339	2.592	2.828	3.118	3.323
500	1.283	1.648	1.965	2.334	2.586	2.820	3.107	3.310
∞	1.282	1.645	1.960	2.326	2.576	2.807	3.090	3.291

APPENDIX D – MEAN HRV OF THE SUBJECTS FROM THE CUH DATABASE DURING THE OFCS

The following figures in this appendix represent the MRR signal of the 23 subjects of the CUH database computed in 60-second windows with 1-second shift, as explained in Chapter 4. The first 15 figures correspond to the allergic subjects, and the rest to the non-allergic subjects.

In order to ease the comparison process, the HRV range is the same for all the subjects (60 – 165 bpm). Background area has been shaded in grey, and each one of the check-ups in blue. From the minute the test is considered finished to the end of the measurement, the plot is shadowed with grey as well.

Allergic subjects

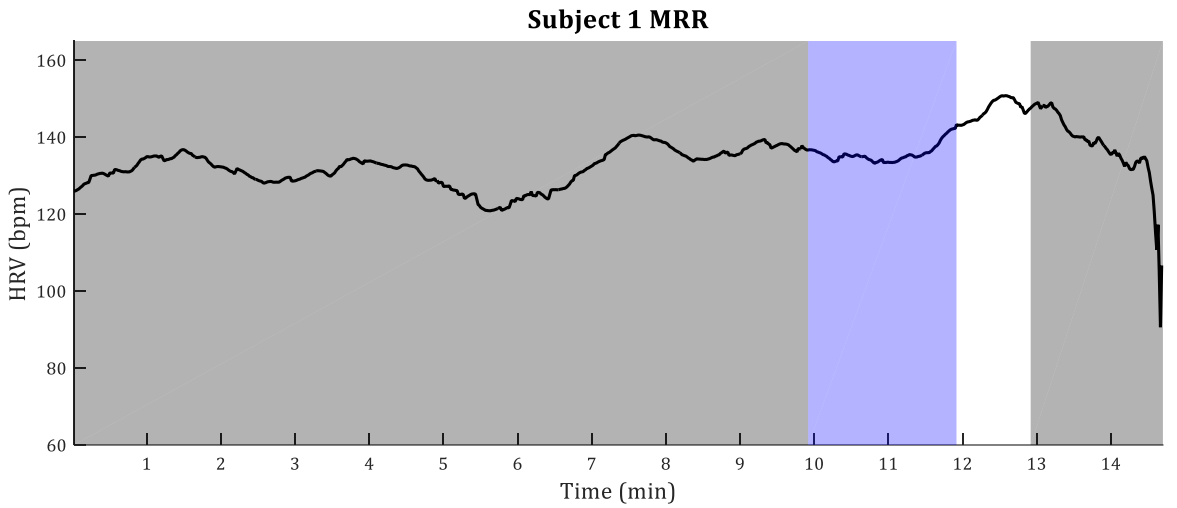

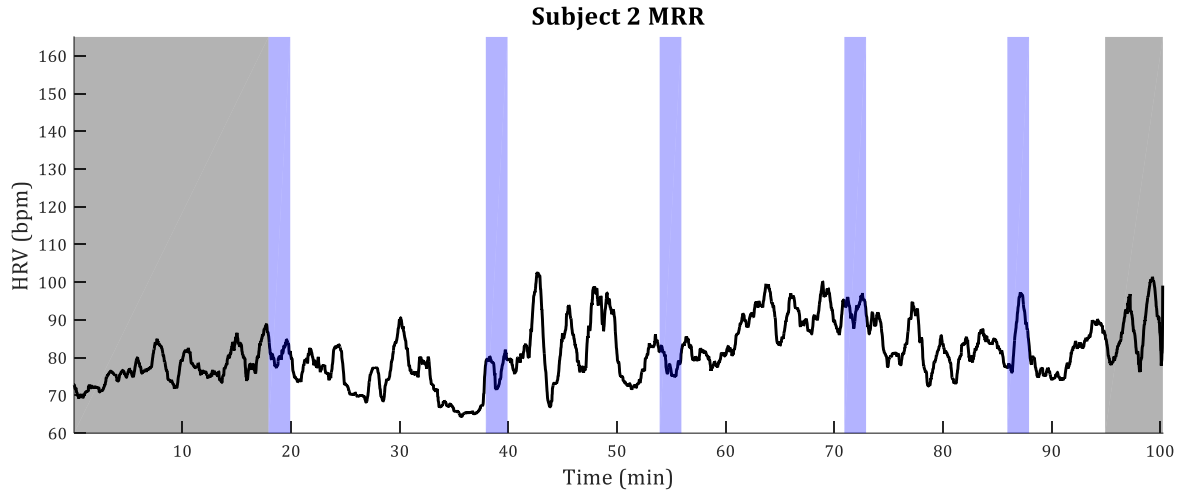

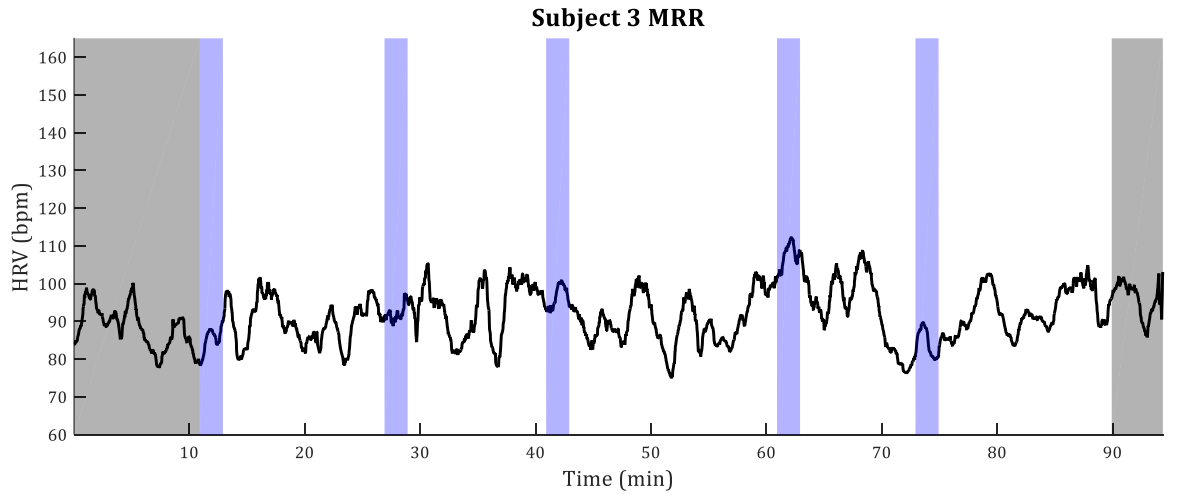

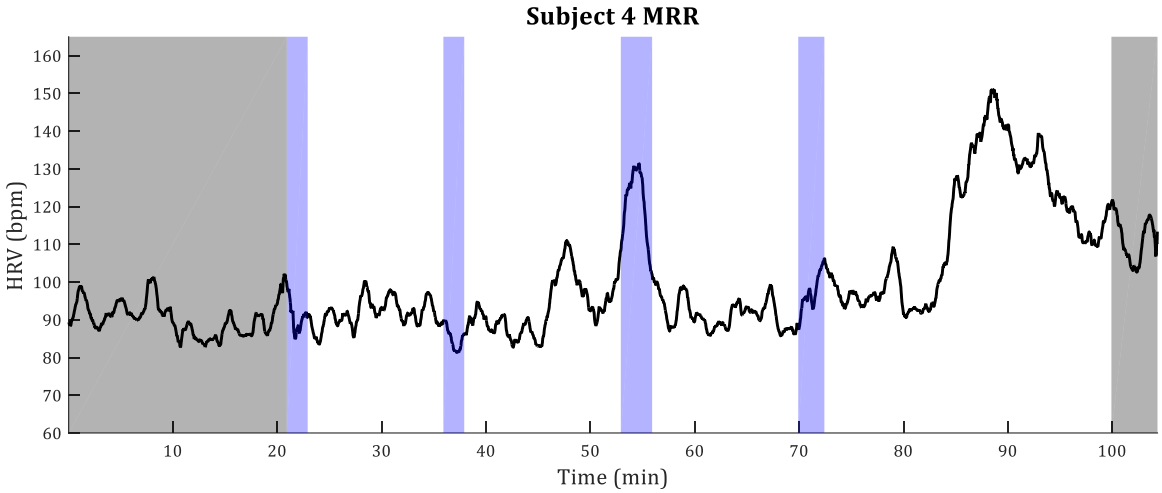
Subject 4 MRR
HRV (bpm)
Time (min)

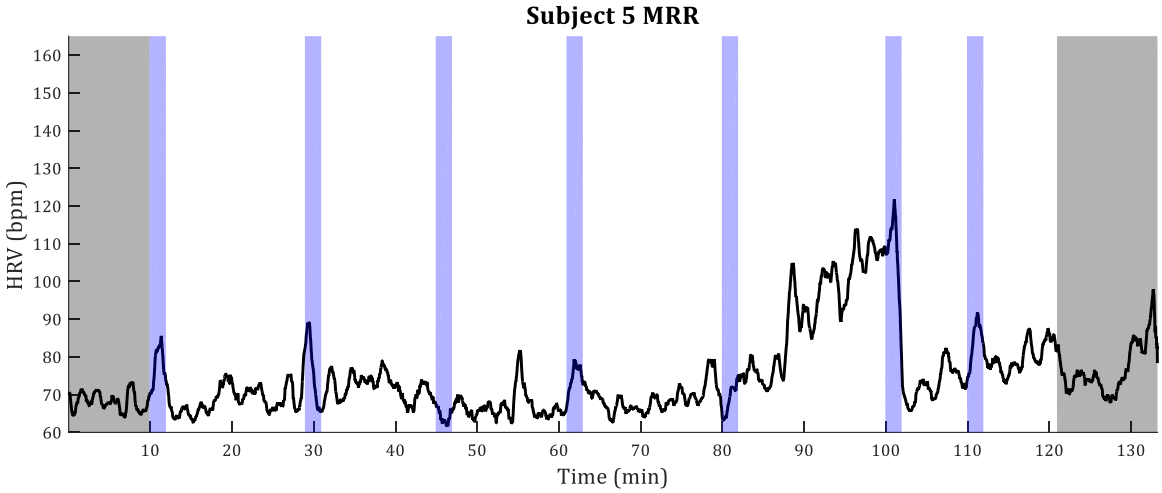
Subject 5 MRR
HRV (bpm)
Time (min)

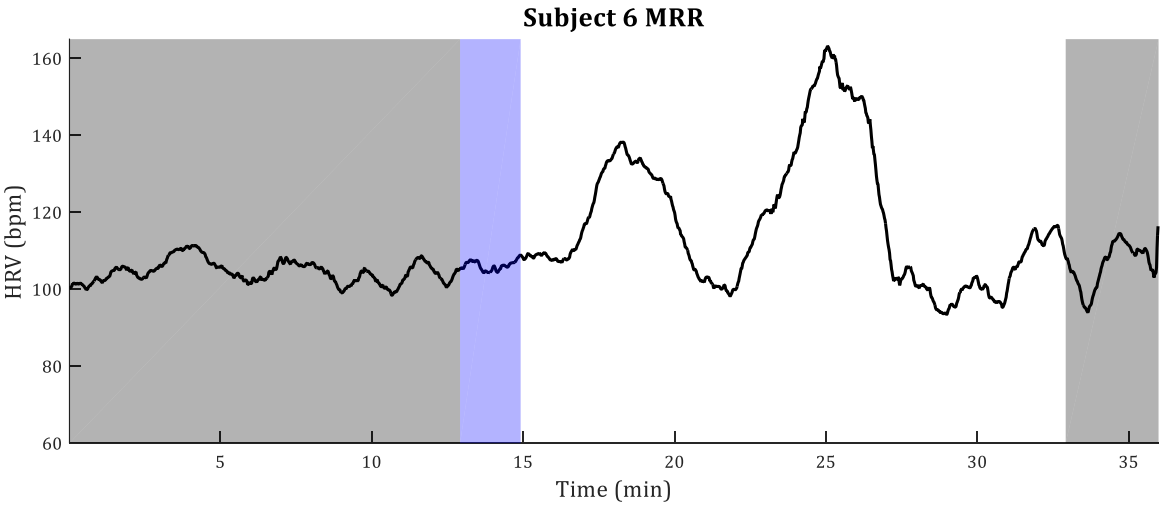
Subject 6 MRR
HRV (bpm)
Time (min)

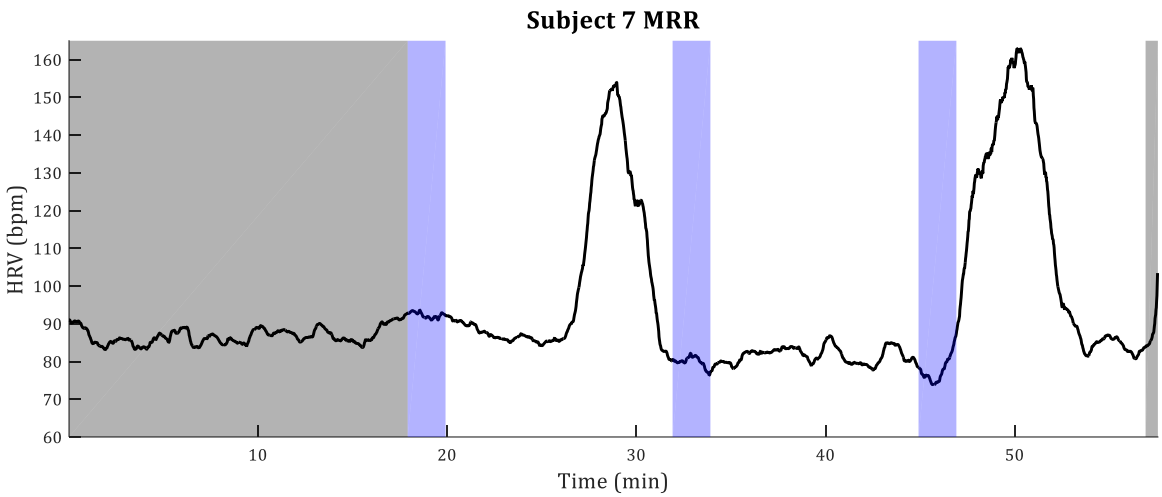
Subject 7 MRR
HRV (bpm)
Time (min)

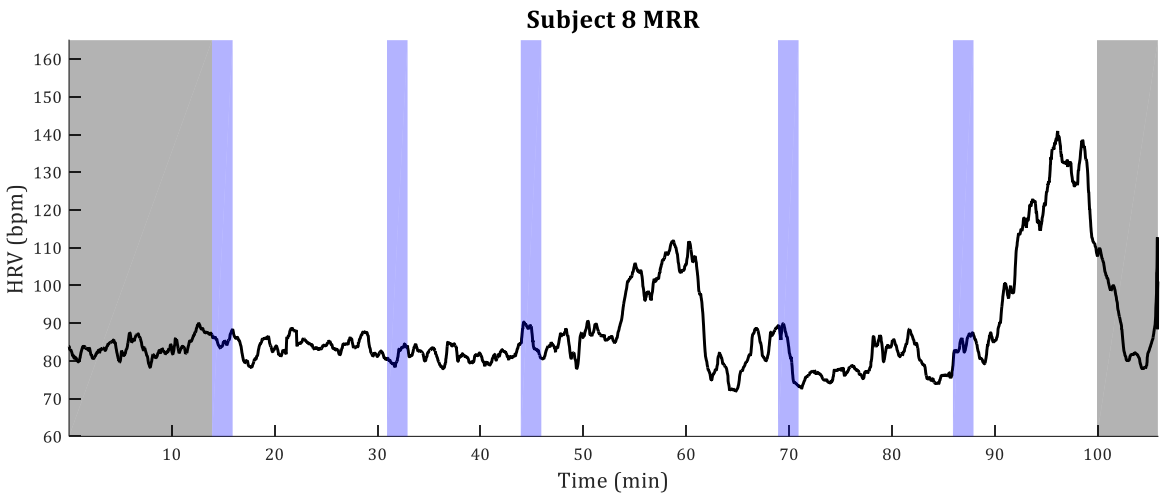
Subject 8 MRR
HRV (bpm)
Time (min)

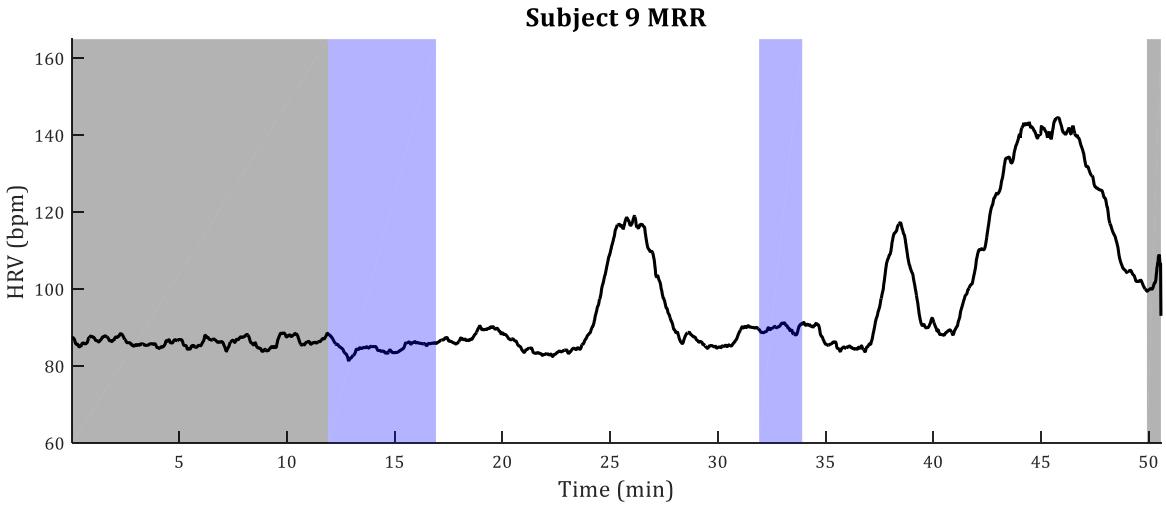
Subject 9 MRR
HRV (bpm)
Time (min)

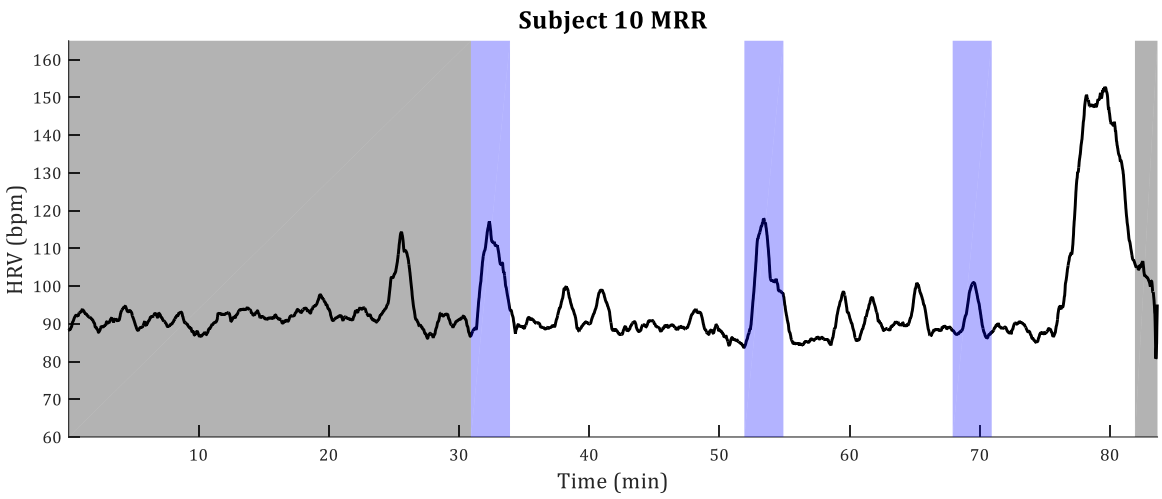
Subject 10 MRR
HRV (bpm)
160
150
140
130
120
110
100
90
80
70
60
10
20
30
40
50
60
70
80
Time (min)

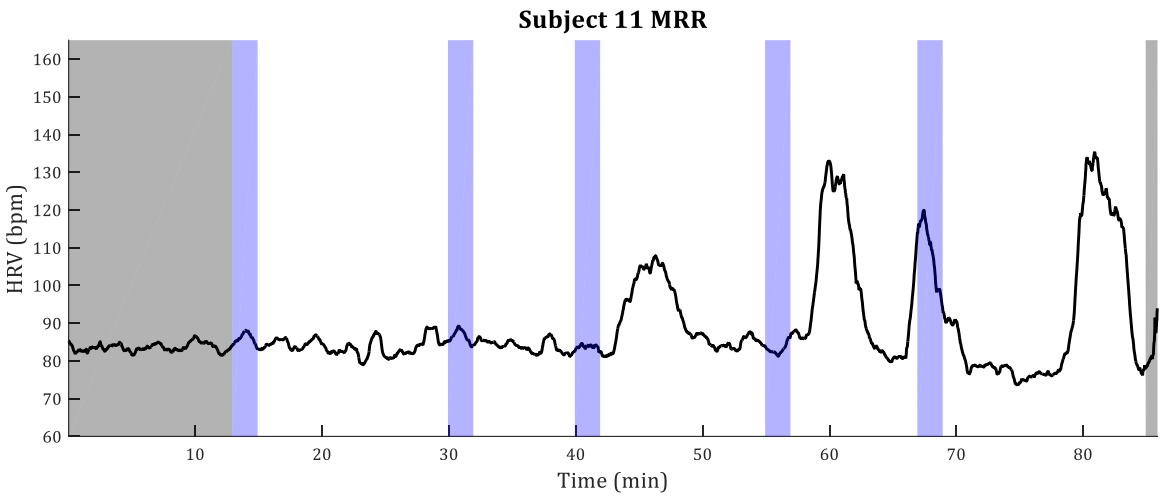
Subject 11 MRR
HRV (bpm)
160
150
140
130
120
110
100
90
80
70
60
10
20
30
40
50
60
70
80
Time (min)

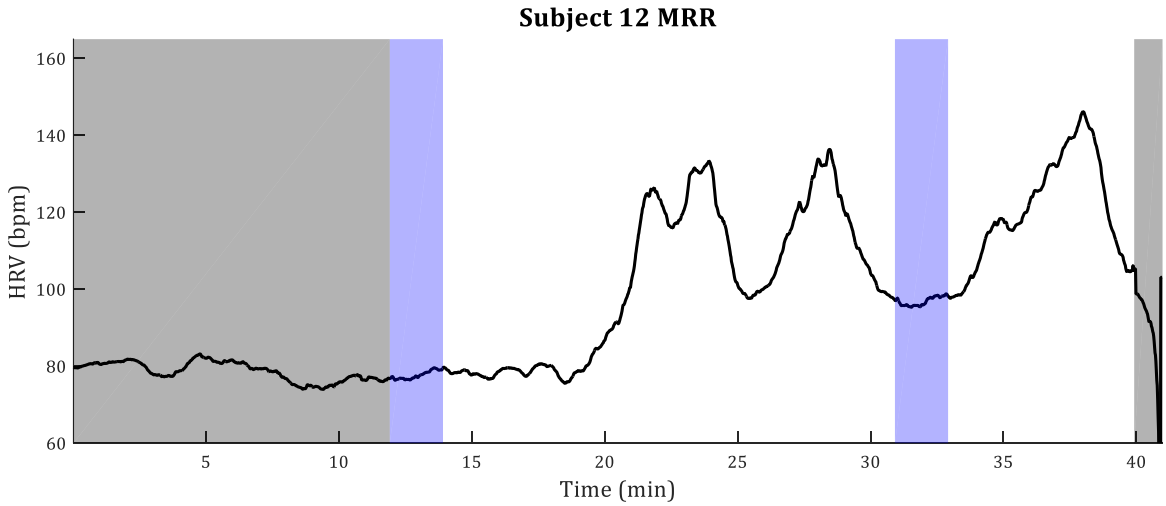
Subject 12 MRR
HRV (bpm)
160
140
120
100
80
60
5
10
15
20
25
30
35
40
Time (min)

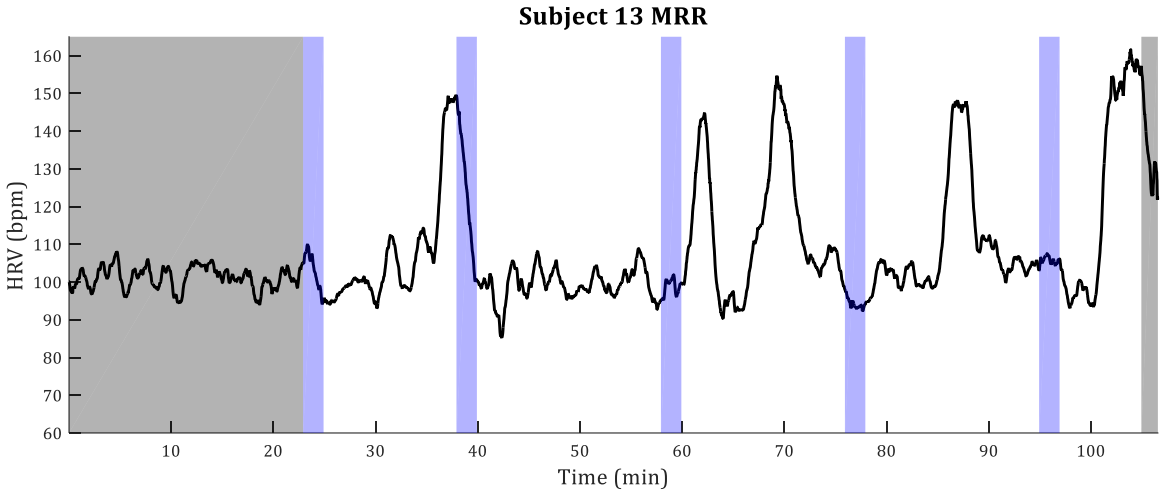
Subject 13 MRR
HRV (bpm)
Time (min)

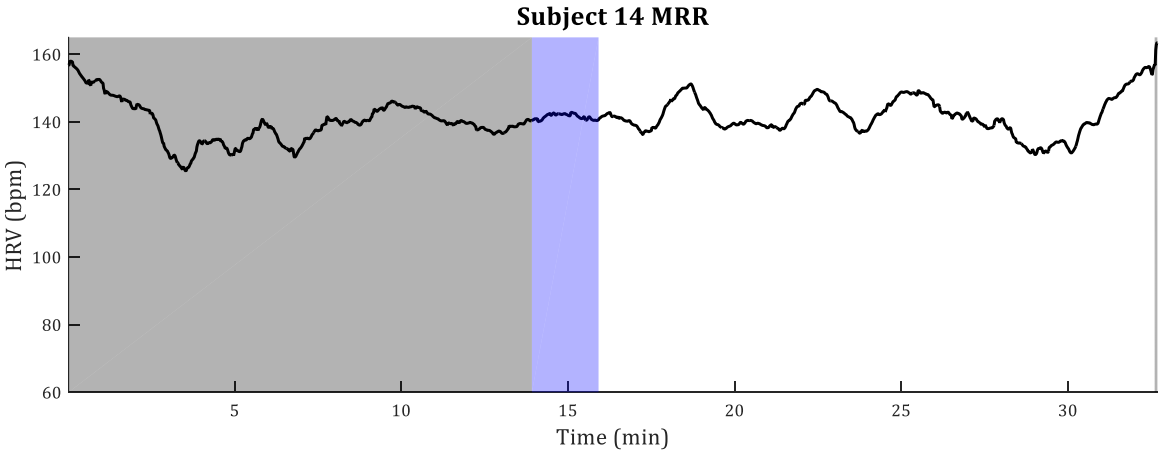
Subject 14 MRR
HRV (bpm)
Time (min)

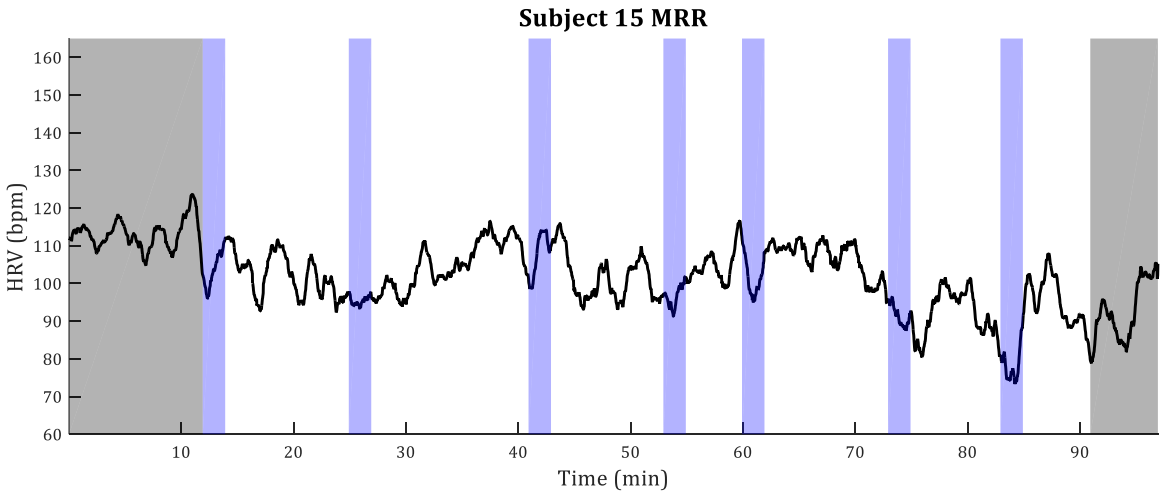
Subject 15 MRR
HRV (bpm)
Time (min)

Non-allergic subjects

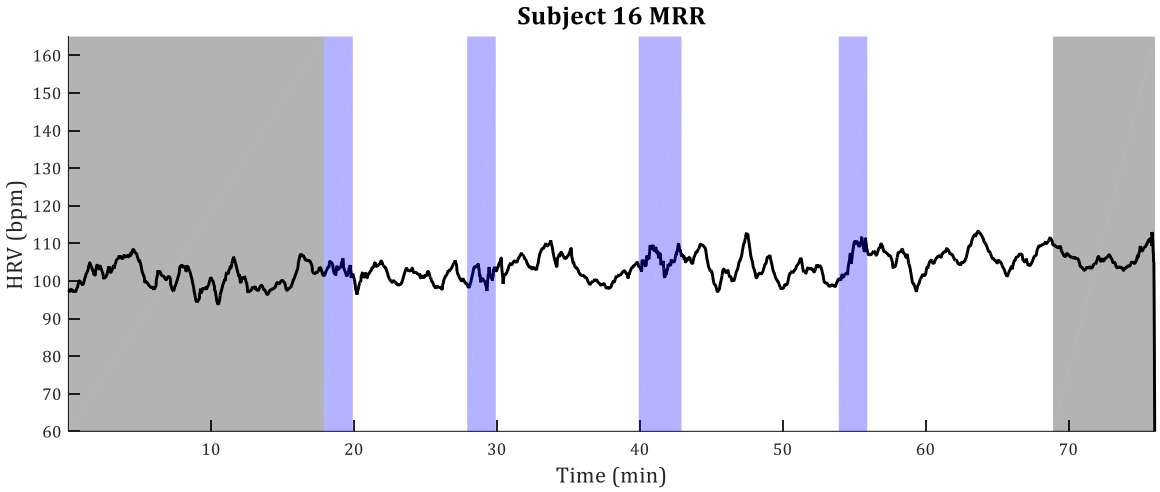

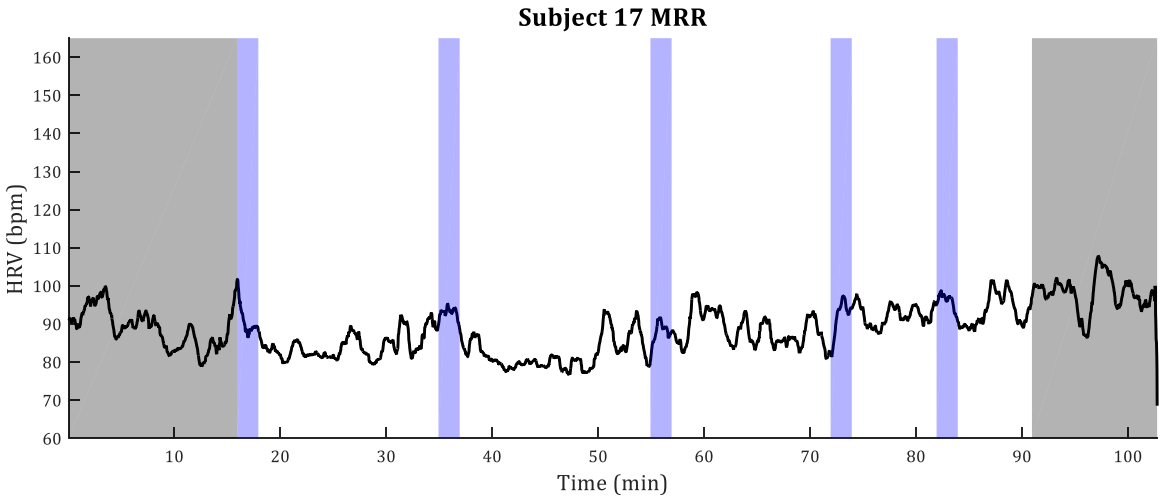

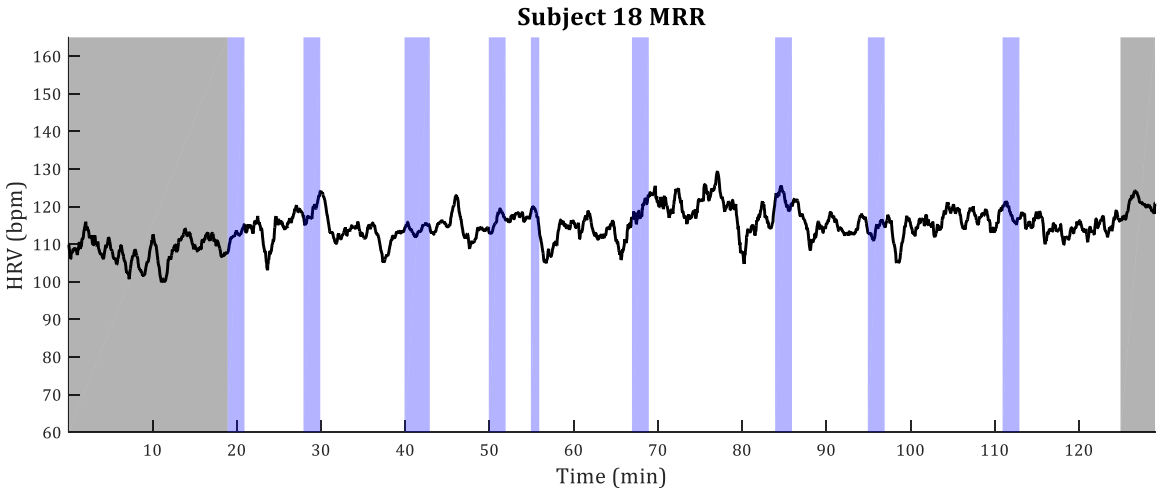

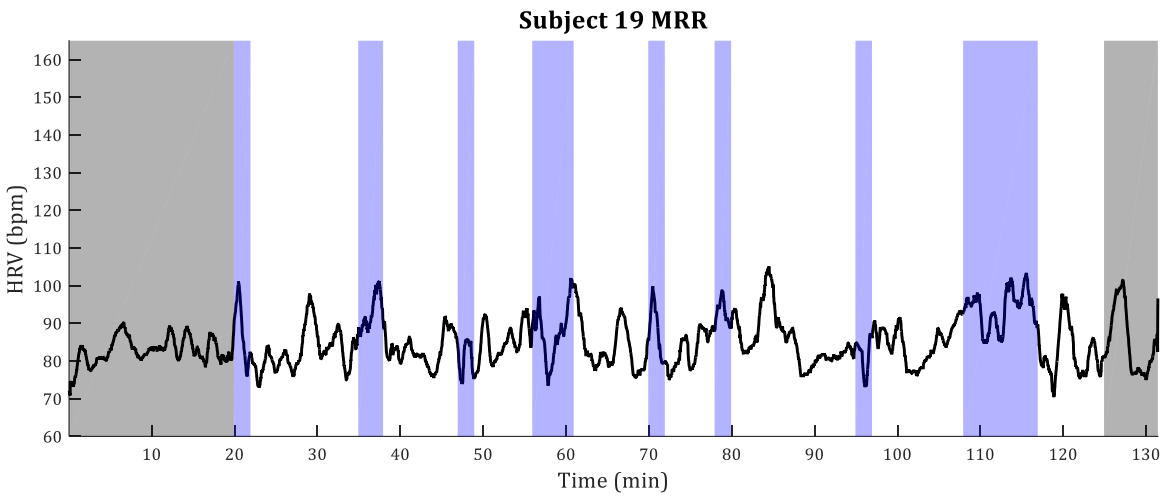
Subject 19 MRR
HRV (bpm)
Time (min)

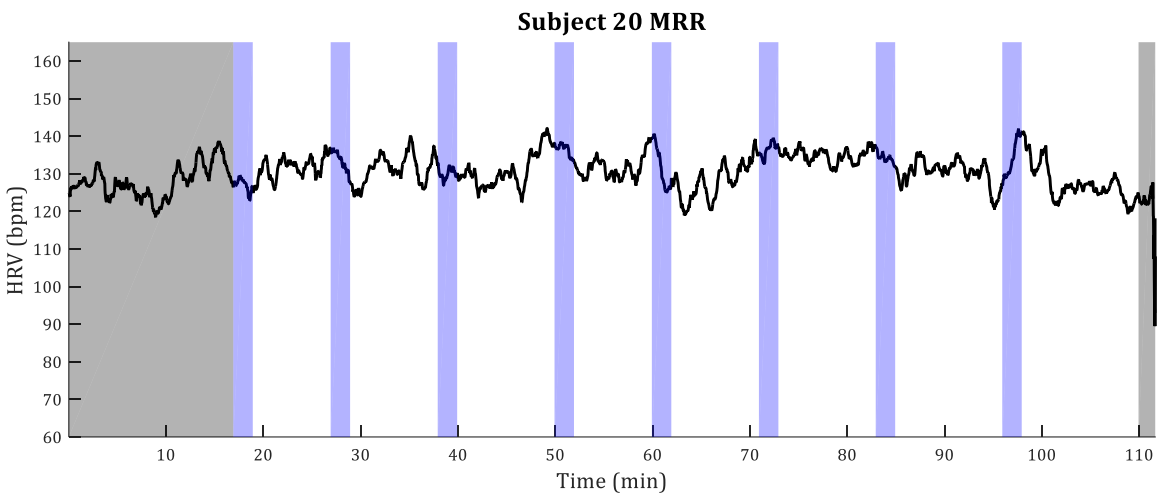
Subject 20 MRR
HRV (bpm)
Time (min)

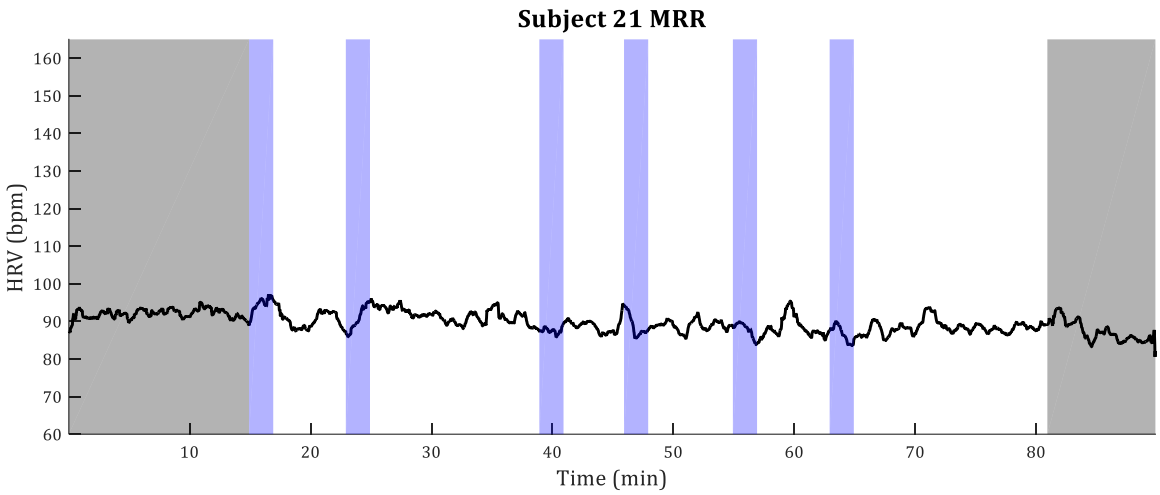
Subject 21 MRR
HRV (bpm)
Time (min)

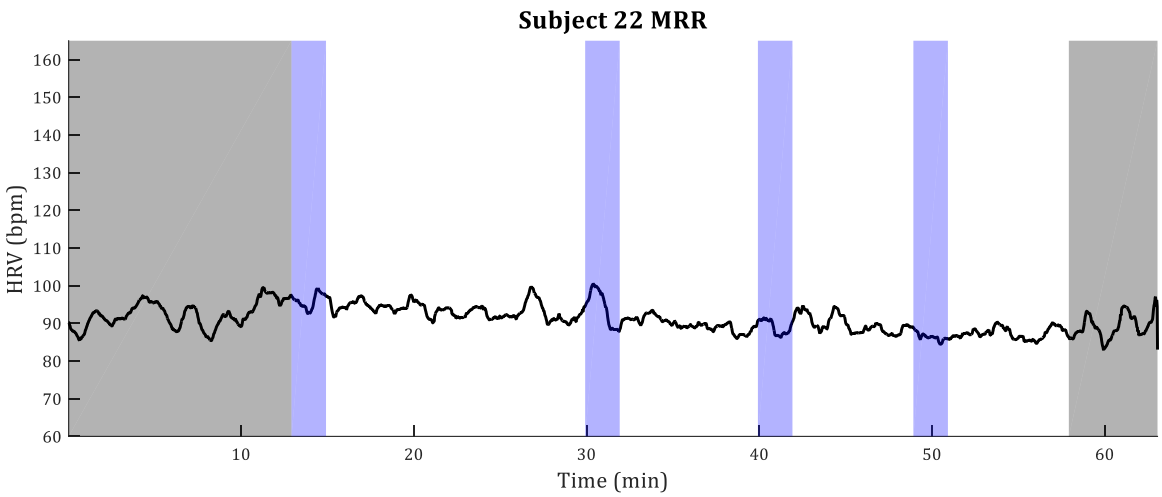
Subject 22 MRR
HRV (bpm)
160
150
140
130
120
110
100
90
80
70
60
10
20
30
40
50
60
Time (min)

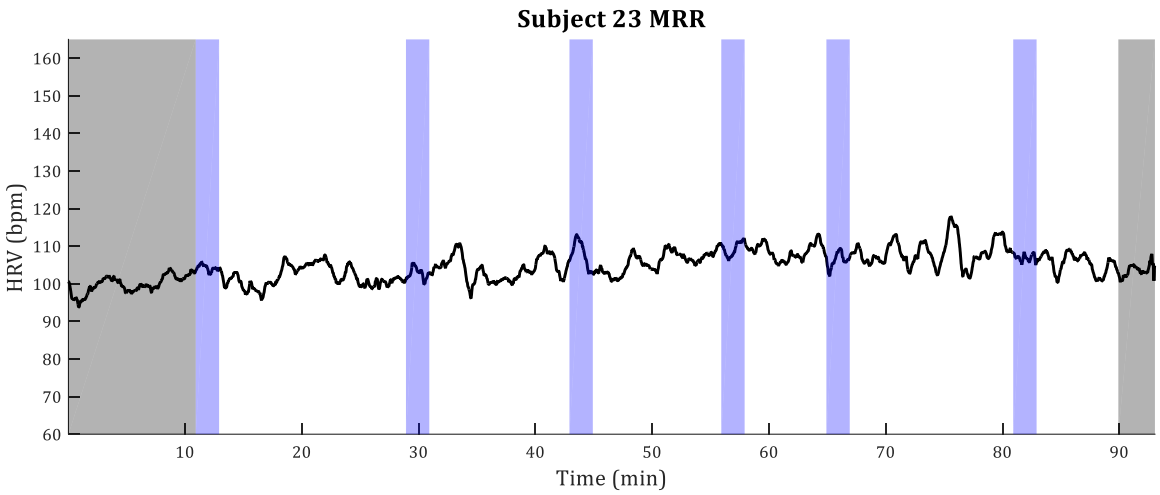
Subject 23 MRR
HRV (bpm)
160
150
140
130
120
110
100
90
80
70
60
10
20
30
40
50
60
70
80
90
Time (min)

APPENDIX E – ETHICAL APPROVAL DOCUMENTS

The following document was presented to the Guadalajara Hospital Ethical Board in order to obtain the ethical approval needed to measure the ECG signal of the patients exposed to the allergy provocation tests. The approval is included next in Spanish.

VALIDACIÓN DE UN ALGORITMO DIAGNÓSTICO DE DETECCIÓN PRECOZ DE LAS REACCIONES ALÉRGICAS MEDIANTE LA MEDICIÓN DE LA VARIABILIDAD CARDÍACA.

Palabras clave

Variabilidad Cardíaca, Reacción Alérgica, Prueba de Provocación.

INTRODUCCIÓN

La variabilidad cardíaca (VC) ha resultado ser una herramienta de gran importancia tanto para investigaciones sobre el sistema nervioso autónomo, como sobre las relaciones entre procesos psicológicos y funciones fisiológicas, o evaluaciones del desarrollo cognitivo y el riesgo clínico [1]. Se han realizado estudios que relacionan esta variabilidad con determinadas enfermedades, como es el caso de pacientes seropositivos o diabéticos [2]; con factores externos que afectan al funcionamiento cardíaco [3]; así como estudios en los que se relaciona el estado mental de los mismos con su variabilidad cardíaca [4], [5].

La prueba de exposición o de provocación (PdE), es la prueba diagnóstica considerada como patrón-oro en algunas patologías alérgicas, como la alergia a alimentos o a medicamentos. En ella al paciente sospechoso de alergia se le administran cantidades progresivamente crecientes del alimento o del fármaco a estudiar para comprobar su tolerancia o su alergia al mismo. La PdE, que se realiza bajo el criterio del alergólogo y con el consentimiento del paciente, consume tiempo y recursos y no está exenta de riesgos por la aparición de reacciones alérgicas potencialmente graves. La indicación de realizar la prueba de exposición se apoya en los resultados obtenidos mediante otros estudios complementarios, tanto in vivo como in vitro, que permiten hacer una estimación aproximativa de la tolerancia del paciente en estudio. Cabe decir que no siempre dichas pruebas complementarias están disponibles. Actualmente no existe ninguna herramienta diagnóstica que ayude a detectar de forma precoz una reacción alérgica y permita reducir el tiempo de realización de una PdE, y disminuya la aparición de reacciones graves.

OBJETIVOS

El **objetivo principal** es validar un algoritmo diagnóstico mediante el uso de un dispositivo automático de medición de FC que permita un diagnóstico precoz en tiempo real de las reacciones alérgicas que aparecen en los pacientes que son sometidos a pruebas de exposición a alimentos o medicamentos. Dicho algoritmo sería capaz de reducir el tiempo de las PdE que se realizan actualmente, así como las dosis necesarias para la detección de alergia. Como **objetivos secundarios**:

- Correlacionar los síntomas presentados por los pacientes con los patrones de VC.
- Objetivar si existen diferencias en cuanto a resultados dependiendo de la edad (niños o adultos)
- Objetivar si existen diferencias en cuanto a resultados dependiendo del tipo de alergia (alimentos o medicamentos).

ANTECEDENTES Y SITUACIÓN ACTUAL

La VC, desde el punto de vista de teoría de la señal, es una métrica de la que puede extraerse información relevante, así como relacionar dicha información con los procesos que influyen en la misma. Debido a la importancia diagnóstica de esta señal y la facilidad con la que es posible obtenerla, su uso ha despertado un gran interés en diversos grupos de perfil ingenieril.

Se han definido una serie de parámetros de la variabilidad cardíaca, calculados tanto en el dominio temporal (SDNN, RMSSD, pNN50, índice triangular, TINN, etc.) como en el dominio de frecuencia (VLF, LF, HF, ratio LF/HF, etc.) [6], gracias a los que es posible, no sólo ayudar al diagnóstico de determinadas enfermedades, sino fomentar el estudio de las mismas con el fin de correlacionar variaciones de dichos parámetros, con diversos estados tanto de salud física, como mental de los pacientes. Así, se han realizado estudios en pacientes seropositivos o diabéticos [2]; correlaciones con factores externos que afectan al funcionamiento cardíaco [3]; así como estudios en los que se relaciona el estado mental de los mismos con su variabilidad cardíaca [4], [5]

Algunas de las investigaciones más importantes y recientes en el ámbito de aplicación de la variabilidad cardíaca se resumen a continuación:

- En el trabajo presentado por Mikko et al. [7], se propone un sistema de monitorización de la señal electrocardiográfica nocturna no invasivo. Este sistema está compuesto por 8 electrodos textiles dispuestos en línea en una sábana de una cama. La novedad de este trabajo estriba en el uso de electrodos textiles y en la disposición de los mismos, de manera que la comodidad del paciente se ve beneficiada sin perjudicar la eficiencia del sistema.
- Scully et al. [8], proponen el uso de un teléfono móvil para la medida de la frecuencia respiratoria, la variabilidad cardíaca y la saturación de oxígeno en sangre. A partir de este trabajo y debido a la, cada vez mayor, potencia computacional de los teléfonos móviles, es posible desarrollar diversos sistemas de monitorización cuya principal ventaja es el ahorro económico en dicha monitorización, así como la implicación directa de los pacientes en su propio cuidado tras un proceso de información de los mismos.
- En [9], Pecchia et al. realizan un estudio de los parámetros “short-term” (Media de los intervalos RR, SDNN, RMSSD, pNN50, Potencia total del espectro, VLF, LF, HF y ratio LF/HF) de la variabilidad cardíaca para la discriminación de pacientes sanos, de pacientes con insuficiencia cardíaca. Con este objetivo proponen un modelo de clasificación basado en los parámetros de la variabilidad de la frecuencia cardíaca escogidos.
- Con respecto al diseño de dispositivos, en [10] se explica la propuesta de Massagram et. al. para el diseño de un chip dedicado exclusivamente a la medida de la variabilidad cardíaca. La ventaja de este chip es que, al ser específico para la medida de la variabilidad de la frecuencia cardíaca, tanto el consumo de potencia, como el tiempo de proceso están optimizados para la realización de esta medida.
- Por último, en [11] se realiza un estudio de los parámetros “long-term” de la variabilidad cardíaca (típicamente tomados durante 24 h.) para detectar condiciones físicas de los individuos a partir del

uso de algoritmos de computación inteligente. Como ejemplo de aplicación de este estudio, se ha empleado el mismo para el análisis de pacientes afectados por Parkinson.

Puede deducirse, a partir de los trabajos comentados, el interés que despierta el estudio de la variabilidad cardíaca, tanto desde el punto de vista de métodos de análisis, como desde el punto de vista de aplicabilidad de su estudio.

El algoritmo diagnóstico se ha diseñado a partir de los datos obtenidos tras la realización de 24 PdE a alimentos en pacientes pediátricos en el hospital de Cork (Irlanda). Durante dichas pruebas se adquirieron las señales electrocardiográficas de los pacientes con un dispositivo inalámbrico llamado Shimmer [12]. Este dispositivo está compuesto por un microprocesador y una serie de periféricos, entre otros, un accesorio para la medida del ECG con 3 electrodos y una antena Bluetooth a través de la que se enviaban los datos del dispositivo a un PC en tiempo real, para ser almacenados en el mismo. Una vez adquiridas dichas señales, se realizó un análisis de las mismas y se correlacionó con el resultado de la PdE: positivo (paciente alérgico) o negativo (paciente no alérgico).

El presente estudio parte de un estudio previo realizado por la University College Cork (Irlanda) en el que se evaluó la variación de 18 parámetros de la variabilidad cardíaca, tanto del dominio temporal (media, desviación estándar, NN50, etc.), como de la frecuencia (VLF, LF, HF, etc.). Tras dicho estudio, se comprobó que el parámetro cuya variación presentaba más correlación con la presencia de una reacción alérgica, era la media de la variabilidad cardíaca, calculada en ventanas de un minuto con un desplazamiento de 1 segundo.

El resultado de este estudio, por lo tanto, es el diseño de un algoritmo diagnóstico de detección precoz de reacciones alérgicas a partir de la media variabilidad de la frecuencia cardíaca. Los resultados obtenidos muestran un 100 % de especificidad (9/9 pacientes clasificados como no alérgicos) y un 93.33 % de sensibilidad (14/15 pacientes clasificados como alérgicos) en este número reducido de pacientes y se muestran en la Tabla 1.

Tanto el diseño del algoritmo, como las pruebas realizadas con el mismo se desarrollaron en modo offline en un PC. Actualmente se ha implementado el algoritmo diagnóstico en el dispositivo Shimmer. Por lo tanto, gracias al uso de dicho dispositivo, es posible medir el electrocardiograma, calcular la variabilidad cardíaca y detectar reacciones alérgicas en tiempo real; así como enviar los datos obtenidos a un PC y generar mensajes de alerta en caso de detección. En este estudio se puede, por lo tanto, validar el funcionamiento de dicho algoritmo funcionando en tiempo real durante pruebas reales.

Así mismo, como puede observarse en la tabla I, todos los pacientes de los que se obtuvieron datos son niños, por lo que se pretende comprobar el funcionamiento del sistema en adultos y en pruebas de alergias a medicamentos, con el fin de detectar las posibles diferencias, primero, entre niños y adultos y, segundo, entre alergias alimentarias y medicamentosas.

APLICABILIDAD Y UTILIDAD PRÁCTICA DE LOS RESULTADOS

Como puede observarse en la tabla I los resultados obtenidos pueden reducir tanto la duración de las pruebas de provocación, como el número de dosis necesarias para detectar una reacción alérgica.

El sistema puede generar una alarma al detectar una reacción, por lo que el personal sanitario encargado de supervisar este tipo de pruebas puede ser avisado en el momento en el que empiecen los primeros síntomas, sin necesidad de que esta progrese en el tiempo. Esto permite incrementar la seguridad del paciente, permitiendo un control más estrecho del mismo con una mayor autonomía del personal sanitario y disminuyendo la posibilidad de reacciones graves.

BIBLIOGRAFÍA

[1] G. G. BERNTSON et al., "Heart rate variability: Origins, methods, and interpretive caveats," *Psychophysiology*, vol. 34, no. 6, pp. 623-648, Nov. 1997.

[2] I. M. Benseñor, M. Eira, E. L. Dorea, E. M. Dantas, J. G. Mill, and P. a. Lotufo, "Heart Rate Variability in HIV Patients, Diabetics, and Controls: The AGATAA Study," *ISRN Vascular Medicine*, vol. 2011, pp. 1-8, 2011.

[3] U. Rajendra Acharya, K. Paul Joseph, N. Kannathal, C. M. Lim, and J. S. Suri, "Heart rate variability: a review.," *Medical & biological engineering & computing*, vol. 44, no. 12, pp. 1031-51, Dec. 2006.

[4] H. M. Seong, J. S. Lee, T. M. Shin, W. S. Kim, and Y. R. Yoon, "The analysis of mental stress using time-frequency distribution of heart rate variability signal.," *Conference proceedings : ... Annual International Conference of the IEEE Engineering in Medicine and Biology Society. IEEE Engineering in Medicine and Biology Society. Conference*, vol. 1, pp. 283-5, Jan. 2004.

[5] A. Begum, A. Mobyen Uddin, P. Funk, and R. Filla, "Mental State Monitoring System for the Professional Drivers Based on Heart Rate Variability Analysis and Case-based Reasoning," in *Federal Conference on Computer Science and Information Systems (FedSIS)*, 2012, pp. 35-42.

[6] M. Malik, "Heart rate variability. Standards of measurement, physiological interpretation, and clinical use.," Mar. 1996.

[7] M. Peltokangas, J. Verho, and A. Vehkaoja, "Night-time EKG and HRV monitoring with bed sheet integrated textile electrodes.," *IEEE transactions on information technology in biomedicine : a publication of the IEEE Engineering in Medicine and Biology Society*, vol. 16, no. 5, pp. 935-42, Sep. 2012.

[8] C. G. Scully et al., "Physiological parameter monitoring from optical recordings with a mobile phone.," *IEEE transactions on bio-medical engineering*, vol. 59, no. 2, pp. 303-6, Feb. 2012.

[9] L. Pecchia, P. Melillo, M. Sansone, and M. Bracale, "Discrimination power of short-term heart rate variability measures for CHF assessment.," *IEEE transactions on information technology in biomedicine : a publication of the IEEE Engineering in Medicine and Biology Society*, vol. 15, no. 1, pp. 40-6, Jan. 2011.

[10] W. Massagram, N. Hafner, M. Chen, L. Macchiarulo, V. M. Lubecke, and O. Boric-Lubecke, "Digital Heart-Rate Variability Parameter Monitoring and Assessment ASIC," *IEEE Transactions on Biomedical Circuits and Systems*, vol. 4, no. 1, pp. 19-26, Feb. 2010.

[11] C.-wei Lin, J.-S. Wang, and P.-choo Chung, "Mining Physiological Conditions from Heart Rate Variability Analysis," *IEEE Computational Intelligence Magazine*, vol. 5, no. 1, pp. 50-58, Feb. 2010.

[12] Shimmer, "SHIMMER (Sensing Health with Intelligence, Modularity, Mobility, and Experimental Reusability)." [Online]. Available: http://www.shimmer-research.com/. [Accessed: 19-Mar-2013].

DISEÑO DEL ESTUDIO

Estudio observacional prospectivo que evidencia los cambios en la frecuencia cardíaca durante una reacción alérgica.

Participantes

Departamento de electrónica, Universidad de Alcalá:

Raquel Gutiérrez Rivas,

Juan Jesús García Domínguez

Sección de Alergia, Hospital Universitario de Guadalajara

Arantza Vega Castro

Ana Alonso Llamazares

Juan Mª Beitia Mazuecos

Mª Belen Mateo Borrega

Sección de Cardiología, Hospital Universitario de Guadalajara

Javier Balaguer

Servicio de Pediatría, Hospital Universitario de Guadalajara

Alfonso Ortigado

Pacientes

Pacientes que sean sometidos a pruebas de exposición o provocación con alimentos y/o medicamentos como protocolo diagnóstico. Los pacientes cuyo resultado sea positivo serán utilizados como casos y los pacientes con estudio negativo serán los controles.

Criterios de Inclusión

- Pacientes de la Sección de Alergia del Hospital de Guadalajara, en estudio por sospecha de alergia a alimentos y/o medicamentos, que como resultado de la práctica clínica habitual vayan a ser sometidos a una prueba de exposición.
- No límite de edad.
- Pacientes (o tutores en caso de menores) que hayan dado su consentimiento a la realización de la PdE.
- Pacientes (o tutores en caso de menores) que hayan dado su consentimiento a la participación en este estudio.

Criterios de Exclusión

- Pacientes que rehúsen su participación en el estudio.
- Pacientes en los que concurra alguna de las situaciones que contraindique la realización de una Prueba de exposición.
- Pacientes con patologías cardíacas

Material

- Material y espacio físico habitual de la Sección de Alergia para la realización de pruebas de exposición en la práctica clínica habitual.
- Dispositivo inalámbrico Shimmer, compuesto por un microprocesador y periféricos (medida del ECG con 3 electrodos, antena Bluetooth)
- PC con sistema operativo diagnóstico.

Método

1. Valoración del paciente y toma de constantes previa al inicio de la prueba de exposición: TA, FC, SatO2
2. Colocación del dispositivo Shimmer con medición de electrocardiograma.
3. Realización de las pruebas de exposición según protocolo habitual de la Sección de Alergia, en dosis crecientes, con intervalos variables de 30 a 60 minutos (según el alérgeno a estudio).
4. Obtención de la variabilidad cardíaca. Esta señal se obtiene midiendo el ECG de forma continua, detectando los picos R del mismo, y calculando la frecuencia cardíaca equivalente a cada uno de los intervalos. Posteriormente, se calcula la media de estos valores, promediando todos los intervalos presentes en una ventana de 60 segundos con un desplazamiento de 1 segundo, es decir, en cada segundo se obtiene la media de la variabilidad cardíaca del minuto transcurrido. Esta señal está representada en color azul en las Figuras 2 y 3.
5. Tras cada dosis (zonas sombreadas en verde en las figuras 2 y 3), se calcula la media de la variabilidad de la frecuencia cardiaca entre el intervalo de tiempo entre la presente dosis y la dosis anterior o, en caso de ser la primera dosis, entre esta dosis y el inicio de la prueba. El valor resultante será utilizado en el intervalo entre la presente dosis y la siguiente, a este valor le llamaremos media de la variabilidad cardíaca, o MVC. El valor de la MVC está representado por una línea verde en las figuras 2 y 3.
6. A partir de cada nueva toma, se compara la variabilidad cardíaca con la MVC obtenida en el punto 4. Se calcula el factor que relaciona la diferencia entre la VC con el tiempo durante el que son diferentes. Cuanta más diferencia exista entre ambos valores, y cuanto mayor sea el tiempo durante el que se dé esta circunstancia, mayor será el valor de dicho factor.

   Se ha establecido un umbral para este factor a partir de las pruebas realizadas hasta el momento. En el momento en el que el factor supere dicho umbral, se considerará que se está dando una reacción alérgica. Se muestra un ejemplo de esta situación en la Figura 2. En dicha figura, la zona sombreada en rojo indica el momento a partir del cual el factor supera el umbral predeterminado.

Variables de estudio

Variable principal

Variabilidad de la frecuencia cardíaca

Variables secundarias

Datos de filiación
- Edad
- Sexo

Datos de diagnóstico
- Reacción sistémica inicial
- Alérgeno responsable

Datos de la Prueba de Exposición
- Duración
- Número de dosis/mg administrados
- Síntomas presentados

Tamaño de la muestra

Se realizarán 20 pruebas en una fase inicial. Dependiendo de los resultados obtenidos durante la realización éstas, necesitarán realizarse cambios en el algoritmo de detección para asegurar su funcionamiento óptimo. Una vez se consiga un funcionamiento correcto, se llegará a 150 muestras para validar el funcionamiento del algoritmo final.

Análisis de datos

Se realizará un estudio de sensibilidad, especificidad, valor predictivo positivo y negativo, y curva ROC (Figura 1) para comprobar la capacidad diagnóstica del algoritmo diseñado. Para esta evaluación se definen los siguientes términos:

- Verdadero positivo (VP): Paciente alérgico, clasificado por el algoritmo como alérgico.
- Verdadero negativo (VN): Paciente no alérgico, no clasificado por el algoritmo como alérgico.
- Falso positivo (FP): Paciente no alérgico, clasificado por el algoritmo como alérgico.
- Falso negativo (FN): Paciente alérgico, no clasificado por el algoritmo como alérgico.

		Sujeto	
		Alérgico	No alérgico
Clasificado como:	Alérgico	VP	FP
	No alérgico	FN	VN

En función de estos parámetros, se define:

- Sensibilidad: Proporción de VP identificados del total de alérgicos

$$Se = VP/(VP + FN)$$

- Especificidad: Proporción de VN identificados del total de no alérgicos

$$Es = VN/(FP + VN)$$

- Valor predictivo positivo: Proporción de VP sobre el total de clasificados como alérgicos

$$VP+= VP/(VP + FP)$$

- Valor predictivo negativo: Proporción de VN sobre el total de no clasificados como alérgicos

$$VP-= VN/(FN + VN)$$

Para el análisis de la curva ROC, se representa el resultado obtenido sobre una gráfica en la que el eje X indica la especificidad y el eje Y, la sensibilidad. Cuanto más cercano esté nuestro resultado de la esquina superior derecha (Se=100 % y Es=0 %), mejor es el resultado. Cualquier punto que se encuentre en la diagonal de esta gráfica (Se=Es) o por debajo, indica que la prueba no tiene capacidad diagnóstica.

Se estudiarán, así mismo, las posibles diferencias entre os resultados obtenidos con pruebas realizadas a niños y a adultos, así como entre pruebas de exposición a alimentos y a medicamentos.

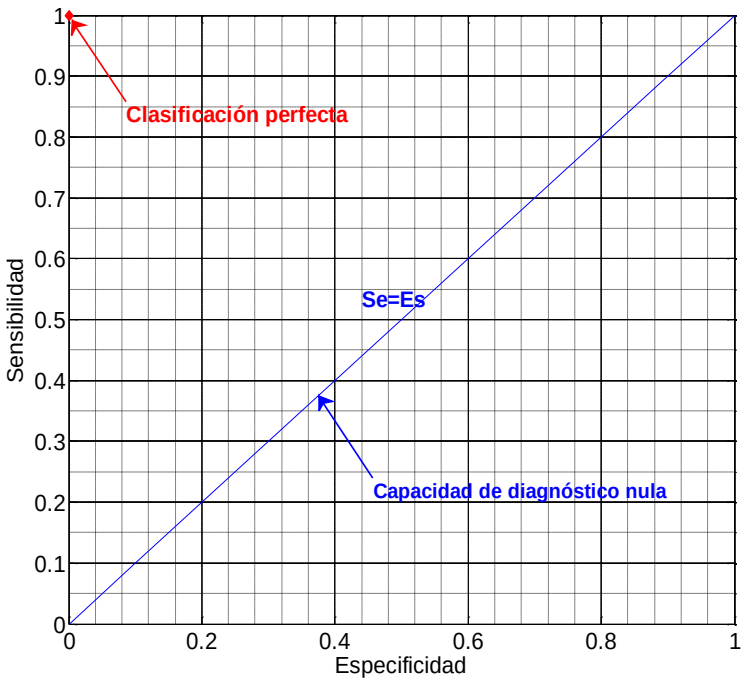

Figura 1. Representación de la curva ROC

ASPECTOS ÉTICOS

La prueba de exposición se realizará según la práctica clínica habitual en todos los participantes por lo que no se altera el manejo rutinario del paciente. A los pacientes que se sometan a esta prueba se les proporcionará información escrita y verbal y deberán firmar el correspondiente consentimiento informado según está protocolizado en la Sección de Alergia

A los pacientes que participen en el estudio se les proporcionará información escrita y verbal sobre los contenidos del proyecto y deberá ser recogida su aceptación para participar en el mismo, mediante la firma del correspondiente consentimiento informado.

Debido a que el dispositivo de medida está alimentado eléctricamente por una batería, se encuentra completamente aislado de la red eléctrica, por lo que el presente estudio no conlleva ningún riesgo adicional a los riesgos propios de una provocación, salvo las molestias que pueda sufrir el paciente por los electrodos empleados en la medida del electrocardiograma.

LIMITACIONES DEL ESTUDIO

En caso de producirse algún tipo de complicación durante la provocación para la que sea necesaria la medida del electrocardiograma, se retirará el dispositivo empleado para el estudio, por lo que no se dispondrá de los datos de ECG a partir de este momento.

Por otra parte, debido a que la correcta obtención de la variabilidad cardíaca pasa por la correcta detección de los complejos QRS del electrocardiograma, en caso de existir movimientos excesivos por parte del paciente, pueden aparecer artefactos en el ECG y, por lo tanto, no detectarse correctamente la variabilidad cardíaca. Sin embargo, se realiza un promediado de esta señal, lo que reduce el efecto de las detecciones erróneas de los complejos QRS.

COSTES

La realización del estudio no supone coste extra añadido a la prueba de exposición que se realiza de forma habitual en la Sección de Alergia del Hospital.

El coste del dispositivo, material informático, análisis de datos, etc. será sufragado por una beca de Formación de Personal Investigador (FPI) de la Universidad de Alcalá.

Tabla 1. Resultados del algoritmo de detección de alergia

Paciente			¿Alérgico?	Alérgeno	¿Detección correcta?	Duración total de la prueba	Instante de detección	Número total de dosis	Dosis para la detección
ID	**Edad**	**Sexo**							
1	18 meses	M	Sí	Trigo	Sí	0 h. 13 min.	11 min	1	1
2	6 años	M	Sí	Cacahuete	Sí	1 h. 35 min.	37 min.	5	2
3	9 años	M	Sí	Huevo	Sí	1 h. 30 min.	1 h. 03 min.	5	4
4	1 año	M	Sí	Leche	Sí	1 h. 40 min.	1 h. 21 min.	4	4
5	8 años	M	Sí	Cacahuete	Sí	2 h. 00 min.	1 h. 15 min.	7	5
6	9 años	F	Sí	Cacahuete	Sí	0 h. 33 min.	14 min.	1	1
7	6 años	M	Sí	Soja	Sí	0 h. 57 min.	27 min.	3	1
8	5 años	M	Sí	Cacahuete	Sí	1 h. 40 min.	50 min.	5	3
9	8 años	F	Sí	Huevo	Sí	0 h. 50 min.	42 min.	2	2
10	3 años	M	Sí	Leche	Sí	1 h. 22 min.	1 h. 16 min.	3	3
11	6 años	F	Sí	Cacahuete	Sí	1 h. 25 min.	58 min.	5	4
12	5 años	F	Sí	Leche	Sí	0 h. 40 min.	21 min.	2	1
13	3 años	F	Si	Leche	Sí	1 h. 45 min.	59 min.	5	3
14	1 año	M	No	Leche	Sí	1 h. 33 min.	--	4	--
15	6 años	M	No	Huevo	Sí	1 h 31 min.	--	5	--

16	10 años	M	No	Huevo	Sí	2 h. 05 min.	--	9	--
17	4 años	F	No	Soja	Sí	2 h. 05 min.	--	8	--
18	8 años	M	Sí	Soja	No	0 h. 33 min.	--	1	--
19	6 años	M	No	Cacahuete	Sí	2 h. 10 min.	--	8	--
20	7 meses	F	No	Leche	Sí	0 h. 44 min.		2	--
21	9 meses	F	Sí	Trigo	Sí	1 h. 31 min.	14 min.	7	--
22	4 años	F	No	Trigo	Sí	1 h. 21 min.	--	6	--
23	2 años	M	No	Cacahuete	Sí	0 h. 58 min.	--	4	--
24	18 meses	F	No	Leche	Sí	1 h. 38 min.	--	6	--

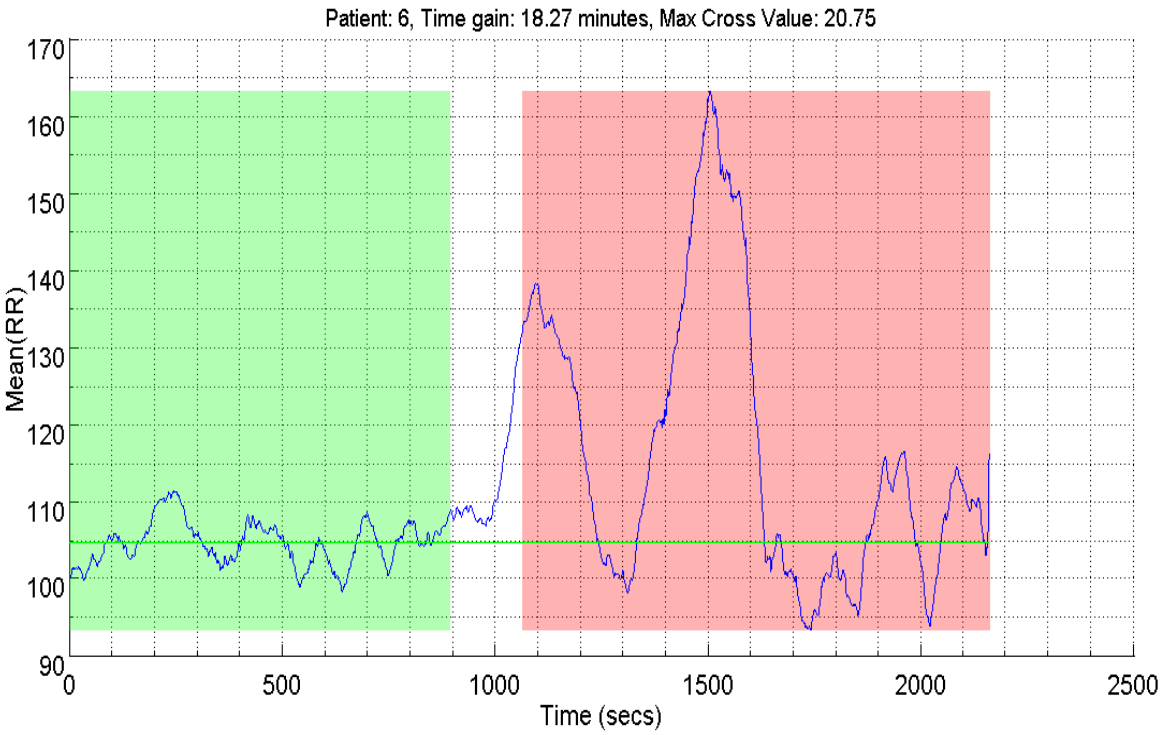

Figura 2. Ejemplo de detección de reacción alérgica

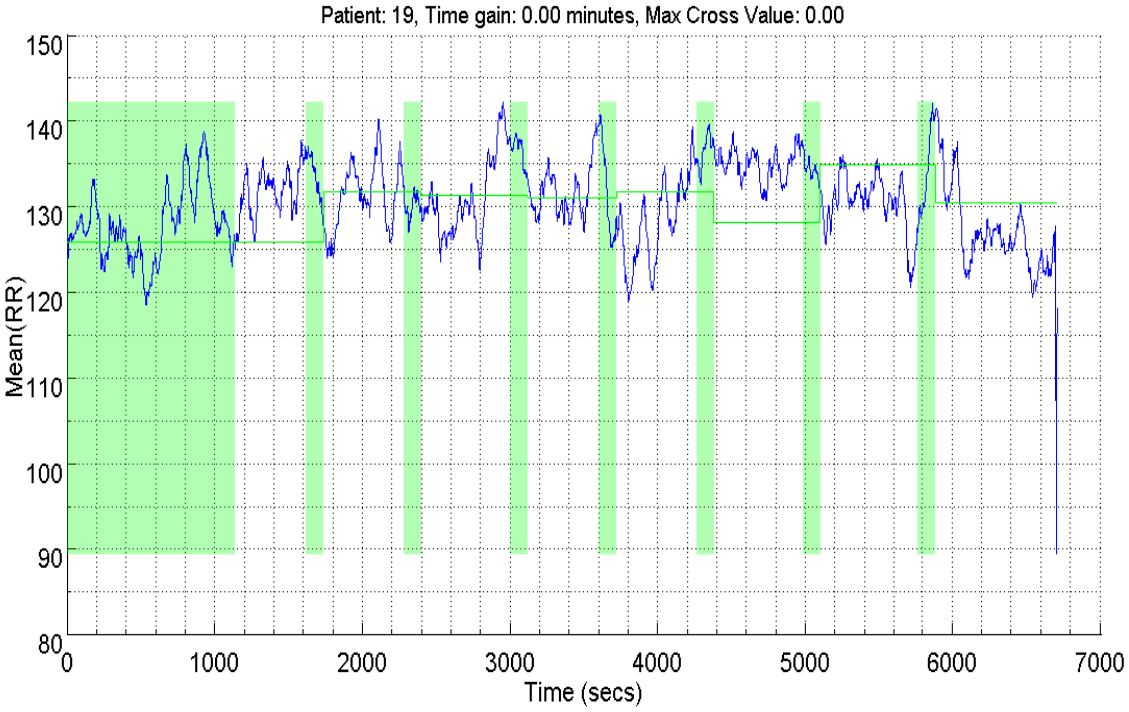

Figura 3. Ejemplo de paciente no alérgico

APPENDIX F – INFORMED CONSENTS

Patient or, if underage, guardians, who wanted to participate in the data collection process had to read and sign two of the three following documents. First one is the informed consent to carry out the food allergy tests, and the second one for drug tests. Depending on the kind of test, they must sign one of these documents, even if the ECG signal is not recorded. Finally, participants (or guardians) of the data collection process must sign the third document, which is the informed consent of this research. Note that all the documents are in Spanish.

F.1 Informed consent for a Food Allergy Test

CONSENTIMIENTO INFORMADO PARA LA REALIZACION DE ESTUDIOS DE ALERGIA A ALIMENTOS

Nombre del paciente …….

Documento Nacional de Identidad ……..

Nombre del médico que informa …….

Fecha ……. /…… /…….

En virtud del artículo 10 de la ley General de Sanidad es obligatorio que usted sea informado de su enfermedad, así como de las distintas opciones diagnósticas y terapéuticas, y de las ventajas e inconvenientes de las mismas.

Tras el estudio de alergia a alimentos que se le ha realizado creemos necesaria la realización de una prueba de tolerancia.

La prueba de tolerancia consiste en la administración de cantidades del alimento sospechoso de producir alergia, progresivamente crecientes, hasta llegar a la cantidad que se toma habitualmente en una comida. Con esta prueba comprobamos que el paciente no es alérgico al mismo, o bien sabiendo que es alérgico determinamos que cantidad de alimento puede tomar el paciente sin presentar ninguna reacción.

El alimento se administrará a lo largo de la mañana, bien de forma directa, o bien camuflado en un puré, yogurt u otro medio que consideremos necesario. El paciente debe permanecer en observación durante toda la prueba, sin poder abandonar el hospital hasta que nuestro personal lo autorice.

La prueba de tolerancia no está libre de riesgo. Pueden aparecer síntomas similares a los que presentó con anterioridad cuando comió el mismo alimento, aunque al comenzar con cantidades pequeñas estos son generalmente más leves. En ocasiones Los síntomas desaparecen sin necesidad de tratamiento. Otras veces administraremos medicación para combatir la reacción alérgica presentada (corticoides, antihistamínicos orales o intramusculares). Es excepcional la necesidad de tratamiento con adrenalina. Por ello estas pruebas se realizan en medio hospitalario, por personal especializado, siguiendo los protocolos e indicaciones de la especialidad, con la cobertura sanitaria adecuada.

En caso de no realizarse la prueba de tolerancia con alimentos no podremos confirmar la existencia o no de alergia al mismo y, ante la duda, prohibiremos la administración de dicho alimento, tanto crudo como cocinado, en cualquier preparado alimenticio.

DECLARACIONES Y FIRMAS

Declaro que:

He sido informado de forma comprensible de la naturaleza y riesgos del procedimiento mencionado, así como de sus alternativas. He podido formular todas las preguntas que he creído convenientes y doy mi consentimiento voluntario para la realización del estudio, pudiendo, no obstante, revocarlo en cualquier momento.

Firma del paciente **Firma del médico**

CONSENTIMIENTO SUBROGADO

Firmado por el representante legal del paciente ya sea por minoría de edad, incapacidad legal o incompetencia.

Nombre ……..

Documento Nacional de Identidad ……..

En calidad de (padre, madre, tutor) ..…… autorizo la realización del procedimiento mencionado.

Firma del representante legal:

F.2 Informed consent for a Drug Allergy Test

CONSENTIMIENTO INFORMADO PARA LA REALIZACION DE ESTUDIOS DE ALERGIA A MEDICAMENTOS

Nombre del paciente …….

Documento Nacional de Identidad ……..

Nombre del médico que informa …….

Fecha ……. /…… /…….

INFORMACIÓN

- El estudio de alergia a medicamentos se completará con la realización de pruebas de tolerancia ante la negatividad o inexistencia de las pruebas cutáneas. La prueba de tolerancia consiste en la administración de cantidades de fármaco progresivamente crecientes para verificar que el paciente no es alérgico a dicho medicamento.
- Estas pruebas no están libres de riesgo. Aunque raramente pueden aparecer síntomas estos son generalmente menores. En ocasiones excepcionales pueden aparecer complicaciones graves. Por ello estas pruebas se realizan en medio hospitalario, por personal especializado, siguiendo los protocolos e indicaciones de la especialidad, con la cobertura sanitaria adecuada.
- Una vez finalizado el estudio de tolerancia a un medicamento no quiere decir que en un futuro más o menos lejano no pueda sensibilizarse al mismo.

DECLARACIONES Y FIRMAS

Declaro que:

He sido informado de forma comprensible de la naturaleza y riesgos del procedimiento mencionado, así como de sus alternativas. He podido formular todas las preguntas que he creído convenientes y doy mi consentimiento voluntario para la realización del estudio, pudiendo, no obstante, revocarlo en cualquier momento.

Firma del paciente **Firma del médico**

CONSENTIMIENTO SUBROGADO

Firmado por el representante legal del paciente ya sea por minoría de edad, incapacidad legal o incompetencia.

Nombre ……..

Documento Nacional de Identidad ……..

En calidad de (padre, madre, tutor) ……. autorizo la realización del procedimiento mencionado.

Firma del representante legal:

F.3 Informed consent for the data collection process

VALIDACIÓN DE UN ALGORITMO DIAGNÓSTICO DE DETECCIÓN PRECOZ DE LAS REACCIONES ALÉRGICAS MEDIANTE LA MEDICIÓN DE LA VARIABILIDAD CARDÍACA.

HOJA DE INFORMACIÓN PARA EL PACIENTE

El Hospital de Guadalajara en colaboración con la Universidad de Alcalá está realizando un estudio cuyo objetivo principal es validar un algoritmo diagnóstico mediante el uso de un dispositivo automático de medición de frecuencia cardíaca que permita un diagnóstico precoz en tiempo real de las reacciones alérgicas que aparecen en los pacientes que son sometidos a pruebas de exposición a alimentos o medicamentos. Dicho algoritmo sería capaz de reducir el tiempo de las pruebas alérgicas que se realizan actualmente, así como las dosis necesarias para la detección de alergia.

El presente estudio parte de un estudio previo realizado por la University College Cork (Irlanda) en el que se evaluó la variación de 18 parámetros de la variabilidad cardíaca.

Se han realizado estudios que relacionan esta variabilidad con determinadas enfermedades, como es el caso de pacientes seropositivos o diabéticos, con factores externos que afectan al funcionamiento cardíaco; así como estudios en los que se relaciona el estado mental de los mismos con su variabilidad cardíaca.

Para realizar el estudio se le colocará al paciente, durante toda la prueba de provocación un dispositivo Shimmer con medición de electrocardiograma.
Debido a que el dispositivo de medida está alimentado eléctricamente por una batería, se encuentra completamente aislado de la red eléctrica, por lo que el presente estudio no conlleva ningún riesgo adicional a los riesgos propios de una provocación, salvo las molestias que pueda sufrir el paciente por los electrodos empleados en la medida del electrocardiograma.

CONSENTIMIENTO INFORMADO

A la vista de lo anterior, deseo hacer constar que he recibido suficiente información y he podido hacer las preguntas pertinentes acerca de los estudios en los que se solicita mi colaboración.

He sido informado que toda la información personal y familiar dada por mí y los resultados que se deriven de estos estudios serán tratados de forma estrictamente confidencial y no se mostrarán a terceros sin mi consentimiento.

Acepto que la información derivada de los estudios a realizar sea incluida en un fichero informático.

Comprendo que mi participación en este estudio es voluntaria y que puedo abandonarlo en cualquier momento, sin dar explicaciones, y sin que esta decisión afecte a los cuidados médicos que haya de recibir.

La información relativa al tratamiento, comunicación y cesión de los datos de carácter personal, se ajustará a lo dispuesto en la Ley Orgánica 15/1999, de 13 de diciembre, de Protección de Datos de Carácter Personal. Según la citada Ley, el consentimiento para el tratamiento de sus datos personales y para su cesión es revocable. Por lo tanto, en cualquier momento usted puede ejercer su derecho de acceso, rectificación, oposición y cancelación de sus datos dirigiéndose a: Dra. Arantza Vega, de la Sección de Alergia del Hospital Universitario de Guadalajara.

DATOS DEL PACIENTE O DE FAMILIAR EN PRIMER GRADO (en el caso de pacientes menores de edad)

Nombre y Apellidos del paciente: _____

DNI: _____

Nombre y Apellidos de quien firma el consentimiento informado (si no es el paciente):

_____

DNI: _____

Relación con el paciente (si no firma el paciente): _____

Nombre y Apellidos del médico que da la información: _____

Firma del paciente o representante legal: Firma del médico:

_____ _____

BIBLIOGRAPHY

[ABRB03] Aberer, W.; Bircher, A.; Romano, A.; Blanca, M.; Campi, P.; Fernandez, J.; … Demoly, P. (2003). Drug provocation testing in the diagnosis of drug hypersensitivity reactions: general considerations. *Allergy*, *58*(9), 854–863

[AdJC09] Adnane, Mourad; Jiang, Zhongwei; & Choi, Samjin. (2009). Development of QRS detection algorithm designed for wearable cardiorespiratory system. *Computer Methods and Programs in Biomedicine*, *93*(1), 20–31

[Afon93] Afonso, Valtino X. (1993). ECG QRS Detection. In Willis J. Tompkins,Univ.of Wisconsin-Madison (Ed.), *Biomedical digital signal processing* (pp. 236–264). Upper Saddle River, NJ, USA: Prentice-Hall, Inc.

[AhMA12] Ahmad, Ida Laila binti; Mohamed, Masnani binti; & Ab Ghani, Norul Ain binti. (2012). Development of a concept demonstrator for QRS complex detection using combined algorithms. In *2012 IEEE-EMBS Conference on Biomedical Engineering and Sciences* (pp. 689–693). Langkawi: IEEE

[Asso98] Association for the Advancement of Medical Instrumentation American National Standards Institute. (1998). *Testing and reporting performance results of cardiac rhythm and ST-segment measurement algorithms*. Airlington, VA: Association for the Advancement of Medical Instrumentation

[BGIC13] Bailón, Raquel; Garatachea, Nuria; de la Iglesia, Ignacio; Casajús, Jose Antonio; & Laguna, Pablo. (2013). Influence of running stride frequency in heart rate variability analysis during treadmill exercise testing. *IEEE Transactions on Bio-Medical Engineering*, *60*(7), 1796–805

[BeAF12] Begum, Shahina; Ahmed, Mobyen Uddin; & Filla, Reno. (2012). Mental State Monitoring System for the Professional Drivers Based on Heart Rate Variability Analysis and Case-based Reasoning. In *2012 Federated Conference on Computer Science and Information Systems (FedCSIC)* (pp. 35–42). Wroclaw: IEEE Comput. Soc

[BEDD11] Benseñor, Isabela M.; Eira, Margareth; Dorea, Egídio Lima; Dantas, Eduardo M.; Mill, José Geraldo; & Lotufo, Paulo a. (2011). Heart Rate Variability in HIV Patients, Diabetics, and Controls: The AGATAA Study. *ISRN Vascular Medicine*, *2011*, 1–8

[BTEG97] Berntson, Gary G.; Thomas Bigger, J.; Eckberg, Dwain L.; Grossman, Paul; Kaufmann, PeterG.; Malik, Marek; … Der molen, Maurots W. (1997). Heart rate variability: Origins, methods, and interpretive caveats. *Psychophysiology*, *34*(6), 623–648

[ChCC06] Chen, Szi-Wen; Chen, Hsiao-Chen; & Chan, Hsiao-Lung. (2006). A real-time QRS detection method based on moving-averaging incorporating with wavelet denoising. *Computer Methods and Programs in Biomedicine*, *82*(3), 187–95

[ChPa00] Chimene, M. F.; & Pallas-Areny, R. (2000). A comprehensive model for power line interference in biopotential measurements. *IEEE Transactions on Instrumentation and Measurement*, *49*(3), 535–540

[ChKS12] Choi, Changmok; Kim, Younho; & Shin, Kunsoo. (2012). A PD control-based QRS detection algorithm for wearable ECG applications. *Conference Proceedings : ... Annual International Conference of the IEEE Engineering in Medicine and Biology Society. IEEE Engineering in Medicine and Biology Society. Conference*, *2012*, 5638–41

[CTCL11] Chou, Chia-ching; Tseng, Shao-yen; Chua, Ericson; Lee, Yaw-chern; Fang, Wai-chi; & Huang, Hsiang-Cheh. (2011). Advanced ECG processor with HRV analysis for real-time portable health monitoring. In *2011 IEEE International Conference on Consumer Electronics -Berlin (ICCE-Berlin)* (pp. 172–175). IEEE

[Chri04] Christov, Ivaylo I. (2004). Real time electrocardiogram QRS detection using combined adaptive threshold. *Biomedical Engineering Online*, *3*(1), 28

[JRLJ11] De Jonckheere, J.; Rakza, T.; Logier, R.; Jeanne, M.; Jounwaz, R.; & Storme, L. (2011). Heart rate variability analysis for newborn infants prolonged pain assessment. *Conference Proceedings : ... Annual International Conference of the IEEE Engineering in Medicine and Biology Society. IEEE Engineering in Medicine and Biology Society. Conference*, *2011*, 7747–50

[EyDB12] Eyal, Shuli; Dagan, Yoni; & Baharav, Anda. (2012). Sleep in the Cloud: On How to Use Available Heart Rate Monitors to Track Sleep and Improve Quality of Life. In *Computing in Cardiology (CinC)* (pp. 329–332). Krakow: IEEE

[FFRM12] Farahabadi, A.; Farahabadi, Eiman; Rabbani, Hossein; & Mahjoub, Mohammad Parsa. (2012). Detection of QRS complex in electrocardiogram signal based on a combination of hilbert transform, wavelet transform and adaptive thresholding. In *Proceedings of 2012 IEEE-EMBS International Conference on Biomedical and Health Informatics* (Vol. 25, pp. 170–173). IEEE

[Foxl05] Foxlin, Eric. (2005). Pedestrian tracking with shoe-mounted inertial sensors. *IEEE Computer Graphics and Applications*, *25*(6), 38–46 http://doi.org/10.1109/MCG.2005.140

[FJJY90] Friesen, G. M.; Jannett, T. C.; Jadallah, M. a; Yates, S. L.; Quint, S. R.; & Nagle, H. T. (1990). A comparison of the noise sensitivity of nine QRS detection algorithms. *IEEE Transactions on Bio-Medical Engineering*, *37*(1), 85–98

[FMSN14] Furuya, Masaki; Masuda, Yuta; Sato, Kei; Nishibe, Toshihiro; Yana, Kazuo; & Ono, Takuya. (2014). Long and short term QT-RR interval co-variability in type 2 diabetes. In *2014 36th Annual International Conference of the IEEE Engineering in Medicine and Biology Society* (pp. 38–41). IEEE

[GhGG08] Ghaffari, A.; Golbayani, H.; & Ghasemi, M. (2008). A new mathematical based QRS detector using continuous wavelet transform. *Computers & Electrical Engineering*, *34*(2), 81–91

[GAGH00] Goldberger, A. L.; Amaral, L. A. N.; Glass, L.; Hausdorff, J. M.; Ivanov, P.Ch.; Mark, R. G.; … Stanley, H. E. (2000). PhysioBank, PhysioToolkit, and PhysioNet: Components of a New Research Resource for Complex Physiologic Signals. *Circulation 101 (23)*, *101*(23), e215–e220

[GSCR12] Goya-Esteban, R.; Sarabia-cachadina, Elena; De la cruz-Torres, Blanca; & Rojo-Alvarez, Luis. (2012). Heart Rate Variability Non Linear Dynamics in Intense Exercise. In *Computing in Cardiology (CinC)* (pp. 177–180). Krakow: IEEE

[GKLE12] Gradl, Stefan; Kugler, Patrick; Lohmuller, Clemens; & Eskofier, Bjoern. (2012). Real-time ECG monitoring and arrhythmia detection using Android-based mobile devices. *Conference Proceedings : ... Annual International Conference of the IEEE Engineering in Medicine and Biology Society. IEEE Engineering in Medicine and Biology Society. Conference*, *2012*, 2452–5

[GFJC11] Gutierrez, Raquel; Fernandez, Samuel; Jesus Garcia, J.; Carlos Garcia, J.; & Marnane, Liam. (2011). Monitoring vital signs and location of patients by using ZigBee wireless sensor networks. In *2011 IEEE SENSORS Proceedings* (pp. 1221–1224). Limerick: IEEE h

[GSGM14] Gutierrez, Raquel; Spagnol, Christian; Garcia, J.Jesus; Marnane, Liam; & Popovici, Emanuel. (2014). Low complexity QRS detectors for performance and energy aware applications. In *IEEE-EMBS International Conference on Biomedical and Health Informatics (BHI)* (pp. 256–259). Valencia: IE

[HWSS11] Hayano, Junichiro; Watanabe, Eiichi; Saito, Yuji; Sasaki, Fumihiko; Kawai, Kiyohiro; Kodama, Itsuo; & Sakakibara, Hiroki. (2011). Diagnosis of sleep apnea by the analysis of heart rate variation: a mini review. In *Annual International Conference of the IEEE Engineering in Medicine and Biology Society. IEEE Engineering in Medicine and Biology Society. Conference* (Vol. 2011, pp. 7731–4). Boston, MA: IEEE

[HJHJ15] Homin Park; Jongjun Park; Hyunhak Kim; Jongarm Jun; Sang Hyuk Son; Taejoon Park; & JeongGil Ko. (2015). ReLiSCE: Utilizing Resource-Limited Sensors for Office Activity Context Extraction. *IEEE Transactions on Systems, Man, and Cybernetics: Systems*, *45*(8), 1151–1164

[HWCT12] Hu, Sheng; Wei, Hongxing; Chen, Youdong; & Tan, Jindong. (2012). A real-time cardiac arrhythmia classification system with wearable sensor networks. *Sensors (Basel, Switzerland)*, *12*(9), 12844–12869

[HNVB07] Hu, Xiao; Nenov, Valeriy; Vespa, Paul; & Bergsneider, Marvin. (2007). Characterization of interdependency between intracranial pressure and heart variability signals: a causal spectral measure and a generalized synchronization measure. *IEEE Transactions on Bio-Medical Engineering*, *54*(8), 1407–17

[HuLi05] Huang, Jin; & Ling, C. X. (2005). Using AUC and accuracy in evaluating learning algorithms. *IEEE Transactions on Knowledge and Data Engineering*, *17*(3), 299–310

[IeVM08] Ieong, Chio In; Vai, Mang I.; & Mak, Peng Un. (2008). ECG QRS Complex detection with programmable hardware. *Conference Proceedings : ... Annual International Conference of the IEEE Engineering in Medicine and Biology Society. IEEE Engineering in Medicine and Biology Society. Conference*, *2008*, 2920–3

[IMLD12] Ieong, Chio-in; Mak, Pui-In; Lam, Chi-pang; Dong, Cheng; Vai, Mang-i; Mak, Peng-un; … Martins, Rui P. (2012). A 0.83- μW QRS detection processor using quadratic spline wavelet transform for wireless ECG acquisition in 0.35- μm CMOS. *IEEE Transactions on Biomedical Circuits and Systems*, *6*(6), 586–95

[Ito13] Ito, Komei. (2013). Diagnosis of food allergies: the impact of oral food challenge testing. *Asia Pacific Allergy*, *3*, 59–69

[JZLQ15] Jin, Min; Zhou, Xiang; Luo, Enze; & Qing, Xiongzhi. (2015). Industrial-QoS-Oriented Remote Wireless Communication Protocol for the Internet of Construction Vehicles. *IEEE Transactions on Industrial Electronics*, *62*(11), 7103–7113

[JiCh15] Jin, Zhanpeng; & Chen, Yu. (2015). Telemedicine in the Cloud Era: Prospects and Challenges. *IEEE Pervasive Computing*, *14*(1), 54–61

[KIKP14] Karmakarl, Chandan; Imaml, Mohammad Hasan; Khandokerl, Ahsan; & Palaniswamil, Marimuthu. (2014). Influence of Psychological Stress on QT Interval. In *Computer in Cardiology Conference (CinC)* (pp. 1009–1012). Cambridge, MA: IEEE

[Kenn13] Kennedy, Harold L. (2013). The evolution of ambulatory ECG monitoring. *Progress in Cardiovascular Diseases*, *56*(2), 127–32

[KhBJ13] Khiari, Bochra; Ben Braiek, Ezzedine; & Jemni, Mohamed. (2013). R-wave detection using EMD and bionic wavelet transform. In *2013 International Conference on Electrical Engineering and Software Applications* (pp. 1–5). IEEE

[KöHO02] Köhler, Bert-Uwe; Hennig, Carsten; & Orglmeister, Reinhold. (2002). The principles of software QRS detection. *IEEE Engineering in Medicine and Biology Magazine : The Quarterly Magazine of the Engineering in Medicine & Biology Society*, *21*(1), 42–57

[KABB13] Kowalski, M. L.; Asero, R.; Bavbek, S.; Blanca, M.; Blanca-Lopez, N.; Bochenek, G.; … Makowska, J. (2013). Classification and practical approach to the diagnosis and management of hypersensitivity to nonsteroidal anti-inflammatory drugs. *Allergy*, *68*(10), 1219–1232

[KWVK07] Kumar, Mohit; Weippert, Matthias; Vilbrandt, Reinhard; Kreuzfeld, Steffi; & Stoll, Regina. (2007). Fuzzy Evaluation of Heart Rate Signals for Mental Stress Assessment. *IEEE Transactions on Fuzzy Systems*, *15*(5), 791–808

[LeKL11] Lee, SangJoon; Kim, Jungkuk; & Lee, Myoungho. (2011). A real-time ECG data compression and transmission algorithm for an e-health device. *IEEE Transactions on Bio-Medical Engineering*, *58*(9), 2448–55

[LANC14] Lewandowski, Jacek; Arochena, Hisbel; Naguib, Raouf; Chao, Kuo-Ming; & Garcia-Perez, Alexeis. (2014). Logic-Centred Architecture for Ubiquitous Health Monitoring. *IEEE Journal of Biomedical and Health Informatics*, *2194*(c), 1–1

[LWSG12] Liou, Shih-hao; Wu, Yi-heng; Syu, Yi-shun; Gong, Yi-lan; Chen, Hung-Chin; & Pan, Shing-Tai. (2012). Real-Time remote ECG signal monitor and emergency warning/positioning system on cellular phone. In Pan,Jeng-Shyang, Chen,Shyi-Ming, & Nguyen,Ngoc Thanh (Eds.), *Intelligent Information and Database Systems Lecture Notes in Computer Science* (Vol. 7198, pp. 336–345). Berlin, Heidelberg: Springer Berlin Heidelberg

[Lomb76] Lomb, N. R. (1976). Least-squares frequency analysis of unequally spaced data. *Astrophysics and Space Science*, *39*(2), 447–462

[Lowr00] Lowry, Richard. (n.d.). VassarStats: Website for Statistical Computation Retrieved November 19, 2015, from http://vassarstats.net/index.html

[MaMe09] Malarvili, M. B.; & Mesbah, Mostefa. (2009). Newborn seizure detection based on heart rate variability. *IEEE Transactions on Bio-Medical Engineering*, *56*(11), 2594–603

[MKAV11] Mamaghanian, Hossein; Khaled, Nadia; Atienza, David; & Vandergheynst, Pierre. (2011). Compressed sensing for real-time energy-efficient ECG compression on wireless body sensor nodes. *IEEE Transactions on Bio-Medical Engineering*, *58*(9), 2456–66

[MILP12] Melillo, Paolo; Izzo, Raffaele; De Luca, Nicola; & Pecchia, Leandro. (2012). Heart rate variability and renal organ damage in hypertensive patients. In *Annual International Conference of the IEEE Engineering in Medicine and Biology Society. IEEE Engineering in Medicine and Biology Society. Conference* (Vol. 2012, pp. 3825–3828). San Diego, CA: IEEE

[MoMa01] Moody, G. B.; & Mark, R. G. (2001). The impact of the MIT-BIH Arrhythmia Database. *IEEE Engineering in Medicine and Biology Magazine*, *20*(3), 45–50

[MFVC02] Moraes, Jctb; Freitas, M. M.; Vilani, F. N.; & Costa, E. V. (2002). A QRS complex detection algorithm using electrocardiogram leads. In *Computers in Cardiology* (pp. 205–208). IEEE

[MuMM13] Mukhopadhyay, S. K.; Mitra, M.; & Mitra, S. (2013). ECG signal processing: Lossless compression, transmission via GSM network and feature extraction using Hilbert transform. In *2013 IEEE Point-of-Care Healthcare Technologies (PHT)* (pp. 85–88). IEEE

[Muno15] Munoz Diaz, Estefania. (2015). Inertial Pocket Navigation System: Unaided 3D Positioning. *Sensors*, *15*(4), 9156–9178

[MPJZ15] Munoz Diaz, Estefania; de Ponte Müller, Fabian; Jiménez, Antonio R.; & Zampella, Francisco. (2015). Evaluation of AHRS Algorithms for Inertial Personal Localization in Industrial Environments. In *IEEE International Conference of Industrial Technology (ICIT)* (pp. 3412–3417). Sevilla (Spain): IEEE

[MuGo14] Munoz Diaz, Estefania; & Gonzalez Mendiguchia, Ana Luz. (2014). Step Detector and Step Length Estimator for an Inertial Pocket Navigation System. In *Indoor Positioning and Indoor Navigation (IPIN 2014)* (pp. 1–6). Korea: IEEE

[MHAB14] Muraro, Antonella; Halken, S.; Arshad, S. H.; Beyer, K.; Dubois, a. E. J.; Du Toit, G.; … Sheikh, a. (2014). EAACI Food Allergy and Anaphylaxis Guidelines. Primary prevention of food allergy. *Allergy: European Journal of Allergy and Clinical Immunology*, *69*(5), 590–601

[NEBA12] Nielsen, Dorthe B.; Egstrup, Kenneth; Branebjerg, Jens; Andersen, Gunnar B.; & Sorensen, Helge B. D. (2012). Automatic QRS complex detection algorithm designed for a novel wearable, wireless electrocardiogram recording device. In *2012 Annual International Conference of the IEEE Engineering in Medicine and Biology Society* (Vol. 2012, pp. 2913–2916). IEEE

[PBTK10] Pal, S.; Bhattacharyya, D.; Tomar, G. S.; & Kim, T. (2010). Wireless Sensor Networks and Its Routing Protocols: A Comparative Study. In *2010 International Conference on Computational Intelligence and Communication Networks* (pp. 314–319). IEEE

[PaMi12] Pal, Saurabh; & Mitra, Madhuchhanda. (2012). Empirical mode decomposition based ECG enhancement and QRS detection. *Computers in Biology and Medicine*, *42*(1), 83–92

[PaTo85] Pan, J.; & Tompkins, W. J. (1985). A real-time QRS detection algorithm. *IEEE Transactions on Bio-Medical Engineering*, *32*(3), 230–6

[PBDT14] Pani, Danilo; Barabino, Gianluca; Dessi, Alessia; Tradori, Iosto; Piga, Matteo; Mathieu, Alessandro; & Raffo, Luigi. (2014). A Device for Local or Remote Monitoring of Hand Rehabilitation Sessions for Rheumatic Patients. *IEEE Journal of Translational Engineering in Health and Medicine*, *2*(November 2013), 1–11

[PMSB11] Pecchia, Leandro; Melillo, Paolo; Sansone, Mario; & Bracale, Marcello. (2011). Discrimination Power of Short-Term Heart Rate Variability Measures for CHF Assessment. *IEEE Transactions on Information Technology in Biomedicine*, *15*(1), 40–46

[PZZX09] Phyu, Myint Wai; Zheng, Yuanjin; Zhao, Bin; Xin, Liu; & Wang, Yi Sheng. (2009). A real-time ECG QRS detection ASIC based on wavelet multiscale analysis. In *2009 IEEE Asian Solid-State Circuits Conference* (pp. 293–296). IEEE

[PuLL12] Puteh, Saifullizam; Langensiepen, Caroline; & Lotfi, Ahmad. (2012). Fuzzy ambient intelligence for intelligent office environments. In *2012 IEEE International Conference on Fuzzy Systems* (pp. 1–6). Brisbane, QLD: IEEE

[Rang01] Rangayyan, Rangaraj M. (2001). *Biomedical Signal Analysis*. IEEE

[RiKW01] Rijnbeek, P. R.; Kors, J. A.; & Witsenburg, M. (2001). Minimum Bandwidth Requirements for Recording of Pediatric Electrocardiograms. *Circulation*, *104*(25), 3087–3090

[SLYJ14] Shifeng Fang; Li Da Xu; Yunqiang Zhu; Jiaerheng Ahati; Huan Pei; Jianwu Yan; & Zhihui Liu. (2014). An Integrated System for Regional Environmental Monitoring and Management Based on Internet of Things. *IEEE Transactions on Industrial Informatics*, *10*(2), 1596–1605

[Shim00a] Shimmer. (n.d.-a). SHIMMER (Sensing Health with Intelligence, Modularity, Mobility, and Experimental Reusability) Retrieved December 11, 2015, from http://www.shimmer-research.com/

[Shim00b] Shimmer. (n.d.-b). Shimmer ECG Module Retrieved from http://www.shimmer-research.com/wp-content/uploads/2012/10/Shimmer-ECG-Promo-Sheet.pdf

[SuMu14] Suryadevara, Nagender K.; & Mukhopadhyay, Subhas C. (2014). Determining Wellness through an Ambient Assisted Living Environment. *IEEE Intelligent Systems*, *29*(3), 30–37

[Task96] Task Force of the European Society of Cardiology the North American Society of Pacing Electrophisiology. (1996). Heart Rate Variability : Standards of Measurement, Physiological Interpretation, and Clinical Use. *Circulation*, *93*(5), 1043–1065

[TeEB15] Tentori, Monica; Escobedo, Lizbeth; & Balderas, Gabriela. (2015). A Smart Environment for Children with Autism. *IEEE Pervasive Computing*, *14*(2), 42–50

[TrDu15] Truong, Hong-linh; & Dustdar, Schahram. (2015). Principles for Engineering IoT Cloud Systems. *IEEE Cloud Computing*, *2*(2), 68–76

[Twom13] Twomey, Niall. (2013). *Digital Signal Processing and Artificial Intelligence for the Automated Classification of Food Allergy*. National University of Ireland

[TTHM14] Twomey, Niall; Temko, Andriy; Hourihane, J.Ob; & Marnane, W. P. (2014). Automated Detection of Perturbed Cardiac Physiology During Oral Food Allergen Challenge in Children. *IEEE Journal of Biomedical and Health Informatics*, *18*(3), 1051–1057

[VaLS12] Valenza, Gaetano; Lanatà, Antonio; & Scilingo, Enzo Pasquale. (2012). Oscillations of heart rate and respiration synchronize during affective visual stimulation. *IEEE Transactions on Information Technology in Biomedicine : A Publication of the IEEE Engineering in Medicine and Biology Society*, *16*(4), 683–90

[Webb93] Webb, Andrew R. (1993). *Statistical Pattern Recognition*. *SIAM Review* (Second Edi, Vol. 35). John Wiley & Sons, Ltd

[WiJK47] Wilson, Frank N.; Johnston, R.; & Kossmann, Charles E. (1947). The substitution of a tetrahedron for the Einthoven triangle. *American Heart Journal*, *33*(5), 594–603

[XiAZ13] Xia, Henian; Asif, Irfan; & Zhao, Xiaopeng. (2013). Cloud-ECG for real time ECG monitoring and analysis. *Computer Methods and Programs in Biomedicine*, *110*(3), 253–9

[Xili14] Xilinx, Inc. (2014). *7 Series FPGAs Overview, Product Specification*

[YaSQ13] Yan, Ruqiang; Sun, Hanghang; & Qian, Yuning. (2013). Energy-Aware Sensor Node Design With Its Application in Wireless Sensor Networks. *IEEE Transactions on Instrumentation and Measurement*, *62*(5), 1183–1191

[ZhLi09] Zhang, Fei; & Lian, Yong. (2009). Wavelet and Hilbert transforms based QRS complexes detection algorithm for wearable ECG devices in wireless Body Sensor Networks. In *2009 IEEE Biomedical Circuits and Systems Conference* (pp. 225–228). IEEE

[ZhWu08] Zheng, Huabin; & Wu, Jiankang. (2008). Real-time QRS detection method. In *HealthCom 2008 - 10th International Conference on e-health Networking, Applications and Services* (pp. 169–170). Singapore: IEEE

[ZDPL14] Zheng, Ya-Li; Ding, Xiao-Rong; Poon, Carmen Chung Yan; Lo, Benny Ping Lai; Zhang, Heye; Zhou, Xiao-Lin; … Zhang, Yuan-Ting. (2014). Unobtrusive sensing and wearable devices for health informatics. *IEEE Transactions on Bio-Medical Engineering*, *61*(5), 1538–54

[ZAAB12] Zidelmal, Zahia; Amirou, Ahmed; Adnane, Mourad; & Belouchrani, Adel. (2012). QRS detection based on wavelet coefficients. *Computer Methods and Programs in Biomedicine*, *107*(3), 490–6

[ZoCh09] Zong, Cong; & Chetouani, Mohamed. (2009). Hilbert-Huang transform based physiological signals analysis for emotion recognition. In *2009 IEEE International Symposium on Signal Processing and Information Technology (ISSPIT)* (pp. 334–339). IEEE